22296-6001-RU-02
1 OCTOBER 1974

FINAL REPORT 3

DESIGN/COST TRADEOFF STUDIES

EARTH OBSERVATORY SATELLITE SYSTEM DEFINITION STUDY (EOS)

PREPARED FOR

NATIONAL AERONAUTICS AND SPACE ADMINISTRATION
GODDARD SPACE FLIGHT CENTER

IN RESPONSE TO
CONTRACT NAS5-20519

TRW
SYSTEMS GROUP

ONE SPACE PARK • REDONDO BEACH, CALIFORNIA 90278

22296-6001-RU-02
1 OCTOBER 1974

FINAL REPORT 3

DESIGN/COST TRADEOFF STUDIES

EARTH OBSERVATORY SATELLITE SYSTEM DEFINITION STUDY (EOS)

PREPARED FOR

NATIONAL AERONAUTICS AND SPACE ADMINISTRATION
GODDARD SPACE FLIGHT CENTER

IN RESPONSE TO
CONTRACT NAS5-20519

TRW
SYSTEMS GROUP

ONE SPACE PARK • REDONDO BEACH, CALIFORNIA 90278

CONTENTS

		Page
1.	INTRODUCTION	1-1
2.	MISSION AND REQUIREMENT SUMMARY	2-1
2.1	Mission Definition	2-1
2.1.1	EOS-A Baseline Mission	2-2
2.1.2	Mission Model	2-4
2.1.3	Advanced Missions	2-6
2.2	General Design Objectives	2-6
2.3	Orbit and Launch Vehicle Considerations	2-6
2.3.1	Orbit Selection	2-6
2.3.2	Launch Vehicle Selection	2-11
3.	OBSERVATORY MODULAR DESIGN CONCEPTS	3-1
3.1	Observatory Conceptual Arrangement	3-1
3.1.1	The Modular Concept	3-2
3.1.2	Modular Size and Modularity Level	3-5
3.2	Mechanical Interfaces	3-12
3.2.1	Observatory to Launch Vehicle	3-12
3.2.2	Observatory to Shuttle	3-14
3.2.3	Modules to Observatory	3-16
3.2.4	Umbilical Connections	3-17
3.2.5	Contamination Considerations	3-19
3.3	Thermal Control Concept and Interfaces	3-21
3.4	Power Interfaces	3-23
3.4.1	Structural Harness	3-23
3.4.2	Module Interfaces	3-23
3.4.3	Summary	3-25
3.5	Data Interfaces	3-25
3.5.1	Data Bus System Operation	3-26
3.5.2	Data Bus Characteristics	3-26
3.5.3	Data Bus Format	3-27
3.6	EMC Control	3-27
3.7	ACS Concept and Mission Peculiars	3-29
3.7.1	Attitude Determination	3-29

CONTENTS (Continued)

		Page
	3.7.2 Attitude Control Implementation for Mission Flexibility	3-30
3.8	Propulsion – Modular Concept	3-35
3.9	Telemetry, Tracking, and Command	3-37
	3.9.1 Introduction	3-37
	3.9.2 Communications System	3-38
	3.9.3 Data Handling System	3-42
3.10	Wideband Communications Module Concept and Mission Peculiars	3-43
	3.10.1 Introduction and Baseline Description	3-43
	3.10.2 Accommodation of Advanced Missions	3-45
3.11	Electric Power Concept and Mission Peculiars	3-47
	3.11.1 Electric Power Concept	3-50
	3.11.2 Selected EPS Configuration	3-51
	3.11.3 Thermal Considerations	3-55
	3.11.4 Solar Array Modularity	3-55
4.	EOS-A BASELINE OBSERVATORY SYSTEM	4-1
4.1	EOS-S Mechanical Configuration	4-1
	4.1.1 Delta Configuration	4-2
	4.1.2 Titan Configuration	4-2
	4.1.3 Payload Accommodation	4-5
	4.1.4 Mechanical Design Features	4-5
	4.1.5 Alternate Configurations	4-7
4.2	EOS-A Electrical Design	4-10
4.3	Performance Requirements and Allocations	4-13
	4.3.1 Mission Operational Modes	4-14
	4.3.2 Error Allocation Groundrules and Approach	4-16
	4.3.3 Error Terms and Allocations	4-17
4.4	ACS Operation	4-20
4.5	Redundancy and Reliability	4-26
4.6	Observatory Mass Properties	4-33
	4.6.1 Thor-Delta Configurations	4-39
	4.6.2 Titan Configuration	4-39

CONTENTS (Continued)

		Page
5.	EOS-A BASELINE INSTRUMENT DESIGN	5-1
5.1	Thematic Mapper	5-1
5.1.1	Configuration/Performance Summary	5-1
5.1.2	Design Details	5-3
5.2	High Resolution Pointable Imager (HRPI)	5-9
5.2.1	Design Detail	5-10
5.2.2	HRPI Configuration/Performance Summary	5-13
5.3	Data Collection Module	5-18
6.	EOS-A BASELINE MODULE/SUBSYSTEM DESIGNS	6-1
6.1	Communications and Data Handling Module	6-1
6.1.1	Introduction	6-1
6.1.2	System Requirements and Capabilities	6-2
6.1.3	System Description	6-2
6.1.4	System Performance	6-11
6.1.5	Equipment Description	6-13
6.2	Attitude Determination Module	6-32
6.2.1	Inertial Reference Unit	6-33
6.2.2	Star Tracker Assembly	6-34
6.2.3	Magnetometer	6-35
6.2.4	Sun Sensor Assembly	6-36
6.2.5	Transfer Assembly	6-36
6.2.6	Data Interface Unit	6-37
6.2.7	Power Control Unit	6-37
6.3	Actuation Module	6-37
6.3.1	Reaction Wheels	6-37
6.3.2	Magnetic Torquers	6-40
6.3.3	Reaction Wheel Electronics Assembly	6-43
6.3.4	Valve and Magnetic Torquer Electronics	6-44
6.3.5	Description of EOS-A Propulsion Configuration	6-45
6.4	Power Module	6-48
6.4.1	Introduction	6-48
6.4.2	Detailed Description	6-49

CONTENTS (Continued)

		Page
6.4.3	Power Control Unit	6-51
6.4.4	Battery Assembly	6-57
6.4.5	Diode Assembly	6-59
6.4.6	Power Disconnect Assembly	6-59
6.4.7	Power Converters	6-59
6.5	Electrical Integration	6-61
6.5.1	Power Distribution	6-61
6.5.2	Signal Distribution	6-63
6.5.3	Observatory Harness Configuration	6-63
6.5.4	Module Harness Configuration	6-67
6.5.5	EMC Controls	6-67
6.6	Solar Array and Drive Module	6-70
6.6.1	Solar Cell Array	6-72
6.6.2	Solar Array Drive	6-73
6.7	Wideband Communication Module	6-76
6.7.1	Introduction	6-76
6.7.2	System Summary	6-77
6.7.3	Requirements Versus Capability	6-79
6.7.4	Wideband Communication System Performance	6-79
6.7.5	Wideband Communication Equipment Description	6-83
6.8	Spacecraft Structure and Mechanisms	6-95
6.8.1	Spacecraft Structure	6-95
6.8.2	Mechanisms	6-114
6.9	Payload Structure	6-122
6.9.1	Design Requirements and Philosophy	6-122
6.9.2	Structural Description	6-123
6.9.3	Structural Analyses	6-125
6.10	Thermal Control	6-128
6.10.1	Design Requirements	6-128
6.10.2	Baseline Structure Thermal Control Design	6-129
6.10.3	Baseline Module Thermal Control Design	6-136
6.10.4	Module/Sensor to Structure Interface	6-138
6.10.5	Comment on Titan and Thor-Delta Configuration Thermal Design	6-139
6.10.6	Summary	6-139

CONTENTS (Continued)

		Page
7.	EOS-A BASELINE INTEGRATION AND TEST CONCEPT	7-1
	7.1 Qualification	7-5
	7.2 Acceptance	7-8
8.	EOS-A BASELINE GROUND SUPPORT EQUIPMENT	8-1
	8.1 Electrical Ground Support Equipment	8-1
	8.2 Mechanical Ground Support Equipment	8-9
9.	EOS-A BASELINE GROUND DATA MANAGEMENT DESIGN	9-1
	9.1 Low Cost Ground Station	9-1
	9.1.1 Operational Characteristics	9-1
	9.1.2 Acquisition Equipment	9-4
	9.1.3 Direct Display	9-5
	9.1.4 Record and Process	9-5
	9.1.5 System Engineering and Integration	9-7
	9.2 Operational Control Center	9-7
	9.3 Baseline Central Data Processing Facility Design	9-14
	9.3.1 User Requirements	9-17
	9.3.2 CDPF Functions and Interfaces	9-19
	9.3.3 Information Management System and Data Services Laboratory	9-22
	9.3.4 Image Processing System	9-24
	9.3.5 Image Processing System Hardware Baseline	9-30
	9.3.6 Operational Considerations	9-35
10.	COSTING EVALUATION	10-1
	10.1 Costing Approach	10-1
	10.2 Cost Tradeoffs	10-2

ILLUSTRATIONS

		Page
2-1	EOS Mission Model	2-5
2-2	Launch Vehicle Payload Capability (Sun-Synchronous Orbits)	2-11
3-1	EOS Modular Concepts	3-3
3-2	EOS Titan and Thor-Delta Configurations	3-7
3-3	Typical Modes of Spacecraft Maintenance	3-9
3-4	Baseline Modular Block Diagram	3-10
3-5	Alternate Schemes of Supporting EOS to the Launch Vehicle	3-13 3-13
3-6	Module Attachment Interface Arrangement	3-17
3-7	Observatory Umbilical Connections	3-18
3-8	Sample Thermal Control System	3-22
3-9	Module Power Interface	3-24
3-10	Typical Module Power Interface	3-25
3-11	Data Handling Concept	3-26
3-12	Bus Formats	3-28
3-13	Star Tracker Geometry	3-30
3-14	Attitude Estimation Block Diagram	3-31
3-15	Attitude Control Functional Block Diagram	3-32
3-16	Actuation Requirements for Growth Missions	3-33
3-17	Actuation Sizing	3-35
3-18	Block Diagram — Communications and Data Handling Module Baseline Design	3-38
3-19	Addition of Redundant Communication Equipment	3-40
3-20	Addition of Equipment for Synchronous Operation	3-41
3-21	EOS-A Wideband Communications Module Block Diagram	3-44
3-22	MODS Conditioning	3-48
3-23	Micro Controller for the High-Speed Multiplexer	3-48
3-24	TDRSS Impact on Wideband Communications	3-49
3-25	Electrical Power Subsystem Simplified Block Diagram	3-52
3-26	Battery Voltage Limit Curve	3-53
4-1	Baseline Thor-Delta EOS	4-3
4-2	Baseline Titan EOS	4-4

ILLUSTRATIONS (Continued)

		Page
4-3	Thor-Delta EOS-A Alternate Concept	4-8
4-4	Delta Configuration for Titan Launch	4-9
4-5	EOS-A System Block Diagram (Minimum Redundancy)	4-11
4-6	EOS-A System Block Diagram (Nominal Redundancy)	4-12
4-7	Generic Sequence of Events and Attitude Control Modes	4-21
4-8	Sun Acquisition Mode	4-22
4-9	Star Acquisition and Attitude Determination	4-23
4-10	Earth Hold Mode	4-24
4-11	Orbit Injection/Trim Mode	4-25
4-12	Normal Mode	4-24
4-13	Safe Mode	4-26
4-14	Nominal Redundancy Configuration Reliability Block Diagram	4-29
4-15	Minimum Redundancy Configuration Reliability Block Diagram	4-32
5-1	Thematic Mapper Scan Geometry	5-1
5-2	Scanning Optics Schematic	5-3
5-3	Chromatic Optics Schematic	5-4
5-4	Thematic Mapper Block Diagram	5-5
5-5	Filter Gain and Phase Characteristics	5-6
5-6	Linear Image Plane Thematic Mapper	5-7
5-7	Thematic Mapper Radiation Cooler Configuration	5-9
5-8	HRPI Electronics Block Diagram	5-11
5-9	Calibration Insertion	5-12
5-10	HRPI Scan Orientation	5-13
5-11	HRPI Configuration (Side View)	5-13
5-12	Prism Array Spectral Separation	5-14
6-1	Communications and Data Handling Module (Thor-Delta)	6-1
6-2	Communication and Data Handling Module Baseline Data	6-6
6-3	Omni Antenna Coverage	6-7
6-4	Communications Modulation Spectra	6-8
6-5	S-Band TT and C Receiver	6-17
6-6	S-Band 2-Watt TT and C Transmitter	6-22
6-7	Data Handling Block Diagram (Baseline Configuration — Redundant)	6-23

ILLUSTRATIONS (Continued)

		Page
6-8	Baseline Command Decoder – Simplified Block Diagram	6-25
6-9	Command Format	6-26
6-10	Typical Modulation Waveforms	6-28
6-11	Attitude Determination Module	6-32
6-12	Attitude Determination Module Block Diagram	6-33
6-13	Actuation Module for Thor-Delta and Titan	6-38
6-14	Actuation Module (Minimum Redundancy)	6-41
6-15	Orbit Transfer/Orbit Adjust – Bilevel RCS Configuration (Titan Configuration)	6-46
6-16	Orbit Adjust – Single Level RCS Configuration	6-46
6-17	Power Module and Interface Block Diagram	6-48
6-18	Electric Power Module Block Diagram	6-50
6-19	Perspective View of Power Module	6-51
6-20	1.0 Kw PWM Regulator	6-52
6-21	Typical Efficiency – PWM Regulator	6-52
6-22	Battery Voltage Limit Switch	6-53
6-23	Battery Voltage Limit Curves	6-54
6-24	Power Regulator Unit Select and Fault Isolation	6-55
6-25	Battery Third Electrode Cell Voltage Detector	6-55
6-26	Power Control Safe Mode Logic	6-57
6-27	Electric Power Module Bus Protection Assembly	6-58
6-28	Secondary Power Converter	6-60
6-29	Redundant Primary Power Bus Protection Concept	6-62
6-30	Detailed Module Electrical Interfaces	6-65
6-31	Wire Harness Concept	6-66
6-32	Solar Array and Drive Module Block Diagram	6-71
6-33	Solar Array and Drive Module Perspective	6-71
6-34	EOS-A Solar Array Drive	6-75
6-35	EOS-A Wideband Communications Module Perspective	6-77
6-36	EOS-A Wideband Communications Block Diagram	6-78
6-37	Power Loss Curves	6-81
6-38	Degradation Due to Transmission Filtering Versus Filter Cut-Off Frequency f for QPSK	6-81

ILLUSTRATIONS (Continued)

		Page
6-39	Antenna Gimbal Drive and Electronics	6-85
6-40	Direct Modulation Design	6-86
6-41	Wideband Data Handling Equipment	6-88
6-42	MODS Conditioning	6-90
6-43	Micro-controller for the High-Speed Multiplexer	6-90
6-44	EOS-A Wideband CDPF Data Format – Thematic Mapper	6-92
6-45	EOS-A Wideband System CDPF – HRPI	6-93
6-46	Speed Buffer Data Format (One Swath)	6-94
6-47	Speed Buffer (LCGS) Partitioning (Includes a line stripper and formatting)	6-94
6-48	EOS-A Baseline Configuration (Titan)	6-97
6-49	EOS-A Baseline Configuration (Thor-Delta)	6-98
6-50	Power Module Structural Configuration	6-105
6-52	Analytical Model of Titan Observatory Configuration	6-111
6-53	Analytical Model of Thor-Delta Observatory Configuration	6-111
6-54	Analytical Model of Power Equipment Module	6-112
6-55	Latch Mechanism, Power Driven EOS MEM/Module Interface	6-115
6-56	Latch Mechanism, Power Driven Internal Concept	6-116
6-57	Tailoring of the Attachment Fitting for Selective Constraint	6-119
6-58	Thor-Delta Version Solar Array Deployment	6-121
6-59	Spring Actuated Hinge	6-122
6-60	Pitch Angle Uncertainty Thermal/Structural	6-127
6-61	Observatory Thermal Features	6-134
6-62	Module Thermal Features	6-136
7-1	Pilot Model EOS-A Integration and Test Flow	7-3
7-2	Flight EOS-A Integration, Test, and Launch Operations Flow	7-4
8-1	Module Test Concept	8-1
8-2	Data Bus Simulators	8-2
8-3	System Test Concept	8-3

ILLUSTRATIONS (Continued)

		Page
9-1	LCGS Functional Block Diagram	9-2
9-2	Acquisition Equipment Subsystem	9-4
9-3	LCGS Minimal Cost Record and Process Configuration	9-6
9-4	LCGS Facilities Configuration	9-7
9-5	EOS Control Center Design Concept	9-11
9-6	EOS Control Center Multiple Operations Design Concept	9-15
9-7	Baseline Ground Data Handling System Interfaces	9-20
9-8	CDPF Functional Structure	9-21
9-9	NASA Data Processing Facility System Overview	9-23
9-10	Baseline Functional Image Processing System Design	9-26
9-11	Error Correction Subsystem Hardware Complement	9-31
9-12	Estimation, Formatting, and Film Generation Subsystem Hardware Complement	9-33
9-13	Formatting and Tape Generation Subsystem Hardware Complement	9-36
9-14	Production Timeline	9-36

TABLES

		Page
2-1	System Output Quality Requirements	2-3
2-2	System Output Quantity Requirements	2-3
2-3	Advanced Mission Characteristics	2-7
2-4	General Design Objectives/Guidelines for EOS	2-8
2-5	Effect of Orbit Selection on HRPI Coverage	2-10
3-1	Post-EOS-A Missions and Design Impacts	3-41
3-2	Subpanel Power (watts)	3-56
3-3	Power per Unit Weight (watt/lb) for Two Array Substrates, Three Glass Thickness, Three Altitudes, Three Life Times	3-57
4-1	EOS Configurations	4-1
4-2	Attitude Estimation Specification	4-18
4-3	Attitude Control Specification	4-19
4-4	Ephemeris Specification (Earth Pointing Mode - 1σ)	4-19
4-5	Thematic Mapper Scan Angle (1σ)	4-19
4-6	Thermal/Structural Specifications	4-19
4-7	Redundancy Configurations	4-28
4-8	Properties of Redundancy Configurations	4-28
4-9	Thor-Delta EOS-A Observatory Weight Summary (716 km Circular Sun-Synchronous Orbit)	4-34
4-10	Titan IIIB EOS-A Observatory Weight Summary (716 km Circular Sun-Synchronous Orbit)	4-35
4-11	Detail Spacecraft Weight Breakdown (Non-serviceable Minimum Redundancy Case)	4-36
4-12	EOS-A Mass Properties Characteristics	4-38
4-13	Δ Weight Breakdown	4-40
5-1	Thematic Mapper Characteristics Summary	5-2
5-2	Weight Tabulation	5-8
5-3	Cooler Radiation	5-8
5-4	HRPI Component Weight Tabulation	5-15
5-5	HRPI Performance Summary	5-15
6-1	Requirements versus Capabilities	6-3
6-2	S-Band Telemetry, Tracking, and Command Parameters	6-12

TABLES (Continued)

		Page
6-3	Command Uplink Power Budget	6-14
6-4	Telemetry Downlink Power Budget	6-19
6-5	Characteristics of Candidate Computers	6-30
6-6	Software Modules and Storage Estimates	6-31
6-7	Attitude Determination Module Equipment List	6-32
6-8	Thor-Delta and Titan Actuation Module Hardware List	6-39
6-9	Actuation Module Equipment List (Minimum Redundancy)	6-40
6-10	EOS-A Battery Characteristics	6-58
6-11	Hardline Signal Interconnections	6-64
6-12	Umbilical Interconnections	6-64
6-13	EOS-A Solar Array Physical Characteristics	6-73
6-14	EOS-A Solar Array Sizing Factors	6-74
6-15	EOS-A Solar Array Performance Characteristics	6-73
6-16	Requirements vs. Capabilities for EOS-A Wideband Communications Module and Data Handling	6-80
6-17	RF Link Analysis Summary	6-82
6-18	Power Flux Density Analysis Summary	6-83
6-19	EOS-A Wideband Communications and Data Handling Module Equipment List	6-83
6-20	Maximum Expected Flight Loads (g's)	6-99
6-21	EOS Observatory Titan Configuration Stiffness Sensitivity Study	6-113
6-22	Description of Observatory Modes - Titan Serviceable Version (5000 pounds)	6-113
6-23	Description of Observatory Modes - Thor-Delta Non-serviceable Version (2500 pounds)	6-113
6-24	Summary of Minimum Margins of Safety	6-114
6-25	Allowable Pointing Tolerance and Drift Rates (Thermal/Structural)	6-123
6-26	Summary of Minimum Margins of Safety	6-129
6-27	General EOS-A Observatory System Thermal Design Requirements and Functions	6-130
6-28	Specific EOS-A Observatory System Thermal Design Requirements	6-130
6-29	Structure TCS Performance Factors, Control Parameters and Methods	6-131

TABLES (Continued)

		Page
6-30	Study Summary of Structural Thermal Control Module	6-133
6-31	EOS-A Baseline Thermal Design Description and Function	6-135
6-32	Module Structure Heater Power Requirements	6-137
7-1	Overview of EOS Baseline and Conventional Test Programs	7-2
9-1	LCGS Thematic Mapper Compaction Alternative	9-3
9-2	Control Center New Equipment	9-10
9-3	Multi-operations Control Center Additional Equipment	9-13
9-4	EOS User Data Requirements	9-18
9-5	EOS CDPF Baseline Data Loading	9-19

GLOSSARY

AC	Alternating Current
ACS	Attitude Control System
A/D	Analog to Digital
ADM	Attitude Determination Module
BCU	Bus Controller Unit
BTU	British Thermal Unit
BVL	Battery Voltage Level
CCT	Computer Compatible Tape
CDPF	Central Data Processing Facility
CONUS	Continental United States
CPU	Central Processing Unit
CRT	Cathode Ray Tube
DC	Direct Current
DCS	Data Collection System
DIU	Data Interface Unit
DMA	Direct Memory Access
DSC	Data Services Laboratory
DSCS II	Defense Satellite Communication System - II
EI	Electrical Integration
EIRP	Effective Isotropic Radiated Power
EGSE	Electrical Ground Support Equipment
EMC	Electromagnetic Compatibility
EMI	Electromagnetic Interference
EOS	Earth Observatory Satellite
EP	Electric Power
EROS	Earth Resources Observatory Satellite
ERTS	Earth Resources Technology Satellite
FLTSATCOM	Fleet Satellite Communications
FSS	Flight Support System
GCS	Gimbal Control Subassembly
GFE	Government Furnished Equipment
GSFC	Goddard Space Flight Center
HDDT	High Density Digital Tape

HDMR	High Density Multirack Recorder
HRPI	High Resolution Pointable Imager
IMS	Information Management System
IPS	Image Processing System
IRU	Inertial Reference Unit
IST	Integrated Systems Test
LCGS	Low Cost Ground Station
LRM	Land Resources Management
MGSE	Mechanical Ground Support Equipment
MODS	Multimegabit Operational Data System
MOMS	Multimegabit Operational Multiplexer System
MMD	Mean Mission Duration
MSS	Multispectral Scanner
MTTF	Mean Time to Failure
NASA	National Aeronautics and Space Administration
NDPF	NASA Data Processing Facility
OAO	Orbiting Astronomical Observatory
OBC	On-Board Computer
OBP	On-Board Processor
OGO	Orbiting Geophysical Observatories
PCM	Pulse Code Modulation
PCU	Power Control Unit
PROM	Programmable Read Only Memory
PWM	Pulse Width Modulation
RCP	Registration Control Point
RCS	Reaction Control System
RF	Radio Frequency
ROM	Read Only Memory
RWEA	Reaction Wheel Electronics Assembly
SAMS	Shuttle-Attached Manipulator System
SAMSO	Space and Missile Systems Organization
SEOS	Synchronous Earth Observatory Satellite
SMM	Solar Maximum Mission
SPMS	Special Purpose Manipulator System

SRU	Space Repairable Unit
SSA	Sun Sensor Assembly
STA	Star Tracker Assembly
TA	Transfer Assembly
TCS	Thermal Control System
TDRSS	Tracking and Data Relay Satellite
TM	Thematic Mapper
TWT	Travelling Wave Tube
USAF	United States Air Force
USN	United States Navy
USB	Unified S-Band
WBCDH	Wideband Communications and Data Handling Assembly
WBCM	Wideband Communications Module
WBCS	Wideband Communications System

1. INTRODUCTION

This document presents the results of design/cost tradeoff studies conducted during the EOS System Definition Studies. These studies have dealt with the definition of a basic modular spacecraft capable of supporting a variety of operational and/or research and development missions, with deployment either via conventional launch vehicles or by means of the Shuttle (with provisions for on-orbit resupply or retrieval).

Tradeoff studies have been conducted at three interwoven levels during the study:

1) Subsystem Tradeoffs. Wherein the optimum (in accordance with program objectives) approach to a given subsystem has been sought; often not impacting decisions in other subsystems or at the spacecraft (or system) level.

2) Spacecraft Tradeoffs. Concerned with spacecraft-level design considerations (e.g., most effective arrangement of subsystem modules, optimum launch vehicle interface), and including subsystem issues which affect the total spacecraft.

3) System Tradeoffs. Including tradeoffs which extend beyond the subsystem/spacecraft level; for example, conventional launch versus Shuttle launch/resupply/retrieval; more spacecraft redundancy versus more frequent Shuttle flights, on-board complexity versus GDHS cost, etc.

This report deals specifically with the spacecraft subsystem and GDHS tradeoffs. Key system-level tradeoffs are identified and discussed where they have been resolved. However, the major system tradeoffs related to Shuttle application will be reported in Report 6*.

A keynote in carrying out this system definition study has been achieving multimission applicability. Designs have been configured with the GSFC-supplied baseline as a point of departure. A review of the basic missions (documented in Section 2 of this report) has provided a basis for establishing the range of requirements which the modular concept must span. Due to time constraints, detailed consideration has been limited to lower altitude missions directly serviceable by the Shuttle.

*"Space Shuttle Interfaces/Utilization"

Building upon these mission requirements, a review of the requirements for modularity was undertaken. Partitioning of the spacecraft into separately assembleable and serviceable entities keeping in mind the impact of changes between missions of mission-peculiar elements was re-evaluated. The level of modularity has not received detailed consideration because top-level reasoning confirms GSFC's choice and a more thorough evolution would require consideration of the impact on orbit servicing; a task to be carried out in the study's second half.

The mechanical, thermal, power, data and electromagnetic compatibility aspects of modularity have been studied and the results are presented in Section 3. These have led to the baseline approach to modularity we recommend. Using this concept we have synthesized an observatory for performing the EOS-A mission as defined in the contract documentation. This observatory design is presented in Section 4. The payload for this mission is covered in Section 5, and details of the module designs appear in Section 6. Sections 7, 8, and 9 deal with observatory integration and test, ground support equipment, and ground data management, respectively. In Section 10 we present details of our cost tradeoff methodology and results.

Our study has been carried out using a task-order approach. The detailed results of most of these tasks are presented in two appendices to this report. Thus, while this volume deals primarily with conclusions and recommendations, the supporting details for these assertions will be found in the appropriate appendix section.

2. MISSION AND REQUIREMENT SUMMARY

2.1 MISSION DEFINITION

The overall objective of the EOS program is to "develop economical, multi-purpose, modular systems to carry observing techniques of the late 1970's and 1980's for earth and ocean surveys, pollution detection and monitoring, and weather and climate prediction (Reference 1)." In developing system and spacecraft designs in pursuit of these objectives, we have also focussed on the goal of evolving a basic modular spacecraft and subsystem modules applicable to a variety of space observation missions.

The general objective in spacecraft and subsystem development is flexibility of application, with the Land Resources Management (LRM) mission a primary flight application. To this end, three mission categories have been dealt with in design:

1) LRM Mission. Implemented primarily with multi-spectral imaging instruments and su -synchronous low altitude orbits. Payloads are relatively well-defined.

2) Specified Advanced Missions. These missions, defined by the study contract, include: SEOS (Synchronous Earth Observatory Satellite, SMM (Solar Maximum Mission), and SEASAT. These missions distinctly differ from the LRM case. Payloads are artially defined.

3) General Future Missions. Broad future mission classes have been hypothesized in subsystem design to test the flexibility of the module designs.

Primary emphasis has been on meeting the requirements of the LRM mission with designs adaptable (or usable as-is) for the other missions. In this regard, specific attention has been paid to missions listed in 2) above, while those missions identified in 3) have provided range-of-requirements guidelines.

---

(1) EOS PDG Final Report, NASA/GSFC, October 1973.

*The five-band MSS mission is included within the general category.

2.1.1 EOS-A Baseline Mission

A major influence in the direction of the EOS system study has been the study specification (Reference 2), in which requirements were defined for a specific LRM observatory, EOS-A, having a payload including two imaging instruments: the thematic mapper (TM) and high resolution pointable imager (HRPI). In the succeeding sections of this report this particular case has received emphasis as a well-defined typical LRM application.

The basic EOS-A mission objective, delineated in Reference 1, can be summarized as:

- Development of instruments and spacecraft systems to make measurements leading to thematic maps of the earth
- Generation of an LRM data base via space observations
- Demonstration of the use of this data base in resource management.

The baseline payload defined by the EOS system study RFP includes two precision imaging instruments: the thematic mapper and high resolution pointable imager. In addition, a data collection system will provide for gathering of data from earth-based remote sensing platforms.

The most basic specification on system performance comes from requirements upon the system output products as defined in Reference 2 (see Tables 2-1 and 2-2). These quality and quantity specifications have been pivotal in evolving system and subsystem requirements for EOS-A (see Section 4.3).

Quality requirements are specified in linear (rather than angular) terms. Consideration of the impact of these requirements on instrument design leads to one of the significant tradeoffs in orbit selection (refer to Report No. 1 of this study): instrument size, weight, and cost all depend on orbital altitude.

---

(2) "Specifications for EOS System Definition Studies," GSFC Document EOS-410-02, 13 September 1973.

Table 2-1. System Output Quality Requirements

	Geometrically Corrected*		Geometrically Uncorrected**	
Swath width	185 km	48 km	185 km	48 km
Spatial resolution				
Visible	30 m	10 m	30 m	10 m
Thermal	120 m	--	120 m	--
Linearity (μrad)	0.2 IFOV	0.2 IFOV	0.2 IFOV	0.2 IFOV
Band-to-band registration	0.1 IFOV	0.3 IFOV	0.3 IFOV	0.3 IFOV
Position accuracy (without ground control points)	±450 m	±450 m	±170 m	±170 m
Position accuracy (with ground control points)	--	--	±15 m	±15 m
Relative radiometric accuracy				
Visible				
Tape	±1.6%	±1.6%	±1.6%	±1.6%
Film	±5%	±5%	±5%	±5%
Thermal				
Tape	±1K	--	±1K	--
Film	±3K	--	±3K	--

*Includes radiometric correction, earth rotation correction, line-length adjustment, correction for earth curvature, and predicted emphemeris.

**Additionally includes use of best-fit ephemeris from measured data.

Table 2-2. System Output Quantity Requirements

Product	Data Volume	No. of Data Users	No. of Formats
HDDT (uncorrected)	10^{10} to 10^{12} bits/day	2 to 10	--
HDDT (corrected)	10^{10} to 10^{12} bits/day	2 to 10	--
CCT (corrected)	10^{9} to 10^{10} bits/day	10 to 100	1 to 5
Black and white positive/negative*	20 to 200 scenes/day	5 to 50	1 to 3***
Black and white prints		5 to 10	1 to 3***
Color positive/ negative**	10 to 100 scenes/day	2 to 20	1 to 3***
Color prints		2 to 10	1 to 3***

*First generation product - 241 mm (9.5-inch)

**Second generation product - 241 mm (9.5-inch)

***Enlargement to standard map scales

Another related constraint in orbit selection comes from the lighting condition imposed by instrument data quality considerations. Illumination studies have resulted in selecting an 11 am descending node orbit.

Another mission goal considered in orbit selection studies is frequent re-viewing of selected earth targets. Using the thematic mapper the revisit frequency is necessarily limited by the swath width and the requirement for overlap of adjacent swaths. However, by selecting orbits giving appropriately interlaced swath patterns, the 30 to 45 degree offset capability of the HRPI can be employed to provide very frequent re-imaging of selected areas.

2.1.2 Mission Model

The mission model is a key factor in system-level decision processes (e.g., launch vehicle selection, Shuttle utilization philosophy). Reference 3 defines a mission model for the system definition study, with EOS-A (as defined above) as the first flight. The majority of the work reported in this report is based on this initial mission model.

During the course of the study, the mission model was updated by GSFC personnel. Figure 2-1 is a mission model received from NASA/GSFC on 14 June 1974, and modified somewhat during subsequent verbal discussions. It defines four basic missions, including the Earth Resource Observation System (EROS) and other related satellites which are candidates for modular implementation. The first mission (EROS) is of primary concern.

As now defined, EOS-A and EOS-A prime instruments are the five-band multi-spectral scanner (MSS) and the thematic mapper.* According to Figure 2-1, this payload will be succeeded by the thematic mapper plus HRPI combination (denoted EOS-B, B prime), which will later go operational. However, this model was augmented during discussions at

---

(3) "Statement of Work for EOS System Definition Studies," GSFC Document EOS-410-01, 13 September 1973.

*In all subsequent discussions, EOS-A will refer to the thematic mapper, HRPI payload unless otherwise noted.

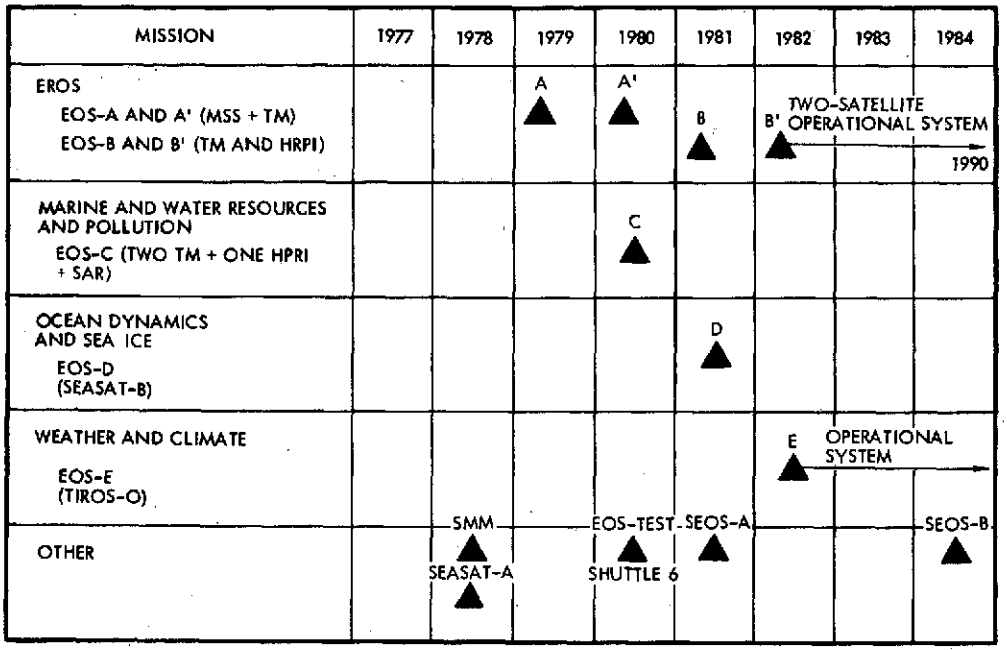

Figure 2-1. EOS Mission Model (June 1974)

GSFC on 22 June 1974 to include two candidate EROS operational/R&D missions:

1) Two MSS instruments giving adjacent swaths on a single satellite. Additional payload includes three wideband tape recorders (to support the MSS's, with one redundant); a wideband communications and data handling system, and a thematic mapper (R&D payload). This satellite will be orbited to provide global coverage with a 9-day cycle (degrading from 17 days if one MSS is inoperative). The satellite will have a relatively high degree of redundancy.

2) Two satellites, each with a single LSS launched so that the two-satellite system gives global coverage in 9 days (degrading from 17 days if one satellite is inoperative). Additional payload for each spacecraft includes two wideband tape recorders, a wideband communications and data handling system, and a thematic mapper (R&D payload). Each identical satellite will be relatively nonredundant, redundancy being provided at the spacecraft level.

The choice of which of these missions to implement is affected significantly by areas beyond the scope of this document (e.g., mission cycle costs, Shuttle use optimization) and will be treated in Study Report No. 5.

2.1.3 Advanced Missions

As noted earlier, SMM, SEASAT, and SEOS have been considered in system design as potential applications of the modular spacecraft. Characteristics and potential payloads for these missions are summarized in Table 2-3.

2.2 GENERAL DESIGN OBJECTIVES

The data requirements associated with the mission definition (e.g., Tables 2-1 and 2-2) are a primary design driver. No less important are the general design objectives summarized in Table 2-4. Foremost among these objectives are low cost, application flexibility, launch vehicle flexibility (conventional and Shuttle), and capability for orbital supply and retrieval via Shuttle. These goals have been a key consideration in system, spacecraft, and subsystem design activities reported in this document. They have led to looking beyond EOS-A in formulating functional and performance requirements.

2.3 ORBIT AND LAUNCH VEHICLE CONSIDERATIONS

A detailed presentation of orbit and launch vehicle tradeoffs and selection factors appears in Report No. 1 of this study. This section summarizes some of the major selection factors presented in Report No. and focusses on EOS-A.

2.3.1 Orbit Selection

A nominally circular orbit of the kind sought for EOS and related applications can be specified with four parameters:

1) Altitude
2) Inclination
3) Local time at nodal crossing
4) Phasing of the satellite in orbit relative to the earth's rotation.

In sun-synchronous orbits the third parameter is important in defining the lighting conditions of the subsatellite point and the fourth parameter in establishing the phase of repeating swaths on the earth's surface. For

Table 2-3. Advanced Mission Characteristics

Spacecraft	Mission Description	Typical Payload Instruments[1]	Payload Characteristics and Requirements[1], [2]			Data Rates	Attitude Control[2]		Orbit and Launch Vehicle
			Weight (lb)	Volume (cu. ft.)	Power (watts)		Orientation	Performance	
SEASAT	Demonstrate space monitoring of ocean surface conditions	• Synthetic aperture radar • Passive microwave radiometer • Infrared imager • Data collection system	500	600	500	0.5 kbit/sec to 10 Mbit/sec	Earth-pointing	0.25 deg accuracy	Low altitude, non-sun synchronous orbit (baseline is 391 n mi, 82 deg inclined); Thor-Delta launch for this payload
Solar Maximum Mission (SMM)	Study fundamental mechanism and effects of solar flares	• Ultraviolet magnetograph • EUV spectrometer • X-ray spectrometer • Hard X-ray imager • Low-energy polarimeter	1430	13.5	175	5 kbits/sec	Sun-pointing	5 arc-sec accuracy; 1 arc-sec drift in 5 minutes	300 n mi, 33 deg including orbit; Thor-Delta launch
Synchronous Earth Observatory Satellite (SEOS)	Resource and weather monitoring from stationary platform; timely warnings and alerts	• Large aperture survey telescope • Microwave sounder • Framing camera • Atmospheric sounder and radiometer	2640	350	145	60 Mbit/sec	Earth-pointing with scan	Point to 5 arc-sec (1σ) stability; 1 arc-sec (1σ) in 12 minutes	24-hour geostationary; latitude and longitude stationkeeping; launched on Shuttle or large conventional launch vehicle with "Tug" stage

NOTES: (1) Data from the following reports:

- "SEASAT-A Phase I Study Report," W. E. Scull, NASA/GSFC, August 1973.
- "Solar Maximum Mission (SMM) Conceptual Study Report," NASA/GSFC Report X-703-74-42, January 1974.
- "Synchronous Earth Observation Satellite (SEOS)," NASA/GSFC Document, 1974.
- "Payload Characteristics for Gap Filler (5-band MSS) Mission," TRW Memo EOS-109, June 1974.

(2) Data from "SMM, SEASAT, ERS and SEOS Instrument Tables," NASA/GSFC, 1974.

Table 2-4. General Design Objectives/Guidelines for EOS

Design Objective	Motivation	Design Provisions
Low-cost spacecraft and module designs	Minimum per spacecraft costs as well as overall program costs	Use of existing proven components; designs not optimized for performance, weight, etc., at expense of cost
Orbital resupply and/or retrieval	Reduced cost through reuse of instruments, structure, and spacecraft modules	Modular design, with provisions for on-orbit replacement; transition ring provides Space Shuttle interface
Capability for conventional launch	Initial EOS launch prior to Shuttle; possible use for operational payloads in 1980's	Launch vehicle interface compatible with Shuttle and conventional launch vehicles
Commonality potential	Reduced costs by sharing costs among many missions	Requirement definition for future missions; delineation of mission-peculiar and universal modules
Simplified management approach	Reduced costs through appropriate innovative management techniques	Awareness of test, reliability and quality assurance, subcontracting alternatives and relation to designs; commonality provisions
Application flexibility	Ease in adapting designs to longer/shorter missions, other mission types, etc.	Flexibility internal to modules; ease in adding redundancy; space for mission-peculiar hardware
Spacecraft orbital survival	Assure spacecraft survival until it can be resupplied or retrieved by Shuttle	Design to avoid single-point failures preventing retrieval or resupply; safe mode
Graceful incorporation of technological advances	Cost/schedule effective use of new developments in subsystem technology area	Modularity in design; noncritical electrical/mechanical interfaces (e.g., use of data bus, power bus)
Graceful incorporation of advanced payloads	Use of new R&D payloads without developing/manufacturing a new spacecraft	Incorporation of new payloads into existing structure via Shuttle resupply; retrieval for major payload update

equatorial, earth-synchronous orbits only the fourth term is important; this establishes the longitude at which the satellite parks.

The payload/mission of EOS-A requires particular illumination conditions which implies a sun-synchronous orbit with appropriate phasing (an 11 a.m. descending node has been selected as the baseline).

Altitude selection relates to a number of factors including:

- Swathing patterns
- Instrument swath widths
- Required overlap of swaths
- Re-visit frequency using offset pointing HRPI
- Spacecraft and payload design impact
- Launch vehicle capability

- Drag makeup requirements
- Shuttle resupply/retrieval capability
- Ground station visibility

Launch vehicle and Shuttle characteristics impose certain constraints on orbit selection. Performance capabilities of the conventional launch vehicles considered are functions of altitude so that specification of a given payload will limit the achievable orbit. Generally, the goal of using the least expensive launch vehicle will be achieved most easily if the lowest acceptable orbit is selected.

Shuttle resupply/retrieval considerations have a bounding effect on orbit altitude selection. It is desirable to permit the Shuttle to approach the spacecraft in its operational orbit, thus allowing retrieval or resupply without the use of spacecraft propulsion (therefore allowing retrieval/resupply with a lower level on spacecraft redundancy).

The primary factors affecting orbit altitude selection are those related to the swathing patterns. These topics are detailed in Report No. 1 of this study. The major points to be considered are:

- By selecting one of a set of discrete altitudes the spacecraft orbital period can be synchronized with the earth's rotational period in such a way that a repeating ground trace is established.
- The minimum number of days in which the trace pattern can be made to repeat is directly related to the instrument swath width and the required overlap. For the range of orbits considered for EOS-A (185 km swath width), this repeat time must be at least 15 days.
- By appropriate selection from among the discrete altitudes giving repeating traces, interlacing swath patterns can be innovated. The interlace pattern can materially affect the minimum interval between successive images using HRPI.

Table 2-5 illustrates the last point for a set of orbits giving a 17-day trace repeat period and between 14 and 15 orbits per day. Our selected design baseline for Titan launch is Case 9, a good selection for a HRPI offset capability of 45 degrees. However, with offset angles limited to 30 degrees, Case 10 would be a better selection (and would not significantly change any other system design, performance, or cost parameter).

Table 2-5. Effect of Orbit Selection on HRPI Coverage

Ease	Altitude (n mi)	Days for Repeating Coverage	
		30-deg HRPI Offset	45-deg HRPI Offset
1	471.1	12	7
2	460.8	7	4
3	450.0	5	4
4	439.3	4	3
5	428.6	4	3
6	418.0	5	3
7	407.5	5	3
8	397.1	9	3
9	386.7	9	2
10	367.4	4	3
11	366.2	6	3
12	356.0	7	3
13	345.9	5	4
14	335.9	6	4
15	325.9	8	6
16	316.0	11	11

Orbit selection for an operational mission may require other factors to be considered. For example, use of a dual MSS payload to give the 9/17 coverage defined in Section 2.1.2 favors a particular type of orbit with particular swath characteristics, further constraining orbit altitude selection.

Each of the advanced missions specified has particular orbit requirements. SEOS requires a geostationary (24-hour) orbit to provide full coverage of CONUS with a short revisit period. SMM, a solar observation spacecraft, can be launched into a low orbit with an inclination selected to maximize the orbited payload.* SEASAT orbits are selected

*Alternatively, a high-inclination sun-synchronous terminator (dawn-dusk) orbit can be selected to maximize sun viewing time.

to give a good range of global coverage (i.e., high inclination) and desirable swathing; however, constancy of solar illumination is neither required or desired (diurnal variations are sought).

The five-band MSS mission is a particular LRM case subject to the same selection criteria and procedures used with other earth resource missions.

2.3.2 Launch Vehicle Selection

The conventional launch vehicles defined in Reference 3 are the Thor-Delta 2910 and the Titan III-D. This study has also considered the Thor-Delta 3910 and the Titan III-B, with the latter a promising alternative to the more expensive Titan III-D. Figure 2-2 shows the payload capability of each alternative. The design tradeoffs have developed viable launch vehicle interfaces for both launch vehicle types. Studies have shown direct injection into the final operating orbit to be desirable with the Thor-Delta but inappropriate with the Titans which do not have a multiple burn capability.

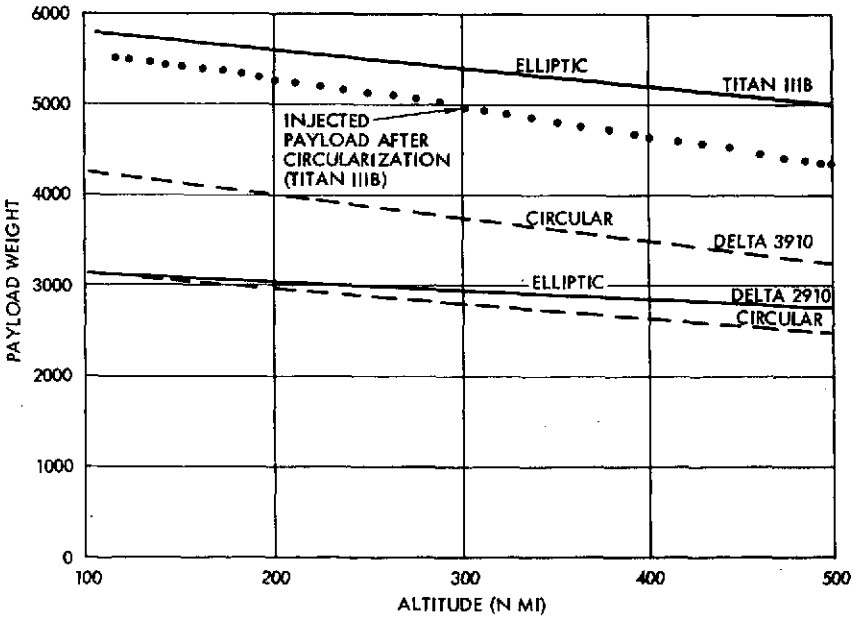

Figure 2-2. Launch Vehicle Payload Capability (Sun-Synchronous Orbits)

3. OBSERVATORY MODULAR DESIGN CONCEPTS

The basic EOS modular observatory has been configured with mission flexibility, low cost, and commonality as major criteria. The resulting observatory concepts are summarized in this section and particularized to EOS-A in later sections.

3.1 OBSERVATORY CONCEPTUAL ARRANGEMENT

The EOS concept is to provide a basic spacecraft with a broad capability to support a wide range of missions which, together with a set of mission-peculiar equipment, comprises the total observatory. To maximize the cost effectivity, the spacecraft is comprised in turn of a set of standardized subsystems, independently packaged and tested (i.e., modules), which, for Shuttle-era flights, may be exchanged within the Shuttle Orbiter payload bay after rendezvous and capture of the observatory by Shuttle. By this in-orbit updating and/or replacement of spacecraft and payload modules, and by the use of the same spacecraft with minimum modifications to support a number of missions, the overall cost of a comprehensive earth observation program can be minimized.

The major goal is to arrive at a spacecraft configuration that can serve the broadest possible spectrum of potential missions, with the constraint that the first flights be launched by conventional launch vehicles, during the pre-Shuttle era (perhaps even in the Shuttle era, if more cost-effective). A second goal is provision for retrieval by Shuttle and return to earth for refurbishment (or on-orbit resupply) if it is shown that retrieval/refurbishment (or resupply) is less costly than total replacement. These goals are addressed in the following configuration concepts.

To perform the tradeoffs necessary to attain the desired goals, spacecraft configurations for both Thor-Delta and Titan class launch vehicles, with the Thor-Delta observatories Titan-compatible and both types Shuttle-compatible.

3.1.1 The Modular Concept

The concept of modularizing a spacecraft is a cost-effective solution for the diversity of missions anticipated for the EOS program. By self-containing each major payload-independent spacecraft subsystem to the greatest extent possible, a flexible spacecraft evolves which can accommodate many different payload complements and orbit parameters while impacting only payload-dependent (mission-peculiar) subsystems. Furthermore, modularity makes feasible the in-orbit serviceability of the observatory by Space Shuttle for maintenance or updating purposes. The cost of accomplishing diverse and extended earth observatory missions can be significantly reduced by the simplification of configuration alteration and the capability for in-orbit maintenance.

In conducting this study of the modular concept for EOS the following guidelines have been adopted:

- The overall technical feasibility and cost-effectiveness are reinforced by applying established technology and existing hardware where appropriate.
- In configuring the observatory, inherent restraints upon growth and flexibility of the spacecraft or subsystems are avoided.
- Emphasis is placed on minimizing recurring costs of hardware elements, e.g., no highly optimized designs or excessively tight tolerances, or application of exotic materials where conventional materials meet the requirements.
- An effort to standardize subsystem modules and/or components for common applicability to baseline and future EOS configurations.
- Sufficient design margin to minimize testing procedures without sacrificing confidence in functional ability.
- Generally employ simplified concepts where options exist.

A basic modular spacecraft consisting of five standard subsystem modules supported by a structure is shown in Figure 3-1.

Each of the modules will be structurally independent, removable from the spacecraft by means of Shuttle-SPMS* compatible latches, or

*Special-purpose manipulator system, part of the Shuttle equipment to accommodate EOS; see Section 3.2.1.

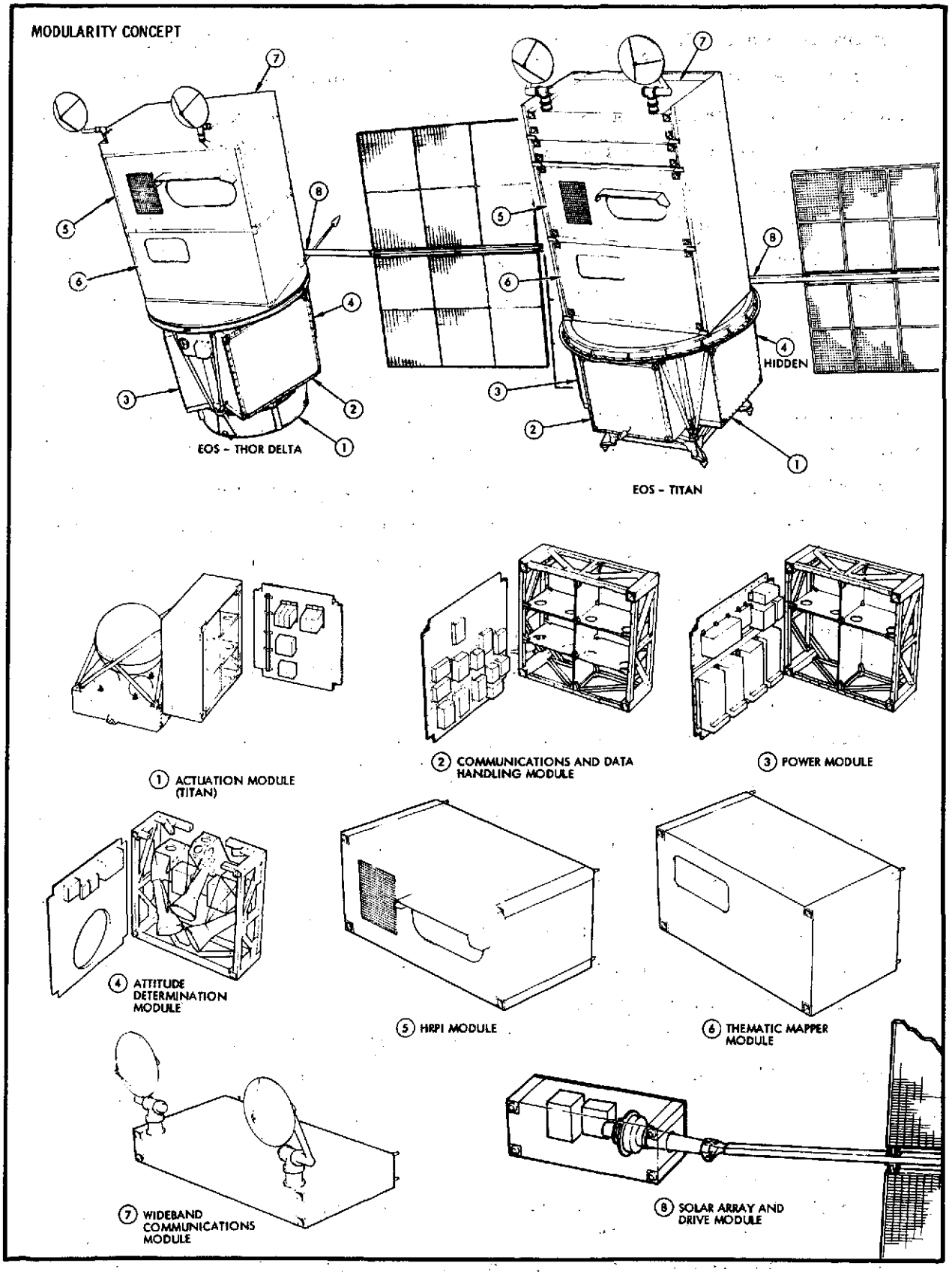

Figure 3-1. EOS Modular Concepts

simply bolted in place for non-Shuttle regurbishable versions of EOS. Four of the modules have a structure similar in construction, with its internal configuration varied as required for each subsystem. The module structures are not required to contribute to fundamental spacecraft structural integrity,* facilitating simplification in definition and implementation of module fixation to the basic structure. The actuation module is somewhat different in configuration from the other subsystems with its tankage envelope requirements. The solar array drive structure is entirely different than the other four.

The size and placement of the various modules were defined in the study proposal and were re-examined during the study; the most satisfactory and cost-effective configuration remains a standard 48 x 48 x 18 inch size, common to both Titan and Thor-Delta versions of EOS. The Delta version, due mainly to fairing diameter constraints, mounts three standard modules in a triangular fashion, while the Titan baseline version uses a four-sided arrangement.** The Delta version is envisioned as nonrefurbishable in-orbit but retrievable by Shuttle. A refurbishable version with the triangular module arrangement would introduce some difficulty in SPMS compatibility for actuation module removal; the SPMS is presently envisioned for rectangular latch location accommodation only. An alternate approach, discussed in Section 4.1.5, would use four somewhat smaller modules in a rectangular arrangement similar to the Titan EOS. However, the additional weight necessary and the smaller modules makes this alternative less attractive.

The general observatory configurations each consist of a spacecraft section including a transition ring, independent of payload, and a forward payload section which is designed to be readily altered by reconfiguring its basic structure for accommodation of various payloads. For the baseline HRPI and thematic mapper with a wideband communication and

---

*An exception may be the actuation module which provides a primary load path in one configuration.

**Note that the triangular Delta configuration can be Titan launched.

data collection system payload, the Titan and Delta payload sections are similar. Payload module construction is similar to the standard modules of the spacecraft functions. The payload modules will be cantilevered at the thermally-benign anti-earth side of the structure using standard attachment mechanisms (see Section 6.9). For Delta launches, because of the limited payload capability, the payload module structure will be deleted and the instruments bolted directly to the payload structure at the anti-earth side, maintaining the same thermal interfaces as if they were module structures. The solar array/drive module is attached to the outside rear of the payload structure also with standard attachments.

Figure 3-2 depicts the EOS Titan and Delta configurations for the EOS-A mission.

3.1.2 Module Size and Modularity Level

Studies by Aerospace Corporation and others have shown that in-orbit servicing is the most economical among three possible modes of spacecraft program maintenance (Figure 3-3).* The modular concept provides this capability. The selection of module size has additional impact on overall costs for operational programs.

A key factor to reducing unit costs is the size of the production run. By standardizing modules as far as practicable, and by producing as many as possible in a single run, their unit costs are minimized. Thus, a module should be usable for many diverse missions with minimum change. By isolating those system elements that are independent of payload characteristics such a goal may be satisfied. Furthermore, by grouping these payload-independent elements into subsystem related functions, a logical module complement is derived. Such a module may be specified, procured, tested, and stockpiled for later synthesis of operational observatories.

*These studies focussed on multisatellite system in coplanar geostationary orbits, using a Shuttle-Tug combination. Conclusions are not necessarily applicable to low-altitude EOS operations.

THOR-DELTA CONFIGURATION

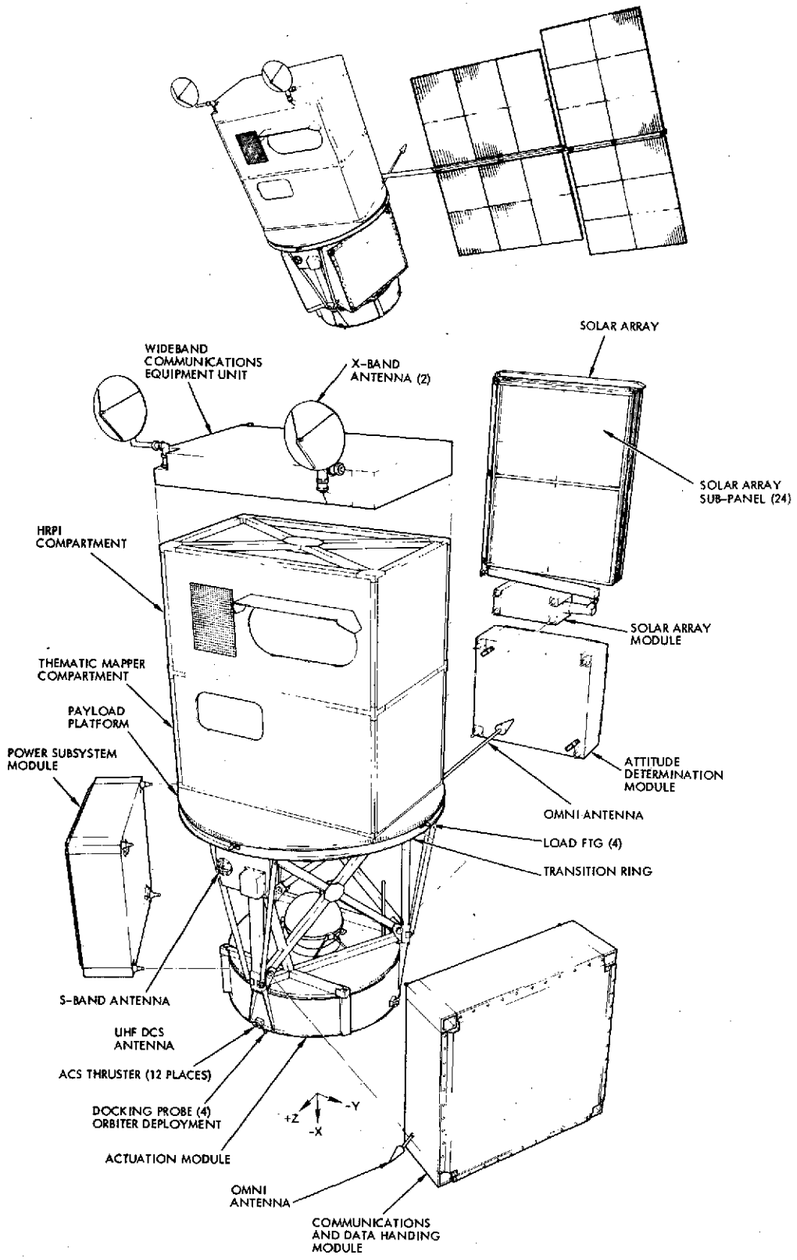

TITAN CONFIGURATION

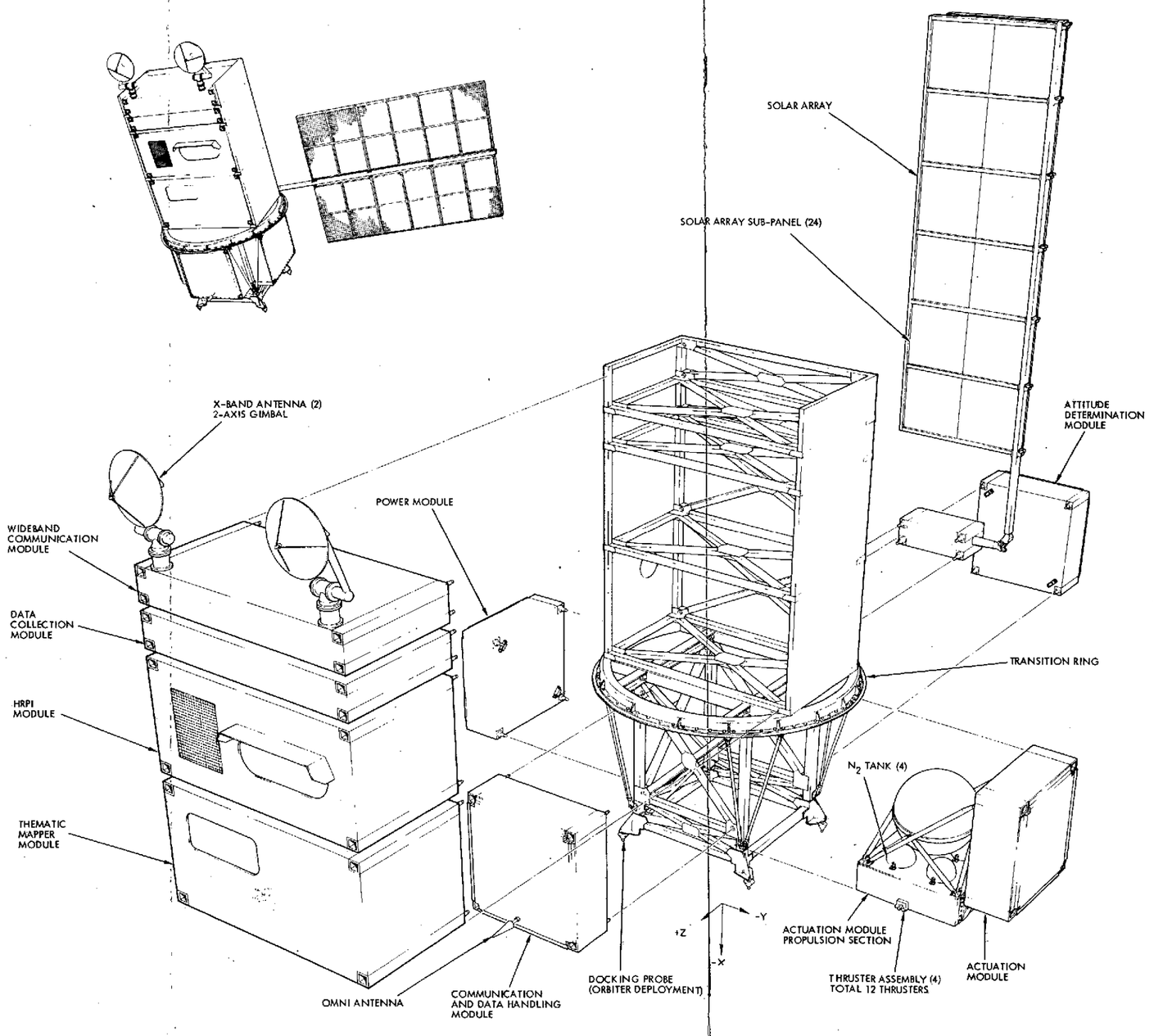

Figure 3-2. ECS Thor-Delta and Titan Configurations

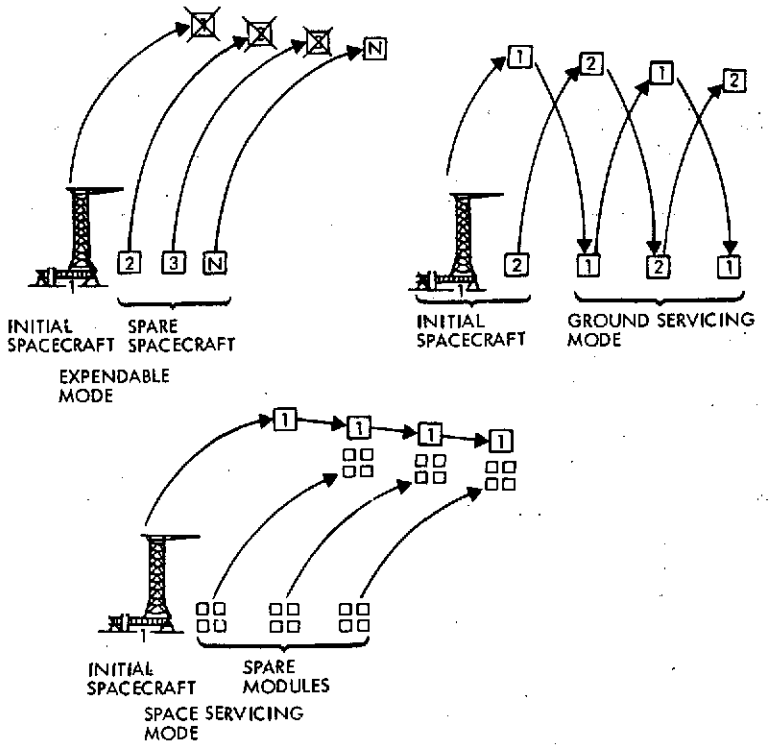

Figure 3-3. Typical Modes of Spacecraft Maintenance

The baseline design shown in Figure 3-4 has followed this guideline. A typical basic spacecraft is composed of five standardized modules:

- Electric power module, containing the power control unit and sufficient batteries to support the mission payload
- Communication and data handling module, with receivers, transmitters, omni antennas, and computer
- Attitude determination module, with star trackers, inertial reference unit, magnetometer, and sun sensor
- Solar array and drive module, containing array drive and drive electronics and supporting a mission-dependent solar array
- Actuation module, with momentum wheels, magnetic torquers, nitrogen attitude control system, and hydrazine orbit maintenance system. The capacities of the elements of this module are payload-dependent.

These allocations of observatory equipment were arrived at without specifically constraining module size or consideration of in-orbit exchange. While it is expected that in-orbit replacement of a payload instrument is a

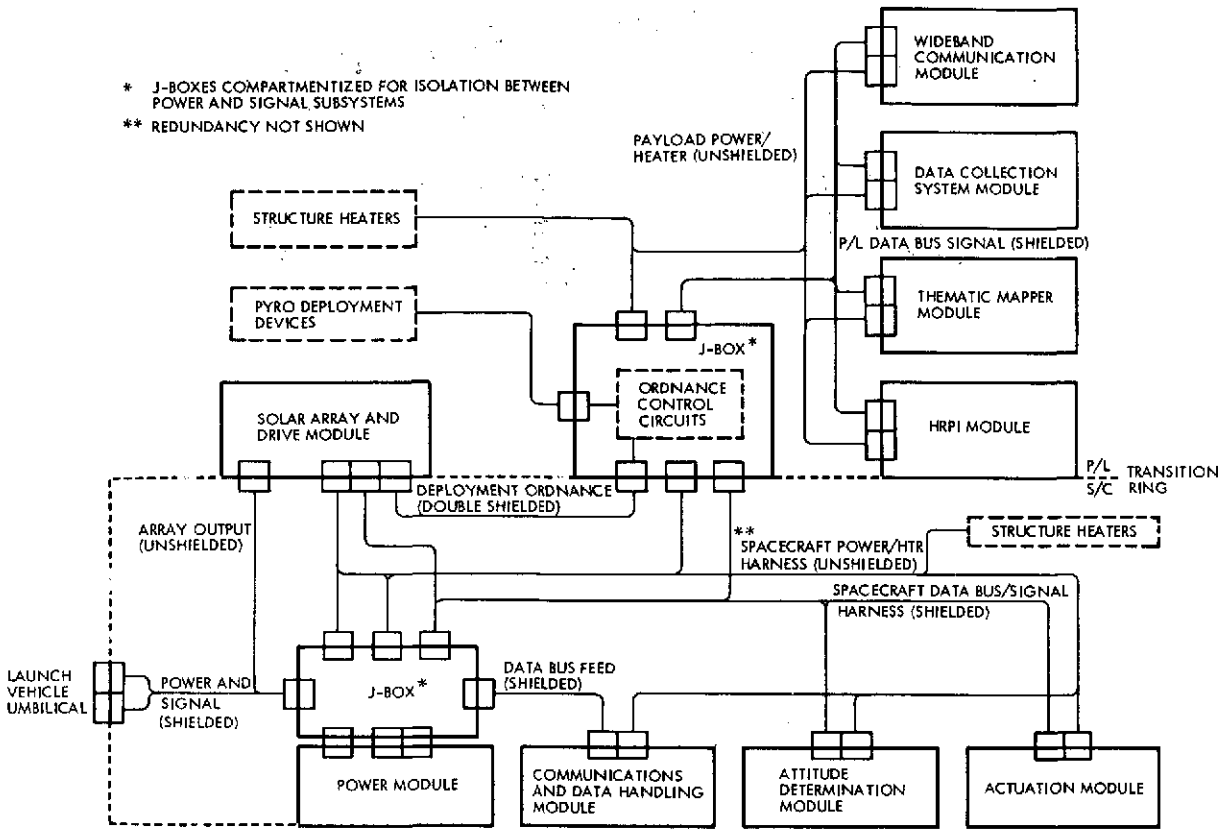

Figure 3-4. Baseline Modular Block Diagram

valuable capability, it is less clear that in-orbit exchange of the relatively large modules is as desirable. Studies of spacecraft anomalies over the last decade show that a major percentage were repairable, but after the infant mortality period there are few failures due to wearout or exhaustion of consummables (References 5 and 6). Without extensive (and expensive) ground testing to wring out infant mortality and without very extensive instrumentation for fault diagnosis, isolation of failures to significant observatory elements (i.e., standardized modules) appears to make sense. At the same time these standardized modules appear to be at an economical level for procurement, as discussed above.

---

(5) Use of Space Shuttle to Avoid Spacecraft Anomalies, Planning Research Corporation Systems Sciences Company, May 1974.

(6) "Demonstrated Orbital Reliability of TRW Spacecraft," TRW Systems Report 0-00735, 73-2286.145, December 1973.

With the Shuttle's large payload bay and relatively high weight capability for low earth orbits, its capabilities should present no constraint to module size for in-orbit servicing within the Shuttle. For servicing at altitudes which the Shuttle itself cannot achieve (as studied in Reference 7) which must be done remotely, the optimum space replaceable unit (SRU) is probably smaller than our standard modules because of the high cost per pound of attaining these high orbits. Such a conclusion was reached in a SAMSO study for a serviceable spacecraft at geosynchronous orbit, although these results were tempered by considerations of numbers of spacecraft to be serviced by a single Shuttle/Tug flight (Reference 7).

Certainly large serviceable modules provide an overall simpler, lighter structure and fewer module attachment mechanisms. The great advantage of in-orbit payload replacement dictates development of a module exchange mechanism (i.e., SPMS) capable of handling SRU's at least as large as payload instruments, and as long as that capability exists in the Shuttle the spacecraft modules might as well be space serviceable too. Only when the observatory is initially launched by a conventional launch vehicle (e.g., Thor-Delta), where its limited payload capability dictates as light a spacecraft as is cost effective without requiring redesign or redevelopment of the spacecraft elements will the serviceability features be deleted.

To arrive at a specific set of standard module dimensions requires consideration of spacecraft configurations and constraints presented by Thor-Delta initial launches. The first three modules in the above list, together with the actuation module, comprise the spacecraft. Since the actuation module is payload-dependent its volume is variable, so for Thor-Delta compatible spacecraft it is desirable to arrange the first three modules around the cross-section of the dynamic envelope. This determines module width. Module depth is determined by the size of the

(7) "In-Space Servicing of a DSP Satellite (U)," TRW Systems Report 16439-6514-TE-01, March 1974.

largest subsystem element that may have to be accommodated, such as batteries or momentum wheels, and module length must be adequate to contain all the equipment. The choice of 48 x 48 x 18 inch modules satisfies the above requirements and allows significant room for growth.

3.2 MECHANICAL INTERFACES

Interfaces of particular concern are those between observatory and launch vehicle, between observatory and Shuttle, and within the observatory, between modules and the observatory structure. Included are contamination considerations.

3.2.1 Observatory to Launch Vehicle

In providing the greatest practical degree of configuration flexibility and minimizing growth constraints, we have retained the transition ring concept of the GSFC demonstration model design. The transition ring is the interface between spacecraft functions and mission-peculiar payload elements. All structural, dynamic, thermal, and electrical interaction between spacecraft and payload may be clearly defined and specified at the transition ring interface. The transition ring also has the capability of providing a standardized structural interface with launch vehicles and the Shuttle Orbiter, independent of the particular EOS configuration for a given mission.

The early versions of EOS will tend to be payload limited because of the limited capabilities of the more economical candidate launch vehicles. With the transition ring concept, where primary observatory loads are transmitted to the launch vehicle through the transition ring (see Figure 3-5a), the spacecraft only supports its own mass. The transition ring adapter is a major piece of structure, and there is a potential flyout problem at observatory separation from the launch vehicle.

The aft adapter concept requires a slightly higher weight spacecraft structure since all observatory loads go through the spacecraft. This added weight plus the weight of the adapter, is to be traded against the equivalent payload penalty of the transition ring adapter. For Thor-Delta, where total payload capability to early EOS mission orbits is

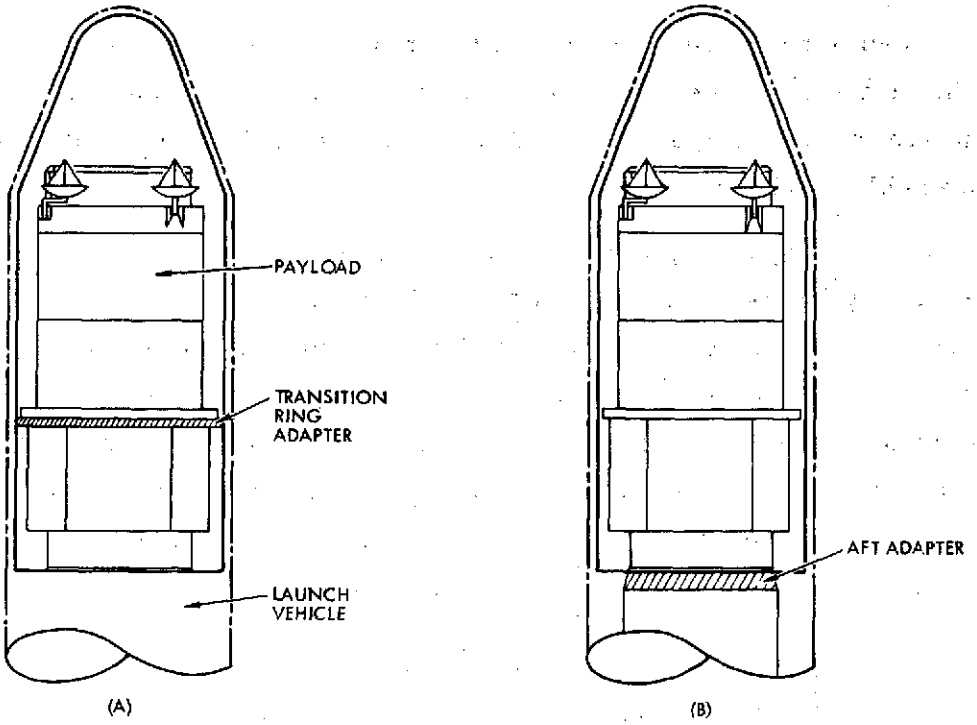

Figure 3-5. Alternate Schemes of Supporting EOS Observatories to Launch

somewhat limited (see Section 3 of Report 1), the aft adapter provides an additional 280 pounds of payload capability:

		Weight (lb)
Equivalent weight penalty of transition ring adapter*		430
Weight of aft adapter	100	
Additional spacecraft structural weight	50	
Net payload penalty with transition ring adapter		280

* Based on preliminary analysis by McDonnell Douglas on their use of a portion of the standard 96-inch Delta fairing as a transition ring adapter; includes the equivalent exchange ratio that would be realized if that portion of the fairing were jettisoned at the same time as the forward portion.

Even with a separate transition ring adapter designed for minimum weight there would be a net payload penalty if launch loads are picked up at the transition ring adapter. A similar analysis of the Titan shows a comparable payload penalty.

By making the spacecraft structure strong enough to withstand total observatory loads on Delta launches, this same structure may be used for later missions where more on-board propulsion may be required; with the transition ring used as the primary load path. The spacecraft will already be structurally adequate to accommodate the higher actuation module weights. Thus, a single spacecraft structure may be able to serve for Thor-Delta launches, Shuttle launches, and even Titan launches if a transition ring adapter is developed for the latter case.

In every case, however, a transition ring is included in the configuration to enable observatory retrieval by Shuttle.

3.2.2 Observatory to Shuttle

The basic mechanical interfaces between EOS and Shuttle are provided by the Flight Support System (FSS) which consists of a transition ring cradle to support the observatory during launch and return to earth, a docking adapter for observatory erection and retention during module exchange, and a Special Purpose Manipulator System (SPMS) to perform the module exchange (References 8, 9). In addition, the Shuttle-Attached Manipulator System (SAMS), part of the standard orbiter equipment, assists in maneuvering the observatory in and out of the docking adapter. The FSS is being studied by Rockwell International under another contract.

(8) "Shuttle/Typical Payload Interface Study, Final Report," North American Rockwell Space Division, Report SD 72-SA-0194, 30 October 1972, Contract NAS5-23093.

(9) "Design Definition Studies of Special Purpose Manipulator System for Earth Observatory Satellites," SPAR/DSMA Report R.592, prepared for GSFC, January 1974.

In addition to the transition ring interface with Shuttle, a key aspect of the observatory modular concept is the technique for in-orbit observatory refurbishment by module replacement. Early versions of EOS are not likely to be refurbishable in orbit due to weight and volume constraints of the Thor-Delta launch vehicle. However, the spacecraft and its subsystems will be designed for in-orbit replacement, and for the non-refurbishable versions the additional mechanisms for replacement will be deleted, giving a weight reduction of 380 pounds. For the payload modules, the module structures will also be eliminated, to save weight; but for both subsystem and payload modules the thermal interfaces will be identical regardless of in-orbit replacement capability.

The mechanical interface between EOS and the docking adapter will consist of four drogue probes hard mounted to the EOS aft structure. The docking adapter contains the clasping mechanisms and will be normalized to the EOS temperature prior to docking to assure mechanical compatibility. There will be a drogue to adapter socket assignment since the umbilical connection must be positioned for mating (Section 3.2.4). For the serviceable configurations an additional set of drogue probes will be mounted to outer panel of the command and data handling module, for use during exchange of the actuation module. The SAMS would rotate the observatory 90 degrees and dock it to the docking adapter such that the observatory axis is normal to the SPMS, permitting actuation module removal and replacement.

Support and retention of EOS within the Shuttle bay will be accomplished through three pin-like load fittings at the transition ring station. These fittings are mounted to an I-cross section ring which is the transition ring, which in turn can be used as a grappling hold by the SAMS for observatory handling. The FSS transition ring cradle will have compatibile mechanisms to support the observatory load fittings. Compared to complete encirculation of a transition ring by a clam shell type clamp, the three-point suspension provides a simplier FSS cradle; no longer would an elevating motion be required for the transition ring to clear the clamp, nor would thermal distortion and fabrication tolerances between the ring and clamp be critical.

3.2.3 Modules to Observatory

The module attachment scheme adopted for interfacing with the observatory structure involves the following considerations:

- Provisions for launch load transfer and rigid body stiffness in orbit
- Thermal resistance to minimize interaction between module and spacecraft structure
- Accountability for misalignment due to fabrication tolerances
- Maintenance of alignment after attachment of critical elements such as attitude determination and payload sensors
- The ability to provide closure and separation forces for the electrical connector
- Simplicity and reliability of operation in considering limitations of the SPMS and astronaut/operator
- Immunity from cold welding, corrosion, contamination, lubrication life, and outgassing and damage susceptibility difficulties
- Minimum weight per attachment fitting.

The attachment interface arrangement, as presently conceived, consists of four identical probe-like mechanisms mounted to the rear of the module assembly. Each of the probes has a mating female socket attached to the spacecraft frame structure. By selective clearance, each of the four fittings is constrained in only those directions indicated in Figure 3-6. Each male probe uses an attach bolt which is turned by SPMS until a predetermined torque is reached, mating the electrical connectors and securely bolting the module to the structure. Module removal is accomplished in a similar manner with SPMS, except SPMS must provide the connector disengagement forces. Section 6.9.2.1 details this mechanism. An alternate approach to the module attachment mechanism, which provides connector demating forces without imposing these forces on the SPMS but rather on the module itself, is currently under study.

The insertion of a module into EOS by SPMS, as presently envisioned, will require astronaut/operator guidance during the final few inches of

travel due to the tolerance buildup involved in all of the systems. Whether he receives his cues visually (TV), by proximity sensors, tactile feedback, or some combination, is yet to be determined. With our attach design, the SPMS is only required to grapple the module for transport and provide each latch with rotational motion. All modules, including the solar array and SAR antenna, will have identical attachment mechanisms, permitting operation with either SPMS or SAMS with a special-end effector.

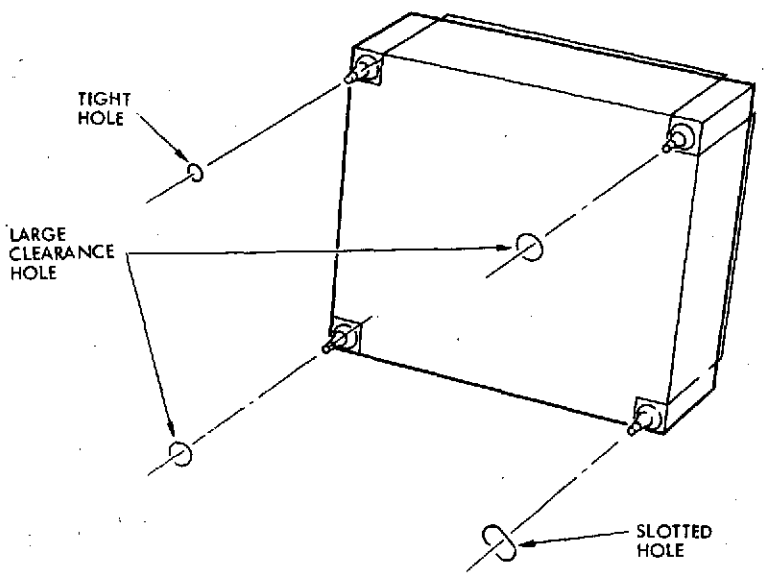

Figure 3-6.
Module Attachment Interface Arrangement

3.2.4 Umbilical Connections

At certain times during the EOS mission it is necessary to couple to the observatory with an umbilical cable for telemetry exchange and power connections. The following cases require umbilical attachment (see Figure 3-7):

1) Prior to launch - aft adapter, conventional launch vehicle
2) Prior to launch - transition ring adapter, conventional launch vehicle
3) Shuttle Bay - while retained in the flight position
4) Erected for module exchange while docked to Shuttle
5) Docked to Shuttle on side - while exchanging aft module.

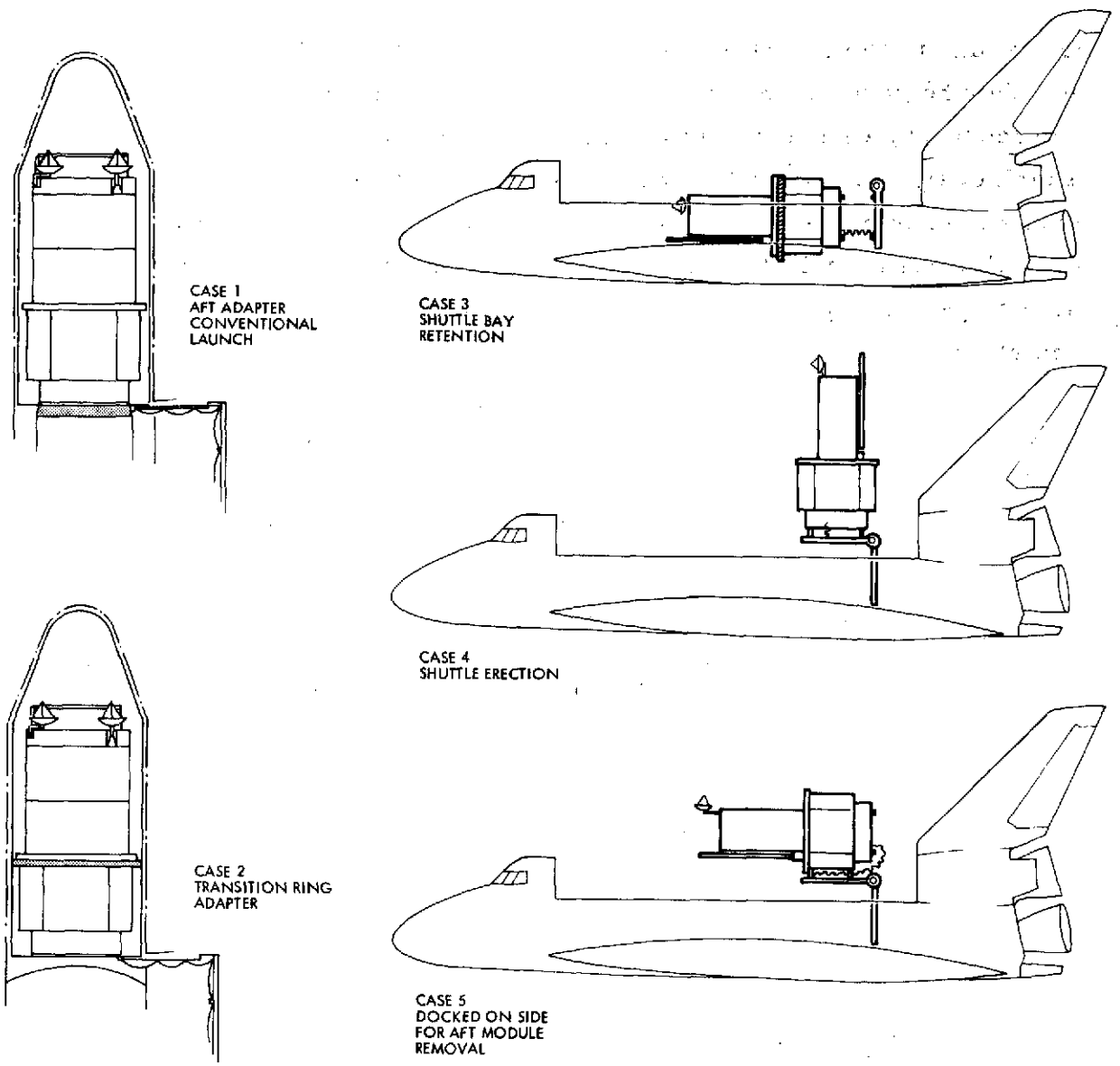

Figure 3-7. Observatory Umbilical Connectors

Although each case has a preferable location for the umbilical connection, it is desirable to have a single connector for the observatory design. Locating the connector on the aft end of the observatory structure accommodates the cases identified without unreasonable requirements on the umbilical cables and attach/detach mechanisms. For prelaunch checkout and observatory maintenance (Cases 1 and 2) using the Delta or Titan vehicles, the umbilical is unplugged by a mechanism from the launch gantry. A door is provided in the fairing for this purpose. During launch the observatory is autonomous.

For a Shuttle-launched mission (or during retrieval) the observatory is secured in the bay by its transition ring (Case 3), and the umbilical comes from the docking adapter of the FSS.

A mechanism within the docking adapter, supplied by the FSS, will plug and unplug the umbilical when EOS is docked (Case 4). The umbilical connector will also require a mechanical latch to ensure positive engagement when EOS is secured in the Shuttle bay by the retention system. (The docking adapter backs away 2 inches while the umbilical remains attached.)

Thus, the umbilical mechanism supplied as part of the FSS docking platform must engage the connector with a positive latch after docking, release the mated connection during Shuttle flight, and unlatch and disengage the umbilical prior to EOS release.

Case 5 is peculiar to a version of EOS requiring aft end module removal access - not presently a baseline configuration - but a possible alternate. Here, the umbilical would require a few feet of service loop (as opposed to a few inches for the other cases) to allow the observatory to be re-docked on its side by means of auxiliary docking drogues on one of its spacecraft modules. The location of the connector on the EOS structure may also be altered depending on the aft module design.

It is estimated that the umbilical will have 50 pin connections and be conventional in design with the exception of its positive mechanical latch which will be mutually selected with the FSS contractor to assure compatibility.

3.2.5 Contamination Considerations

The observatory will have several components which are particularly susceptible to contamination, either particulate or condensed volatiles. Star tracker optics, payload sensor optics, the payload radiative cooler surfaces and ultra precision bearings, are dependent on a clean environment for maximum performance. In the case of HRPI or Thematic Mapper or similar spectroradiometric instruments, degradation effects are particularly complex to take into account since the deposits on optical

surfaces are generally spectrally variant, causing wavelength-dependent attenuation which affects the total optical train and is, therefore, difficult to calibrate in addition to reducing overall sensitivity. Internal calibration sources are limited in providing confidence for post-launch calibration since the deposits on optics may be spatially distributed, essentially requiring an extended source at infinity for adequate calibration which is impractical with internal sources. Also, the internal calibration lamps and their associated optics are questionable in spectral and intensity stability. The sun has been utilized for calibration in the past, but due to its orders of magnitude greater brightness then intended targets, has produced limited success. The moon has been suggested as a calibration source since it has a stable albedo and approximately the proper brightness. Preliminary investigation indicates that the observatory could be commanded to view the full moon, if desirable, at infrequent intervals (an opportunity occurs once every 28 days).

Prevention of contamination has classically been approached with procedures such as clean room conditions during spacecraft-to-launch vehicle mating, and in some cases, jettisonable covers. The Space Shuttle era will introduce new problems in contamination control. The Shuttle bay cannot practically be maintained at a high level of cleanliness due to its short turnaround between missions and operational modes. Also, its reaction control thrusters and its many lubricated mechanisms pose new problem areas. One suggestion has been to include as part of the EOS flight support system an internal shroud or cocoon-like tent to protect the observatory. However, this approach appears difficult to implement and costly in terms of weight and associated handling equipment complexity. For our baseline approach, we are recommending commandable covers over all critical elements which can be closed during Shuttle proximity. Although this adds additional complexity to the observatory in terms of mechanisms and command sequences, it appears mandatory unless the contamination environment, yet to be defined, proves otherwise.

One special problem with covering optics is the requirement to vent the associated cavities during launch and retrieval. Whether this is

done with purge gas or integral filters is yet to be determined. Protection during retrieval is desirable since the accurate analysis of deposits accumulated on optics during extended space operational periods is an important data point in accessing future requirements for contaminant avoidance.

3.3 THERMAL CONTROL CONCEPT AND INTERFACES

The EOS thermal control system (TCS) has been guided by the following general TCS requirements/objectives:

- Modules thermally decoupled from structure
- Accommodates wide range of experiments and missions
- Accommodates module replacement in orbit
- Limits structural temperature gradient and fluctuation to preserve alignment
- Minimum total program cost but with a reasonable risk factor.

Modularity requires that individual module thermal design be essentially independent. Since mechanical interfaces are not ideal, a major consideration was the determination of the allowable impact of these interfaces on the structure/module thermal designs and the design to meet these requirements. Conductive interaction is achieved by controlling mechanical module/structure coupling and temperature gradient across the interface. Multilayer insulation (MLI) between module and structure minimizes radiative interaction.

Each module has its own independent thermal control system consisting of a temperature-controlled heater and high efficiency multilayer insulation blankets over all surfaces except for the radiating area, which has a low α_s/ϵ coating (see Figure 3-8). Thermal design details of each module (attitude determination, actuation including propulsion, electrical power, communication and data handling, solar array and drive, and wideband communications and data handling) are described in Appendix A, Section 5.5.

The payload and subsystem structural frames (including the transition ring) each have independent thermal control systems consisting of

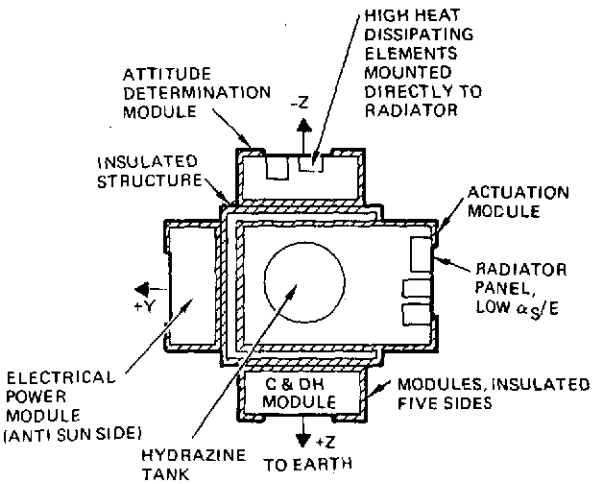

Figure 3-8.
Sample Thermal Control System

multilayer insulation blankets, sandwiching between structural numbers, and several independently-controlled heaters. Temperature level, distribution, and fluctuations are constrained to limit thermal distortion.

This module thermal control approach provides design flexibility by allowing replacement/substitution of modules without thermally impacting the overall TCS. Modularity can also reduce test costs by the elimination of acceptance thermal vacuum tests.

The selected thermal control system is designed for near-earth 11:00 a.m. node/sun phase sun-synchronous reference orbit with heater power level and radiator area optimally sized for this orbit. Other near-earth orbits, 6:00 a.m. to 12:00 a.m. node/sun phasing, are accommodated but with some heater power penalty; node/sun phasing between 12:00 noon to 6:00 p.m. is thermally accommodated by reversing the spacecraft's direction in orbit and maintaining an anti-sun side. Non-sun-synchronous orbits are similarly accommodated.

Major TCS interfaces are:

- TCS/Launch Vehicle. Provision for on-stand conditioner air, limitation of internal shroud temperature during ascent and limitations of Observatory attitude during orbital injection from shroud jettison, are generally necessary.

- TCS/Natural Environment. TCS accommodates environments resulting from mission timeline for the considered near-earth orbits and node/sun phasing.

- Structure/Module. Thermal isolation requirements between each module (and sensor) and structural (payload and subsystem) are detailed in Appendix A, Section 5.5. This isolation is achieved by a combination of mechanical isolation and temperature gradient control. Heat flow at each module/structure interface must be less than 1 watt.

- Payload Structure/Transistion Ring. Appropriate payload structure/transition ring isolation and transition ring temperature control are provided to limit heat flow at this interface.

- TCS/Shuttle. During retrieval/resupply, power may be required from the Shuttle to avoid extreme module cool-down, depending upon the length of the servicing operation (see Appendix A, Section 5.5).

3.4 ELECTRICAL INTERFACES

The power interface concept must provide consistency with the program goals of modularity and commonality while maintaining established performance and reliability requirements.

3.4.1 Structural Harness

The payload harness is dual redundant with diode isolation at the load to remove load faults and line breakers in the power module to protect against harness shorts. The breakers in the power module are magnetically driven and may be operated open or reset by control signals. The spacecraft power distribution is similar to the payload, with the exception that the two breakers for the dual redundant harness may not be opened simultaneously by signals through the data interface unit. Complete disconnect of spacecraft power may be obtained only by hardwire control through the umbilical. The purpose of this feature is to avoid inadvertant shutdown of the spacecraft while in flight. Individual spacecraft module harnesses fan out from a junction box near the power module in the spacecraft. The harnesses to the modules in the payload fan out from a junction box near the transition ring in the payload structure. This permits the separate assembly and test of spacecraft and payload systems. All modules obtain power through dedicated buses from the spacecraft junction box.

A separate heater bus is also routed to each module to maintain module temperatures during maintenance and resupply. This bus is routed to the umbilical at the spacecraft junction box so that removal of the power module will not interrupt the minimal module temperature control required during resupply.

3.4.2 Safe Mode Bus

A means is provided for causing the observatory to enter the safe mode (sun bathing) as a result of any predefined failure condition anywhere

in the observatory. This is accomplished by a line common to all modules which is normally held at a logical "high" level by a medium impedance source in the power module. An unsafe condition in any module can be used to ground this line (provided provision was made for this prior to launch). All modules continually sense the level of this line and automatically enter their predefined safe condition whenever the line goes low. For our EOS-A design we have identified only one condition for entering the safe mode (an enduring negative energy balance) but the scheme is inherently modular and places no constraints on how it is applied in future missions.

3.4.3 Power Interfaces

The prime power distributed to all modules is specified at 28 ± 7 volts. Studies of expected power system performance indicate a maximum expected range of 26 to 32.5 volts for orbits below 900 nautical miles. The expected range for the geostationary orbit does not exceed 22 to 32.5 volts assuming a possible 60 percent depth of discharge under normal operating conditions.

Prime power is isolated from secondary power in each module by a regulated converter which provides ±5 percent regulation full load to 50 percent load. Individual regulators at the black box level will provide closer tolerance on supply voltages where required. The primary power and heater bus interface to each module is shown in Figure 3-9. This design allows either bus to power the module equipment independent of the selected redundancy within the module.

The design presently incorporates one converter to power all equipment within the module (except the data interface unit). Each data interface unit has a separate converter so that a single-point failure in the equipment will not prevent commanding of the module. The isolation of the primary power bus for load faults is accomplished by the fuses shown in Figure 3-10. Paralleling of the fuses provides redundancy for a fuse opened in launch vibration. The diode in series with one fuse prevents current flow in that leg until the other fuse has opened. Each fuse may then be sized for a reasonable fault current to minimize the effect

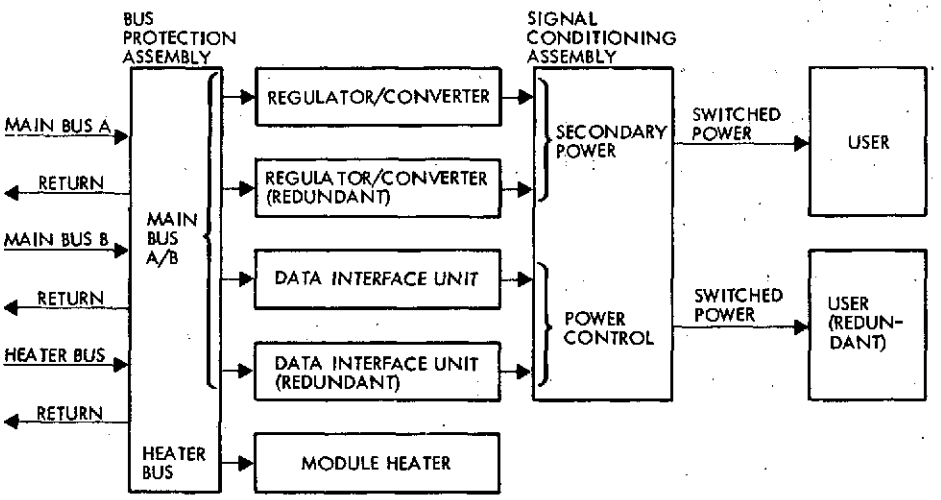

Figure 3-9. Module Power Interface

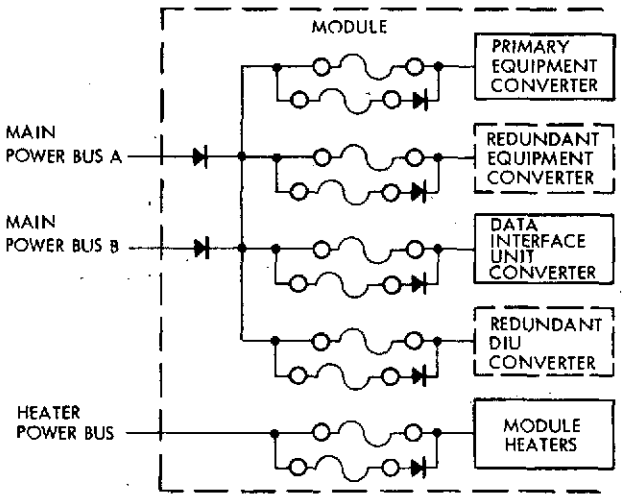

Figure 3-10.
Typical Module Power Interface

on the primary power bus. Use of the diode does not significantly increase the time required to open the line after a fault occurs. If the fuses were simply paralleled, the current required to open them would be approximately twice the current rating of one fuse and could result in loss of effectiveness of the fuse protection approach.

Input filters to all modules concist of EMI feedthrough capacitors and an optimized two-stage LRC networks. These filters are designed to maintain line noise 6 dB below EMI requirements and also minimize cold start transients. Normal activation of a module will be a soft start, that is, the filters will be charged and operation is initiated by control of the switching transistor in the regulator.

3.4.3 Summary

The power subsystem design provides a standard interface for each observatory module. Fault isolation prevents failures in any module from affecting another module. Individual power harnesses may be reconfigured with minimum difficulty.

The input filter design in each module maintains control of harness noise signals and also minimizes the amplitude of cold-start transients. The low dynamic impedance of the battery, main regulator filter, and minimum common main power bus length effectively eliminate significant dynamic coupling between modules.

3.5 DATA INTERFACES

Data transfer between electrically-isolated payload and spacecraft modules for EOS are handled by an AC-coupled party line data bus system. Figure 3-11 shows a simplified block diagram of the system. This system,

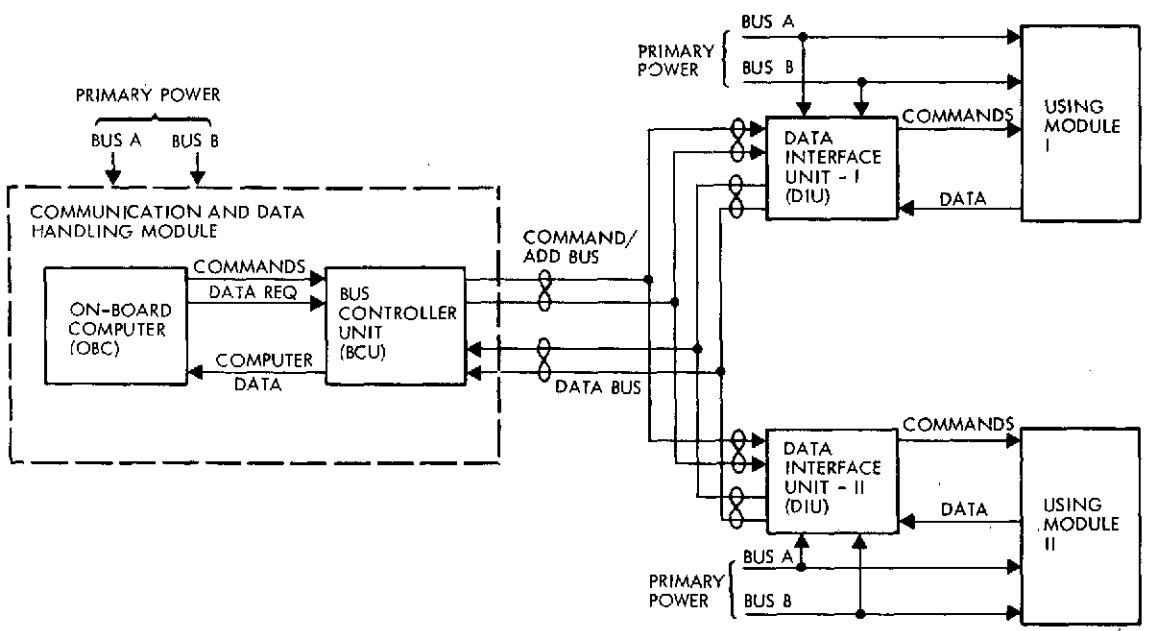

Figure 3-11. Data Handling Concept

including data interface units in each module and an on-board computer for control, provides adequate flexibility to accommodate all proposed future missions.

3.5.1 Data Bus System Operation

The data bus system, comprising the bus controller unit (BCU) and data interface units (DIU), is under control of the on-board computer located in the communications and data handling module. Each DIU receives power from the primary power bus and communication between it and the BCU is conducted on an AC-coupled bus.

If it is necessary for one module to transfer data to another module, data is requested from the first module by the computer via the BCU. The computer then outputs the data as a computer command via the bus to the second module where it is internally decoded.

3.5.2 Data Bus Characteristics

The data bus is operated as a four-wire full duplex system. Computer commands are transmitted from the bus controller on one wire pair and computer data and telemetry are received by the bus controller on the other wire pair. The bus bit rate is 1.024 Mbit/sec.

3.5.3 Data Bus Format

The format used for transmission of data on the bus is illustrated in Figure 3-12. As shown, 24 bits are used for addressing a data interface unit with a request for information whereas 32 bits are required for a command. Return data needs no address as it is timed by the computer and bus controller. The word length is 8 bits for telemetry and 16 bits for computer data.

3.6 ELECTROMAGNETIC COMPATIBILITY CONTROL

The observatory will consist of a number of replaceable spacecraft subsystem and experimental modules which must not only be mutually compatible during orbital operation but must also be electromagnetically compatible with existing and future launch and resupply vehicles. The required degree of compatibility will be achieved by limiting the magnitude of all extraneous electromagnetic emissions, by protecting all sensitive input signals and/or control circuitry from external influences, and by minimizing the number of input/output interfaces at both the observatory and module level. Electrical systems grounding concepts, case and

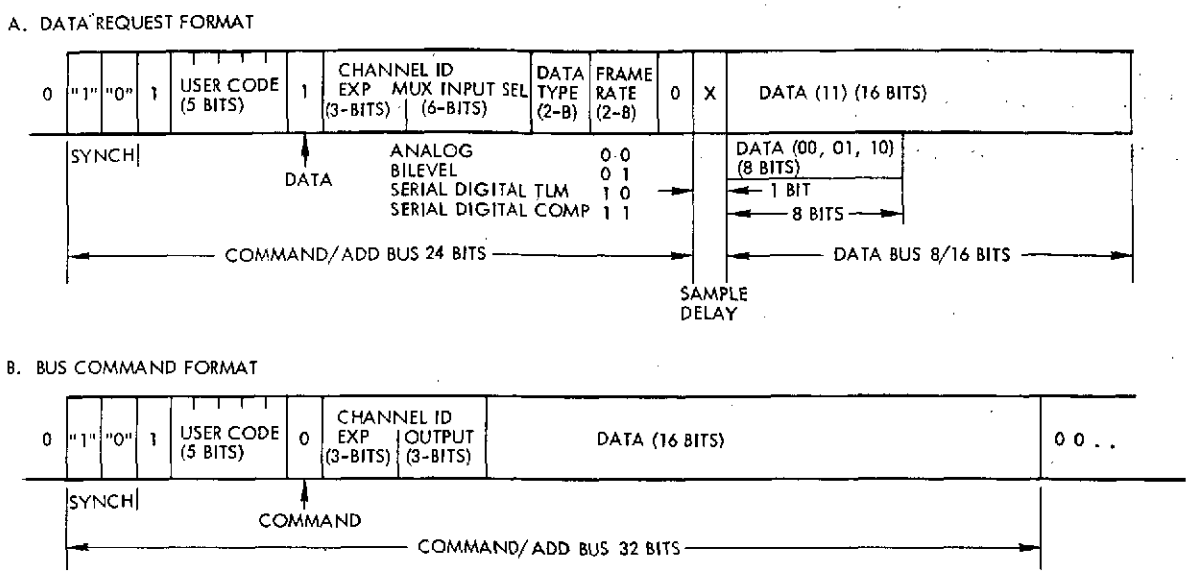

NOTES:
USER CODE (5 BITS) IDENTIFIES THE DIU OR MODULE
CHANNEL ID IDENTIFIES THE DATA REQUEST CHANNEL WITHIN THE DIU

Figure 3-12. Bus Formats

cable shielding criteria, electrical bonding methods, specification controls, etc., have been selected which will ensure an electromagnetically compatible system with adequate margins between output interference emission levels and input susceptibility levels. Each operational module will be treated as an independent, functionally operational entity with input/output filtering, shielding, or bandwidth limitations applied at its interfaces as needed, thus allowing future functional redesign of any mission-peculiar module without serious effects on the compatibility margins of other modules. The controls and criteria which have been selected for the EOS are summarized in Section 6.5 and will be detailed in the applicable module and systems specifications.

The primary DC power and party line data bus distribution subsystems will have single-point grounds. Also, single-point grounding will be employed for low level analog sensor circuits and high current control circuits. Subsystem circuitry wholly contained within a given module will, with some exceptions, employ multiple-point grounding using the module radiator panel and support structure as the ground reference

plane and return path for secondary power and signal currents within the module. The grounding methods will:

- Prevent the injection of high level circulating currents into common structural elements
- Reduce the magnetic field sensitivity of low level sensor/amplifier circuits
- Allow for stable and efficient subsystems operation at high audio and radio frequencies.

3.7 ACS CONCEPT AND MISSION PECULIARS

3.7.1 Attitude Determination

Operation of the ACS and ground processing of payload data requires a means of precise attitude determination. A qualitative comparison of candidate attitude determination approaches show the stellar-based system to be preferred for the range of potential applications. The stability requirements imposed by EOS-A payload performance require a precision inertial reference unit with appropriate updates. Star mappers, ideal for an earth-pointing mission, are a poor choice for inertial pointing. The system using a precision sun sensor does not offer unlimited sun-orbit geometries, nor does it yield data in eclipse. Fixed star trackers, appropriately mounted, appear to offer the best solution. The selected attitude determination design uses as sensors a three-axis rate integrating gyro package and two body-fixed star trackers to provide periodic gyro rate bias updates. This sensor information is processed by the onboard digital computer which integrates the gyro rates to provide attitude and establishes optimal attitude estimates at the star tracker update times. Figure 3-13 illustrates the star tracker geometry in an earth-pointing mission. Normal operation requires two star trackers. A third star tracker is shown for use as an optional redundant standby unit. The star trackers are positioned on the spacecraft so that a large swath including many stars is viewed on the celestial sphere with minimum radiant interference from the sun, and can provide suitable data for inertial pointing.

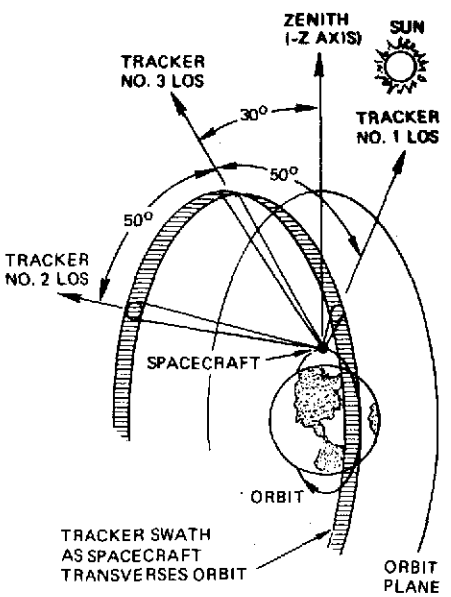

Figure 3-13
Star Tracker Geometry

The on-board attitude estimation procedure is illustrated in Figure 3-14. On-board spacecraft attitude estimation during earth-pointing is performed by a digital computer which receives IRU data input every 200 mseconds and star tracker information every 3 to 10 minutes. The IRU measured gyro rates are corrected within the computer for their bias drift rates, and the result kinematically integrated to yield an inertial attitude estimate. When a predetermined star enters a tracker field of view, the symbolic switch "S" closes and both the inertial attitude and the gyro drift rates are updated. Ground ephemeris data are provided periodically to a time-dependent ephemeris model which, along with the inertial attitude estimate, yields an estimate of spacecraft attitude in geocentric coordinates. This data is issued in the earth-pointing mode to steer the spacecraft and in pitch to maintain the pitch axis normal to the apparent ground track. Yaw steering is employed to maintain the payload scan plane normal to the image velocity vector.

3.7.2 Attitude Control Implementation for Mission Flexibility

The above-defined concept is implemented in a manner which facilitates the accommodation of a broad variety of missions (earth-pointing, sun-pointing, stellar-pointing) and spacecraft configurations with minimum changes. A key feature is the grouping of attitude sensing functions within one invariant module (attitude determination module) and actuation functions, including propulsion, in another module (actuation module) which can change internally from mission to mission if required. Each module is functionally configured to be applicable to any of the generic mission types delineated. Software functions are mechanized in the on-board computer with the communications and data handling module (Figure 3-15).

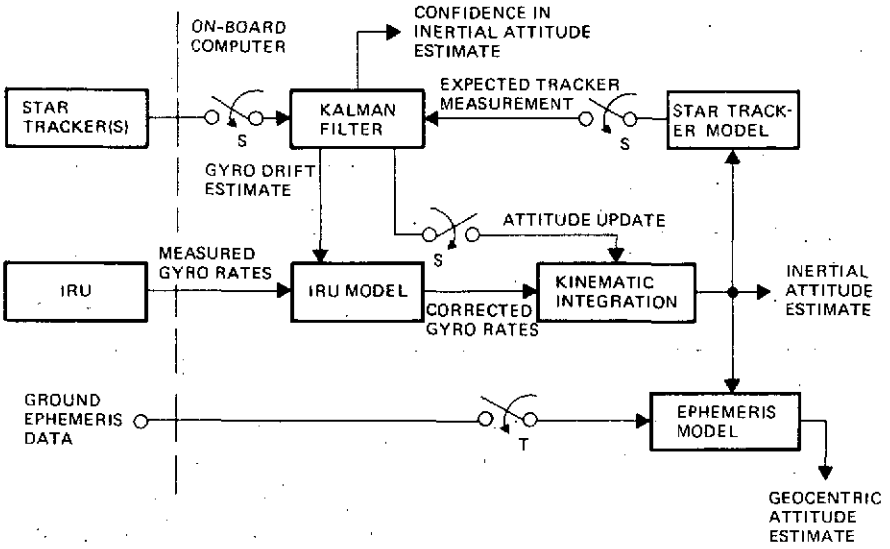

Figure 3-14. Attitude Estimation Block Diagram

3.7.2.1 Attitude Determination Module

The attitude determination module is designed to be used in any of the mission-types considered, without redesign. Provisions exist for added redundancy (e.g., three star trackers, six gyro assemblies) and for special elements (e.g., a precision null-seeking sun sensor) which could be needed for certain missions, without requiring these elements to be included in more basic applications. Minor related changes (generally simplifications) would be made in the on-board computer software for missions which are not earth-pointing.

3.7.2.2 Actuation Module

The actuation module is designed for multi-mission applicability in the sense that space is provided for actuation having a wide range of sizes. Actuation electronics have been designed to drive all units within the selected range.

Of particular interest in determining the required space within the module are the reaction wheels and magnetic torquers.* In order to meet these requirements a hypothetical worst-case disturbance model was developed.

*Thrusters are relatively easy to accommodate from a size standpoint. The major propulsion impact is from tankage.

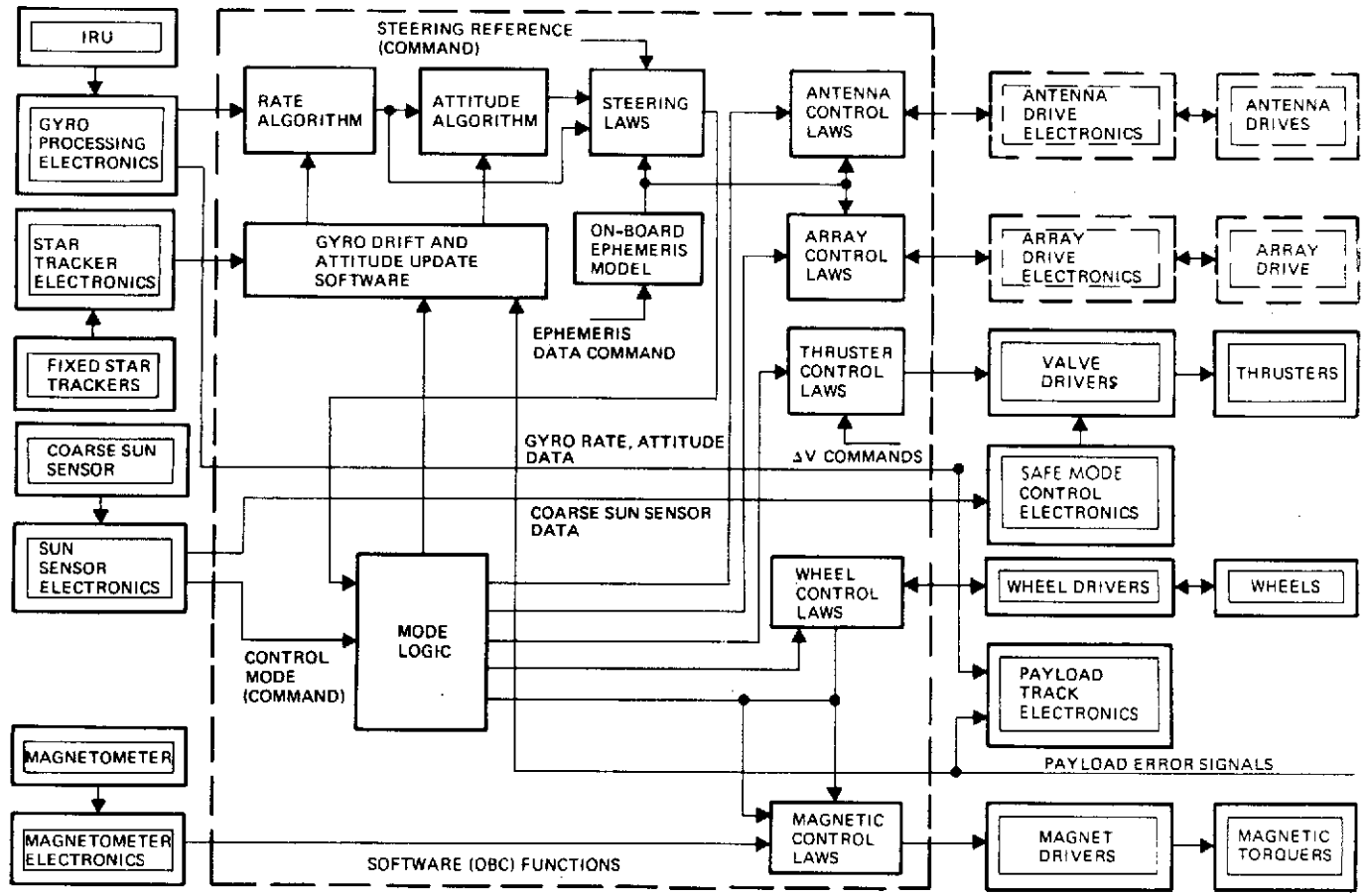

Figure 3-15. Attitude Control Functional Block Diagram

The four cases plotted in Figure 3-16a are bounding disturbance torque models. A 4 kw solar array with its center of pressure offset 33 feet from the spacecraft mass center has been used to develop the worst-case pressure torques, as well as the worst-case inertia product produced gravity gradient torques. Torques approaching 0.02 ft-lb (as specified in the RFP-provided ACS specification) are unlikely in a geostationary orbit. Moreover, torques as high as 0.2 ft-lb will occur in low orbits only when a very large spacecraft (e.g., 100,000 slug-ft^2

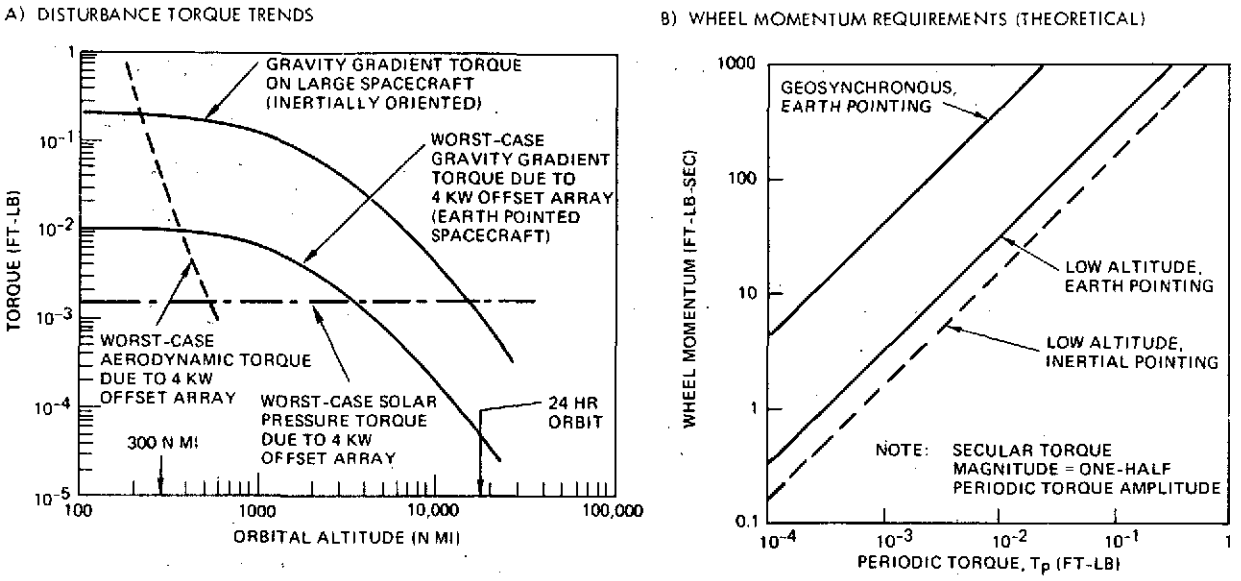

Figure 3-16.

Actuator Requirements for Growth Missions

inertial differences) is inertially pointed (and then will tend to be at twice orbit frequency rather than orbit frequency). We can conclude that torques higher than 0.01 ft-lb will occur only in extreme cases.

Theoretical wheel requirements can be developed as a function of disturbance torque magnitude. Figure 3-16b shows the theoretical wheel momentum (based on storage of the peak periodic momentum plus the secular momentum accomulated during a half orbit) for three cases

with a fixed periodic-to-secular torque ratio of two.* At low altitude (e.g., 900 km), inertial pointing requires somewhat less momentum than earth-pointing, because disturbances will be primarily at twice orbit frequency. The low orbit rate at 24-hour altitude results in large momentum requirements. In reality, with continuous magnetic unloading, the required wheel size will be less than the theoretical value (which applies more accurately when thruster unloading is employed). The design of a combined wheel and magnetic unloading system is discussed in Appendix A, Section 5.2.4.

A similar analysis gives insight into magnetic torquer sizing requirements. Figure 3-16c shows the theoretical lower bound on magnetic moment (based on equating the secular torque to the product of the magnetic moment and the orbital average of the magnetic field amplitude) for two cases. In all cases, actual requirements can be expected to exceed the values indicated here (as exemplified by the specific design of Appendix A, Section 5.2.4.

The disturbance torque ranges and resulting actuator sizing of Figure 3-16 can be translated into more concrete terms. Figure 3-17a shows wheel sizing for an EOS-type earth-pointing mission with a specified wheel-produced slew rate of 2 deg/min. This plot shows wheel momentum and torque requirements for establishing the slew rate and absorbing disturbance torques (secular torques = half of periodic torques). Requirements due to slew increase with spacecraft inertia and as the allowable attitude change during acceleration ($\Delta\theta$) decreases. Requirements due to disturbances are shown for low altitude orbits. Data points (●) are representative existing wheels.

For realistic disturbance levels, three standard wheels should be able to meet the requirements (for example, the two OGO wheels and one other). Extreme cases may require very large wheels, having torques approaching a foot-pound and a momentum capacity of several thousand ft-lb-sec. Requirements for high torque (in excess ov 20 to 40 in.-oz) may necessitate development of new wheels with brushless DC torquers.

---

*The "spec max" and "spec min" limits refer to the ACS specification accompanying the study RFP.

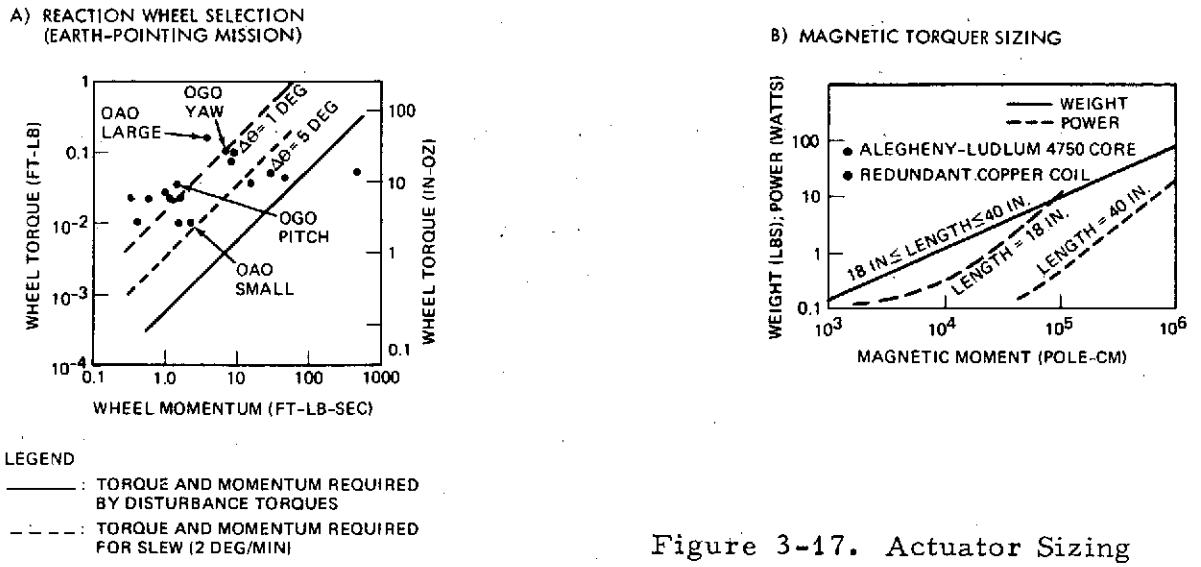

Figure 3-17. Actuator Sizing

Magnetic torquer sizing is similarly exhibited in Figure 3-17b. This plot shows the magnetic torquer weight and power as a function of magnetic moment requirement and is based on a flight-proven design. Again, three standard sizes can meet all realistic requirements now projected.

3.8 PROPULSION - MODULAR CONCEPT

Propulsion system functions consist of orbit transfer, orbit adjust, and attitude control. Attitude control consists of the primary mode of spacecraft attitude control during orbit adjust and transfer maneuvers and backup control for reaction wheels and magnetic torquers during reaction wheel unloading and safe mode control.

In all cases the propulsion hardware is an integral part of the actuation module. Because the module is structurally and thermally self-contained, components and propellant may be added or deleted (within limits of weight and envelope) for future missions with little effect on overall spacecraft design. Propellant mass can be increased slightly by increasing the blowdown ratio for the hydrazine or by increasing the gas pressure for the cold gas.

The modular design also allows changes in tank size and number of tanks to accommodate large changes in propellant loads.

In summary, the actuation module design accommodates the current EOS requirements while providing sufficient flexibility to accommodate anticipated requirements for future missions. This approach takes into account the need for a low-cost, yet highly reliable system, that can add or delete propellant quantity and specific components with minimal impact on the spacecraft design and associated interfaces.

The baseline propulsion system hardware includes a monopropellant hydrazine subsystem to perform the orbit transfer and adjust functions and a cold gas (GN_2) subsystem to perform the reaction control functions. The hydrazine element can be deleted when velocity control is not required. The two elements are combined in a manner which permits sharing of certain components to achieve the most cost-effective implementation. In the baseline configuration the hydrazine tank is pressurized with GN_2 from a line downstream of the high pressure to accommodate both impulse requirements for the reaction control system and pressurization requirements of the hydrazine tank. The considerations which led to this configuration as compared to alternatives are presented in Appendix A, Section 5.3.

The reaction control subsystem must provide spacecraft attitude control during orbit transfer and adjust maneuvers and for attitude control during the operational phases (e.g. backup unloading). The torque requirements for providing these functions differ in some cases by an order of magnitude. In these cases the system must be capable of operation at two levels of thrust. This is accomplished by using a high pressure regulated gas supply for the high thrust and a low pressure regulated gas supply for the low thrust. Typically the high pressure regulators would operate in the 300 to 350 psia range and the low pressure regulators would operate in the 30 to 35 psia range. The arrangement of the thrusters and isolation valves permits either group of six thrusters to provide three-axis control at either the high or low thrust level.

A variation of the propulsion system for use in applications not requiring orbit transfer can be achieved with a smaller hydrazine tank to provide only the propellant necessary for performing orbit adjust maneuvers. With this approach, a lower thrust hydrazine thruster can be used to provide the impulse for the adjust maneuvers. The reduced disturbance torques related to the low thrust hydrazine thruster permits the use of a single level reaction control system.

In general, either of these systems would be sized so that the storage capacity would be adequate for the worst-case anticipated mission requirements. For missions where the requirement is lower, the excess capacity could be used to provided added margin for longer life or for increased mission flexibility, or the tanks could be off-loaded so that booster capability could be more fully utilized.

3.9 TELEMETRY, TRACKING, AND COMMAND

3.9.1 Introduction

The communications and data handling module provides the spacecraft with the capability for receiving, demodulating, and processing information transmitted from NASA ground-based stations. Furthermore, it provides the capability for the on-board collection, formatting, and transmission of spacecraft housekeeping, medium-rate user, and transponded ranging data. Finally, it contains the equipment required to perform all on-board computations.

The module design accommodates the requirements of EOS-A while providing sufficient flexibility to accommodate the requirements of future missions, taking into account anticipated requirements for increased antenna gain, EIRP, data rate, data processing, computer storage, and system reliability, as well as the present and future capabilities of the NASA ground network. With the advent of TDRSS, an alternate communications path to EOS will be established. Again, the modularity of design concept is sufficiently flexible to accommodate TDRSS with a minimum of impact. Figure 3-18 presents an overall block diagram of the communications and data handling module. The following sections present the modularity concept in the communications and data handling system areas.

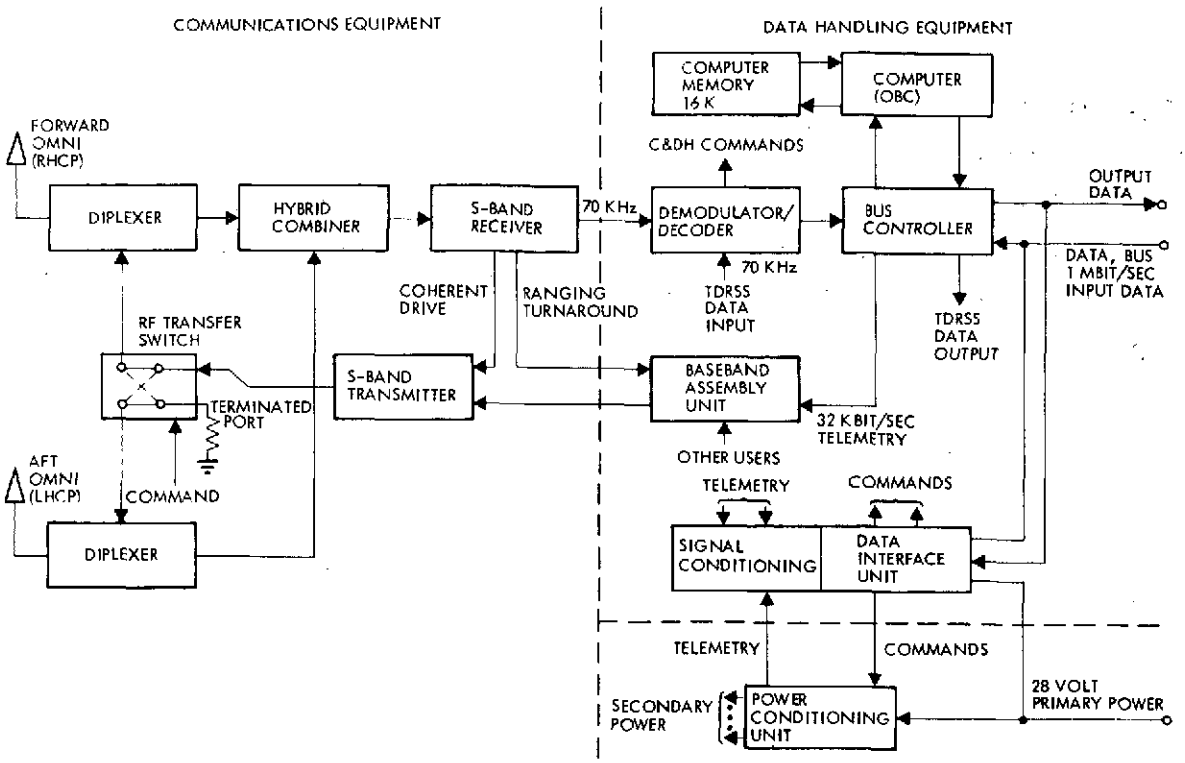

Figure 3-18. Communications and Data Handling Module Baseline Data

3.9.2 Communications System

3.9.2.1 Baseline Design

Figure 3-18 presents the baseline communications organization. This design, making use of flight-proven components, provides for command reception and telemetry transmission via two opposite, circularly polarized omni-directional antennas which, in turn, provide over 97 percent spherical coverage measured relative to the -1.0 dBi point. The outputs from each of the antennas are coupled to a hybrid combining network by means of two diplexers. The hybrid combines the two signals from the diplexers to provide a signal output to an S-band receiver tuned to a frequency located within the 2050 to 2150 MHz range. One output of the hybrid network is terminated. Since one of the antennas is right-hand circularly-polarized and located on the earth-pointing or forward side of the spacecraft and the other is left-hand circularly-polarized and located on the opposite or aft side, an antenna polarization address scheme is implemented, which allows the STDN to command the spacecraft via one of the two antennas, regardless of how the spacecraft is orientated.

The input to the S-band receiver contains command and ranging information in Unified S-Band (USB), STDN-compatible form. The receiver detects this information and provides the command data as an output to a demodulator/decoder unit contained within the data handling system portion of the module. The demodulation/decoder input from the receiver consists of a 70 kHz subcarrier containing 2 kbit/sec command data. The detected ranging data is provided as an output from the receiver to a baseband assembly unit also contained within the data handling subsystem. The baseband assembly unit sums the range data with a 32 kbit/sec, biphase-modulated, 1.024 MHz telemetry subcarrier and a 512 kbit/sec (medium-rate date) direct digital data stream to form the baseband signal which phase modulates the downlink RF carrier.

A frequency reference, coherent with the uplink carrier, is provided as an output from the receiver to the S-band transmitter. This reference, suitably multiplied in frequency, is phase-modulated by the composite baseband signal from the baseband assembly unit. Futhermore, since the downlink carrier is phase coherent with the uplink (with a frequency ratio of 240/221), two-way range rate or doppler information is provided. The S-band transmitter provides a 2-watt RF output which is coupled to the two omni-antennas by means of an RF transfer switch. The switch allows the transmitter to couple its output to either antenna.

3.9.2.2 Accommodation of Advanced Missions

Advanced missions may require operation at higher orbit altitudes with higher data rates and higher system reliability. The addition of redundant equipment to the communications and data handling module communication system to achieve higher reliability is readily accomplished by adding a second S-band receiver to the previously terminated output port of the antenna hybrid combiner network in Figure 3-18, and adding a second transmitter to the previously terminated input port of the RF transfer switch. Figure 3-19 illustrates a fully redundant communications system . Adequate space has been provided within the communications and data handling module to accommodate equipment additions for redundancy.

The baseline design was established using STDN/USB compatible uplink and downlink carrier and subcarrier frequencies, data rates, and

modulation formats. Within this framework, the module design is capable of accommodating a wide range of program requirements, In particular, the baseline system was established for a maximum real-time telemetry data rate of 32 kbit/sec; a maximum medium data rate of 512 kbit/sec; and a maximum uplink data rate of 2 kbit/sec. Since these rates represent the maximum requirements for the spacecraft, the communications system design will accommodate other low altitude requirements (300 to 900 nautical miles).

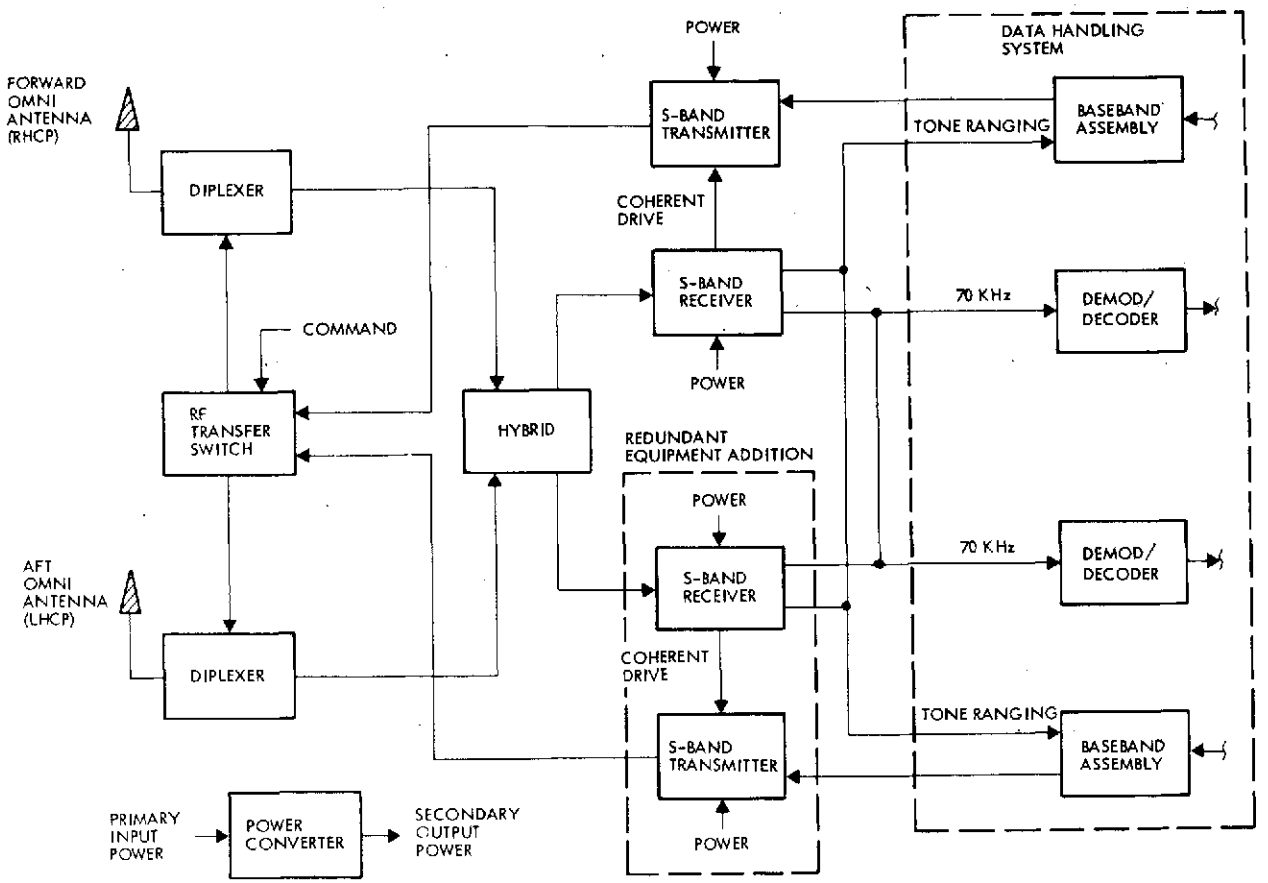

Figure 3-19. Addition of Redundant Communication Equipment

In general, the EOS baseline design can provide more than adequate performance for those missions having an orbit altitude of 1810 km (975 nautical miles) or less. A synchronous mission (such as SEOS) will require an earth coverage, fixed-mounted, 2-foot antenna mounted on the module for operation with the baseline 2-watt transmitter. Table 3-1 lists post-EOS-A missions as well as required design modifications to the

Table 3-1. Post-EOS-A Missions and Design Impacts

Mission	Orbit Altitude (km)	Uplink Antenna	Downlink Antenna	Downlink Transmitter	Weight Impact	Power Impact
SEOS	36,041 (synchronous)	Omni	2-foot dish	2 watts	2.5 lbs	None
SEASAT-A	725	Omni	Omni		None	None
Solar Maximum Mission (SMM)	556	Omni	Omni		None	None
Gap Filler (5-Band MSS)	861	Omni	Omni		None	None
SEASAT-B	723	Omni	Omni		None	None
Advanced SMM	556	Omni	Omni	2 watts	None	None

baseline design. Figure 3-20 shows the system block diagram for synchronous operation. The weight impact of the 2-foot antenna and associated RF switch is 2.5 pounds. Presumably, the spacecraft would be operated at a low data rate capable of being supported by an omni antenna until the spacecraft is properly positioned in synchronous orbit. After this, telemetry and perhaps payload data would be transmitted via the 2-foot antenna.

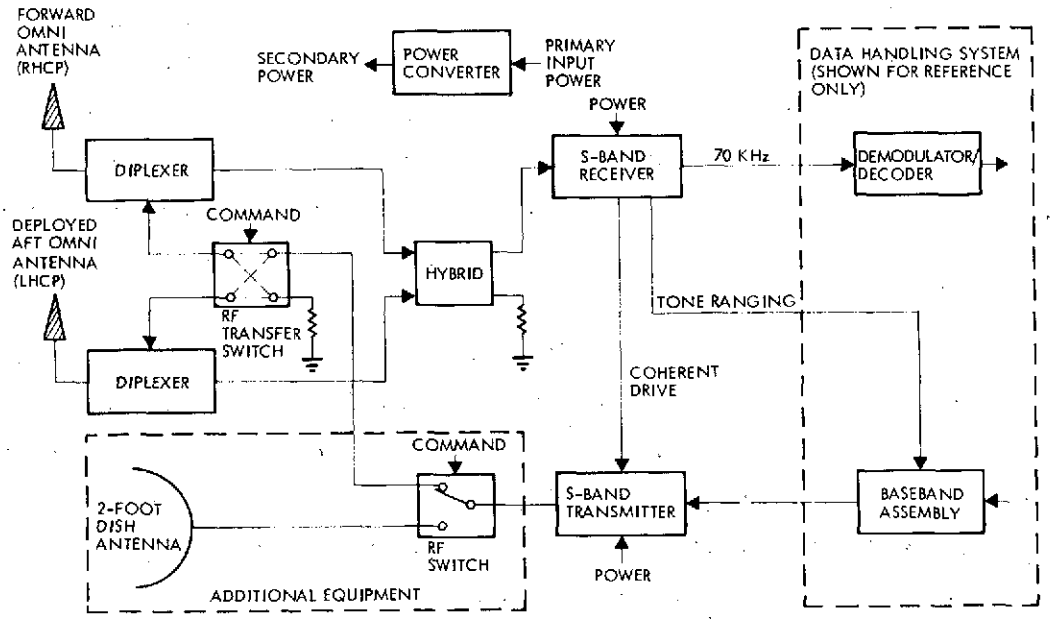

Figure 3-20. Addition of Equipment for Synchronous Operation

Finally, the requirements of TDRSS have no impact on the module design. The forward link from TDRSS is implemented by an appropriate baseband input to the decoder/demodulation unit (Figure 3-18) from a TDRSS-compatible receiver contained within the wideband communications module. Similarly, multiplexed telemetry data is transmitted on the TDRSS return link by providing an output from the bus controller unit to a TDRSS-compatible transmitter also contained within the wideband communications module.

3.9.3 Data Handling System

3.9.3.1 Baseline Design

The data handling equipment comprises several equipments that perform various data handling functions (refer to Figure 3-18). The demodulator/decoder accepts a 70 kHz subcarrier from the S-band receiver, demodulates it and transmits a serial data stream to the bus controller. The bus controller controls the data bus; i. e., it transmits command and interrogation signals to the various digital interface units (DIU's) contained in other modules and accepts telemetry and computer data. The bus controller provides the computer interface (hand-shake) accessing the memory directly through the DMA. Two kinds of data are transferred to the computer memory: data from the demodulator/decoder tagged for storage in the computer memory and requested data (by the computer) from the data bus system. A final function of the bus controller is to provide backup circuits for the telemetry formatting which is normally accomplished in the computer. The computer performs many functions (e. g., telemetry formatting, command and telemetry storage, thermal control, and attitude control system calculations). The baseline nonredundant computer operates with a 16K word memory. The DIU contains the remote command decoder which transfers serial or pulse commands to the user equipment. The DIU also contains a PCM encoder for time-division multiplexing both analog and digital data. The baseband assembly provides the subcarrier for the downlink telemetry and sums all of the downlink data for transmitter modulation.

3.9.3.2 Accommodation of Advanced Missions

The data handling equipment is designed to handle all projected advanced missions (Table 2-3) without design change. The design philosophy is described by component:

- Demodulator Decoder. The principal requirement is the command data rate. The command word is 44 bits long, 15 of these are used for overhead: spacecraft address and priority check. A 29-bit word is transmitted to the bus control unit. The uplink bit word is transmitted to the bus control unit. The uplink bit rate is 2 kbit/sec including overhead, and the net bit rate (maximum) is 1.3 kbit/sec. No future mission is expected to exceed this requirement.

- Bus Controller. The bus controller operates with the data bus at a bit rate of 1 Mbit/sec. Bus occupancy for EOS-A is approximately 25 percent at the highest telemetry rate. No future mission should require full occupancy of the data bus.

- Computer and Memory. CPU duty cycle is presently low (25 percent). Memory requirements are 16K words. The memory can be expanded to as high as 64K words so the computer should be adequate for all future missions and for missions requiring redundancy.

- DIU. The DIU capability is presently seven serial commands, 32 pulse commands, and 64 telemetry data inputs. Eight expanders, each containing the same number of functions as the DIU, may be added to any unit. As many as 32 DIU's can be handled by one bus controller. No future spacecraft or module will exceed this expandable capability.

- Baseband Assembly. The baseband assembly has four spare summation amplifier inputs as well as associated switching capability. No advanced mission should exceed this capability.

3.10 WIDEBAND COMMUNICATIONS MODULE CONCEPT AND MISSION PECULIARS

3.10.1 Introduction and Baseline Description

The equipment provided within the wideband communications module processes the wideband digital data outputted from the spacecraft thematic mapper and HRPI units and transmits it, at a 240 Mbit/sec rate, on an X-band carrier to the NASA STDN. It also processes the thematic mapper and HRPI data to a lower 20 Mbit/sec rate for transmission, via a second X-band link, to low cost ground stations (LCGS). A block diagram of the wideband communications module equipment is shown in Figure 3-21.

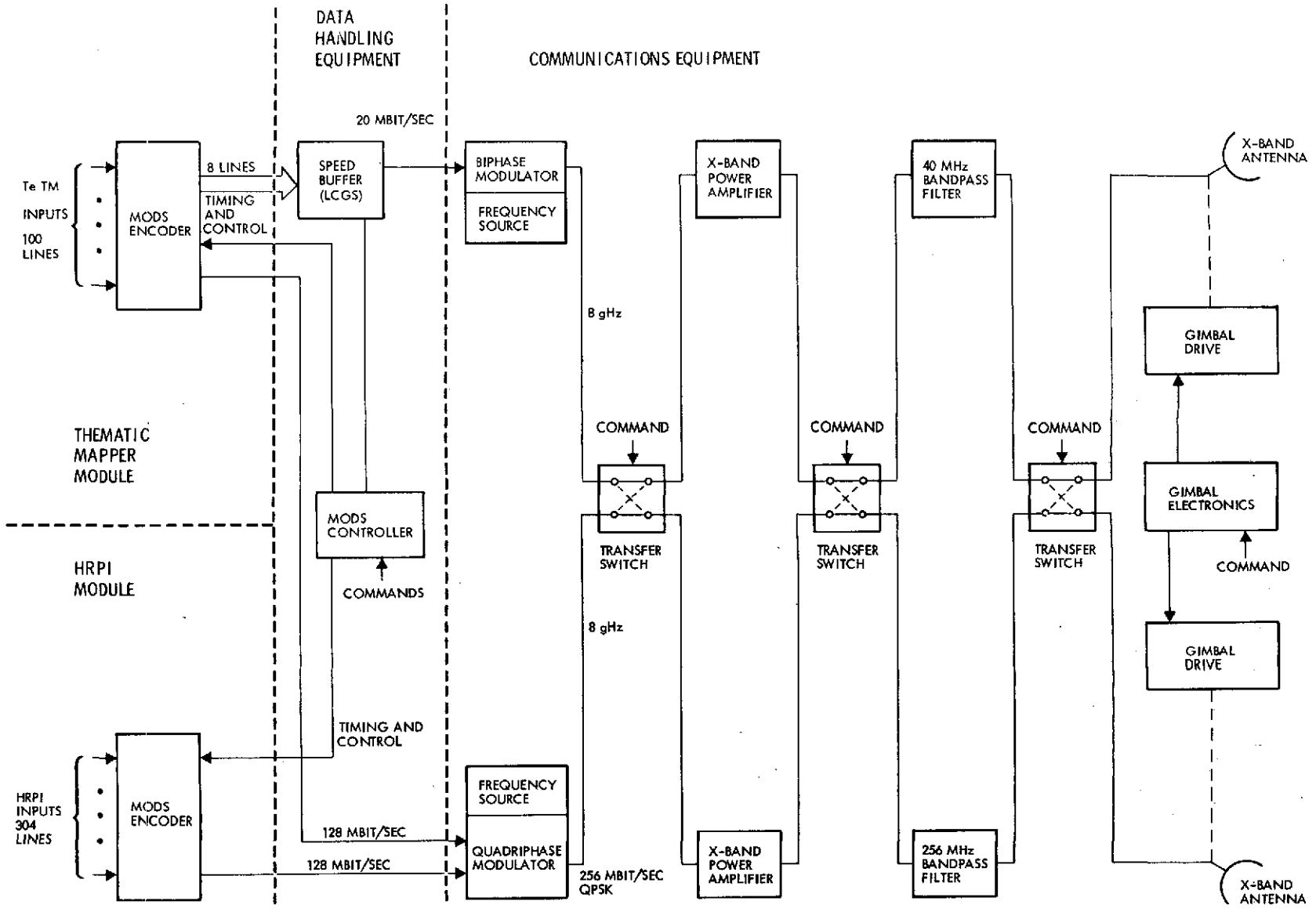

Figure 3-21. EOS-A Wideband Communications Module Block Diagram

Information from the TM unit is provided to the module in two forms. The first is in parallel form on eight lines at 15 Mbit/sec per line. The second is in serial form at 120 Mbit/sec. The parallel information is provided as inputs to an LCGS speed buffer which selects and frames data for transmission to the LCGS at 20 Mbit/sec (or optionally at 15 Mbit/sec).

The output from the speed buffer drives an X-band biphase modulator. The second or serial output from the TM unit is provided as an input to an X-band quadriphase modulator along with a 120 Mbit/sec serial, digital data stream from the HRPI. The two data streams from the TM and HRPI are in synchronism as established by clock signals provided to each of these units from a Multi-megabit Operational Data System (MODS) controller contained within the module. The output from the quadriphase modulator as well as the output from the biphase modulators drive 0.5 watt X-band power amplifiers which have their inputs and outputs cross-strapped by means of RF transfer switches. Each of the amplifiers drive RF, pretransmission bandpass filters which limit the combined 20 and 240 Mbit/sec RF spectra. The outputs from the two filters drive steerable X-band antennas and are coupled to them by means of an RF transfer swtich. Secondary power is provided to all units contained within the module from a power converter unit. Finally, each of the steerable antennas is driven from a biaxial gimbal drive controlled from gimbal drive electronics. Telemetry and command data are provided to and from a remote terminal unit which interfaces with the spacecraft data bus.

3.10.2 Accommodation of Advanced Missions

The baseline design for the wideband communications module equipment is provided in nonredundant form. The RF equipment, as shown in Figure 3-21, however, is capable of being cross-switched and the design therefore, is redundant with respect to the transmission of either the TM or HRPI data. Additional reliability, where required for a particular mission, can be achieved through the use of one or more additional standby units suitably coupled by RF switches. The same consideration can be given to the data handling equipment.

Advanced missions with data requirements and orbit altitudes in the EOS-A range can be readily accommodated by both the digital and RF

equipment with no change to the module design. Missions which require higher data rates than EOS-A or are required to operate at significantly higher altitudes have a direct impact on the RF equipment, particularly in view of the fact that the baseline RF equipment was configured to transmit the maximum EIRP to the ground station with the spacecraft at nadir, without violating the established CCIR maximum power flux density level. This essentially dictates that advanced missions such as SEOS be accommodated by direct replacement of RF equipment to attain higher EIRP's.

The SEOS mission at geostationary altitude requires a 24 dB increase in EIRP which can only be achieved through the use of higher transmitter power levels, larger pointable antennas, or a combination of the two. In order to avoid possible mechanical mounting problems associated with large diameter antennas, it is desirable to keep the antenna diameter reasonably small. This requires the use of 50 to 100 watt TWT amplifiers in place of the present 0.5 watt solid-state amplifiers and, therefore, has a major impact on the module design. A reasonable compromise would be to replace the 0.5 watt amplifiers with 16 to 20 watt TWT's and replace the 2.0-foot diameter antennas with one's having a 5-foot diameter. The module design will accommodate the increase in weight, volume, and power associated with these changes.

The on-board data handling requirements for EOS-A as well as future missions vary from a low of 300 bits/sec for the SEASAT-A pulse compression radar altimeter, to a high of more than 300 Mbit/sec where picture imagers as well as synthetic aperture radar are used. In general, all of the sensor outputs are analog. The A/D conversion accuracy requirement varies from 4 to 10 bits per sample. Housekeeping requirements also vary over a wide range.

With the exception of the speed buffer, the wideband data handling system is designed with modular components so that one design will fit all missions as well as all instruments. Special-purpose signal conditioning boards/slices (a part of the instrument) will probably be necessary in many instances, but the major portion of the system will require only firmware changes in the controlling read only memories (ROM's) to be adapted to different instruments.

Modularization is achieved as follows:

- Standard boards/slices are designed. These sections are combined to perform the desired functions. Figure 3-22 shows how these boards/slices are combined for the baseline system (Te TM and HRPI).
- ROM's or PROM's are used to program minor and major frame events to the following quantization levels (refer to the block diagram, MODS controller, Figure 3-23):

Major Frame Timing:	12 bits (4096) The major frame may be quantized in as many as 4096 minor frame groups
Minor Frame Timing:	9 bits (512) The minor frame may be quantized in as many as 512 word groups.
Word Timing:	Word lengths of 4, 8, 16 and 32 are selectable.

The advent of TDRSS requires the installation of Ku-band RF equipment into the wideband communications module. This equipment may directly replace the X-band RF equipment if the sole method of communications to the ground is via TDRSS or, it may be an adjunct to the X-band equipment if direct-to-ground communications capability is retained. Figure 3-24 illustrates a design which accommodates TDRSS by modular Ku-band equipment.

In addition to the Ku-band equipment, TDRSS-compatible S-band equipment will also be mounted within the module for command reception and telemetry transmission. Again, as indicated in Figure 3-20, this can be accommodated by a modular addition to the baseline equipment.

Modular design as well as ROM control means that future missions and other instruments may very well use the same equipment with no design modiciation.

3.11 ELECTRIC POWER CONCEPT AND MISSION PECULIARS

The electrical power subsystem (EPS), which generates and distributes electrical power, consists of the solar array, batteries, power control unit (PCU), harness, and power switching assemblies. The solar array, with its associated solar array drive assembly is contained in the

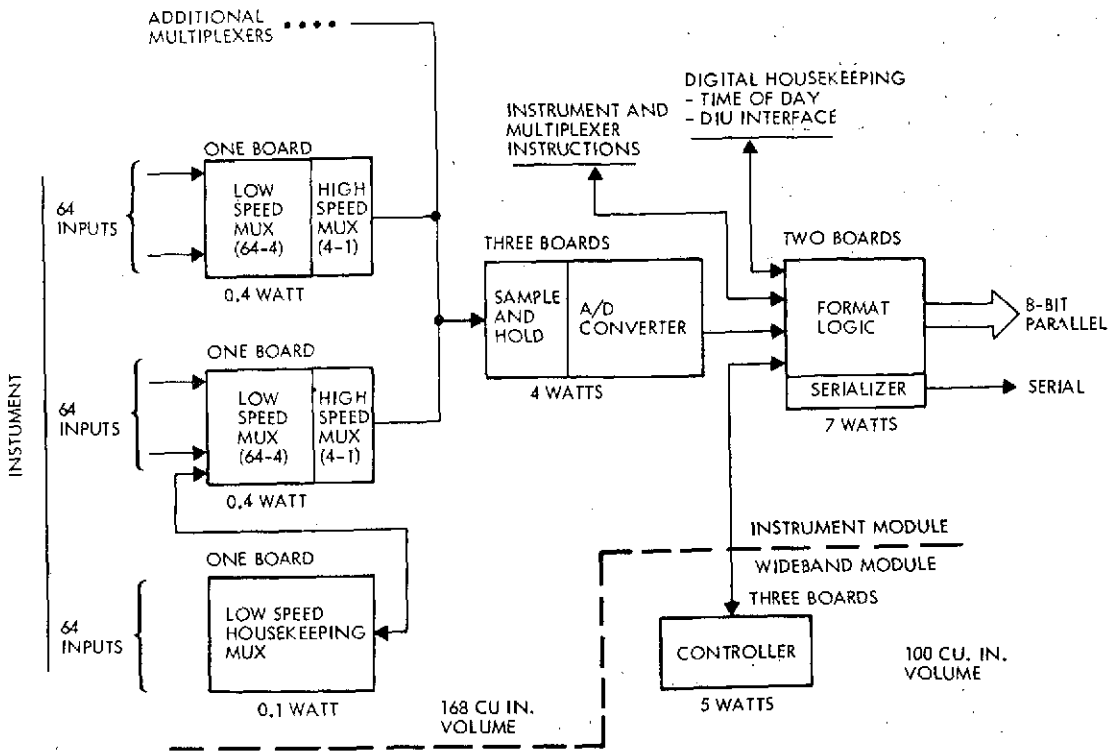

Figure 3-22. MODS Conditioning

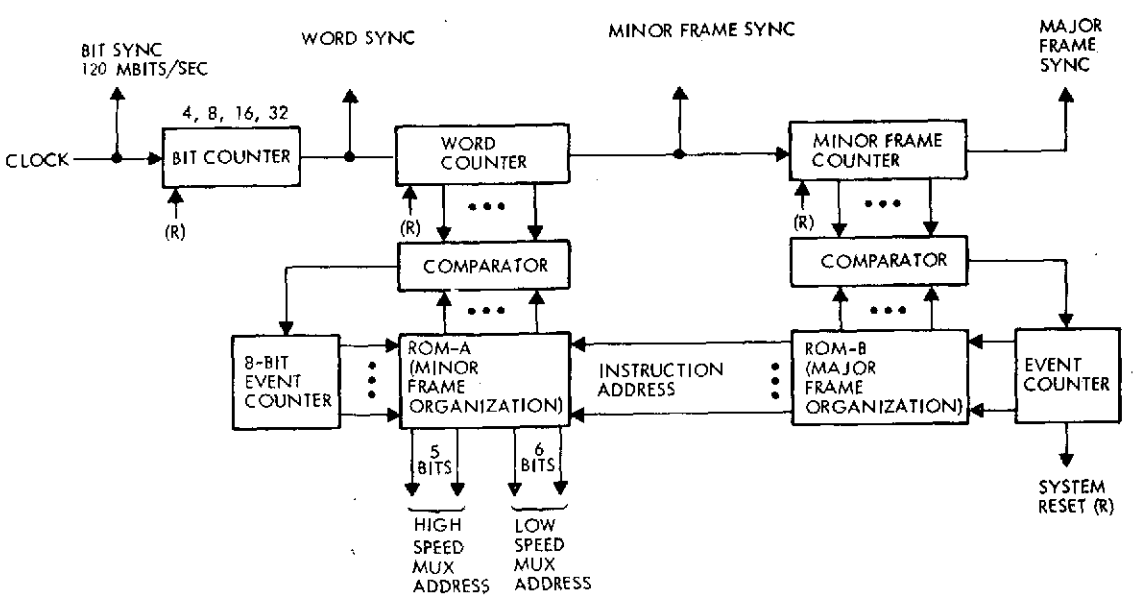

Figure 3-23. Micro-controller for the High Speed Multiplexer

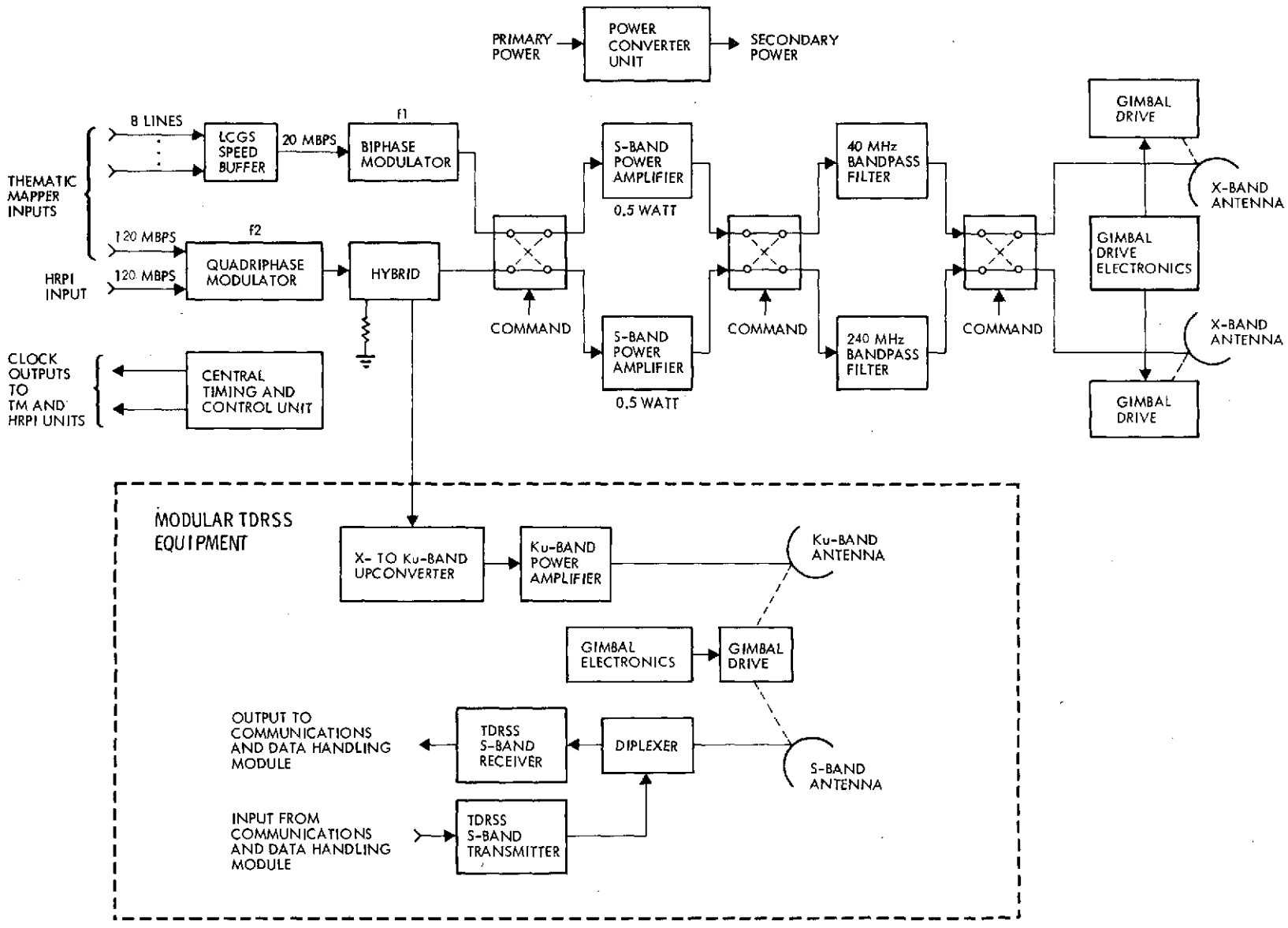

Figure 3-24. TDRSS Impact on Wideband Communications Module

solar array and drive module. Sections 6.4 and 6.6 describe the features of the power module and the solar array and drive module, respectively.

3.11.1 Electric Power Concept

The EOS spacecraft will perform a variety of missions in orbits ranging from low to geostationary altitudes. Major changes in orbit altitide and inclination have a significant effect on the size of electrical power subsystem components , particularly the solar array and batteries. For example, at low altitudes the power required for battery recharge is approximately 33 percent of the end-of-mission solar array power, while at geostationary altitude it is only 15 percent. Solar array maximum temperatures are approximately 15°C greater at low altitudes than at geostationary altitudes due to thermal heat inputs from the earth. These differences, produced by the particular characteristics of individual missions, would normally result in important difference between sets of hardware specifically designed on a minimum-weight, maximum-reliability basis. However, for EOS the design emphasis is directed toward cost-effective, modular hardware. The power subsystem hardware is optimized for the spectrum of EOS missions and is not an optimum size and weight for a specific mission.

The power subsystem, in addition to providing the efficient transfer and control of power, must also be flexible enough to accommodate a variety of load power levels and orbit profiles with a minimum of reconfiguration and adjustment. The configuration must provide automatic operation without dependence upon other subsystems or ground intervention. This latter requirement is of particular importance for low-altitude missions in which the spacecraft is beyond ground control for multiple successive orbits. Finally, the configuration must be simply-conceived to maximize subsystem reliability and minimize nonrecurring costs.

Various candidate power subsystem configurations were examined to determine their applicability to the EOS mission subject to the considerations stated above. Analyzed and traded off were:

- Multiple-battery series charger (PWM-type) with full solar array

- Multiple-battery shunt charger (dissipative-type) with full solar array
- Single-battery series charger (PWM-type) with full solar array
- Single-battery series charger (PWM-type) with split solar array
- Single-battery shunt charger (dissipative-type) with split solar array
- Single-battery series-shunt charger (PWM-type) with full solar array.

The results of these studies are summarized in Appendix A, Section 5.4. The final conclusion of the configuration analyses is that the first subsystem configuration, a version of one developed and flight-proven on the Orbiting Astronomical Observatory (OAO), best satisfies the EOS mission requirements.

3.11.2 Selected EPS Configuration

A simplified block diagram of the selected electrical power subsystem configuration is shown in Figure 3-25. Its operation is as follows. A day/night signal closes contactor K1 upon entering eclipse, shunting out the series PWM regulator. During the initial sunlit portion of the orbit the solar array supplies load current and battery charge current at a voltage determined by the battery. As charging continues the terminal voltage of the batteries will rise. When the voltage of one or both batteries begins to exceed a temperature-compensated battery voltage limit (BVL) an error signal will be generated which will cause the drive circuit of K1 to open the contactor. The series regulator, designed to accommodate the full combination of load and battery charge powers for the EOS mission, will then reset the load bus voltage to the value required by the BVL. With the voltage limited to the BVL level the currents in both batteries will reduce toward stable asypmtotic values as charging (actually overcharging) continues. When the spacecraft enters eclipse the batteries discharge through battery enable/disable relays to the spacecraft loads. The transision from the charge to the discharge modes is smooth and continuous.

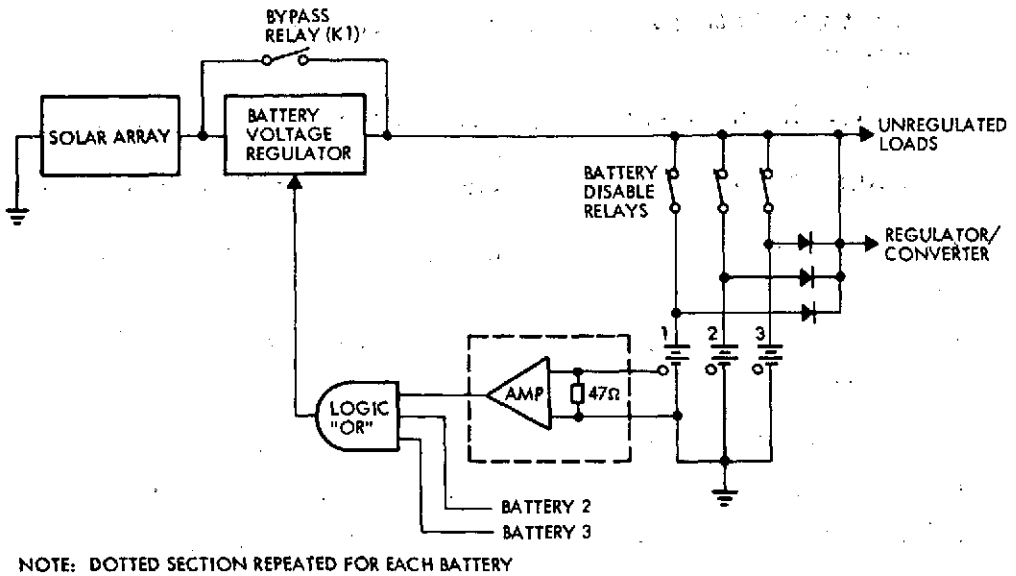

Figure 3-25. Electric Power Subsystem Simplified Block Diagram

The key to successful application of the subsystem configuration to widely differing orbits and power levels is the ability to tailor battery overcharge to provide the proper overcharge ratio (as a function of battery temperature), and to limit battery dissipation in the event of a thermal imbalance within the power module. A family of eight BVL's, spaced equidistantly and essentially linear over a temperature range of 0 to +35°C, is provided (Figure 3-26).

As mission conditions change or as the battery characteristics vary with age and use, the operational BVL can be changed by ground command. During periods of constant sunlight when the batteries need only be trickle-charged at low rates the lower BVL's may be used for charge reduction. This procedure has been effectively applied, under both normal and anomalous operating conditions on the OAO program.

The BVL control mechanism is backed up by two auxiliary protection features. Each battery contains one cell that contains a vendor installed third electrode. As oxygen is generated within the sealed cell a voltage proportional to cell pressure is developed between the third electrode and the negative terminal. When this signal exceeds a reference voltage that corresponds to an over-pressure condition within the cell an

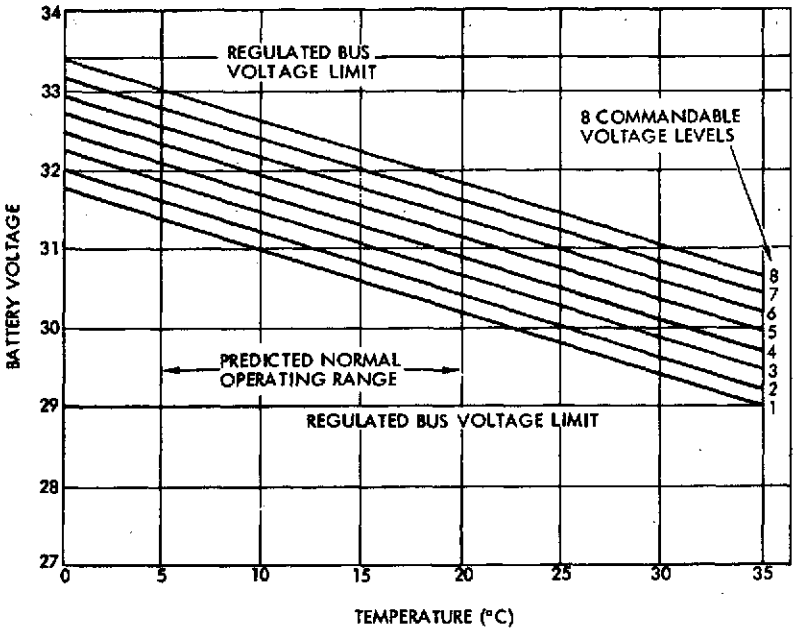

Figure 3-26. Battery Voltage Limit Curves

internal subsystem command is generated which causes the BVL to be switched to the lowest curve of the family. This has the immediate effect of reducing charge current in both batteries to levels which will produce an increase in the rate of oxygen recombination.

The second auxiliary protection feature consists of a charge control switch that is operated by a battery temperature signal. When the temperature of either battery exceeds 35°C (95°F) an internal subsystem command is generated which causes the BVL to switch from its present level to the lowest. When the battery cools to a temperature below 29.4°C (85°F) the BVL is returned to the original level.

The subsystem configuration studies included an assessment of benefit to be obtained by tracking of the solar array maximum power point. Such benefits accrue when the solar array temperature is cold upon emergence from eclipse, and when the solar vector is off-normal to the solar array panels. The presence of a series PWM-type regulator (itself a form of power-point tracker) in the EPS configuration suggests that this form of optimization may be obtained at a small expense of additional cost, complexity, and weight. However, the conclusion drawn

from the investigation (which is summarized in Appendix A, Section 5.4, indicates that the net increase in available solar array power that would be available during the solar array thermal transient is not justified by the increased complexity and cost required for its implementation. Furthermore, since a wide variety of solar aspect angles can be expected to result from the range of proposed missions, it is necessary to design the solar array with a hinge to obtain a nominal offset of the array from the pitch axis. When this preset angle is properly selected for the particular mission, the variation in solar incidence will be less than ±45 degrees for eclipsing orbits. The analysis in Appendix A, Section 5.4 demonstrates that power-point tracking does not provide substantial benefit intil a 45-degree incidence is reached or exceeded and the net power gain is approximately 1 percent.

An attitude control safe mode logic is provided in the power module through monitoring battery change control status and solar array current. This logic is activated if either of two conditions occur:

1) Loss of solar array current (day/night detector) for a period exceeding the maximum eclipse time

2) Two consecutive sunlight periods without the batteries reaching the voltage limit.

The attitude control safe mode logic receives a signal from the day/night detector and starts a 45-minute timer. If the condition persists for 45 minutes and the logic circuit is enabled, the attitude control module safe mode functions will be enabled. If the day/night detector senses solar array current, the 45-minute timer is reset.

When the spacecraft enters eclipse, a signal from the day/night detector starts the two-stage eclipse counter circuit. If the batteries fail to attain sufficient charge by not reaching the battery voltage limit after two eclipse periods, the attitude control module safe mode functions will be enabled when the safe mode logic is enabled. If the batteries reach full charge, the battery voltage limit circuit will reset the logic and the eclipse counter. The eclipse counter can also be reset by ground command.

3.11.3 Thermal Considerations

The performance of the selected EPS configuration depends on the establishment and control of a well-defined thermal interface between the batteries and the power module. While this is generally true for most spacecraft, it is of particular importance for EOS because of the selected method of battery charge control. The problem is stated simply. When multiple parallel battery strings are charged from a common bus it is essential that they each be at or very near a common temperature otherwise there will be imbalanced charge current sharing with the warmest batteries taking the greatest fraction of available charge current. If the temperature difference between batteries is too great the coldest batteries will be charge-starved by the time the warmest reach the BVL. To avoid this problem a firm design requirement must be placed on the thermal control subsystem portion of the power module to assure that the temperature of each battery mounting surface does not differ by more than 2.5°F from the average temperature of all battery mounting surfaces. Otherwise the average temperature of each battery mounting surface should lie within the range of 1.6°C (35°F) to 18.3°C (65°F) to ensure reliable, long-life operation. Battery temperature is controlled with thermal conducting shims between cells which are thermally bonded to a battery baseplate. The baseplate is temperature controlled by the external radiator on the anti-sun surface and electrical resistance heaters.

In consonance with the requirement for precise thermal control it is also necessary to design the batteries in a manner which minimizes thermal gradients within the assemblies. This is not a difficult objective to meet, but only at the expense of a moderate increase in packaging weight in comparison to a conventional weight-optimized design.

3.11.4 Solar Array Modularity

To accommodate the variety of missions encompassed by the modular concept, we have selected a standard solar cell subpanel which can be assembled in various quantities. In establishing the configuration the following factors were considered:

- Power increment (cost and weight non-optimality)

- Variety of launch vehicles (shroud constraints)
- Altitude variations
- Mission duration variations
- Array open circuit voltage (reguires 98 cells in series).

These have led to specific physical and electrical configurations and cell and coverglass selection. The array is attached to a solar array drive module containing a 1 degree of freedom drive mechanism, springs, and associated electronics (see Section 6.6), which is removable for on-orbit servicing. This is described in Section 4.1 and depicted in Figures 4-1 and 4-2.

A nominal subpanel power of 40 watts was selected as the best compromise between a reduction in watt, weight, and cost as subpanel size grows and an average increase of weight and cost due to granularity of array power selection. This is achieved by mounting two strings of three parallel by 98 series cells on a 30 x 28.8 inch substrate. Coverglass requirements depend on orbit altitude and mission duration. Table 3-2 indicates the subpanel power for three life times and three altitudes as a function of coverglass thickness. Based on these values, power (watts) per unit weight (pounds) for two different substrate technologies appears in Table 3-3. Although this table indicates a slight weight advantage for the 6 mil coverglass, handling costs favor a thicker selection. We have chosen 12 mil thick glass at an increase in weight (EOS-A) of about 9 pounds. This will prove a satisfactory choice for orbits up to about 1000 miles.

Table 3-2. Subpanel Power (watts)

Years	300 nautical mi (73°C)			600 nautical mi (66°C)			800 nautical mi (60°C)		
	Glass Thickness								
	6 mil	12 mil	20 mil	6 mil	12 mil	20 mil	6 mil	12 mil	20 mil
0	50.70	50.70	50.70	52.54	52.54	52.54	54.22	54.22	54.22
1	47.76	48.67	49.89	48.23	48.33	48.50	39.64	41.42	43.82
2	44.11	46.39	49.38	47.08	47.11	47.28	37.41	39.53	42.25

Table 3-3. Power per Unit Weight (watt/lb) for Two Array Substrates, Three Glass Thickness, Three Altitudes, Three Life Times

Years	300 nautical mi (73°C)			600 nautical mi (66°C)			800 nautical mi (60°C)		
	Glass Thickness								
	6 mil	12 mil	20 mil	6 mil	12 mil	20 mil	6 mil	12 mil	20 mil
0	18.85/ 27.10	16.57/ 22.40	14.53/ 18.99	19.53/ 28.10	17.34/ 23.77	15.05/ 19.68	20.16/ 28.99	17.89/ 24.52	15.54/ 20.31
1	17.75/ 25.54	16.06/ 22.02	14.30/ 18.69	17.93/ 25.79	15.95/ 21.87	13.90/ 18.16	14.74/ 21.20	13.67/ 18.74	12.56/ 16.41
2	16.40/ 23.59	15.31/ 20.99	14.15/ 18.49	17.50/ 25.18	15.57/ 21.35	13.55/ 17.71	13.91/ 20.01	13.05/ 17.89	12.11/ 15.82

4. EOS-A BASELINE OBSERVATORY SYSTEM

EOS-A system design considerations include mechanical and electrical configurations, performance requirements and allocations, redundancy and reliability, and mass properties.

4.1 EOS-A MECHANICAL CONFIGURATION

Two baseline configurations of the basic EOS spacecraft have been synthesized: 1) a Titan version (Figure 4-1) with a rectangular arrangement of spacecraft modules, and 2) a Thor-Delta version (Figure 4-2) with a triangular arrangement. Both use identical modules for all spacecraft subsystems except for the actuation module. For some missions, it may be desirable to fly the Delta version (triangular) from Titan, in which case it could be serviceable in orbit because of Titan's bigger payload capability. Table 4-1 summarizes EOS configurations in combination with possible launch vehicles.

Table 4-1. EOS Configurations

Configuration		Launch Vehicle		
		Thor-Delta	Titan IIIB	Shuttle
Triangular	Serviceable*		X	X
	Non-serviceable	X**		
Quadrangular	Serviceable			
	Non-serviceable		X**	X

*Serviceable refers to capability for in-orbit module replacement

**These are the Thor-Delta and Titan baseline configurations described in this section.

The mechanical interfaces with the launch vehicle for both the Thor-Delta and Titan configurations are by means of aft adapters, as described in Section 3.2. For later missions where payloads may be heavier, a transision ring adapter may be used as previously described. Space Shuttle mechanical interfaces are also addressed in Section 3.2.

The basic design consists of a spacecraft assembly (subsystem modules plus support structure), transition ring, and payload assembly (instruments and instrument-dependent equipment with an appropriate structure).

4.1.1 Delta Configuration

For Delta (Figure 4-1), the payload assembly accommodates the HRPI, thematic mapper, and wideband communications module, including two side-mounted double-gimballed antennas for unobstructed horizon-to-horizon viewing. A repackaged HRPI (Section 5.2) provides an improved radiator view factor.

The spacecraft assembly uses three standard 48 x 48 x 18 inch subsystem modules. The volume within the triangular-shaped structure is used for orbit-adjust hydrazine propellant storage, with the pneumatics and other attitude control equipment in the actuation module which also includes the hydrazine system.

The solar array is comprised of four identical wings which in turn consist of a group of standard array subpanels; 1 degree of rotational freedom about a fixed clock angle is provided. The large solar array required and the limited storage area within the Delta fairing result in a design that requires a sequenced deployment similar to that performed on several previous spacecraft.

The spacecraft has four probes on its aft surface to mate with the Shuttle docking and deployment platform.

4.1.2 Titan Configuration

The Titan configuration is shown in Figure 4-2. Subsystem modules including solar array panels, are common with the Delta design; however, the instruments mount in different support structures. For the quad configuration the objective has been to make all modules replaceable in orbit using the SPMS and SAMS. These include the three basic subsystem modules, plus the payload instruments, wideband communications, data collection, actuation, and solar array modules. Thus, any subsystem or payload element can be replaced during a Shuttle resupply, except the structure and its thermal control.

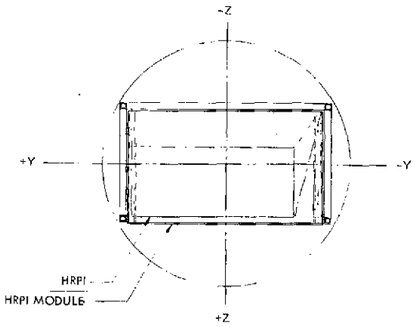

SECTION D-D

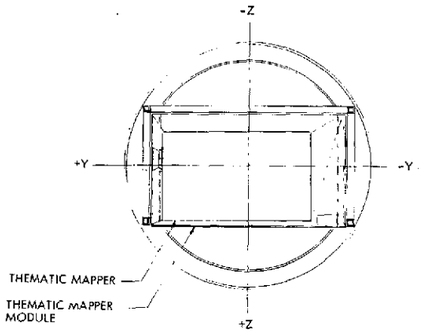

SECTION C-C

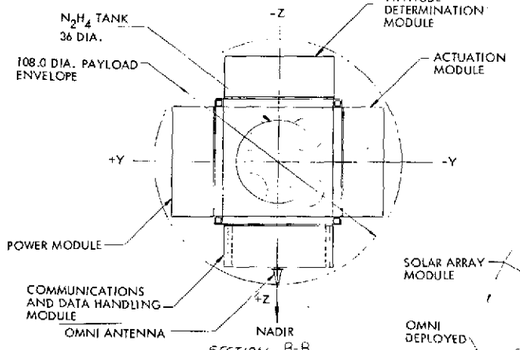

SECTION B-B

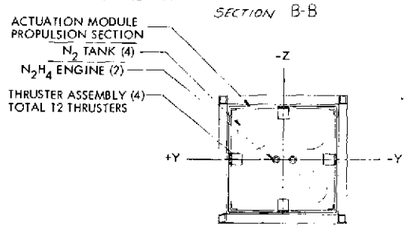

SECTION A-A

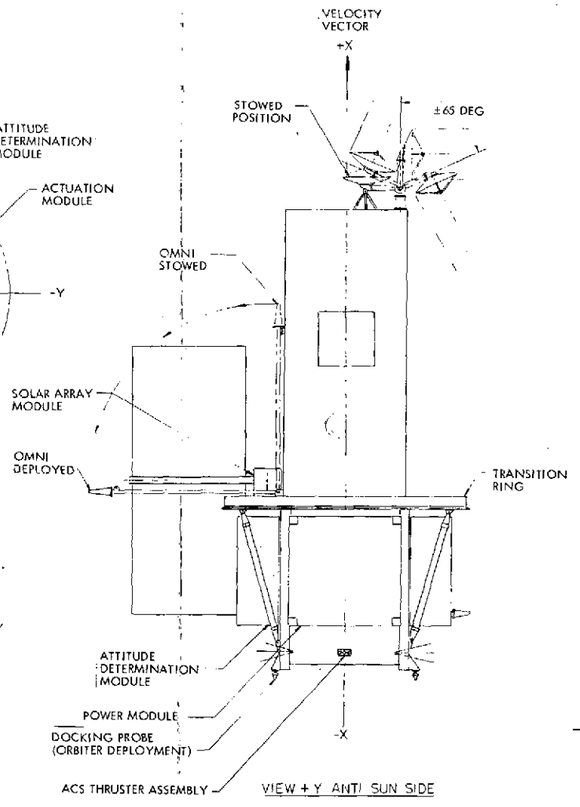

VIEW +Y ANTI SUN SIDE

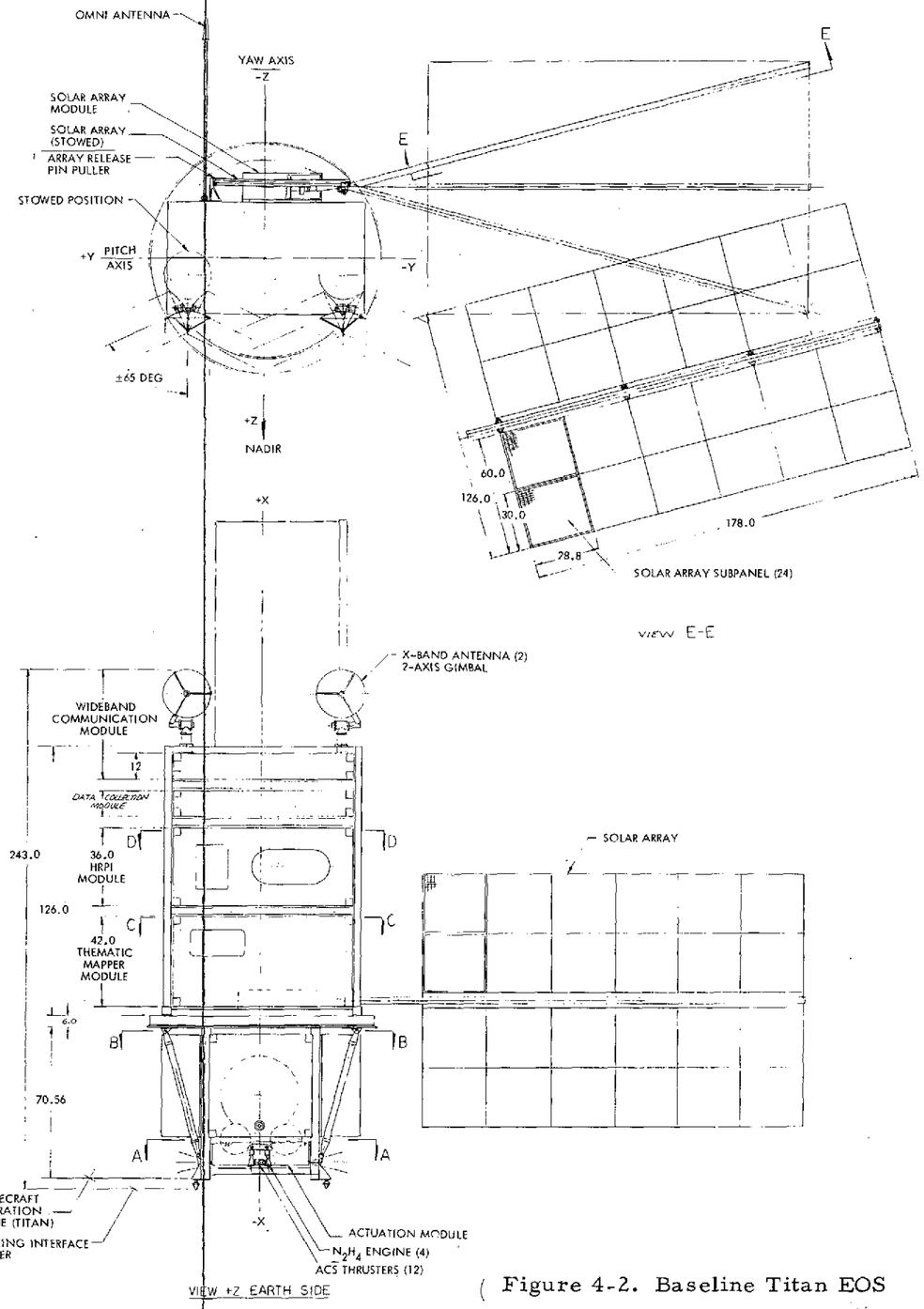

VIEW +Z EARTH SIDE

Figure 4-2. Baseline Titan EOS

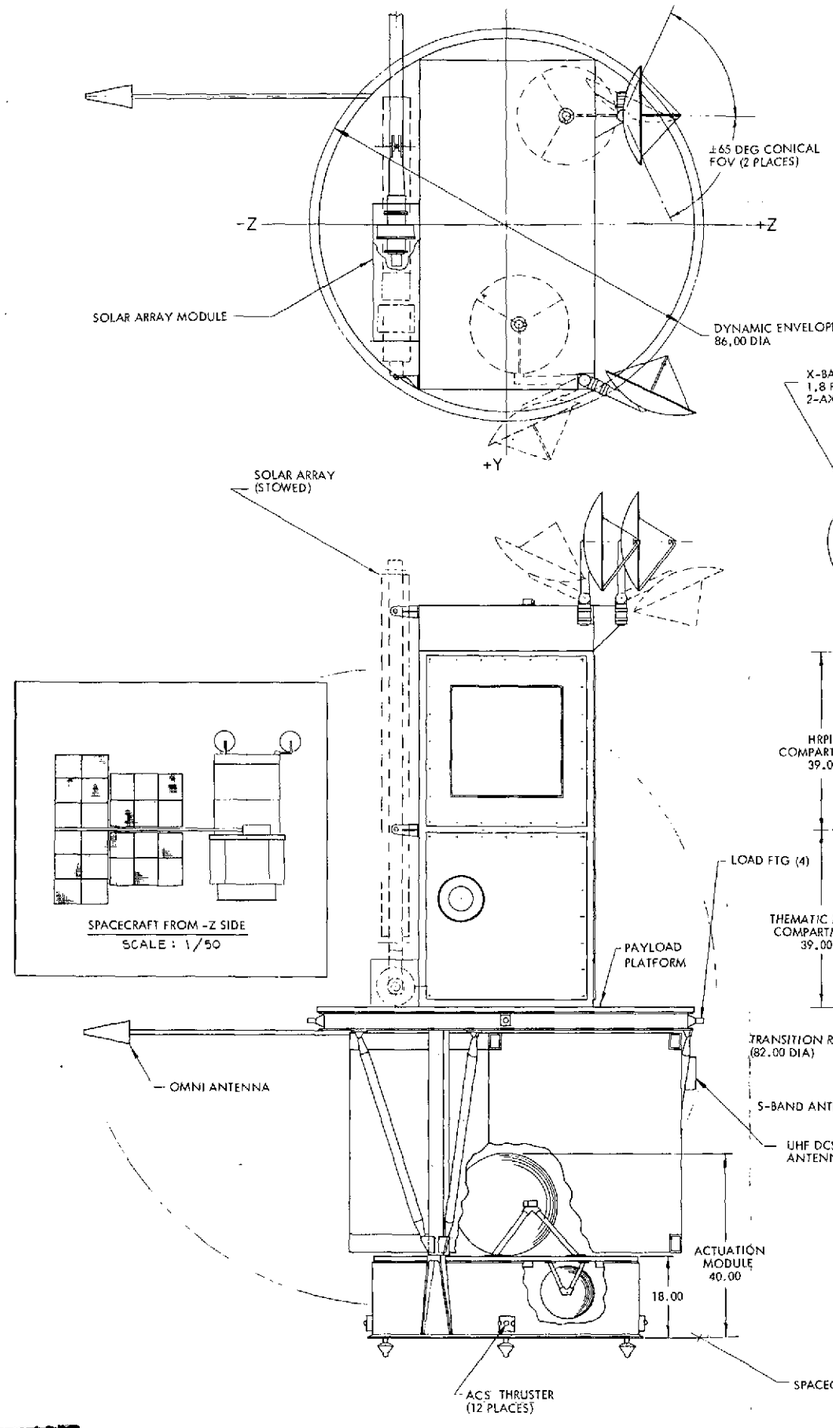

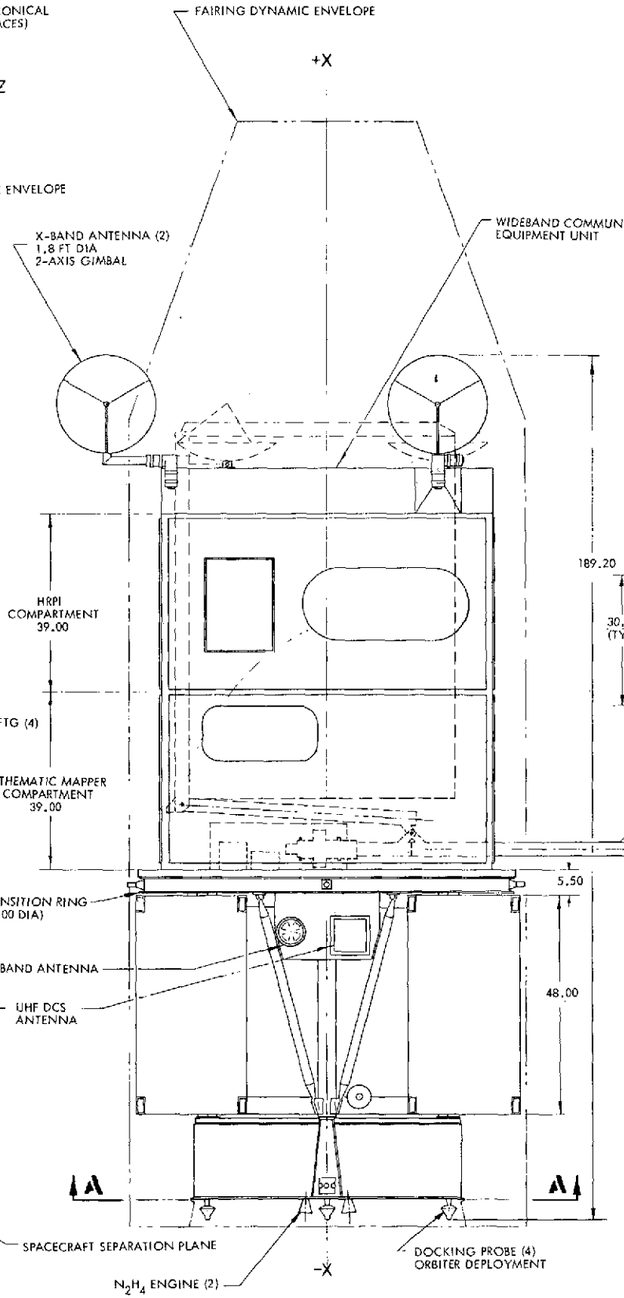

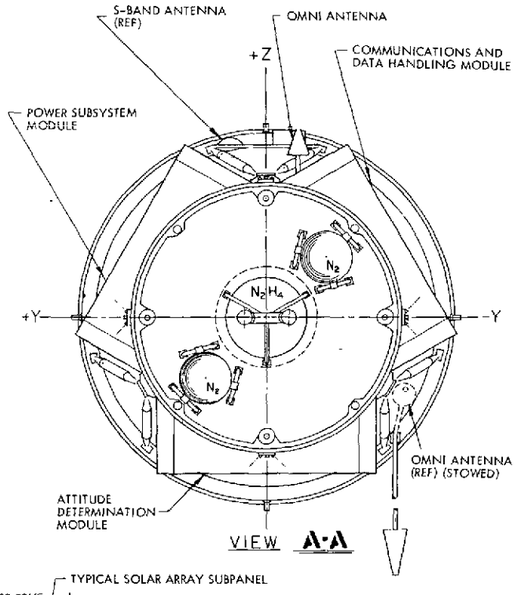

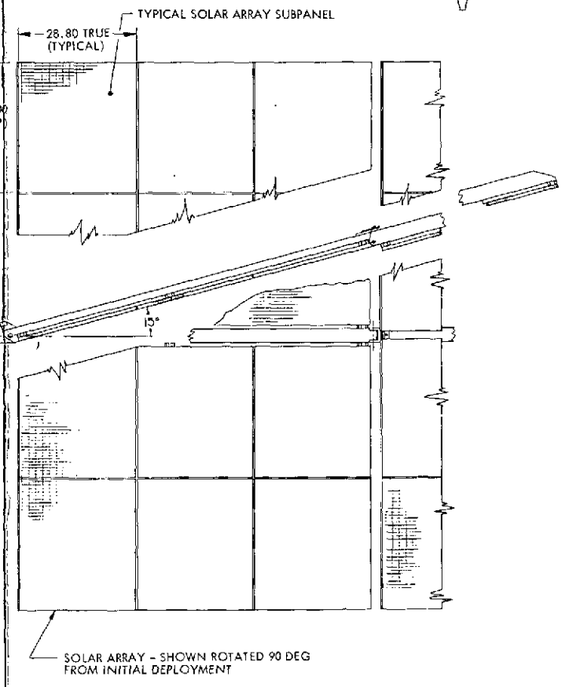

Figure 4-1. Baseline Thor-Delta EOS

4.1.3 Payload Accommodation

The EOS-A baseline observatory payload consists of the:

- Thematic mapper
- High resolution pointable imager
- Wideband communication system
- Data collection system.

The two payload sensors, thematic mapper and HRPI, are multi-spectral imaging scanners with very high resolution and pointing requirements, as described in Section 5. In considering this, the philosophy developed for mounting the instruments enables maintenance of a stable instrument alignment to the attitude determination module. Fixed biases in alignment will be removed by pre-operation calibration. Thus, the latch mechanisms (special-purpose manipulator system (SPMS), and spacecraft structure are relieved of predictable and repeatable absolute alignment on the order of arc-seconds. Once latched and thermally normalized, however, the coordinates must remain stable throughout the orbit.

The thematic mapper will be mounted nearest the attitude determination module since it has the more stringent alignment requirements due to cartographic applications, despite its lower resolution. It is also potentially the heavier of the two instruments.

For our baseline observatories, any of the potential candidate sensor configurations (Section 5) can be accommodated as long as the major axis of its envelope is mounted transversely to the EOS velocity vector. Alternate configurations, with the major axis longitudinal, could be accommodated but require a significant alteration of the spacecraft structure and design philosophy.

4.1.4 Mechanical Design Features

All of the payload modules are installed drawer-fashion into the structure and secured at the anti-earth side. The thematic mapper installation, particularly in a refurbishable version of EOS, is somewhat more

complex owing to its radiative cooler for infrared channels. In order to afford the cooler a clear view of the night sky, a jog to the side during insertion will be required of SPMS prior to latching. This is within the stated capability of the SPMS.

In configuring the wideband communications module with its articulated antennas, an arrangement has been developed which alleviates the requirement for deployment on a hinged boom as originally envisioned. The biaxial pointing drive will have the capability of deploying and retracting the antennas to and from a stowed position without hampering the 65-degree half-cone angle view of each antenna. The elimination of the hinge and its associated waveguide flexure is a significant savings in cost, complexity, and weight. During launch, pyrotechnic devices will secure the antenna appendages to the wideband communication module, relieving the pointing drives from torsional loading. For Shuttle retrieval, a mechanical fastener, similar to commercially available over-center pin pullers, will be used to secure the antennas during entry. The task of operating these retention devices will be the responsibility of the Shuttle-attached manipulator system (SAMS). Other options such as EOS incorporated electromechanical means for operating retention devices for this and other appendages are less attractive due to increased complexity, weight, and cost.

Solar array and omni antenna retention will be accomplished in a similar manner: pyro release for initial deployment and SAMS-actuated mechanical fasteners for Shuttle retrieval. Array deployment will be spring initiated to a positive catch upon removal of the launch restraints. For retraction during Shuttle module exchange operations or retrieval, SAMS will disable the catch and restow the array in its folded position. For EOS retrieval, particularly a Delta version with its more complex folding sequence, it may be more cost-effective to have SAMS jettison the array by pulling a pin at the boom hinge. This decision will be made as the cost of SAMS utilization is established during its development. Again, the philosophy is to keep the spacecraft associated mechanisms simple and to use the versatility of the SAMS manipulator and its human operator.

4.1.5 Alternate Configurations

Two alternate observatory configurations are presented: a four-sided Thor-Delta design, and application of the baseline Thor-Delta design for Titan or Shuttle launch.

4.1.5.1 Four-Sided Thor-Delta

Figure 4-3 shows an EOS-A similar to the four-sided Titan baseline design. The Delta fairing dynamic envelope of 86 inches limits the standard spacecraft modules to 43 x 43 x 14 inches, compared to the 48 x 48 x 18 inch dimensions of the baseline configurations. The actuation module has been divided into two modules: 1) an attitude control module containing the momentum wheels and magnetic torquers in a standard module framework, and 2) an aft-mounted propulsion module containing the hydrazine and nitrogen systems, using the volume within the spacecraft structure.

In the figure, the transition ring is replaced by a three-point support at the station of the transition ring for Shuttle support. Such a design provides a stiffer observatory because the basic bending structure has a larger footprint and the four longerons provide a larger bending modulus, compared to the three-longeron baseline Thor-Delta design. As a result, the spacecraft structure will be slightly lighter than the baseline and provide more growth for hydrazine volume. The interface with the Delta launch vehicle will be simpler because the transition from the circular Delta interface to the four longerons will be easier compared to the three in the baseline.

It is not apparent, however, that the lighter structure will balance the weight of the additional module structure required compared to the Thor-Delta baseline. The smaller modules appear adequate to accommodate the minimum redundancy subsystem equipment complement as presently defined, but do provide less growth capability. Care would have to be taken in configuring the attitude determination module because of the depth of the star trackers and their sun shades; they would have to be allowed to penetrate the inboard surface of the module. Similarly, one magnetic torquer would have to penetrate the attitude control module in order to accommodate a long enough torquer.

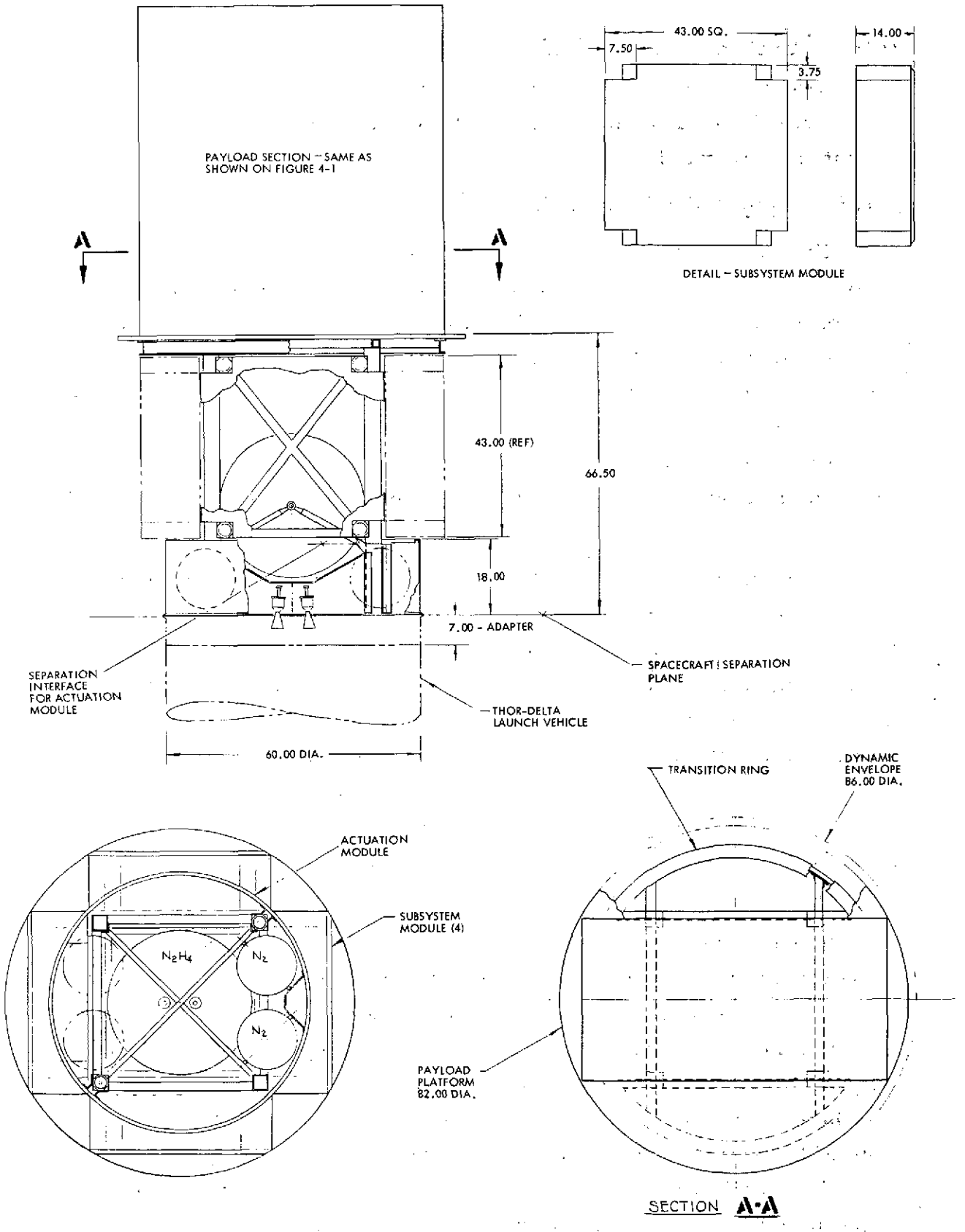

Figure 4-3. Thor-Delta EOS-A Alternate Concept

Because of these disadvantages, this configuration is less favored than the baseline.

4.1.5.2 Thor-Delta Configuration for Titan or Shuttle Launch

The Thor-Delta spacecraft can be adapted for Titan or Shuttle launch by supporting the observatory at the transition ring (Figure 4-4).

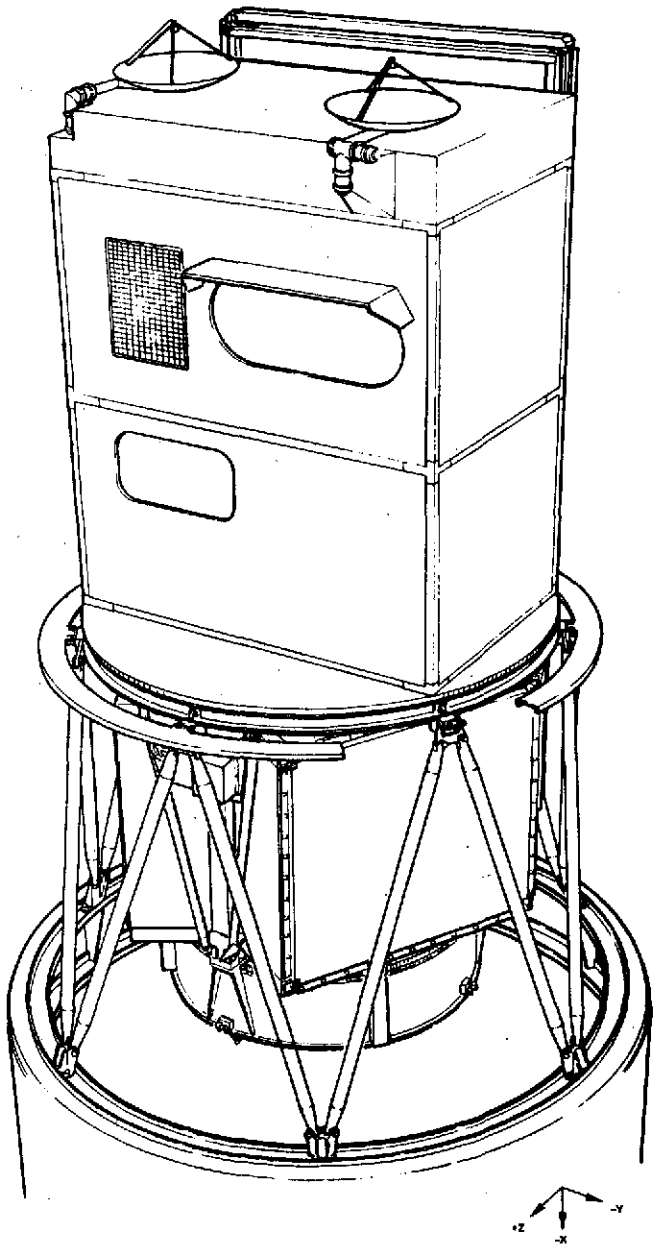

Figure 4-4.
Delta Configuration for Titan Launch

The baseline Thor-Delta design has both a transition ring and an aft adapter. The transition ring is used to support the observatory during Shuttle retrieval while the aft adapter supports the loads during Thor-Delta launch.

The concept of the aft adapter and the transition ring gives a favorable weight trade-off. This additional increase in allowable launch vehicle payload can support a heavier instrument payload or a larger hydrazine complement for later mission orbit adjust requirements.

A transition ring adapter to support the observatory at its transition ring during Titan launches would have to be developed. It would support the observatory at the 82-inch diameter transition and be attached to the Titan.

4.2 EOS-A ELECTRICAL DESIGN

The electrical system block diagram for the minimum and nominal redundancy* EOS-A configurations are shown in Figures 4-5 and 4-6. These designs are discussed in detail in Section 6 and the tradeoffs which led to their selection are in Appendix A. Summarized below are some of the salient features of these designs:

- Wideband Communications. Two 24-inch parabolic antennas point simultaneously to two ground stations: NASA ground station and the LCGS. Pointing is accomplished with a stepper motor gimbal drive under control of the computer. The 240 Mbit/sec wideband data to the NASA ground station is edited by the speed buffer electronics to 20 Mbit/sec for the LCGS. Transmission takes place at X-band by means of 0. 5-watt transmitters.

- Communications and Data Handling. The communications and data handling module provides the command and telemetry communication link between the spacecraft and the ground control station. The module contains the on-board computer which for mats telemetry, stores commands, and backside telemetry data, assists in power and thermal control, and provides computational capability for the ACS and experiments as needed. The on-board computer works in conjunction with a data bus controller which provides the data bus interface with all other modules and also contains independent telemetry formatting capability.

  Polarization diversity is used with two omni antennas, each mounted on appropriate ends of the spacecraft. Transmitter antenna selection is achieved with a commandable RF switch. Both antenna signals are combined in a hybrid for the receiver.

- Solar Array and Drive. Separate module allows replacement as a complete assembly. Multiple slip rings provide low loss power transfer. Array folding mechanism allows array to be stowed for resupply operation.

- Electrical Power. A low impedance bus is established with batteries tied to the main feeder bus. Diode box isolates batteries for parallel connection. Two battery assemblies contain three batteries. Power disconnects controlled by Shuttle throughline.

- Attitude Determination. Contains only mission nonpeculiar ACS equipment applicable to range of missions without modification. Standby redundant precision sensors (FST, IRU).

*Section 4.4 describes redundancy configurations condidered for cost tradeoffs

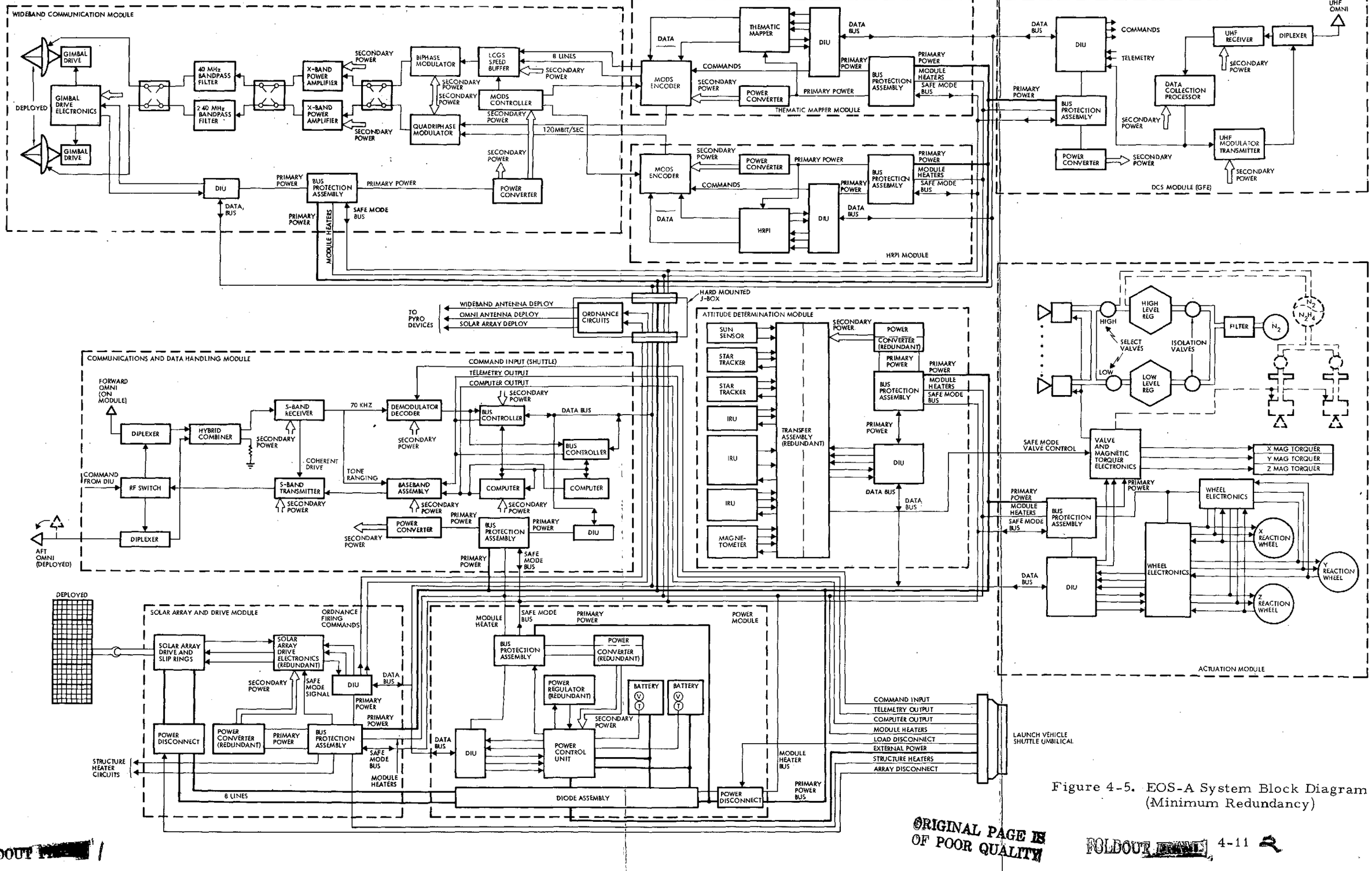

Figure 4-5. EOS-A System Block Diagram (Minimum Redundancy)

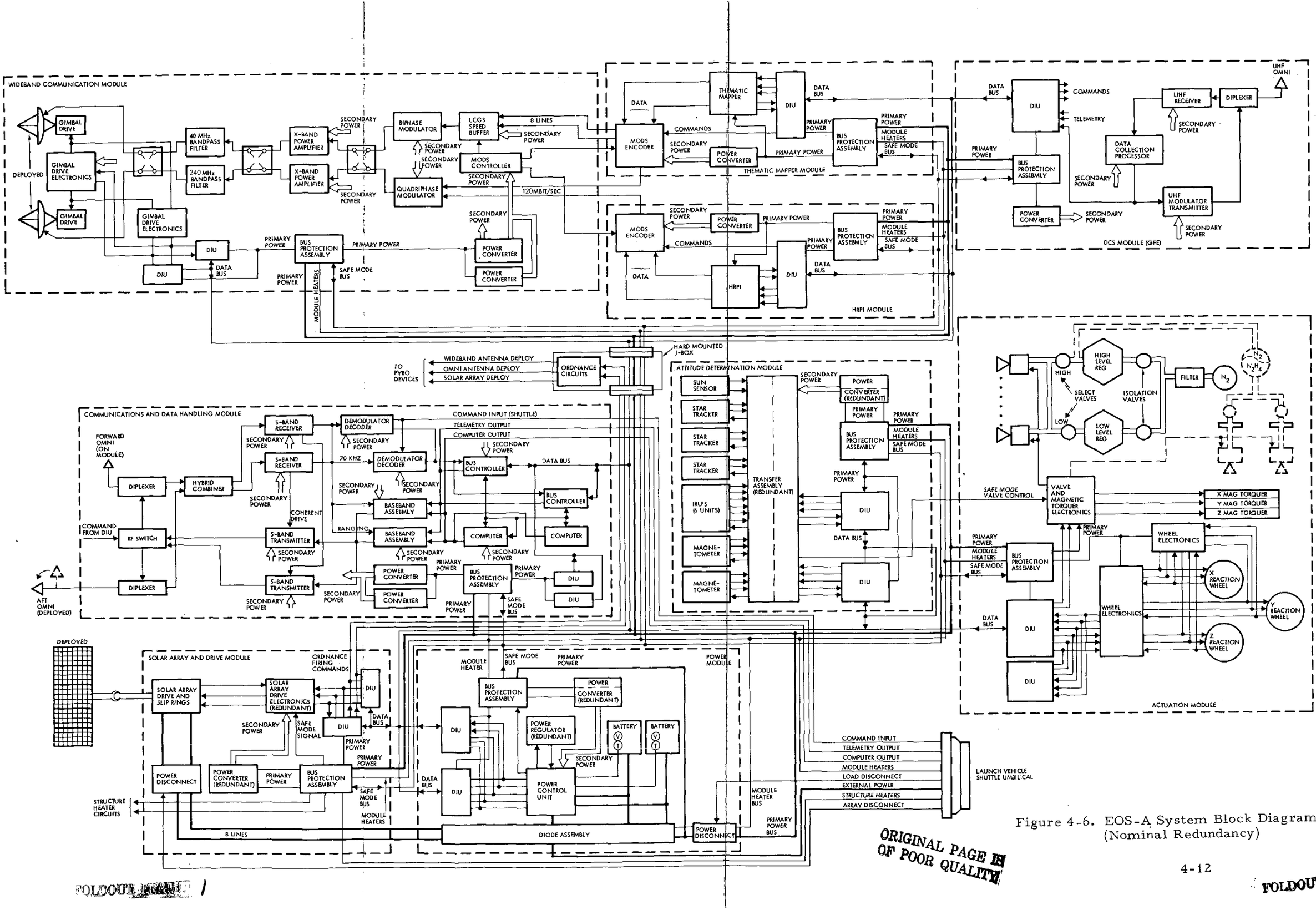

Figure 4-6. EOS-A System Block Diagram (Nominal Redundancy)

- Actuation. Contains all mission-peculiar ACS equipment: reaction wheels, magnetic torquers, pneumatic thrusters selected from standard inventory according to spacecraft characteristics. Functional redundancy employed.

- Data Collection System. The data collection system equipment is contained in the data collection system module and is NASA government-furnished equipment.

- High Resolution Pointing Instrument. The HRPI views a swath 48 km wide with a 10-meter resolution. Pointing capability is up to 30 degrees on either side of nadir. Data is reformatted for X-band transmission. Performs visible and near-visible earth observations.

- Thematic Mappers. The thematic mapper views a swath 185 km wide with a 30-meter resolution. It contains one thermal infrared band. Data is reformatted prior to transmission by X-band links.

4.3 PERFORMANCE REQUIREMENTS AND ALLOCATIONS

Performance requirements have been evaluated and allocated to the various sources of payload pointing error. Emphasis has been given to analysis of the EOS-A system output quality requirements. However, alternate and future missions have also been considered to provide maximum growth and commonality potential. See Appendix A for detailed analysis.

For EOS-A the geometric impact of each error source upon in-track and cross-track errors in locating ground points from the spacecraft has been analyzed. This directly influences the low-cost ground station user. The improvement in performance that results from the use of registration control points whose geodetic location is known was then assessed. This in indicative of the accuracy available to the central data processing facility user, whose ground-based optimal filter essentially removed the predominant source errors.

These results have been used to derive requirement upon the various error contributions:

- Attitude control
- Attitude determination (inertial)

- Ephemeris estimation
- Structural/thermal deformation
- Payload parameters

Both earth-pointing and other missions have been considered, dealing with several representative operational modes.

4.3.1 Mission Operational Modes

4.3.1.1 Earth Pointing

This mode receives primary attention as it is the basic mode for EOS-A with a clear definition of its payload sensors. These sensors comprise a thematic mapper (TM) and a high resolution pointable imager (HRPI). The former has the more stringent geometric/geodetic accuracy requirements due to its use in cartography; hence the TM is assumed to be the requirement driver for EOS-A. The TM points nominally along the spacecraft yaw axis when its scan angle is zero, and sweeps about an axis colinear with the spacecraft roll axis. Each TM image consists of approximately 50 million pixels. Geodetic accuracy denotes the degree to which the TM image can be located upon the surface of the earth. Important to cartographers, a 1 pixel accuracy (30 m, 1σ) is desirable. More stringent is the required geometric accuracy, namely the fidelity or distortion free characteristic of each image. In order to accurately note changes in comparable scenes imaged at different times (e.g., 17 days), a 1σ error less than 1/4 pixel, or 7.5 m, is the goal.

Data from both the TM and the HRPI is telemetered via a wideband communications system to a central data processing facility (CDPF). The primary burden placed upon the CDPF concerns the formation of a "continuous" radiometric image given the 38 million discrete samples. Additionally, the CDPF removes any causal geometric/geodetic effects of significance (e.g., skew caused by earth rotation). To aid in improving its image fidelity, the CDPF makes use of the known locations of 10 or so imaged points per pass. These registration control points (RCP) are assumed uncorrelated and known to 30 m (1σ). Since this accuracy far exceeds that which a spacecraft fixed observer could predict, such points

actually aid in calibrating spacecraft error sources. Once calibrated, the geometric/geodetic accuracy of every pixel can be vastly improved. This improvement depends upon the number and location of the RCP's chosen. For error analysis, it is assumed that ground control points are established at a variety of TM scan angles, and separated in time by no more than 2 minutes. In fact, the first three such points will be assumed about 10 seconds apart so that the predominant bias errors can be removed early in the data-taking pass.

Besides the CDPF, there are other downlink processors of the TM and HRPI radiometric data. These low-cost ground stations (LCGS) perform neither radiometric nor geometric/geodetic corrections. Pictures are formed from the data in an "as received" condition. For many applications, there may be sufficient accuracy to warrant the cost savings and flexibility (e.g., mobile) of LCGS units. For more exacting needs, the CDPF is always available. One assumption regarding the LCGS will be made, however: it is assumed that ground points in two comparable 185 x 185 km scenes can be visually established in order to fix four "almost constant" error sources which largely dominate the geometric/geodetic accuracy.

4.3.1.2 Stellar Inertial

The normal stellar inertial mode uses the same gyro package and star tracker used for the earth-pointing mode. Here it becomes particularly important that the spacecraft exhibit a repeatable attitude in order to observe the emission of very dim stars. Since stellar payloads and the accuracy of their information have not been defined, the required attitude control performance in this mode will be assumed given by the GSFC/NASA values presented in the RFP. It is probable that the basic modular attitude determination system would be used in a "target acquisition" mode with a fine error sensor for precise pointing (see below).

4.3.1.3 Sun Pointing

In a sun pointing mission, it is likely that the star trackers would be removed from the attitude determination module in favor of an accurate sun sensor in order to effect a cost savings. However, no major

change in the accuracy requirement is anticipated. During sunlit times the pointing accuracy in each axis will still be 0.01 deg (1σ), with the stability requirements of the RFP holding during eclipse intervals.

4.3.1.4 Stellar Inertial Mode with Ideal Sensors

In some future missions, it is anticipated that spacecraft attitude information will be derived from the payload itself, with spacecraft sensors for acquisition. Such an attitude reference would, of course, be very accurate, and any significant spacecraft attitude errors would only be the result of non-ideal control system components. The GSFC/NASA specification of the EOS Study RFP cites allowable errors attributed to the control system in such applications; these are repeated at the close of this section.

4.3.2 Error Allocation Groundrules and Approach

In developing a detailed allocation of errors with EOS-A in the baseline mission, several groundrules and observations have been considered, as summarized below:

a) The TM is the primary payload in defining absolute and relative pointing requirements.

b) Known static alignment errors can be compensated in control loops by bias commands to give accuracy TM pointing. Total static errors are observable.

c) Static alignment errors are not critical; alignment should be stable over reasonable period

- Space servicing will be followed by (explicit or implicit) calibration.
- Misalignment of HRPI relative to TM will not be compensated by control offset biases (but will be observable using RCP's in HRPI images).

d) The relative shift of the same ground point over a 17-day period is 5 m (1σ).* This is undoubtedly a conservative estimate for most ground points, but is adequate for our purposes here.

*For example, due to seismic effects.

e) The computational effort required by the software in order to correlate the same ground point on two images depends heavily upon the anticipated size of the search region. It will be assumed that this region is governed by the fact that the anticipated initial in-track and cross-track relative location is 300 m (1σ).

f) Ground software memory requirements are adversely affected by nonorthogonality of the TM scan trace. Estimation errors in spacecraft attitude yaw and ephemeris rates govern the degree of this orthogonality, and it is assumed that 0.01 deg (1σ) "effective" yaw estimation error is acceptable.

In order to develop error allocations, the geometry defining the effect of the various contributors upon TM line-of-sight interaction with the earth's surface was derived. This error model was employed, with a representation of the software by which RCP's are used for error correction (a Kalman filter), to evolve a computer program which rapidly conducts vigorous covariance analyses. The details of these models and the error allocation approach (which includes judgmental factors) are presented in Appendix A.

4.3.3 Error Terms and Allocations

4.3.3.1 Definition of Error Terms

Given the general error signal $\theta(t)$ defined on $0 \leq t \leq T$, the following basic error terms are defined.

a) Bias

$$\theta(0)$$

b) Drift Rate

Define the drift rate, b, to satisfy

$$\int_0^T \left[\theta(t) - \theta(0) - bt\right] dt = 0$$

for T very large. Then

$$b = \frac{1}{T^2} \int_0^T \left[\theta(t) - \theta(0)\right] dt$$

c) Drift Rate Deviation

For $0 \leq T_1 < T_2 \leq T$, define the apparent drift rate as

$$c(T_1, T_2) = \frac{2}{(T_2 - T_1)^2} \int_{T_1}^{T_2} \left[\theta(t) - \theta(T_1)\right] dt$$

Then the drift rate deviation over $\left[T_1, T_2\right]$ is simply

$$\Delta c(T_1, T_2) = c(T_1, T_2) - b$$

While drift rate can be considered as a stationary effect, drift rate deviation arises due to noise sources in the system, and is thus a random variable. The CDPF Kalman filter can successfully calibrate drift rates, but is somewhat at the mercy of drift rate variations.

d) Jitter

$$\sigma_\beta(T_1, T_2) = \left\{ \frac{1}{T_2 - T_1} \int_{T_1}^{T_2} \left[\theta(t) - \theta(T_1) - c(t - T_1)\right]^2 dt \right\}^{1/2}$$

where the jitter can be thought of as "noise" relative to an attitude ramp defined by $\theta(T_1)$ and c.

4.3.3.2 Performance Specifications

Using these error representations, Tables 4-2 through 4-6 define the allocated performance.

Table 4-2. Attitude Estimation Specification*

	Earth Pointing		Stellar Inertial** or Sun Pointing (per axis)
	Roll, Pitch	Yaw	
Bias	15 arc-sec	25 arc-sec	0.05 arc-min
Drift	0.009 deg/hr	0.04 deg/hr	0.004 deg/hr over 1 hr
Drift rate deviation	0.005 deg/hr over 2 minutes	0.015 deg/hr over 2 minutes	0.004 deg/hr for 30 sec $\leq t \leq$ 1 hr
Jitter	0.30 arc-sec rms	1.0 arc-sec rms	2 arc-sec rms for times up to 1 hr

*Accuracy of estimate of attitude of star tracker mounting surface.

**GSFC/NASA RFP spec.

Table 4-3. Attitude Control Specification*

	Earth Pointing		Stellar Inertial** or Sun Pointing (per axis)	Stellar Inertial*** Using Experiment (per axis)
	Roll, Pitch	Yaw		
Bias	7.5 arc-sec	12.5 arc-sec	0.25 arc-min	0.01 arc-sec
Drift	0.005 deg/hr	0.02 deg/hr	0.002 deg/hr over 1 hr	Not applicable
Drift rate deviation	0.0025 deg/hr over 2 minutes	0.007 deg/hr over 2 minutes	0.002 deg/hr for 30 sec $\leq t \leq$ 1 hr	Not applicable
Jitter	0.15 arc-sec rms over 2 minutes	0.5 arc-sec rms over 2 minutes	1 arc-sec rms for times up to 1 hr	0.004 arc-sec rms for times up to 1 hr

*Refers to control using ideal sensors of star tracker mounting surface.
**GSFC/NASA RFP spec when separate attitude estimation module is used.
***GSFC/NASA RFP spec when the experiment becomes the attitude sensor.

Table 4-4. Ephemeris Specification* (Earth Pointing Mode - 1σ)

	Along Roll or Pitch Axes	Along Yaw Axis
Bias	120 m	900 m
Drift	0.15 m/sec	0.50 m/sec

*Accuracy of the ephemeris data used by the CDPF

Table 4-5. Thematic Mapper Scan Angle (1σ)

Bias	7 arc-sec
Jitter (e.g., nonlinearity)	0.45 arc-sec rms

Table 4-6. Thermal/Structural Specifications*

	Earth Pointing		Stellar Inertial/ Sun Pointing
	Roll, Pitch	Yaw	
Bias	30 arc-sec	30 arc-sec	0.25 arc-min
Drift	0.009 deg/hr	0.04 deg/hr	0.002 deg/hr
Jitter	0.3 arc-sec rms	1.0 arc-sec rms	1 arc sec rms

*Refers to error in the estimate of the attitude of the thematic mapper mounting surface relative to that of the star tracker. A fixed bias in yaw can be compensated by an attitude yaw command.

4.4 ACS OPERATIONS

The ACS function is to control the orientation of the EOS spacecraft during all phases of the mission subsequent to separation from the launch vehicle. The mission phases during which the ACS is required to operate include the following:

- Transfer orbit and injection into final orbit
- Sun acquisition
- Payload fine pointing (normal mode)
- Orbit velocity trim
- Orbit deboost
- Shuttle retrieval.

In addition, a safe mode is implemented to automatically reorient the spacecraft and solar array toward the sun for maximum sun illumination upon receipt of a signal indicating a low power condition.

The basic attitude reference for normal operation is a precision three-axis strapdown inertial reference unit capable of providing the high degree of attitude stability required for the broad spectrum of EOS missions. The inertial reference unit gyroscopes provide a measure of spacecraft attitude and rate. The gyro data is periodically updated by a pair of body-fixed star trackers which yield a measure of absolute inertial attitude. The star trackers are mounted to the spacecraft in a skewed position with their fields of view oriented to the anti-sun side of the orbit plane. Ephemeris data from an on-board ephemeris model (updated periodically from the ground) are used to transfer the inertial attitude data measurements into an earth-referenced coordinate system to develop attitude control data for earth pointing missions.

Attitude control torques for fine pointing control during normal operation are obtained from a set of three orthogonal body-fixed reaction wheels. Wheel momentum saturation is prevented by the use of a set of three orthogonal electromagnetic torquers which interact with the earth's magnetic field to create control torques on the spacecraft. High level cold gas thrusters provide control tor ues during other modes of

operation such as acquisition and orbit velocity engine firing which entail relatively rapid reorientation and/or large disturbance torques. These thrusters can also be operated in a low level mode.

Except for the safe mode and direct control via the payload, all control laws and other computational functions related to the attitude and orbit control are implemented by the on-board computer within the communications and data handling module. The on-board computer processes signals from the attitude sensors (gyros, star trackers, etc.) and generates commands for the attitude control torquers (reaction wheels, magnets, thrusters) so as to achieve the desired spacecraft orientation.

4.4.1 Attitude Control Modes and Sequence of Events

A number of control modes are necessary to establish the normal fine pointing operation condition and to ensure the long-term integrity of the spacecraft. The specific sequence of events and associated control modes are booster and mission peculiar. However, the attitude control system modular design incorporates the flexibility to be easily adaptable to the broad spectrum of EOS mission consideration. A general sequence of events and control modes are shown in Figure 4-7.

The general implementation of the attitude control modes and relationship to the sequence of events is discussed in the following paragraphs.

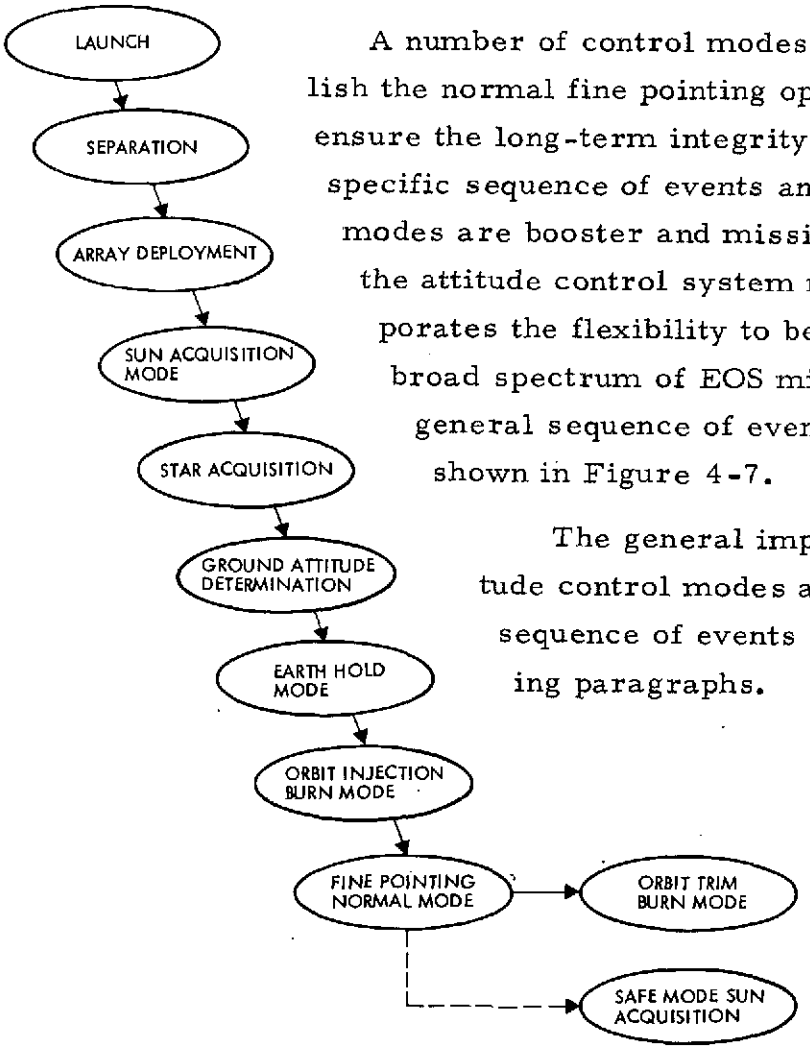

Figure 4-7
Generic Sequence of Events and Attitude Control Modes

4.4.1.1 Launch, Separation, and Array Deployment

During the launch and boost phase of the mission, the only attitude control equipment energized are the gyro spin motors. It is considered desirable to have the gyro spin motors running at this time in order to protect the bearings against vibration-induced damage.

Subsequent to separation of the spacecraft from the booster, an on-board timer initiates array deployment and the sun acquisition mode. The array is deployed and caged with the array plane parallel to the X (roll) spacecraft axis.

4.4.1.2 Sun Acquisition (Figure 4-8)

The purpose of the sun acquisition mode is to reorient the spacecraft to align the -Z axis with the sun for maximum solar array power and a benign thermal condition. Initiation of the sun acquisition mode applies power to the attitude control equipment. The pointing reference is a sun sensor with 2π steradian field-of-view. The gyros are used to control the spacecraft angular rate and null the initial rates at separation. The on-board computer processes sun sensor and gyro data to generate the thruster firing signals required to achieve the desired orientation with respect to the sun. Control logic initiates a preset attitude rate to search for the sun to accommodate the case where the sun is initially outside the sun sensor field-of-view. During eclipse the attitude is held constant under gyro reference control.

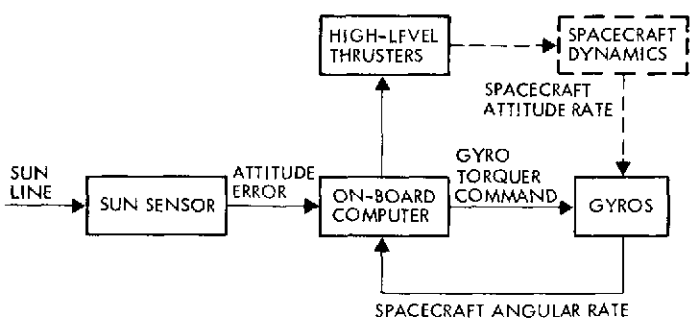

Figure 4-8. Sun Acquisition Mode

4.4.1.3 Star Acquisition and Ground Attitude Determination (Figure 4-9)

Subsequent to sun acquisition, the spacecraft will be reoriented to the proper attitude for orbit injection engine burn (if required). Knowledge of spacecraft attitude is required in order to generate the ground commands for this reorientation. Attitude determination on the ground uses telemetered star position information from the body-fixed star trackers

in conjunction with telemetered data from a triaxial magnetometer which senses spacecraft attitude with respect to the earth's magnetic field. If necessary, a commanded search rate around the sun line can be used to introduce stars into the star tracker's limited field of view. After star tracker acquisition, the spacecraft attitude rate around the sun line is nulled by gyro control.

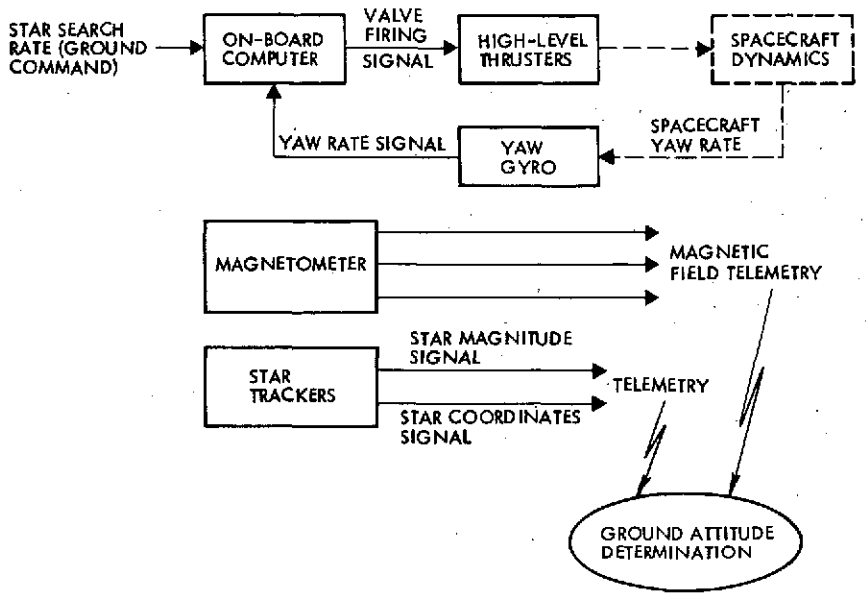

Figure 4-9. Star Acquisition and Attitude Determination

4.4.1.4 Earth Hold (Figure 4-10)

The earth hold mode reorients the yaw axis (+Z) to point at the earth prior to firing of the orbit injection engine. Orientation around the yaw axis is controlled to align the orbit injection engine into the orbit plane. This attitude is held under gyro control in response to pitch, roll, and yaw attitude ground commands derived from the ground computation of spacecraft attitude as described in the previous section. The solar array drive mechanism continuously rotates in response to on-board computer commands so as to maintain the array pointed toward the sun.

4.4.1.5 Orbit Injection/Trim Burn (Figure 4-11)

At the proper point in orbit a ground command is transmitted to initiate the orbit injection engine burn. The spacecraft attitude is held

fixed at the desired orientation by means of the high level thrusters and the gyro reference. During subsequent orbit trim burns, the spacecraft attitude is controlled in the same manner.

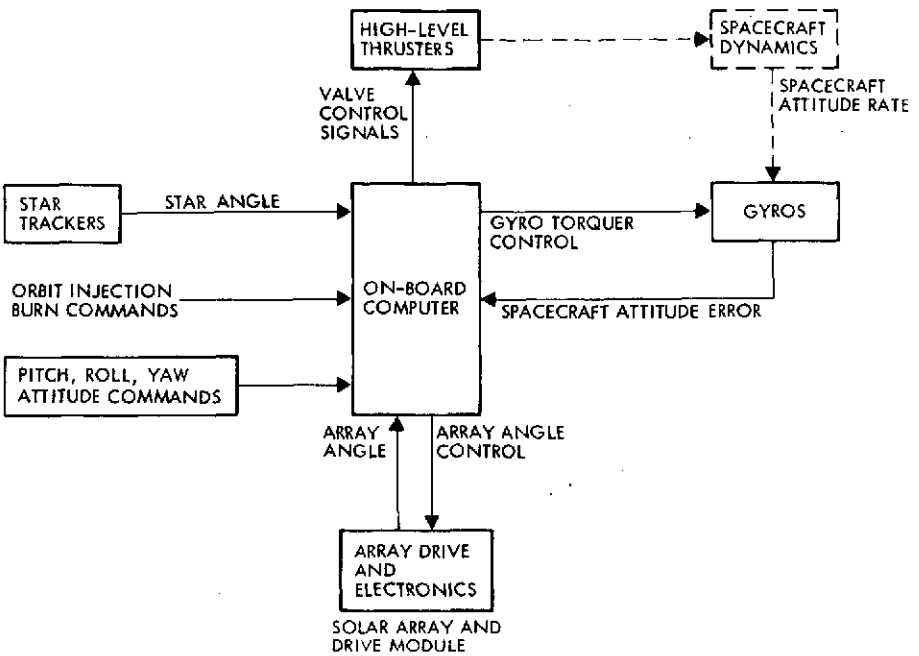

Figure 4-10. Earth Hold Mode

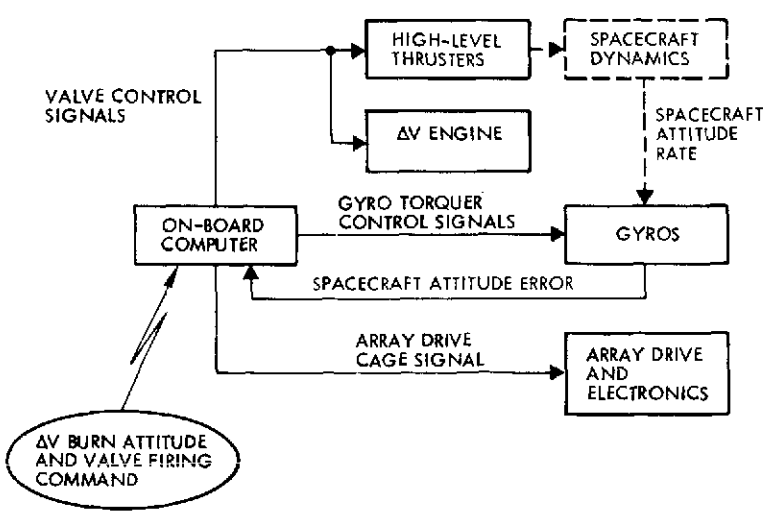

Figure 4-11. Orbit Injection/Trim Mode

4.4.1.6 Normal Mode (Figure 4-12)

Normal mode provides the long-term accurate pointing as dictated by payload requirements. Specific missions may require earth, stellar inertial, or sun pointing. The normal mode attitude reference is a body fixed rate integrating gyro and body-fixed star trackers for periodic update and correction of gyro drift. Three orthogonal reaction wheels provide the basic control torques. Three orthogonal magnetic torquers provide the means for momentum unloading of the reaction wheels. The on-board computer implements the attitude control laws. A triaxial magnetometer provides a measurement of the earth's magnetic field components as an input to the computation of magnetic torquer control signals. The on-board computer incorporates ephemeris, star catalog, and attitude programs which are employed in the attitude control algorithms. These are updated as required by ground command.

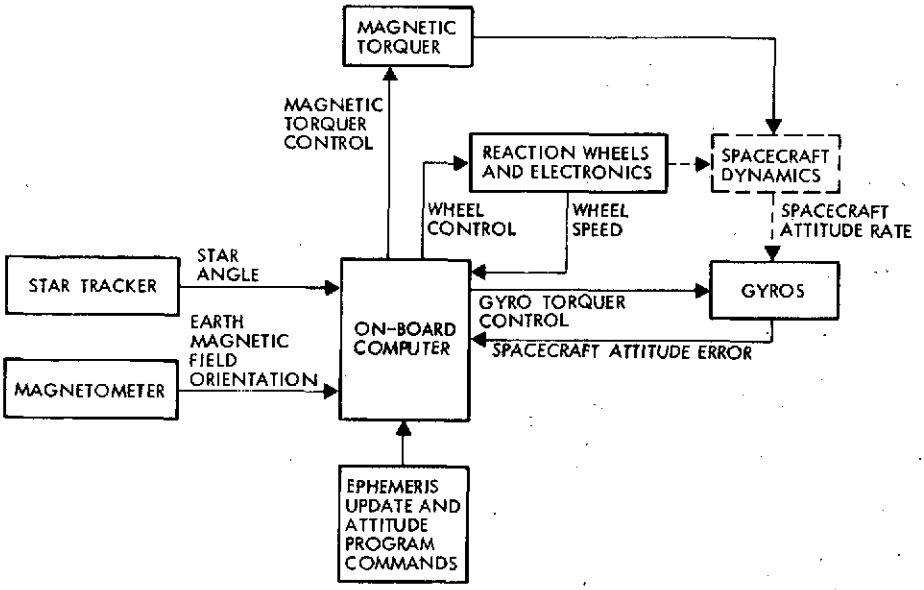

Figure 4-12. Normal Mode

4.4.1.7 Safe Mode (Figure 4-13)

A backup failure mode is provided which automatically orients the spacecraft for maximum sun illumination of the solar array. This mode is initiated by an on-board signal indicating an unsafe low power condition generated within the electric power module and distributed via the safe

bus. During the safe mode the array drive is rotated to the position with the array surface parallel to the spacecraft roll axis and the spacecraft is reoriented to point the -Z axis at the sun. Attitude control is by means of the sun sensor and the low level thrusters. Special-purpose safe mode attitude control electronics replace the on-board computer for attitude control and the gyros, reaction wheels, and magnetic torquers are disabled.

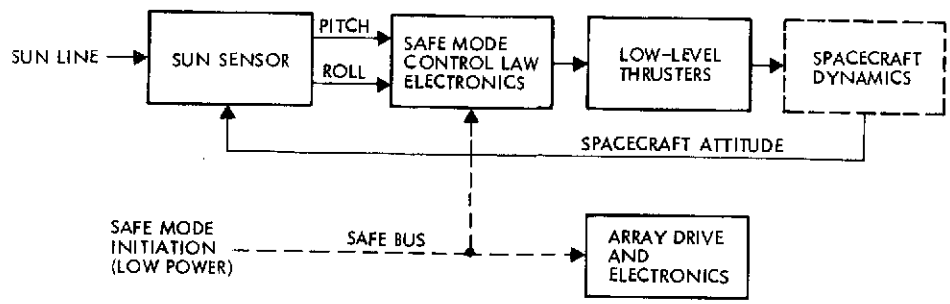

Figure 4-13. Safe Mode

The safe mode provides a benign power and thermal regime which can be held for a long period of time during which the ground can provide failure diagnosis and corrective action, wither via redundant hardware activation or Shuttle servicing. Return from the safe mode to normal control will be command initiated.

4.5. REDUNDANCY AND RELIABILITY

The degree of redundancy (or reliability goals) selected for an EOS-based spacecraft will be based ultimately on the mission objectives and scenario. Satellites intended as research and development tools will be subject to a set of system design criteria which may differ markedly from those for operational satellites. A spacecraft flown prior to the availability of Shuttle resupply/retrieval capability may be given a different level of redundancy than that provided to a vehicle intended to be maintained.

These considerations have led to an EOS design which will accommodate varying degrees of redundancy, selectable in accordance with mission objectives. Key design features making this goal feasible are:

- Implementation of redundancy at the unit/assembly level, rather than internal to black boxes
- Maintenance of appropriate electrical and mechanical interfaces (e.g., modular approach, data bus).
- Avoidance of volumetric constraints within modules, allowing ample redundancy growth capacity.

The level of redundancy chosen is mission-dependent. For a Shuttle-serviced EOS-A servicing costs must be traded off against spacecraft hardware costs. Four redundancy configurations have been defined for the spacecraft, ranging from the minimum level compatible with servicing to a more nominal level of redundancy with most elements of the spacecraft backed up by a standby unit. Table 4-7 characterizes these redundancy configurations. Figures 4-14 and 4-15 show reliability block diagrams for the Minimum and Nominal cases. Table 4-8 summarizes the reliability of those configurations by module. Note that only spacecraft modules (not payload elements) are addressed here. The degree of payload modularity will generally be dependent on the character of the payload elements.*

The basic (i.e., least expensive, lightest) configuration is the one with minimum redundancy for circular orbit servicing. Only the redundancy necessary to ensure against loss (i.e., unserviceability) of the spacecraft via a single failure has been provided. This low degree of replication is made feasible by the attitude control safe mode, which sun-points the spacecraft using hardware which is, for the most part, not employed during normal operation.

Increases in redundancy from the minimum level incur increases in spacecraft weight and cost, but with an accompanying lengthening of expected mission duration prior to failure. Table 4-8 shows normalized cost and incremental weight as a function of mean mission duration (MMD) for several values of design life, where the data are based on the four point designs of Table 4-7 (this MMD does not consider payload failures).

---

*For EOS-A, an R&D mission, the TM and HRPI will be nonredundant, while the wideband communication will have a degree of redundancy similar to that of the spacecraft modules. Operational satellites, however, may have redundant instruments.

Table 4-7. Redundancy Configurations

Configuration	Description	Redundant Equipment
Minimum	Redundancy necessary to assure no single-point failure preventing retrieval	• Power converters in attitude determination, electric power, and solar array and drive modules • Redundant array drive motor, electronics • Internally redundant power control/ regulation in electric power module
Variant 1	Least reliable elements made redundant; MTTF raised to about 18 months	• Redundancy of Minimum case • Redundant transfer assembly, star tracker, gyro in attitude determination module • Redundant on-board computer memory module • Redundant on-board computer central processor unit
Variant 2	Least reliable elements made redundant; MTTF raised to about 24 months	• Redundancy of Variant 1 • Redundant DIU, SCU in actuation module, attitude determination module, communication and data handling module, and electric power module • Redundant power converter in communication and data handling module • Redundant bus controller in communication and data handling module
Nominal	Most electronic assemblies made standby redundant; "typical" redundancy level for long-life satellites	• Redundancy of Variant 2 • Dodecahedron gyros (three in standby) • Redundant magnetometer • Redundant safe mode electronics • Redundant command receiver, telemetry transmitter, baseband assembly • Redundant DIU, SCU in solar array and drive module

Table 4-8. Properties of Redundancy Configurations

Redundancy Configuration	Mean Mission Duration (months)*					Normalized Cost	Incremental Weight (lb)
	T_D = 1 yr	T_D = 2 yr	T_D = 3 yr	T_D = 4 yr	T_D = 5 yr		
Minimum	6.7	8.5	8.9	9.1	9.1	1.00	0
Variant 1	9.5	14.7	17.2	18.3	18.8	1.07	55.8
Variant 2	10.5	17.7	22.0	24.3	25.5	1.11	75.8
Nominal	11.5	21.5	29.9	36.2	40.8	1.18	112.1

*T_D = Design life.

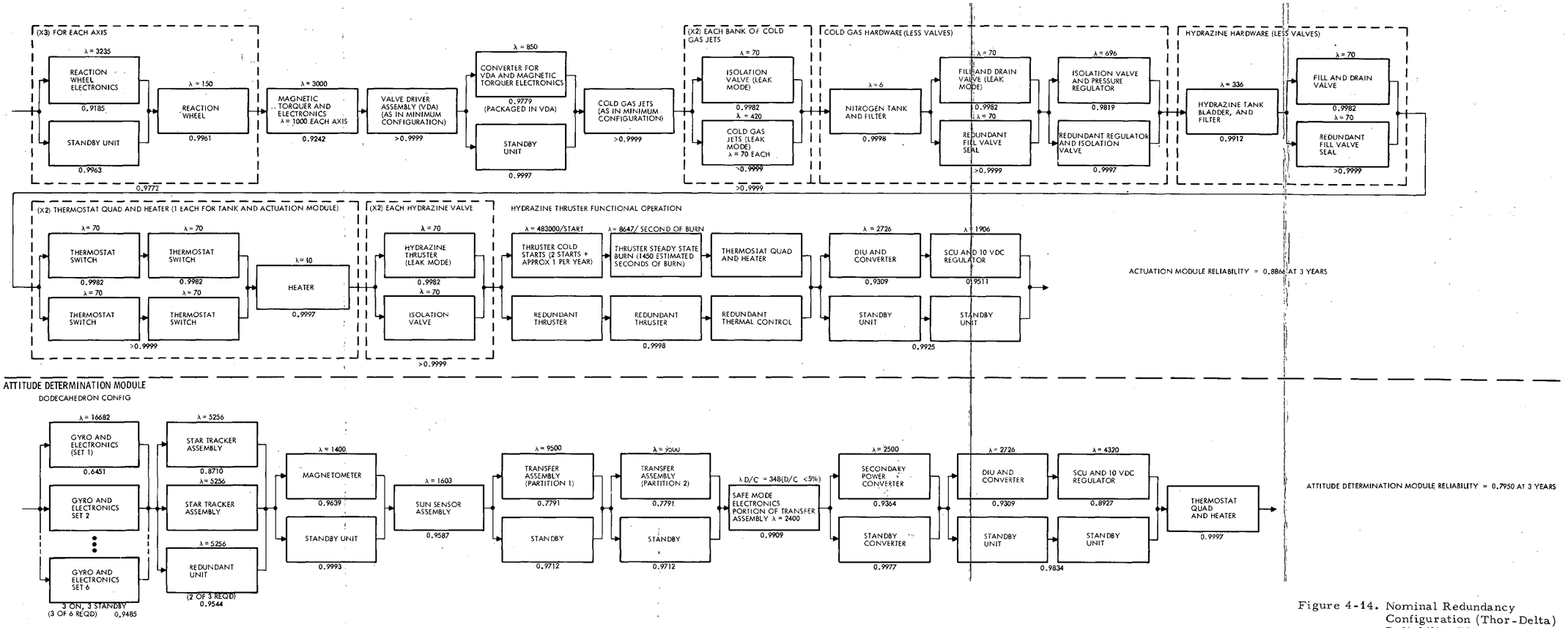

Figure 4-14. Nominal Redundancy Configuration (Thor-Delta) Reliability Block Diagram

FOLDOUT FRAME 1

FOLDOUT FRAME 2

FOLDOUT FRAME 3

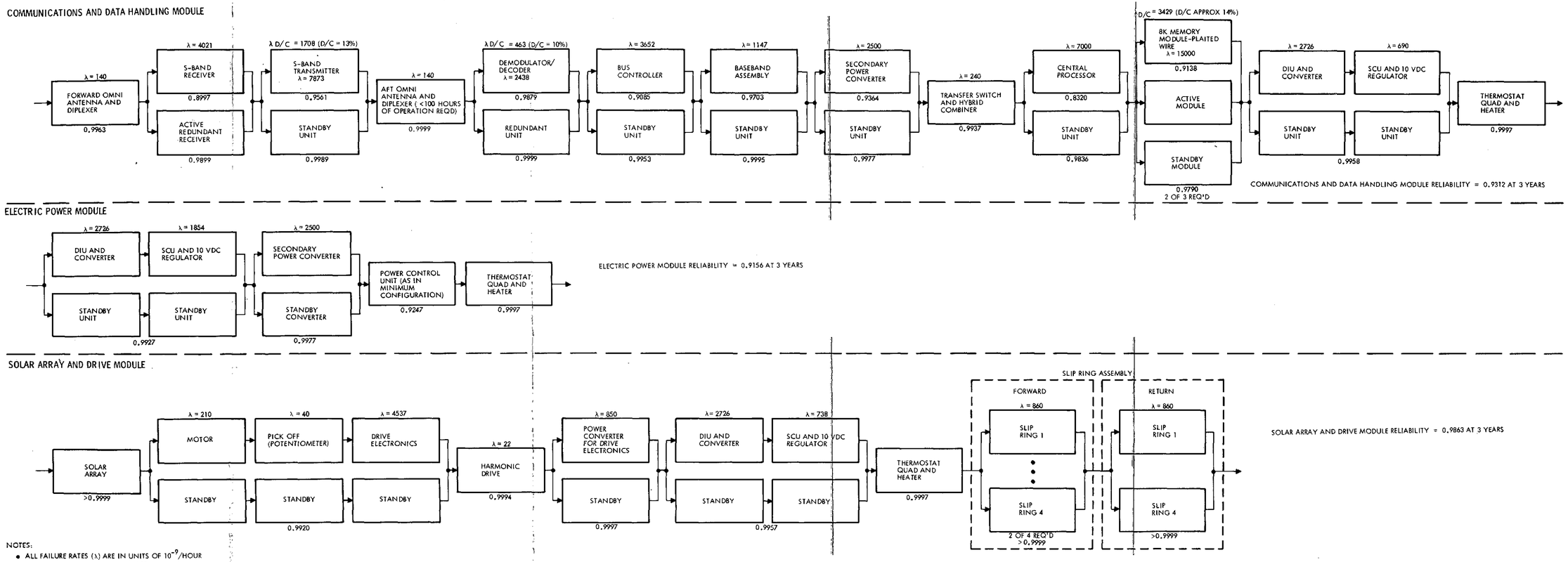

Figure 4-14. Nominal Redundancy Configuration (Thor-Delta) Reliability Block Diagram (continued)

FOLDOUT FRAME

FOLDOUT FRAME 2

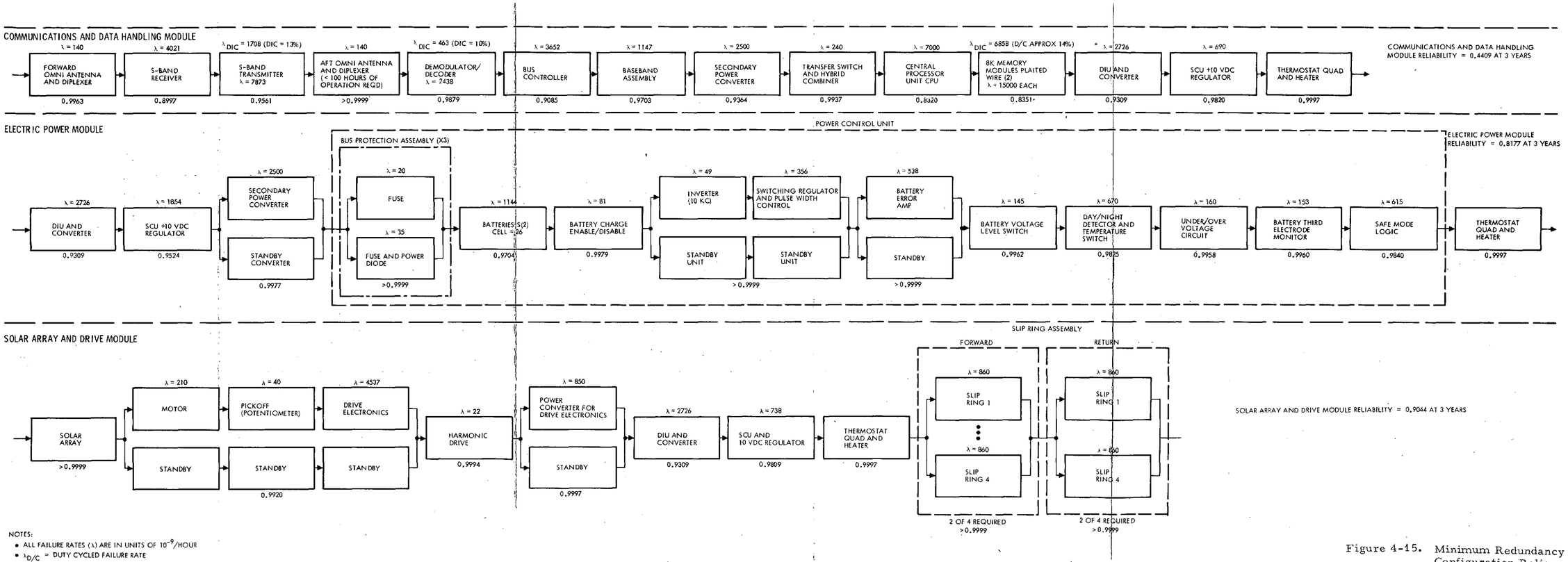

NOTES:

- ALL FAILURE RATES (λ) ARE IN UNITS OF 10^{-9}/HOUR
- $\lambda_{D/C}$ = DUTY CYCLED FAILURE RATE

SPACECRAFT RELIABILITY = 0.0187 AT 3 YEARS

Figure 4-15. Minimum Redundancy Configuration Reliability Block Diagram (continued)

FOLDOUT FRAME 1

FOLDOUT FRAME 2

FOLDOUT FRAME 3

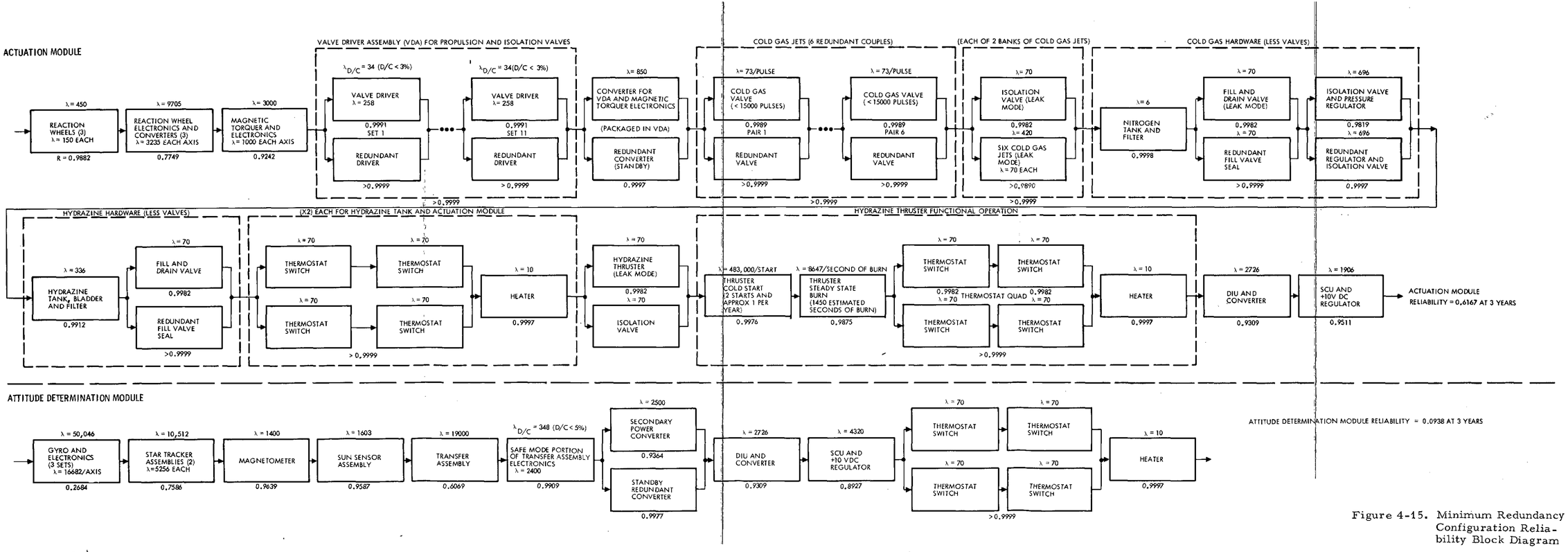

Figure 4-15. Minimum Redundancy Configuration Reliability Block Diagram

FOLDOUT FRAME 1

FOLDOUT FRAME 2

FOLDOUT FRAME 3

Note that for an infinite design life, MMD is identical to mean time to failure (MTTF); hence MMD can be employed in an analgous and more realistic manner in preliminary mission cycle costing analyses.

The baseline design life (established by considerations of degradation in array sizing) is 2 years. From the data presented it is apparent that design life values in the 2 to 3 year range are appropriate if MMD values in the 2-year region are desired for an operational mission. Use of low levels of redundancy will clearly lead to fairly frequent orbital servicing via Shuttle, as will too short a design life. Mission cycle cost tradeoffs, conducted in accordance with Shuttle application studies, will be reported in Study Report No. 6.

Reliability and MMD can be predicted for EOS-A by incorporating the payload reliability data. Using a 3-year design life leads to the following MMD values for EOS-A:

Redundancy	Spacecraft MMD	Observatory MMD
Minimum	8.9	8.2
Nominal	29.9	26.6

where the payload consists of a wideband communications and data handling module (with redundancy consistent with the spacecraft), a thematic mapper, and a HRPI.

4-6. OBSERVATORY MASS PROPERTIES

Mass properties estimates are presented in this section for the EOS-A baseline observatory systems as described in Section 4.1.

The baseline observatory weight summaries are presented in Table 4-9 for the Thor-Delta 2910 and 3910 configurations and in Table 4-10 for the Titan III-B (SSB) version. Detail weight breakdowns of the basic spacecraft elements are tabulated in Table 4-11. Observatory mass property characteristics (i.e., center of mass, moments and products of inertia estimates) for various in-orbit conditions are summarized in Table 4-12. Because of the large payload capability of the

Table 4-9. Thor-Delta EOS-A Observatory Weight Summary
(716 km Circular Sun-Synchronous Orbit)

Item	Launch Vehicle: Serviceability : Redundancy :	Weight (lb)			
		2910 Nonserviceable Minimum	2910 Nonserviceable Nominal	3910 Nonserviceable Minimum	3910 Nonserviceable Nominal
Spacecraft		1403	1512	1625	1734
Basic structure (including modules)		543	543	685	685
Electrical power		256	267	256	267
Electrical harness and connectors		61	61	61	61
Solar array and drive		146	150	146	150
Attitude determination		76	132	76	132
Actuation		58	74	94	110
Pneumatics (N_2)		57	57	57	57
Communication and data handling		41	63	41	63
Thermal control		78	78	78	78
Interstage adapter		87	87	131	131
Mission-Peculiar		511	515	728	732
Orbit adjust system (N_2H_4)		46	50	55	59
Instrument structure		271	271	479	479
Instrument thermal control		64	64	64	64
Instrument harness and connectors		30	30	30	30
Wideband communication and data handling		100	100	100	100
Instruments		690	690	690	690
Thematic mapper (TM)		360	360	360	360
High resolution pointable imager (HRPI)		330	330	330	330
Total Observatory		2604	2717	3043	3156
Launch Vehicle Capability		2625	2625	3685	3685
Contingency (net available)		21	-92	642	529

Table 4-10. Titan III-B EOS-A Observatory Weight Summary
(716 km Circular Sun-Synchronous Orbit)

Item	Launch Vehicle: Serviceability : Redundancy :	Weight (lb) III-B (SSB) Serviceable Minimum	III-B (SSB) Serviceable Nominal	III-B (SSB) Nonserviceable Minimum	III-B (SSB) Nonserviceable Nominal
Spacecraft		2311	2420	2110	2219
Basic structure (including modules)		1186	1186	1002	1002
Electrical power		256	267	256	267
Electrical harness and connectors		66	66	66	66
Solar array and drive		146	150	146	150
Attitude determination		76	132	76	132
Actuation		94	110	94	110
Pneumatics (N_2)		93	93	93	93
Communication and data handling		41	63	41	63
Thermal control		119	119	102	102
Interstage adapter		234	234	234	234
Mission-Peculiar		1856	1860	1450	1454
Circularization and orbit adjust system		457	461	457	461
Instrument structure		1141	1141	770	770
Instrument thermal control		119	119	84	84
Instrument harness and connectors		39	39	39	39
Wideband communication and data handling		100	100	100	100
Instruments		750	750	750	750
Thematic mapper (TM)		360	360	360	360
High resolution pointable imager (HRPI)		330	330	330	330
Data collection system (DCS)		60	60	60	60
Total Observatory		4917	5030	4310	4423
Launch Vehicle Capability		5143	5143	5143	5143
Contingency (net available)		226	113	833	720

Table 4-11. Detail Spacecraft Weight Breakdown (Non-serviceable/Minimum Redundancy Case)

Item	Quantity	Weight (lb)		
		Thor-Delta 2910	Thor-Delta 3910	Titan III-B (SSB)
Electrical Power		256.2	256.2	256.2
Power control unit	1	28.4	28.4	28.4
Secondary power and bus protection	1	10.2	10.2	10.2
Diode assembly	1	2.0	2.0	2.0
Power disconnect assembly	1	2.6	2.6	2.6
Data interface unit	1	4.0	4.0	4.0
Battery (22 ~40 AH cell)	2	209.0	209.0	209.0
Electrical Harness and Connectors		61.0	61.0	66.0
Communications and data handling		9.0	9.0	9.0
Attitude determination		10.0	10.0	10.0
Electrical power		12.0	12.0	12.0
Solar array and drive		8.0	8.0	8.0
Actuation and propulsion		9.0	9.0	9.0
Spacecraft support structure		13.0	13.0	18.0
Solar Array and Drive		146.2	146.2	146.2
Solar array assembly	144 sq. ft.	116.0	116.0	116.0
Drive assembly	1	9.7	9.7	9.7
Drive electronics assembly	2	4.0	4.0	4.0
Power disconnect assembly	1	1.5	1.5	1.5
Data interface unit	1	4.0	4.0	4.0
Secondary power converter	1	6.0	6.0	6.0
J-box	1	5.0	5.0	5.0
Attitude Determination		76.0	76.0	76.0
Star tracker	2	22.0	22.0	22.0
Star tracker shade	2	5.0	5.0	5.0
Magnetometer assembly	1	4.0	4.0	4.0
Inertial reference unit	3	21.0	21.0	21.0
Sun sensor assembly	1	1.0	1.0	1.0
Transfer assembly	1	13.0	13.0	13.0
Data interface unit	1	4.0	4.0	4.0
Power control unit	2	6.0	6.0	6.0
Actuation		57.5	93.5	93.5
Reaction wheel	3	26.4	49.5	49.5
Magnetic torquer	3	13.2	26.1	26.1
Reaction wheel electronics	3	12.0	12.0	12.0
Valve and magnetic torquer electronics	1	1.9	1.9	1.9
Data interface unit	1	4.0	4.0	4.0
Pneumatics		57.1	57.1	93.3
Tankage	2/4	22.5	22.5	45.0
Fill valve	1	0.5	0.5	0.5
Pressure transducer	1	0.5	0.5	0.5
Filter	1	0.5	0.5	0.5
Isolation valve	4	2.4	2.4	2.4
Vent	1	0.6	0.6	0.6
Regulator	2	2.4	2.4	2.4
Thrusters	12	8.4	8.4	8.4
Lines		3.0	3.0	5.0
GN_2	867/1638 lb sec.	16.3	16.3	28.0
Communications and Data Handling		40.4	40.4	40.4
Forward omni	1	0.4	0.4	0.4
Aft omni	1	0.8	0.8	0.8
RF transfer switch	1	0.7	0.7	0.7
Diplexer	2	6.0	6.0	6.0
Hybrid combiner	1	0.1	0.1	0.1
S-band receiver	1	2.5	2.5	2.5
S-band transmitter	1	2.5	2.5	2.5
Demodulator/decoder	1	2.0	2.0	2.0
Bus controller	1	1.3	1.3	1.3

Table 4-11. Detail Spacecraft Weight Breakdown (Non-servicable/Minimum Redundancy Case) (cont'd)

Item	Quantity	Weight (lb)		
		Thor-Delta 2910	Thor-Delta 3910	Titan III-B (SSB)
Communications and Data Handling (cont'd)				
Computer	1	9.0	9.0	9.0
Computer memory	2	4.6	4.6	4.6
Baseband assembly	1	1.3	1.3	1.3
Data interface unit	1	1.2	1.2	1.2
Power converter	1	5.0	5.0	5.0
Coax cable		3.0	3.0	3.0
Spacecraft Structure		543.2	685.2	1001.6
Communication module	1	71.0	71.0	71.0
Attitude determination module	1	62.3	62.3	62.3
Electrical power module	1	80.9	80.9	80.9
Solar array and drive module	1	15.5	15.5	15.5
Actuation and propulsion module	1	30.3	30.3	100.9
Transition ring assembly	1	147.8	181.0	226.0
Lower fram assembly	1	123.2	223.9	404.9
Attach hardware and miscellaneous		12.2	20.3	40.1
Thermal Control		78.6	78.6	101.5
Communication module		12.7	12.7	12.7
Attitude determination module		8.7	8.7	8.7
Electrical power module		18.7	18.7	18.7
Solar array and drive module		7.2	7.2	7.2
Actuation and propulsion module		9.0	9.0	19.7
Transition ring and truss assembly		22.3	22.3	34.5
Interstage Adapter		87.0	131.0	234.0
Separation ring	1	22.6	39.3	---
Shell assembly	1	7.3	13.4	---
Lower ring	1	9.5	18.8	20.6
Separation clamp assembly	1	22.3	29.7	---
Separation band assembly	1	11.3	11.3	---
Springs, pyrotechnics, harness, etc.		6.0	6.0	4.2
Attach hardware and thermal provision		8.0	12.5	20.9
Strut assembly	1	---	---	163.3
Spacecraft interface fittings	4	---	---	25.0
Spacecraft Assembly		1403.2	1625.2	2108.7

Titan III-D (~20,000 pounds for the orbits of interest), a separate tabulation is not presented for this launch vehicle since all of the aforementioned configurations are capable of being launched on this booster.

For all cases, the launch vehicle capabilities and the observatory ΔV requirements are based on a 716 km (386.6 nmi) circular sun synchronous operational orbit. The payload capabilities of the Thor-Delta versions are based on direct injection of the observatory into this orbit. Since the Titan III-B cannot deliver the observatory by direct injection into the required circular orbit, the Titan III-B payload is based on a transfer orbit capability to a 185 x 716 km (100 x 386.6 nmi) sun synchronous orbit. Thus, for this case the circularization ΔV of 481 ft/sec

Table 4-12. EOS-A Mass Properties Characteristics

Configuration/Condition	Weight* (lb)	Center of Mass (in.)**			Moment of Inertia (slug-ft^2)			Products of Inertia (slug-ft^2)		
		$\bar{X}$	$\bar{Y}$	$\bar{Z}$	I_x (Roll)	I_y (Pitch)	I_z (Yaw)	I_{xy}	I_{xz}	I_{yz}
Thor-Delta 2910										
At separation-stowed	2538	80.4	2.3	3.9	329	1162	1238	-43	-101	8
Array deployed (facing +X)	2538	77.2	-4.2	3.9	908	1147	1715	41	- 55	100
Array deployed (facing -Z)	2538	78.1	-4.2	3.0	902	1171	1746	-35	- 67	176
Array deployed (facing -X)	2538	79.0	-4.2	3.9	908	1144	1712	-111	- 80	100
Thor-Delta 3910										
At separation-stowed	3554	80.5	2.1	3.6	451	1619	1728	-54	-108	9
Array deployed (facing +X)	3554	78.2	-2.6	3.6	1036	1606	1606	33	- 62	100
Array deployed (facing -Z)	3554	78.8	-2.6	3.0	1029	1629	2242	-43	- 73	177
Array deployed (facing -X)	3554	79.4	-2.6	3.6	1036	1602	2208	-120	- 87	100
Titan III-B (SSB)										
At separation-stowed	4909	93.6	0.6	-1.6	1101	4148	4432	-73	- 82	12
Array deployed (facing +X)	4598	93.5	-3.2	-1.7	1838	3541	4511	134	61	132
Array deployed (facing -Z)	4598	94.4	-3.2	-0.8	1789	3469	4489	- 2	25	-3
Array deployed (facing -X)	4598	95.2	-3.2	-1.7	1838	3504	4474	-138	7	132

* Thor-Delta Configurations - Based on the direct injection payload capability of the launch vehicle into a 716 km (386.6 nmi) circular sun synchronous orbit.

Titan III-B Configuration - Separated observatory weight based on the payload capability of the launch vehicle to a 185 x 716 km (100 x 386.6 nmi) sun synchronous transfer orbit. Solar array deployed conditions based on observatory weight at beginning of life in 716 km circular sun synchronous oribt.

** Longitudinal center of mass ($\bar{X}$) referenced from the observatory/aft adapter separation plane.
Lateral center of mass ($\bar{Y}$, $\bar{Z}$) referenced from the geometric centerline of the spacecraft.
Coordinate reference axes and notation system are as shown in the layout drawings, Figures 4-1 and 4-2, in Section 4.1.

is provided by the observatory. Deorbit ΔV provision is not included in any of the configurations presented since the Shuttle is capable of rendezvous and retrieval from this operational orbit.

4.6.1 Thor-Delta Configurations

Weight summaries delineating the spacecraft system, the mission peculiars and the science instruments for a non-space-serviceable case are presented in Table 4-9 for two levels of spacecraft equipment redundancies. Reliability estimates associated with the minimum and nominal redundancy cases are presented in Section 4.5.

As noted in Table 4-9, the 2910 is a marginal configuration, whereas the 3910 configuration, due to its greater payload capability, has a comfortable contingency margin. The 3910 weight margin is such that the spacecraft equipment modules could be made space-serviceable and yet retain a contingency margin of approximately 11 percent of the estimated observatory weight. The estimated Δ weight to make the five spacecraft modules (electrical power, attitude determination, solar array and drive, communications and data handling, and actuation modules) space-serviceable is approximately 164 pounds. Should the wideband communication and instrument modules also be made space-serviceable, an additional 321 pounds would be required (see Table 4-13).

In an attempt to maximize the contingency margin, a preliminary weight tradeoff was conducted using a transition ring adapter approach in lieu of the aft adapter concept. The net result of this investigation was that the aft adapter was the minimum weight approach, thus providing the larger contingency margin.

Preliminary observatory weight summaries for alternate payload missions which were conceptually synthesized using the basic Thor-Delta spacecraft bus are summarized in Section 7 of Report 1, "Orbit/Launch Vehicle Tradeoff Studies and Recommendations."

4.6.2 Titan Configuration

Weight summaries for the Titan IIIB serviceable and nonserviceable configurations are presented in Table 4-10 for two levels of spacecraft

Table 4-13. Δ Weight Breakdown

	Δ Weight (lb)
Spacecraft Section	
Provide tie-down and latch hardware for the five serviceable modules	+101.0
Provide additional insulation at module interfaces	+15.0
Provide serviceable module structure for the solar array and drive, and actuation equipment in lieu of mounting equipment directly to the primary structure	+47.6
	+163.6
Instrument Section	
Provide serviceable module structure for the instruments in lieu of mounting the instruments directly to the primary structure	+158.7
Provide tie-down and latch hardware for three science modules	+84.0
Provide additional structural insulation within the module bays	+13.4
Modify the horizontal elements of the basic truss structure between the module bays and modify the structure on the +Z face for module serviceability	+64.9
	+321.0

equipment redundancies. Except for the addition of a data collection system (DCS), the science instrument payload is the same as that of the Thor-Delta configuration.

As noted in Table 4-10, the Titan IIIB is a viable configuration in the nonserviceable or partially serviceable mode. Should the spacecraft equipment modules be made serviceable, the Δ weight increase would be 201 pounds. The net contingency margin available would then be equivalent to ~11 percent of the estimated observatory weight.

In the fully serviceable case wherein the spacecraft modules and the payload modules are all serviceable, the contingency margin is only 226 pounds for the minimum redundancy case and 113 pounds with nominal redundancy. Thus, the fully serviceable configuration is a marginal case.

5. EOS-A BASELINE INSTRUMENT DESIGN

5.1 THEMATIC MAPPER

The baseline thematic mapper for the EOS-A spacecraft which was selected by TRW is the linear image plane scanner. This approach was selected on the basis of preliminary evaluations which showed that this instrument gave data considerably easier to process than the conical scanner and somewhat easier than the object plane scanner. During the course of the study, this opinion did not change and we still believe this to be the best choice for the baseline system by a narrow margin.

However, factors such as reduced altitude, extremely critical weight, or wider swathwidth could drive the preferred approach to either the linear object plane scanner or the conical image plane scanner concepts.

This section, therefore, describes the linear image plane instrument as used in our baseline system design. Comparisons and certain tradeoffs of all instruments are given in Report 1, Section 4.1 and in Report 3, Appendix A, Section 4.1.

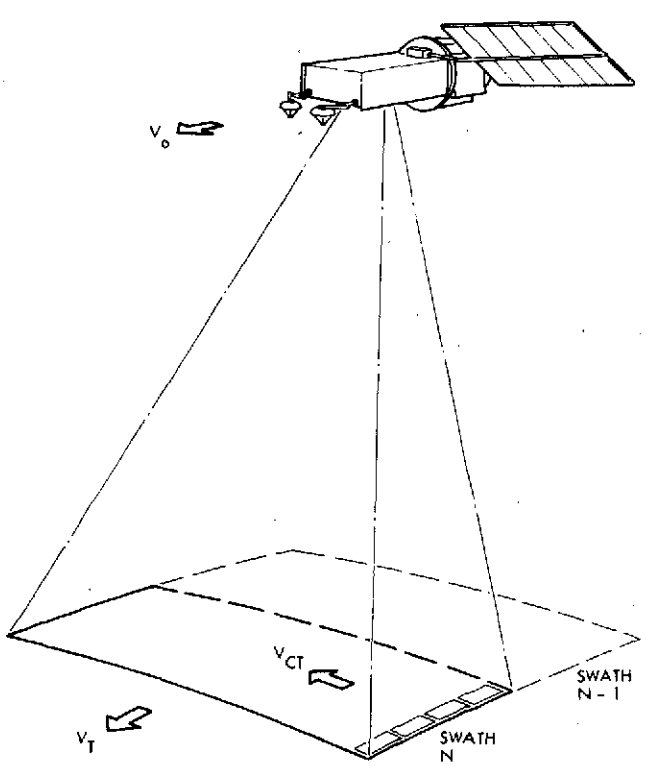

Figure 5-1.
Thematic Mapper Scan Geometry

5.1.1 Configuration/Performance Summary

The thematic mapper scans the ground area below the spacecraft (Figure 5-1), collecting radiation in each of seven spectral bands, and develops analog signals whose magnitude is dependent on the radiation intensity in each band. These signals, along with appropriate synchronization and housekeeping signals, are processed by the MODS unit, which performs the multiplexing and analog-to-digital conversion prior to telemetry to the ground station. As indicated in Figure 5-1, an array of detectors with their fields of view displaced in

the in-track direction is swept in a cross-track direction to cover a 185 km wide area. Scan timing is adjusted such that adjacent scan swaths are contiguous as the spacecraft motion in orbit advances the scanned field in the in-track direction. A summary of the instrument characteristics is shown in Table 5-1.

Table 5-1. Thematic Mapper Characteristics Summary

Design altitude: 717 km

Ground resolution: 30 m

Swath width: 185 km

Sensitivity:

Spectral Band (μm)	Input Radiance (10^{-5} w/cm^2 sr)	S/N at Mininum Radiance
0.5 to 0.6	22 to 363	10
0.6 to 0.7	19 to 297	7
0.7 to 0.8	16 to 231	5
0.8 to 1.1	30 to 363	5
1.55 to 1.75	8 to 66	5
2.1 to 2.35	3 to 39	5
10.4 to 12.6	200 to 265	NEΔT = 0.5°K

Radiometric accuracy: ±10% absolute
± 1% relative (cell/cell and band/band)

Weight: 166 kg (365 lb)
Size: 183 x 97 x 102 cm (72 x 38 x 40 in.)
Power: 110 w
Output signals:

Source	No. of Channels	Data Rate words/sec/channel	Bits/ word
Bands 1 through 6 data	96	115, 165	8
Band 7 data	4	28, 790	8
Housekeeping and Command Verification	50	0.5	8

Modulation transfer function: MTF > 0.5 for a spatial input frequency of 30 m per half cycle

5.1.2 Design Details

5.1.2.1 Optics

A conceptual layout of the linear image plane thematic mapper showing the key optical elements associated with the scanning and imaging functions is presented in Figure 5-2. Light entering the entrance port is reflected off the fixed mirror and directed to the primary mirror. The spherical primary mirror generates an image at focal plane I. As the roof mirror passes in front of the image plane, light from different portions of the scene are sequentially directed to the image cone compensation (ICC) mirror and the balance of the optical train. A secondary effect of this type of image plane scan is that the cone of light leaving the second roof mirror surface is tilted as a function of scan angle. Oscillating mirror ICC compensates for this tilt such that the light distribution at the corrector mirror is constant with scan angle. In order to provide acceptable imagery over the total ±7.38 degree scan field, a Schmidt corrector surface is employed. The final corrected image appears at the entrance to the chromatic optics section.

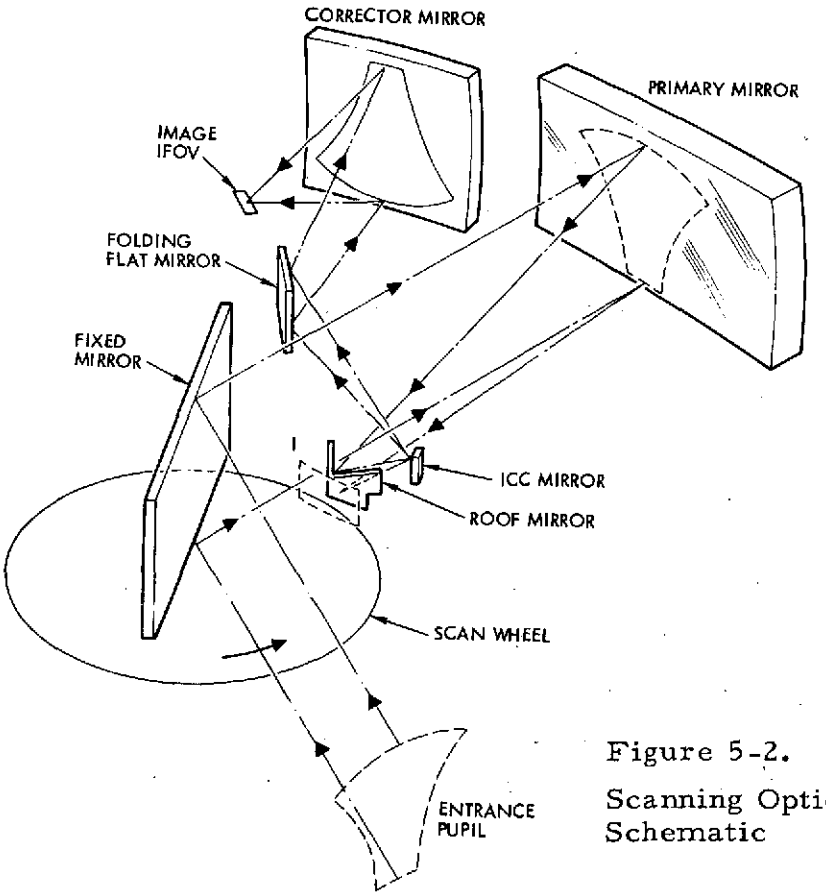

Figure 5-2.
Scanning Optics Schematic

The optical elements associated with the various spectral channels are shown in Figure 5-3. A field dissector directs light from one portion of the image plane to band 1 through 4 detectors, and the balance to band 5 through 7 detectors. The Dichroic mirror reflects the lower wavelength energy to band 5 and 6 detectors, and transmits energy to the band 7 detectors. Spectral filtering is provided by the filters that are positioned over the various detector arrays.

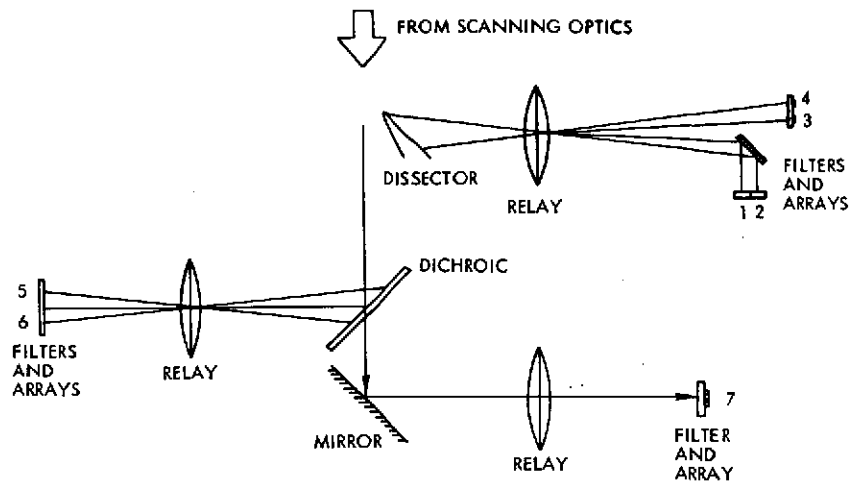

Figure 5-3. Chromatic Optics Schematic

5.1.2.2 Electronics

A block diagram of the thematic mapper electronics is shown in Figure 5-4. Scan wheel motions are controlled by a phase-lock loop. As the wheel rotates, a series of pulses are output from the encoder, which are compared to the pulse train output from the frequency multiplier. Any frequency or phase differences between the two signals are sensed and processed for application to the motor. Frequency matching ensures that the scan wheel rotates at the proper rate, and phase matching ensures that the scan position is nominally in synchronization with the spacecraft clock. In order to minimize the disturbance imparted to the spacecraft as a result of this motion, momentum compensation hardware is included. A counter rotating wheel, of equal but opposite momentum, is driven by an AC motor. Both wheels change rate in response to a ground command that selects the multiplier factor for the frequency multiplier.

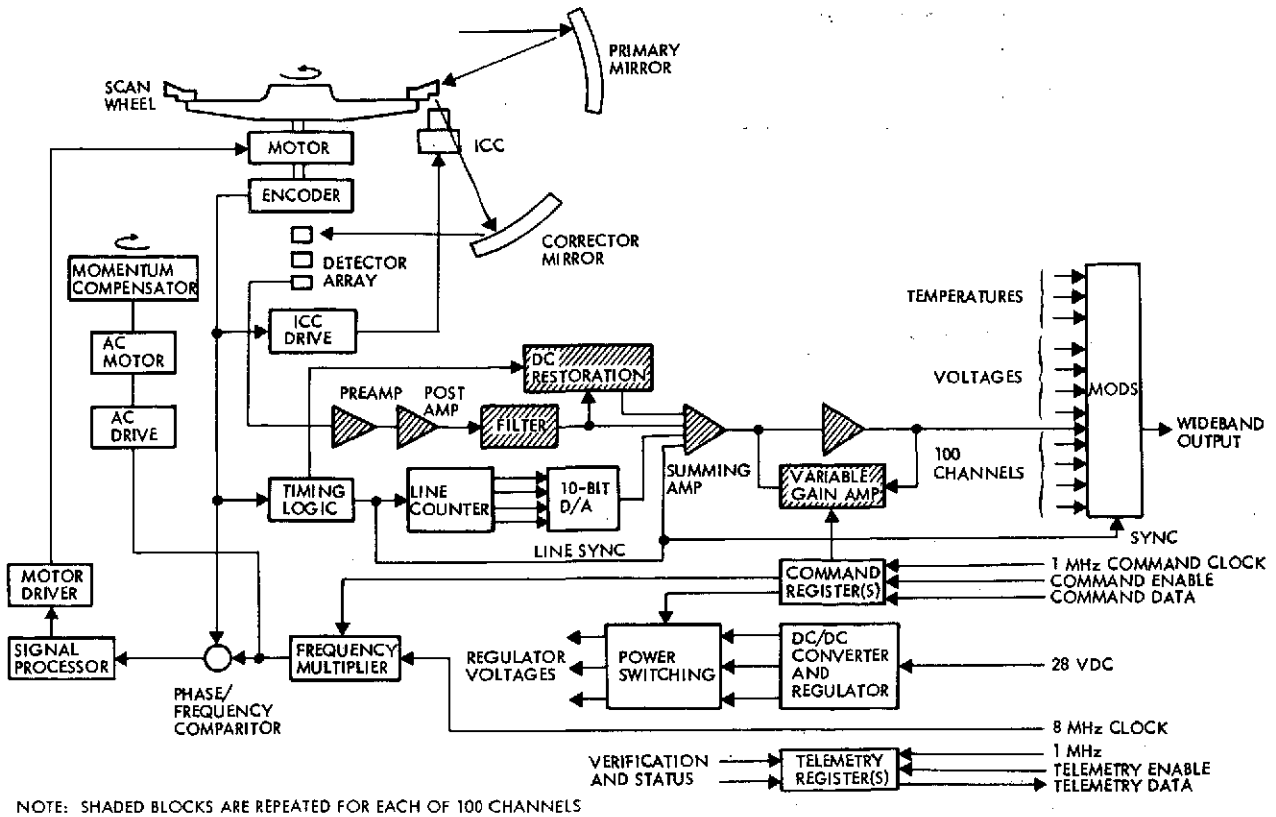

Figure 5-4. Thematic Mapper Block Diagram

Associated with each detector channel is a preamplifier, post-amplifier, filter, DC restorer, summing amplifier, and variable gain amplifier. High-frequency peaking is incorporated in the post-amplifier to compensate for roll-off due to the inherent detector capacitance and preamplifier input impedance. The overall frequency response of detector, preamplifier and post-detector is flat from DC to the input frequency 61.51 kHz. In order to attenuate the higher frequency noise components but provide only minor attenuation at the signal frequency, a fifth order Butterworth filter is used. Figure 5-5 shows the gain and phase characteristics of the filter. At the signal frequency the output is down to 0.95 (~-0.5 dB), and the noise equivalent bandwidth is 77 kHz. If the phase versus frequency response were plotted on linear graph paper, it would be fairly linear indicating a constant time delay for all frequencies within the passband. This time delay is approximately 7.7 μsec.

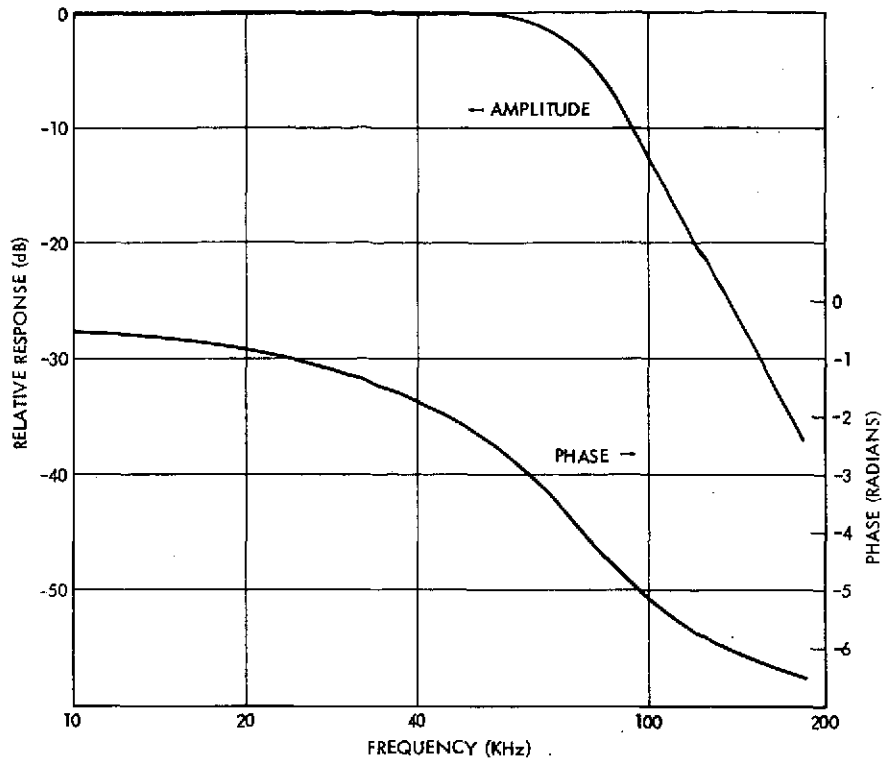

Figure 5-5. Filter Gain and Phase Characteristics

For bands 1 through 6, a DC restoration circuit is included to establish a dark level reference once per scan. If a non-zero output exists at the output of the Butterworth filter, when the detectors are viewing a specially darkened area of the instrument, the DC restorator generates an equal, but opposite voltage. The same compensating bias is held on the restorer output during the balance of the line scan. This action ensures zero output from the summing amplifier for zero radiance input.

The present linear image plane design concept does not define characteristics of the variable gain amplifier in detail, but one promising implementation is described. The variable gain amplifier could exhibit eight fixed gain states in response to ground commands. Total gain range is about 1.95 to 1 with a gain selection resolution of 10 percent. It should be possible, with this resolution, to match the overall response of each set of 16-detector channels to within ±5 percent. This feature has merit for the low-cost ground station in that channel-to-channel gain differences need not be compensated. Only 3-bit command words for each channel are required for gain selection.

5.1.2.3 Mechanical

Figure 5-6 illustrates the basic layout of the thematic mapper package. All instrument components are beryllium with the exception of the aluminum honeycomb baffle and insulation box. The scan wheel and roof mirrors are cored isotropically. Both the primary, pointing, and corrector mirrors are machined and cored from solid pressings. A listing of the weights for the individual elements is tabulated in Table 5-2. Later manufacturers weight estimates indicate a weight of 325 pounds can be attained.

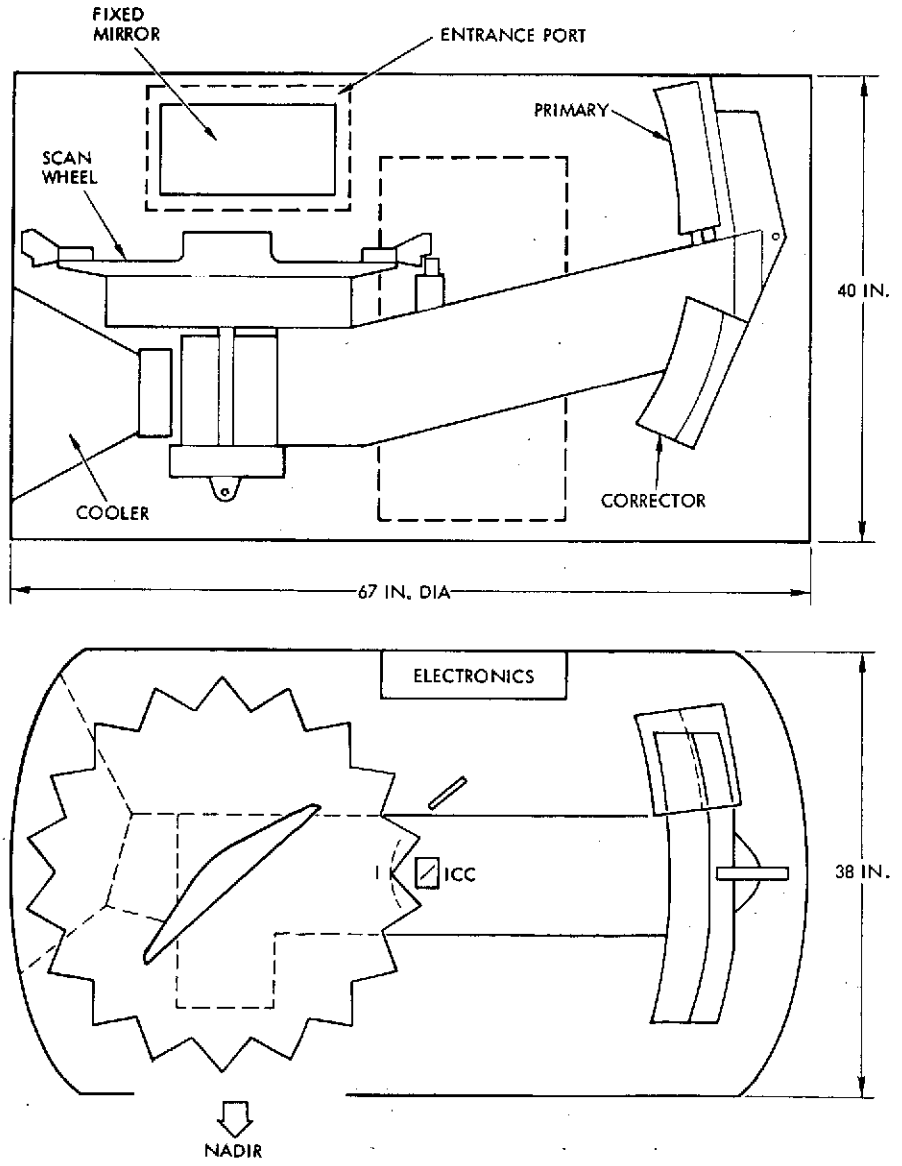

Figure 5-6. Linear Image Plane Thematic Mapper

Table 5-2. Weight Tabulation

Item	Weight (lb)
Main frame	71
Primary mirror plus mount	27
Scan wheel	75
Hardware	15
Thermal isolators	10
Momentum compensator	11
Pointing mirror	30
Corrector mirror plus mount	10
Detector cooler	7
Relay mirrors	7
Electronics	47
Baffle box	55
	365 lb

The radiation cooler is shown in Figure 5-7. This is a two-stage device with a first-stage temperature of ~200°K and a second-stage temperature of ~100°K. The joule heating that is radiated by the cooler is 375 and 2 mw, respectively, for the first and second stages, as indicated in Table 5-3.

Table 5-3. Cooler Radiation

Spectral Band	Stage 1		Stage 2	
1 through 4	80 detectors and 80 FET's	240 mw		
5 through 6	40 FET	120 mw	40 In Sb	0 mw
7	5 FET	15	5 HgCdTe	2 mw
	Total	375 mw		2 mw

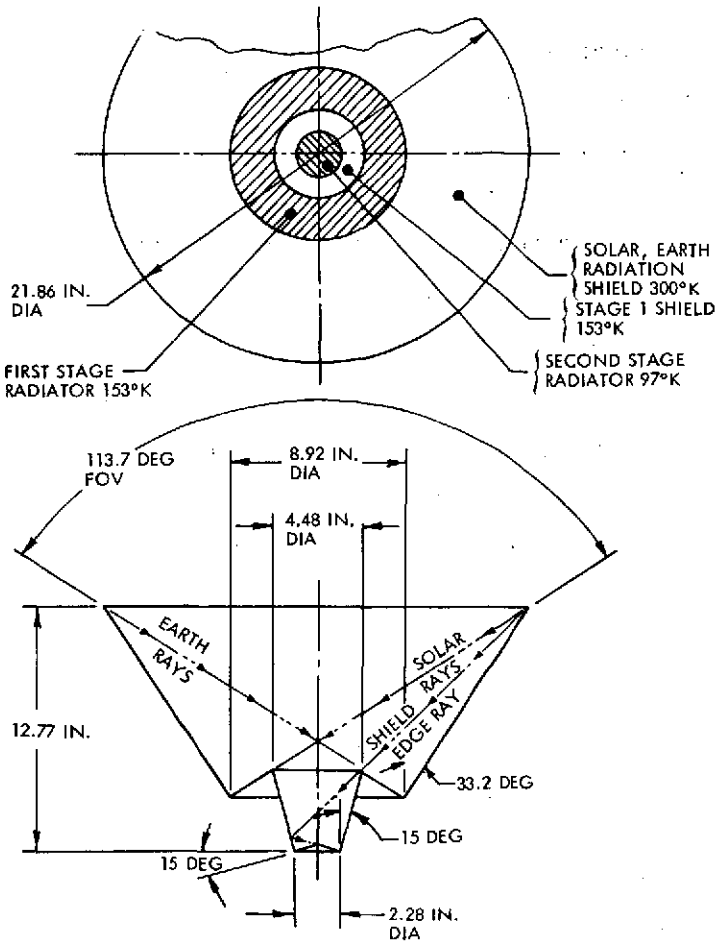

Figure 5-7. Thematic Mapper Radiation Cooler Configuration

5.2 HIGH RESOLUTION POINTABLE IMAGER (HRPI)

Four HRPI designs were considered: the Westinghouse pushbroom approach and three mechanical scanners from Gulton/Te, Honeywell, and Hughes. The pushbroom scanner was selected as a baseline and is described in this section. Comparisons between the selected and alternate approaches are given in Appendix A, Section 4.2.

The baseline HRPI instrument is a solid-state multi-spectral imager. A linear array of 4864 photodiodes in each of four color bands collects image data in a pushbroom scanning mode. Based on the Westinghouse HRPI configuration, the sensor provides ±30-degree cross-track field of view pointing and 10-meter ground resolution. The Westinghouse pointing mirror and telescope have been reoriented to obtain non-skewed off-nadir imagery.

Inherent features of the solid state design are high geometric registration and mechanical reliability. Since image scanning requires no moving parts, vibrational impact on other satellite subsystems is minimal. Detector array sensors offer weight and/or signal-to-noise advantages over corresponding mechanical scanners. Increased detector dwell time results in higher signal-to-noise. (Alternatively, smaller optical systems may be used to achieve the same signal-to-noise as mechanical scanners.)

The baseline HRPI is configured for a 717 km orbit altitude. Using lightweight materials (beryllium optics and structure) and present detector technology, the baseline instrument weights 330 pounds (includes 10 percent contingency). Baseline cost is $16 million. Instrument dimensions are compatible with either the Titan or Thor-Delta launch vehicle.

5.2.1 Design Detail

Each color array has 4864 detectors (19 chips with 256 detectors per chip). Associated with each detector chip are four analog multiplexers (Figure 5-8). Each multiplexer sequentially samples 64 detectors. This results in a total output of 304 parallel analog data lines. The multimegabit operation data systems (MODS), packaged as part of the HRPI electronics, converts the analog signals to a single line of digital data. Interlaced with the digital data are synchronization and housekeeping data.

The MODS control unit receives a timing signal from a spacecraft central control and timing unit. This synchronizes the HRPI and thematic mapper data rates for instrument signal combining (quadriphasing) prior to X-band transmission. The multiplexer address decoder receives the control and timing commands from the MODS control unit and simultaneously controls the 304 analog multiplexers via a 64-element multiplexer control bus.

Data bus commands (mirror pointing, electronic gain, calibration, etc.) are received by the data interface unit (DIU) and translated for instrument function control. HRPI housekeeping information (voltages, temperatures, electronic gain state, etc.) is formatted by the DIU for housekeeping telemetry.

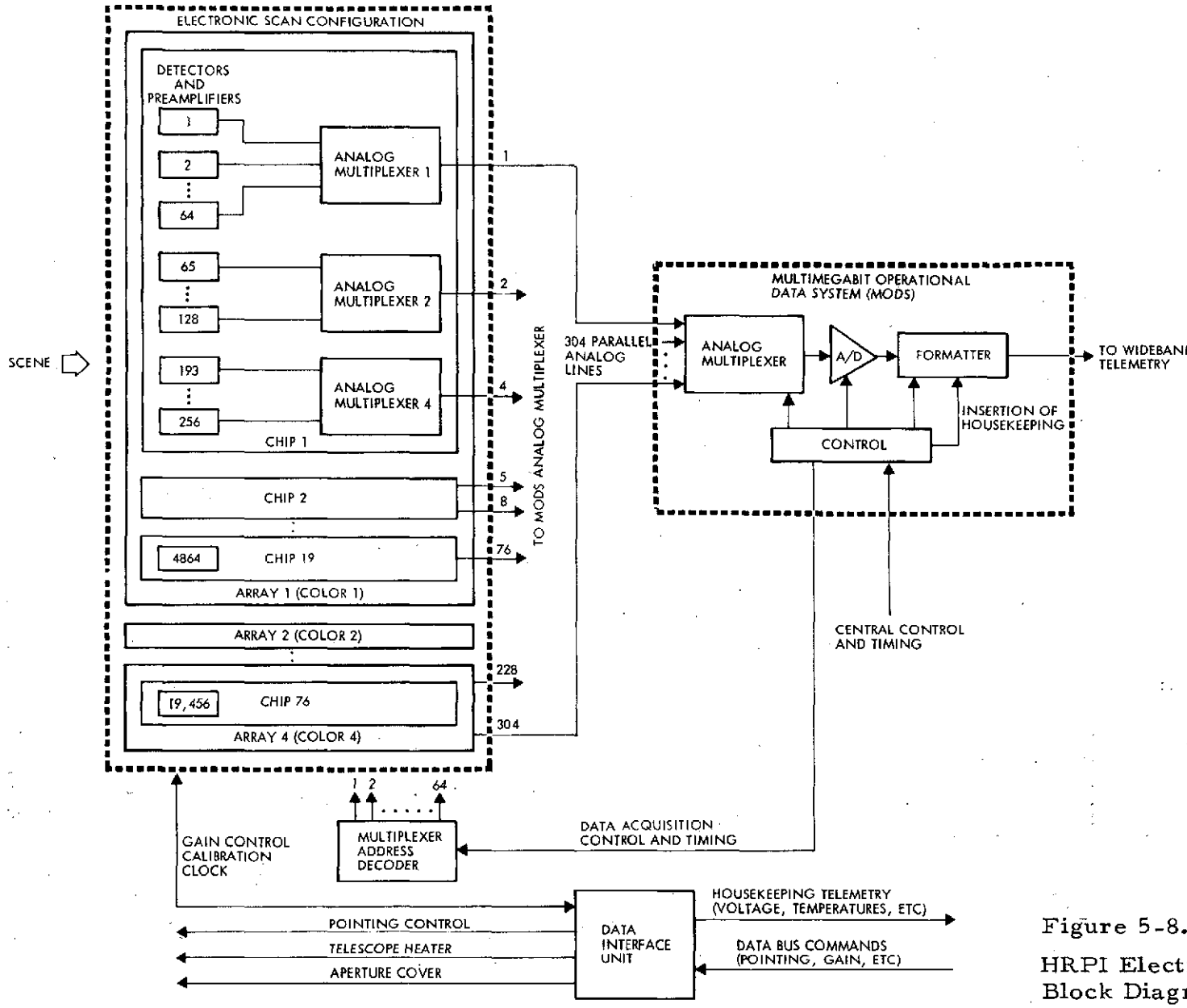

Figure 5-8.

HRPI Electronics Block Diagram

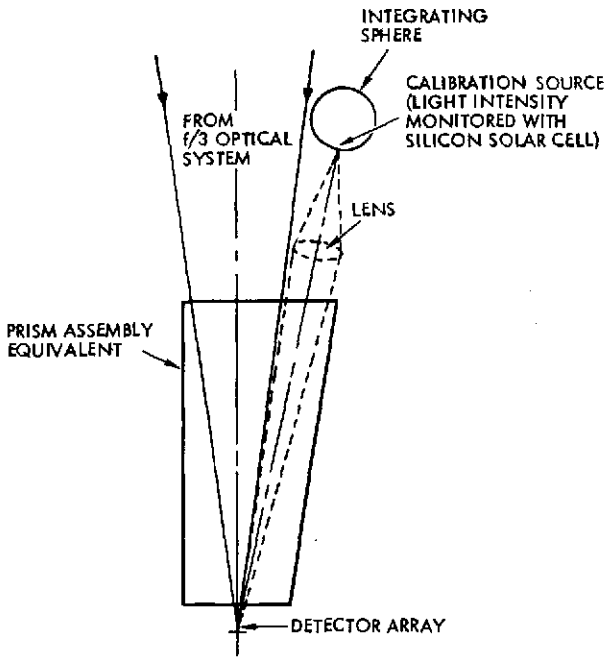

Figure 5-9. Calibration Insertion

Detector dark current and gain variations are calibrated with a shutter and an internal light source. The shutter is mounted between the rear correction lens and prism assemblies. At the end of an image data run, the shutter is closed without halting the wideband data stream. After sufficient collection of dark current data, an internal light source illuminates the detector array (Figure 5-9). The shutter is then opened and the calibration source turned off. This calibration sequence allows the ground data processing facility to collect calibration data immediately after collection of image data without waiting for pointing mirror rotation or aperture cover closure. This minimizes wideband tape recording costs in the ground data processing facility.

The HRPI is mounted at three points with insulating blocks that inhibit heat flow. For the Titan launch vehicle, the instrument is mounted inside a module enclosure. The enclosure, designed for Shuttle operations, has a commandable aperture cover that protects the instrument from contamination during Shuttle approach. The same cover serves as a sun shade when open during normal operation. For the Thor-Delta configuration, the mounting is direct to the spacecraft structure. The sun shade is stationary.

In either case, the HRPI is insulated with a thermal blanket. A $\pm 10^{\circ}C$ swing in spacecraft environment results in a maximum conduction and radiation heat transfer of 10 watts (6 watts surface radiation and 4 watts conduction through mounting blocks). Penetrations in the overall spacecraft thermal shroud allow for heat rejection by the telescope and electronics thermal radiators.

5.2.2 HRPI Configuration/Performance Summary

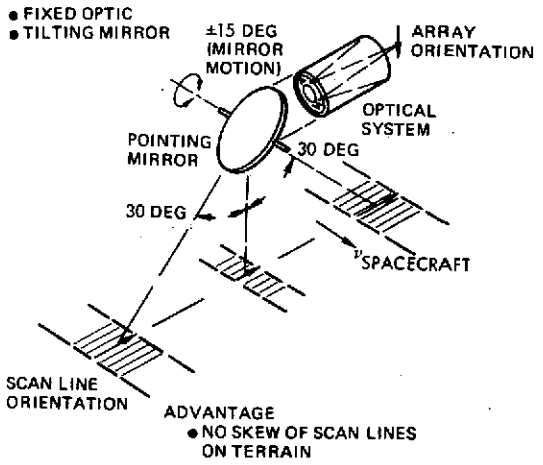

Figure 5-10.
HRPI Scan Orientation

Non-skewed imagery is obtained by orienting the telescope in the cross-track direction and rotating the field of view pointing mirror about the in-flight axis (see Figure 5-10). The 15-inch catadioptric telescope has spherical primary and secondary mirrors (see Figure 5-11). The front corrector lens protects the telescope interior from contamination.

A 15 x 30 inch oval pointing mirror is required to obtain ±30 degree off-nadir pointing. Instrument weight and mirror pointing/momentum compensation power requirements are minimized by using a cored beryllium mirror structure. A 16 x 36 inch oval entrance aperture allows ±30 degree viewing (Figure 5-11). Silver/teflon thermal radiators (α_s = 0.15, ϵ = 0.8) efficiently cool the electronics and telescope.

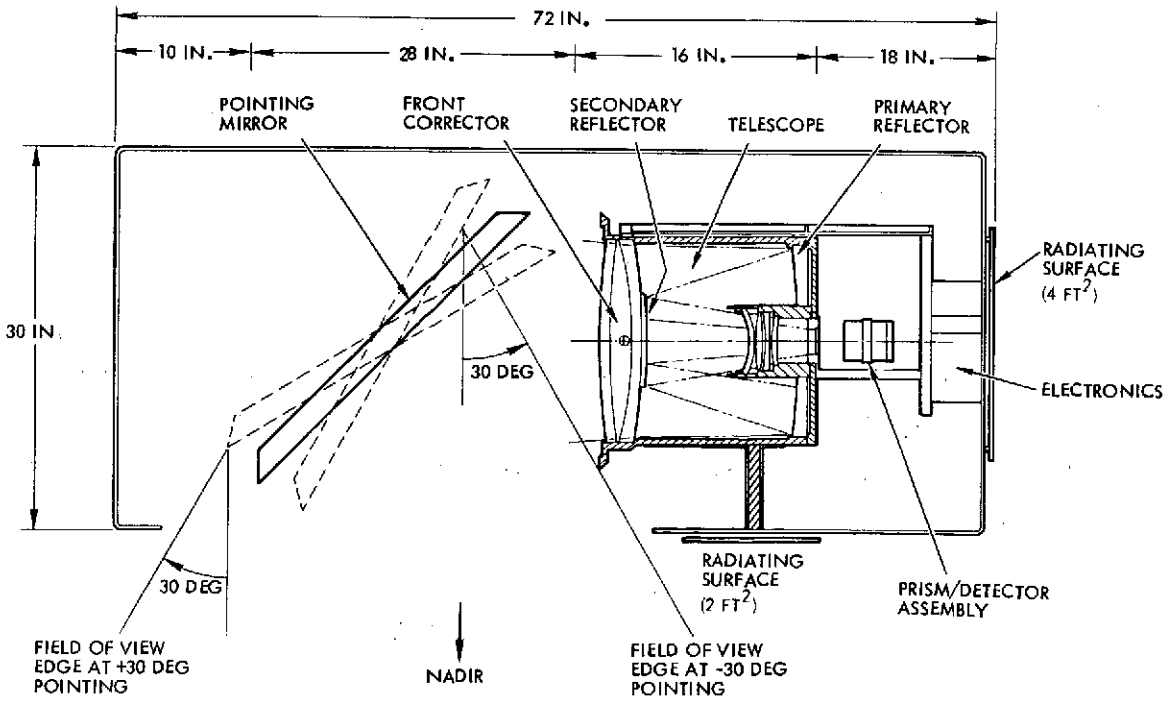

Figure 5-11. HRPI Configuration (Side View)

Light reflected off the pointing mirror passes through the front corrector lens. After reflection by the primary and secondary telescope mirrors and distortion correction by the rear corrector assembly, the scene energy is spectrally separated into four colors and imaged on four linear diode arrays. The six-prism assembly (Figure 5-12) spectrally separates the scene energy with dichroic coatings at relatively low indident angles. This results in high efficiency and low polarization. The prism assembly is cemented in place between the top and bottom of the instrument housing mounting structure. The detector assemblies are mounted to a structure that is thermally coupled to the telescope structure, providing a path for excess heat generated by the detector preamplifier electronics.

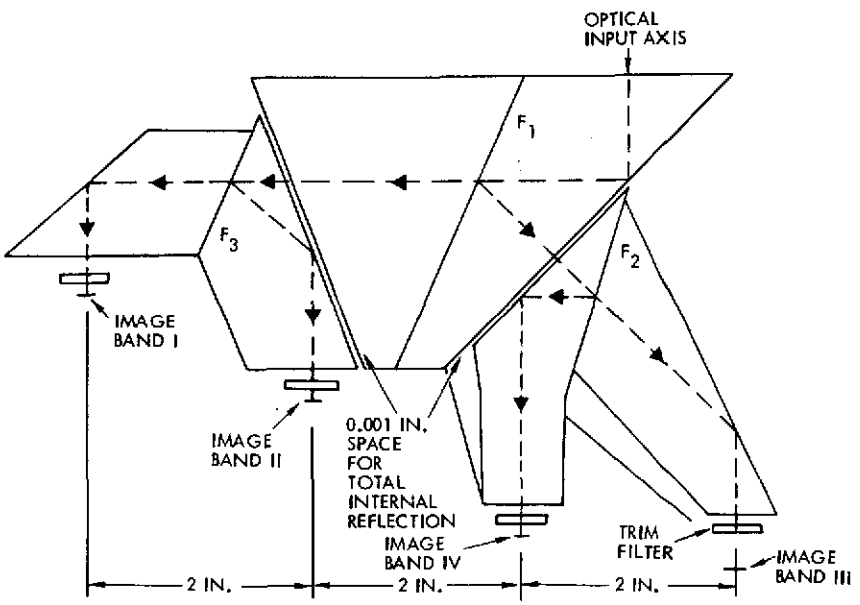

Figure 5-12. Prism Array Spectral Separation

A tabulation of component weights is given in Table 5-4. Key performance parameters are summarized in Table 5-5. The background signal-to-noise (S/N) values were calculated using the following equation and parameter values:

$$S/N = \frac{\pi N (1 - \phi) T}{4 f_{no}^{2}} \cdot \frac{\eta t}{NES}$$

Table 5-4. HRPI Component Weight Tabulation

	Weight (lb)
Telescope assembly	70
Detectors and beam splitter	8
Mirror and pointing assembly	54
Angular momentum compensation	19
Electronics	28
Thermal control	16
Miscellaneous	20
Structure	85
Net	300
Contingency (10 percent)	30
Total	330

Table 5-5. HRPI Performance Summary

Design orbit attitude: 717 km

Field of view (FOV): 3.9 degrees

Cross-track pointability

Range:	±30 degrees
Selectability increment:	0.5 degrees
Repeatability:	±0.1 degrees
Measurability:	±0.05 degrees

Coverage and resolution:

	Pointing Angle (From Nadir)	
	0 Deg	±30 Deg
Swath width (km)	48.6	69.8
Along-track resolution (m)	10	11.8
Cross-track resolution (m)	10	14.2

Linearity: 10 percent of a picture element

Spectral registration: 10 percent of a picture element

Table 5-5. HRPI Performance Summary (Continued)

Spectral performance:

Spectral band number	1	2	3	4
Bandwidth (nanometers)	500-600	600-700	700-800	800-1100
Background radiance (w^2/m^2-sr)	2.2	1.9	1.6	3.0
Background S/N (DC signal/rms noise)	53	47	36	38
Background S/N (13:1 contrast to background; 10 meters/line spatial frequency)	2.5	2.5	2.0	1.9
System MTF	0.16	0.18	0.19	0.17
Quantum efficiency	0.75	0.74	0.69	0.38

Radiometry

Accuracy: 10 percent
Repeatability: 1 percent
Calibration: Dark current plus two gain transfer points, once per data-taking mission

Size:

Cross-track (Y axis) length:	72 inches
Nadir (Z axis) height:	30 inches
Along-track (X axis) width:	25 inches

Weight: 330 pounds

Power:

Voltage-operating range:	28 ±7 VDC
Electronics (power conditioning, amplifiers, data processing):	100 watts
Heater power (maximum):	19 watts
Pointing mirror:	2 watts

Data interface:

Bits/word:	8
Rate (Mbits/sec):	128
Data sampling duty cycle:	0.82

Thermal interface:

Operational environment:	20 ±10°C
Radiative heat transfer:	6 watts to or from spacecraft
Conductive heat transfer:	4 watts to or from spacecraft

where

N = background radiance (Table 5-5)

ϕ = obscuration = 0.25

T = optical transmission = 0.5

f_{no} = optical f-number = 3.0

η = quantum efficiency (Table 5-5)

t = frame time = 1.49 msec

NES = noise equivalent signal = 1.5 μjoules/m^2

The resulting S/N values (Table 5-5) range from 36 to 53. The alternate mechanical scanner designs (Hughes, Te, and Honeywell) have S/N values ranging from 5 to 10. The performance difference is due to the high detector dwell time afforded by the electronically scanned push-broom design.

The sensor data rate is given by

$$\text{data rate} = \frac{n_e \cdot b \cdot n_b}{t_f \cdot \phi_s}$$

where

n_e = number of resolution elements per scan line (4864)

b = number of bits per data sample word (8)

n_b = number of spectral bands (four)

ϕ_s = data sampling duty cycle (0.82)

t_f = line frame time (1.48 msec)

This results is a data rate of 128 Mbits/sec. The purpose of the data sampling duty cycle is to speed up the HRPI data rate to match that of the thematic mapper. This simplifies the combining of the HRPI and the thematic mapper data for spacecraft telemetry.

5.3 DATA COLLECTION MODULE

The data collection module will be provided as government-furnished equipment (GFE) from NASA and will not be discussed here. Refer to Appendix A, Section 4.3 for a preliminary discussion of some of the topics pertinent to the data collection system.

6. EOS-A BASELINE MODULE/SUBSYSTEM DESIGNS

6.1 COMMUNICATIONS AND DATA HANDLING MODULE

6.1.1 Introduction

The communications and data handling (CDH) module (shown in Figure 6-1) contains the equipment required to receive information from and transmit information to, NASA ground stations. It provides the spacecraft with the capability to receive, demodulate, and process uplink command information; collect, process, and telemeter housekeeping and medium-rate user data; coherently transpond range information; and centrally perform on-board computations. Finally, it contains the equipment required to implement and control the spacecraft data bus system.

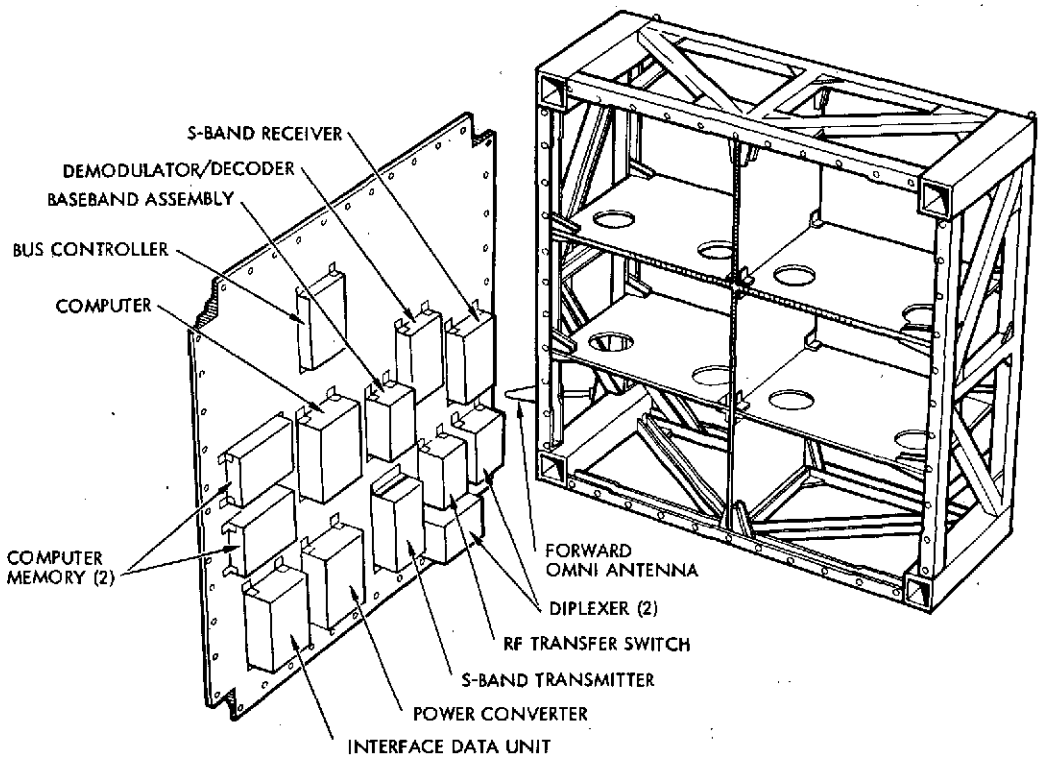

Figure 6-1. Communications and Data Handling Module (Thor-Delta)

The baseline design chosen for EOS-A represents the end product of extensive tradeoffs performed in the areas of on-board communications and data handling. The results of these studies presented in summary form here are presented in detail in Appendix A, Section 5.1.

The design, with or without redundant equipment, provides cost-effective and reliable operation through the use of proven spacecraft equipment and technology. It offers the feature of design modularity, providing a great deal of system flexibility to accommodate post-EOS-A missions with little or no impact to the module design. It can accommodate medium-rate data users (e. g., tape recorders) having rates up to 512 kbits/sec with no impact. Finally, it performs on-board computer processing and storage of telemetry data thereby eliminating the need for a housekeeping data tape recorder.

The following sections present a discussion of the requirements which were used to establish the baseline design and its capabilities. Following this is a discussion of system operation in turn followed by a discussion of system performance. Finally, detailed descriptions of the equipment contained within the module are presented.

6.1.2 System Requirements and Capabilities

A guide to requirements imposed on the CDH module is contained in the "Communications and Data Handling Performance Specification for EOS," (EOS-L-129, revised Section II), dated 30 January 1974. A further guide arises as a result of operating within the framework of the NASA unified S-band system as presented in the "Spaceflight Tracking and Data Network User's Guide Baseline Document," STDN 101.1, dated April 1974, and supplied after contract initiation.

TRW has considered these and other requirements which must be self-imposed. System flexibility and design modularity must be of concern to allow for expansion to meet the objectives of later missions. The interface between the communications and the data handling systems may also impose requirements. Finally, it is important that the system be configured with proven components to ensure cost-effective design. Table 6-1 lists the requirements which were used to configure the CDH module as well as the capabilities of the baseline CDH system design.

6.1.3 System Description

Figure 6-2 presents a block diagram of the baseline design for the communications and data handling module. Uplink data, transmitted from

Table 6-1. Requirements versus Capabilities

Requirement	Reference	Paragraph	Capability
RF Group			
Communications fully compatible with "GSFC Aerospace Data Systems Standards", X-560-63-2	1	2.2.1	Command and telemetry formats compatible with GSFC X-560-63-2
Antenna Polarization			
Antennas singly linearly polarized or dual right and left circular	1	2.2.1	Dual right and left hand circular polarized omni-antennas provided
Transmit Frequency			
Carrier lies in 2200 to 2300 MHz range	1	2.2.1	Transmit carrier lies in 2200 to 2300 MHz range
Receive Frequency			
Carrier lies in 2050 to 2150 MHz range	1	2.2.1	Receive carrier lies in 2050 to 2150 MHz range
RF Characteristics			
• Transmit frequency: TBD ±0.001%	1	2.2.1.1	Transmit carrier stability is one part in 10^5
• Receive frequency: TBD MHz	1	2.2.1.1	Receive carrier lies in 2050 to 2150 MHz range
• Transponder ratio: 221/240	1	2.2.1.1	Uplink to downlink frequency ratio is 221/240
• Transponder sidetone frequency: 500 kHz	1	2.2.1.1	Transponder bandwidth compatible with 500 kHz sidetone frequency
• Command bit rate: 2000 bits/sec	1	2.2.1.1	2 kbit/sec rate, or optionally 1 kbit/sec at reduced cost
• Command modulation: PCM/PSK/FM/PM	1	2.2.1.1	PCM, split-phase-M command data frequency modulates 70 kHz subcarrier. Subcarrier phase modulates carrier.
• Narrowband telemetry rate: Selectable: 32, 16, 8, 4, 2, 1 kbit/sec	1	2.2.1.1	Telemetry rate selectable: 32, 16, 8, 4, 2, 1 kbit/sec
• Narrowband telemetry modulation: Split-phase PCM/PM on subcarrier	1	2.2.1.1	PCM-split-phase/PSK/PM on 1.024 MHz subcarrier
• Medium rate telemetry: 500 kbit/sec maximum	1	2.2.1.1	512 kbit/sec maximum
• Medium rate telemetry modulation: Split-phase PCM/PM	1	2.2.1.1	PCM-split-phase/PM (direct carrier modulation)
• Transmitter power: 2 or 0.2 watts	1	2.2.1.1	2-watt transmitter
• Telemetry data coding: Manchester (split-phase)	1	2.2.1.1	Manchester (split-phase)
Receiver/Demodulator Options			
• Single receiver/demodulator (baseline)	1	2.2.1.2	• Baseline Design: Single receiver/demodulator with RHCP and LHCP antenna diversity combining
• Dual receiver/demodulators with with RHCP and LHCP diversity combining			• Alternate Design: Dual receiver/demodulators with RHCP and LHCP antenna diversity combining
Command Performance			
• Probability of false command execution less than $1x10^{-10}$ for any input condition	1	2.2.1.2	• Probability of false command execution less than $1x10^{-19}$ for input levels of -112 dBm and above
• Probability of good command rejection less than $1x10^{-5}$ over signal range of -105 to -40 dBm	1	2.2.1.2	• Probability of good command rejection less than $1x10^{-5}$ for input levels of -112 dBm and above

Table 6-1. Requirements versus Capabilities (Continued)

Requirement	Reference	Paragraph	Capability
Receiver Combining			
Receiver combining such that highest quality signal used for each bit decision for dual receiver option	1	2.2.1.2	Diversity combining plus receiver squelch ensures highest output signal level into demodulator/decoder for dual receiver operation
Transmitter			
S-band transmitter capable of simultaneously transmitting 32 kbit/sec real-time low rate housekeeping data and 640 kbit/sec of medium rate data	1	2.2.1.3	S-band transmitter capable of simultaneously transmitting 32 kbit/sec of real-time housekeeping data and 512 kbit/sec of medium rate data
Transmitter Data Selection			
Four selectable medium rate modes: 1) Ranging tones (500 kHz) 2) Memory dump (128 kbit/sec) 3) Tape recorder dump (640 kbit/sec) 4) Special instrument data	1	2.2.1.3	Selectable medium rate modes: 1) Ranging tones (500 kHz) 2) Tape recorder dump (512 kbit/sec) 3) Special instrument dump (512 kbit/sec) 4) Computer memory dump is time division multiplexed into 32 kbit/sec housekeeping data
RF Group-Receiver/Demodulator			
Active redundancy for dual receivers/demodulators	1	2.3.1.1	Active redundancy provided
RF Switch			
Transponder transmitter output to be switched by command to an antenna other than that used by a receiver	1	2.3.1.2	RF switch provided to switch transmitter to either antenna
Spherical Antenna Coverage			
Spherical antenna coverage provided	TRW	self-imposed	97 percent spherical antenna coverage provided at -1.0 dBi
Reliable Command Performance			
Reliable command performance provided	TRW	self-imposed	Worst Case Link Margins: Carrier: 49.2 dB Command: 47.3 dB (10^{-6} BER)
Reliable Telemetry Performance			
Reliable telemetry performance provided	TRW	self-imposed	Worst Case Link Margins: Mode 1: 32 kbit/sec housekeeping plus 512 kbit/sec medium rate data: Carrier: 33.8 dB 32 kbit/sec: 7.3 dB (10^{-6} BER) 512 kbit/sec: 8.4 dB (10^{-6} BER) Mode 2: 32 kbit/sec housekeeping plus 500 kHz tone ranging: Carrier: 38.5 dB 32 kbit/sec: 20.5 dB (10^{-6} BER) Ranging: 18.3 dB (5 meter, 1σ)
Simultaneous Command Distribution			
• Bus command rate: 16K commands/sec	2	p. 3, Item 4	All commands processed in any combination at the following rates:
• Computer commands: 62.5 commands/sec	1	2.2.2	Up to 24,000 commands/sec (telemetry = 64 kbit/sec)
• Computer pulse commands: 62.5 commands/sec	2	p. 3 Item 6	Up to 31,875 commands/sec (telemetry = 1 kbit/sec)
• Uplink commands: 50 commands/sec 62.5 commands/sec	1 2	2.2.2 p. 3, Item 5	46.5 commands/sec provided

Table 6-1. Requirements versus Capabilities (Continued)

Requirement	Reference	Paragraph	Capability
Data Acquisition			
• Telemetry data rate: Selectable: 1, 2, 4, 8, 16, 32 kbit/sec Up to 64 kbit/sec	1 2	2.2.2 p. 3, Item 2	Selectable: 1, 2, 4, 8, 16, 32, 64 kbit/sec
• Computer data rate: 32 kbit/sec 64 kbit/sec	1 2	2.2.2 p. 3, Item 3	Telemetry bit rate = 64 kbit/sec
Input Command Message			
Message length: 40 bits Bit rate: 2 kbit/sec Format: Introduction - 39 bits Phase - 1 bit Address - 7 bits Op. code - 2 bits Data - 24 bits Check code - 7 bits	1	2.2.2.1.1	Message length: 43 bits Bit rate: 2 kbit/sec Format: Introduction - 200 bits Phase - 1 bit Spacecraft address - 7 bits Op. code - 2 bits User code: 5 bits Channel ID - 6 bits Data - 16 bits Check code: 7 bits
Bus Configuration			
Three separate buses: 1) Command party line 16 kbit/sec, 125 command/sec 24-bit format 2) Telemetry address party line 128 kbit/sec, 8000 addresses/sec, 16-bit format 3) Telemetry data party line 64 kbit/sec, 8-bit words	1	2.2.2.1	Full duplex, two separate buses 1.024 Mbit/sec, flexible slot assignments Command/address bus Command format: 32 bits Data request format: 24 bits Data Bus Telemetry data: 8-bit words Computer data: Analog bilevel: 8-bit words Serial digital: 16-bit words
Full Duplex, two separate buses 1.024 Mbit/sec, 32K words/sec	2	p. 1	
Supervisory (command/address) 32-bit format continuous Manchester code	2	p. 1	Data clock derived from continuous Manchester code
Reply (Data) 12 to 29-bit format clocked by supervisory clock; delayed 64 to 66 μsec.	2	p. 1	
Remote Units			
• Number of units: 32 64	1 2	2.2.2.1 p. 1	Maximum number of units: 32
• Input power: two wire, 16 kHz square wave from CDH module	1	2.2.2.2	+28 volts from primary power bus
• Remote multiplexer: 64 data channels	1	2.2.2.2.1	64 data channel/data interface unit-expandable to 512 data channels by addition of up to seven expanders
• Remote decoder Command outputs: 64 pulse 4 serial digital	1	2.2.2.2.2	Command outputs: 32 pulse 7 serial digital can be expanded to 256 pulse commands/data interface unit, 56 serial digital by addition of up to seven expanders
On-board Computer			
• Type: general-purpose, digital binary, full parallel organization, one index register	1	2.2.3	General-purpose, digital binary, full parallel organization with one double length accumulator and one index register provided

Table 6-1. Requirements versus Capabilities (Continued)

Requirement	Reference	Paragraph	Capability
• Arithmetic:			
- Fixed point binary - 16-bit data word (min) - Add instruction <5μsec - Multiply instruction - Divide instruction - Double precision add <40 sec - Double precision multiply <200 sec - Four logic instructions: and, or, exclusive or, complement - conditional/unconditional transfers	1	2.2.3.3	- Fixed point binary - 18-bit word - 4μsec/add instruction - 30 μsec/multiply instruction - 60 μsec/divide instruction - <30 μsec/double precision add - Double precision multiply <150 sec - Four logic instructions provided: and, or, exclusive or and complement - conditional/unconditional transfers provided
• Memory:			
- Nonvolatile, expandable to 64K words in 8K word modules	1	2.2.3.1	- Nonvolatile memory provided expandable to 64K words in 8K word modules
- Cycle by cycle power switching of 8K memory modules (100 MW maximum increase in standby power per 8K module)			<100 MW (2-mil plated wire memory) Maximum standby per 8K module
- Protection against illegal write to memory			- Protection against illegal write to memory provided
• Input/Output:			
- 16 maskable interrupts	1	2.2.3.2	16 maskable interrupts provided
- All input/output channels must be able to operate in both DMA mode and program control mode			16 independent cycle steal operations time share one DMA channel

Sources: (1) "Data Handling Performance Specification for EOS," EOS-L-129, Section II, 30 January 1974
(2) NASA "Free Flyer" Multiplex Data Bus Characteristics, 4 June 1974

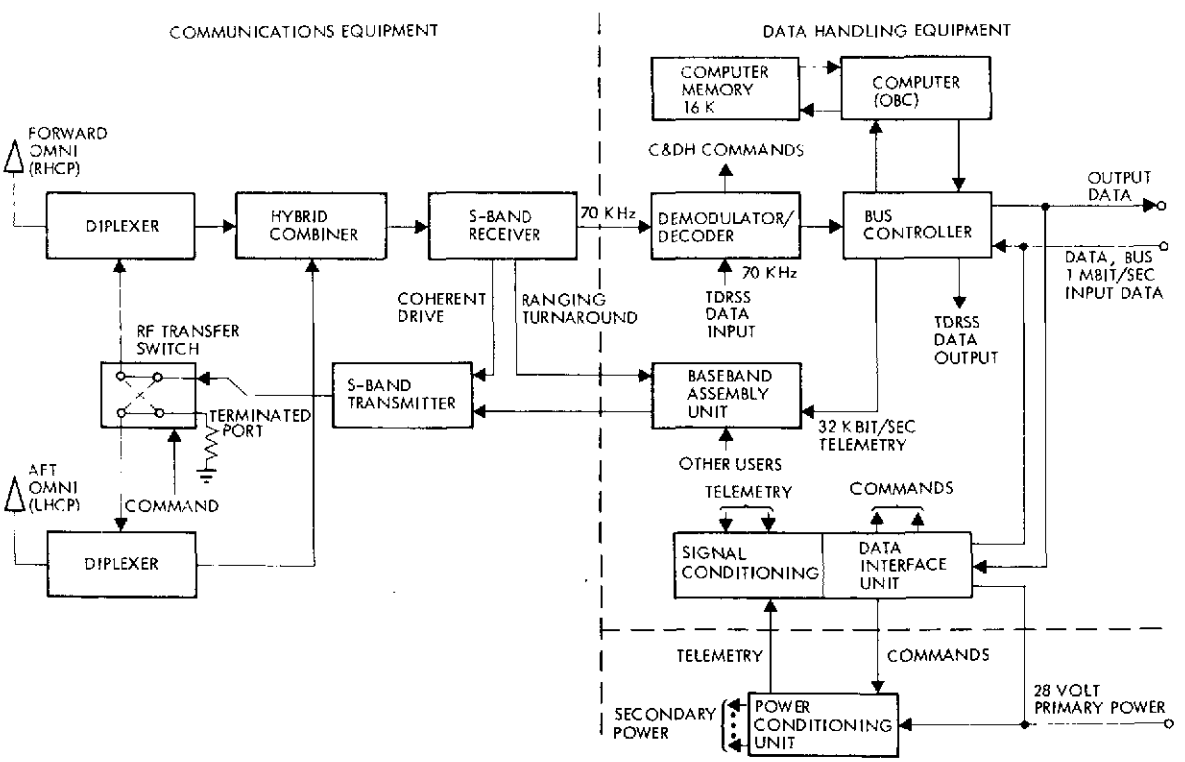

Figure 6-2. Communications and Data Handling Module Baseline Data

NASA STDN stations on a phase-modulated carrier lying within the 2050 to 2150 MHz range is received by one of two omni-directional antennas having opposite senses of circular polarization. One of the antennas is fix-mounted to the earth pointing side of the CDH module while the other is boom-deployed on the opposite or aft side. The outputs from the two antennas are connected by diplexers to a hybrid combiner. Since the ground station will transmit to the spacecraft with either right or left hand antenna polarization, only one antenna will be illuminated at a time. This effectively allows the spacecraft to be commanded via polarization diversity or polarization switching. Since the patterns of the two antenna are orthogonal by virtue of their opposite senses of polarization and since each antenna provides hemispherical coverage, uplink as well as down-link communications can be guaranteed for all orientations of the space-craft relative to the ground. Figure 6-3 illustrates the antenna coverage provided by the two antennas. Further, Section 5.1.2 of Appendix A discusses alternate diversity techniques.

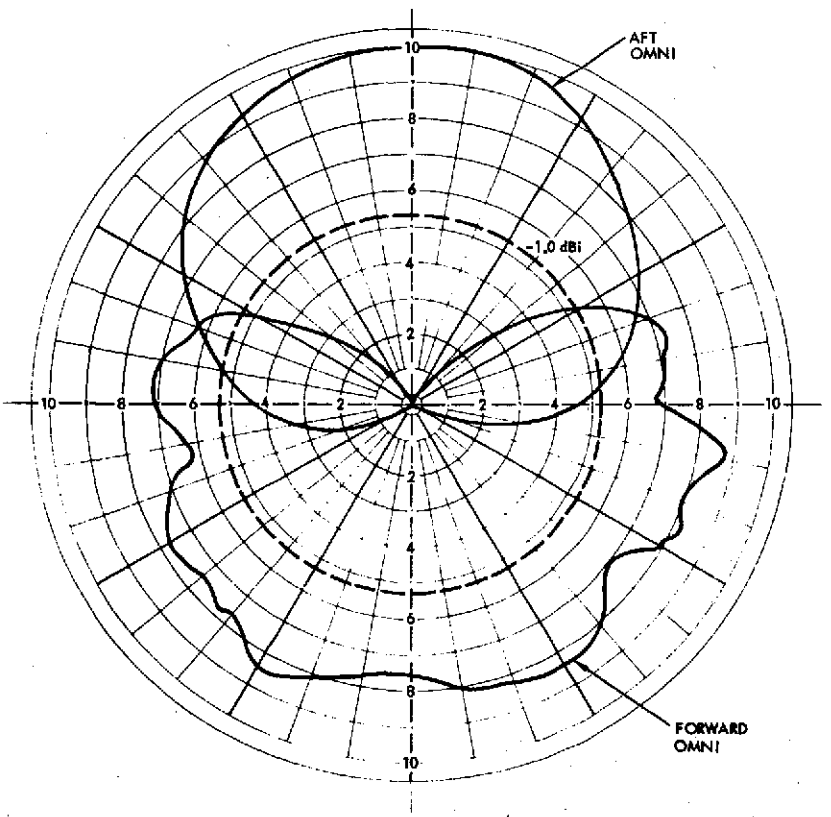

Figure 6-3. Omni Antenna Coverage

The output from the hybrid combiner is coupled into an S-band receiver. The receiver employs a phase-lock loop to acquire, track, and coherently demodulate the uplink carrier. The uplink information, phase-modulated onto the carrier consists of command data and tone ranging data having a PCM/PSK/FM/PM format. Command data having a PCM, split-phase, mark 1 format at 2 kbit/sec frequency modulates a 70 kHz subcarrier which is in turn combined with ranging tones to provide the baseband which phase modulates the uplink carrier. Figure 6-4a illustrates the uplink spectra.

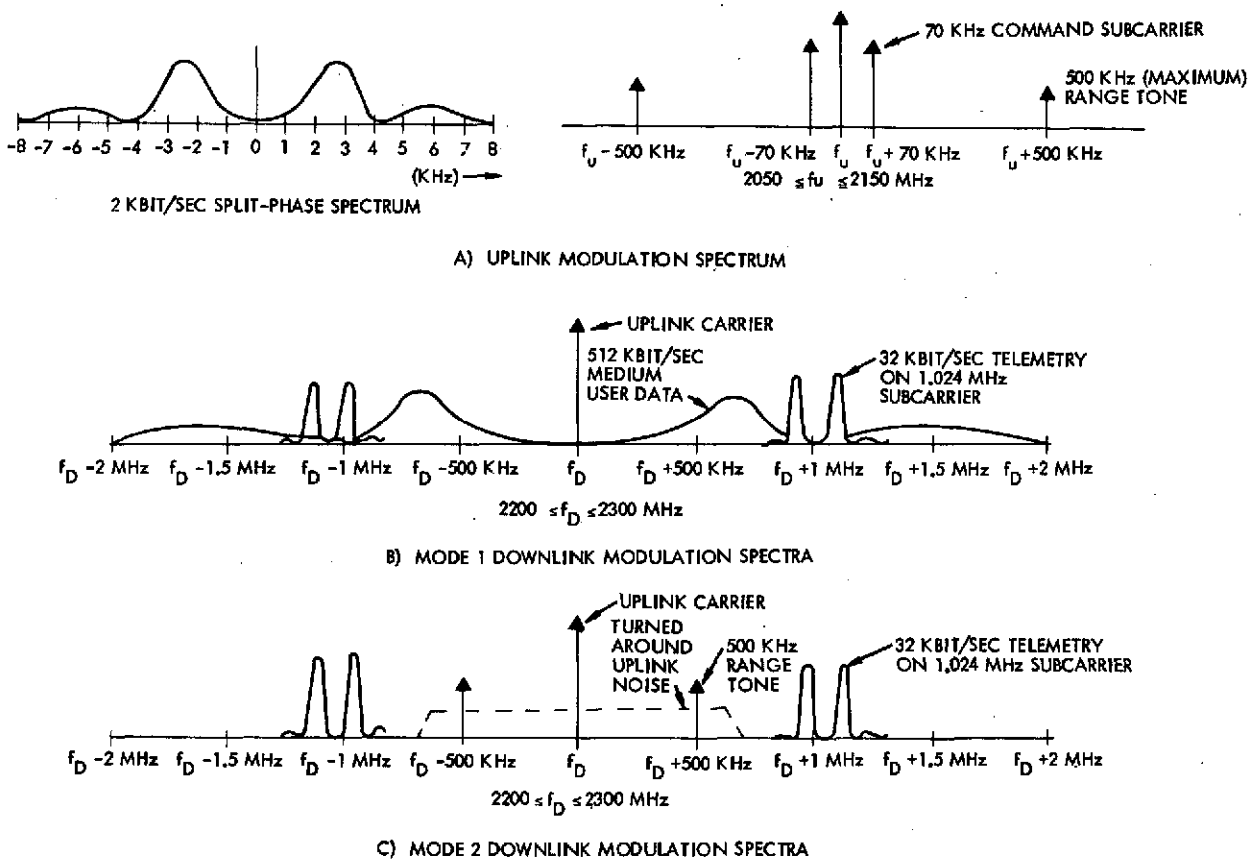

Figure 6-4. Communications Modulation Spectra

The receiver coherently demodulates the uplink carrier and provides three outputs. The command information, present on the 70 kHz subcarrier is provided as an input to a demodulator/decoder unit contained within the data handling segment of the CDH module. Tone ranging data, also demodulated from the uplink carrier, is provided to a baseband

assembly unit where it is combined with telemetry data to form the downlink baseband. Finally, a coherent carrier reference is provided to the transmitter. This reference, when suitably multiplied in frequency, forms the downlink carrier and provides range rate or doppler information.

The demodulator/decoder unit frequency discriminates the 70kHz subcarrier from the receiver and provides it to a 2 kbit/sec bit synchronizer-detector contained within the unit. The output from the synchronizer-detector, consisting of a detected 2 kbit/sec data stream plus clock is provided to a decoder, also contained within the unit. The output from the decoder, representing the output from the demodulator/decoder unit, is provided as an input to the bus controller unit.

The bus controller unit provides the control for the spacecraft data bus. Uplink commands from the demodulator/decoder unit are normally routed through the bus controller unit to the computer (OBC) where they are stored in memory by command time tag. The computer extracts these commands relative to the spacecraft clock and routes them to the bus controller unit which, in turn, sends them out on the spacecraft data bus. Uplink commands, suitably encoded, can be made to bypass the computer and fed directly through the bus controller unit to the data bus.

Each equipment module contained within the spacecraft will interface with the data bus by means of a data interface unit. The data interface units will decode command information sent out on the bus as well as encode telemetry information for transmission via the bus to the bus controller unit. The bus controller unit will format telemetry data from each of the data interface units and output it as a serial digital data stream at 32 kbit/sec to the baseband assembly unit.

In addition to outputting telemetry data in real-time to the baseband assembly unit, the bus controller unit will also output telemetry data to the computer. The computer processes this data with respect to programmed algorithms and limits and stores the resultant information into its associated memory. This allows housekeeping and experiment data to be collected and stored when the spacecraft is out of view of ground stations and effectively eliminates the need for an on-board housekeeping

data tape recorder. When the spacecraft is in view of a ground station, the computer will dump its memory into the bus controller unit where the data will be multiplexed, along with real-time housekeeping data to form the 32 kbit/sec output data stream to the baseband assembly unit.

The baseband assembly unit accepts the 32 kbit/sec data stream from the bus controller unit and split-phase modulates it onto a 1.024 MHz subcarrier which is then combined with medium rate user data, at 512 kbit/sec maximum to form the baseband output to the S-band transmitter. This comprises telemetry mode 1. In telemetry mode 2, the 512 kbit/sec medium rate data is replaced by tone ranging data (500 kHz maximum) from the S-band receiver. Figure 6-4b and c illustrates the downlink RF spectra for the two telemetry modes.

The S-band transmitter takes the composite baseband information from the baseband assembly unit and phase modulates it onto a coherent carrier reference provided from the receiver to provide a coherent downlink. In addition, the transmitter can be commanded into a noncoherent mode in which the carrier reference is provided from an internal oscillator. The RF output from the transmitter, consisting of a 2-watt, PCM/PSK/PM modulated carrier lying within the 2200 to 2300 MHz range, is provided to an RF transfer switch which allows the transmitter to be coupled (via the diplexer) to either of the two omni-antennas.

Power for the CDH module is provided from a central power conditioning unit. In addition, command and telemetry data for the module itself is processed by means of a data interface unit which is tied into the bus controller unit through the data bus.

For those missions requiring higher reliability than that provided by the baseline design, equipment can be added and cross-strapped as required. For example, a redundant receiver can be added by simply connecting it to the terminated port of the hybrid combiner in Figure 6-2. Further, a redundant transmitter can be accommodated by connecting its output to the terminated port of the transfer switch. Missions such as SEOS which require a higher EIRP can be accommodated by mounting a fixed, 2-foot parabolic antenna to the module and connecting it via an RF switch to the 2-watt transmitter.

6.1.4 System Performance

6.1.4.1 Frequency Plan and Modulation Format

The uplink and downlink frequency plan and modulation formats will be compatible with the NASA STDN/USB system. Uplink command data at 2 kbit/sec will be split-phase, mark-encoded, and frequency-modulated onto the USB, 70 kHz command subcarrier. The subcarrier will be summed with tone ranging data and the composite baseband will phase modulate an uplink S-band carrier lying in the 2050 to 2150 MHz range. Figure 6-4a shows the uplink command modulation spectra and Table 6-2 lists some of the command uplink communications parameters as well as the downlink parameters.

Information to be telemetered on the downlink will be transmitted in two modes. In mode 1, real-time data consisting of housekeeping telemetry and on-board computer memory dump information is time-division multiplexed and transmitted at a 32 kbit/sec, maximum rate. In addition, command selectable, medium rate user data at 512 kbit/sec maximum will also be transmitted. The 32 kbit/sec data will split-phase modulate the standard, USB 1.024 MHz subcarrier which will, in turn, phase modulate a downlink S-band carrier lying in the 2200 to 2300 MHz region. The 512 kbit/sec medium rate user data will be split-phase encoded and directly phase modulate the downlink carrier. Figure 6-4b depicts the downlink modulation spectra for mode 1.

In telemetry mode 2, the real-time, 32 kbit/sec telemetry will again split-phase modulate the 1.024 MHz subcarrier which will, in turn, phase modulate the downlink carrier. In place of the 512 kbit/sec, medium rate user data of mode 1, transponded uplink tone ranging data with a 500 kHz maximum, tone frequency will directly phase modulate the carrier. Figure 6-4c shows the modulation spectra for mode 2.

Finally, two-way range rate or doppler information will be provided by coherently heterodyning and phase tracking the uplink carrier by means of a phase-lock loop receiver and providing a coherent reference to the transmitter which, when suitably multiplied in frequency, will provide the downlink S-band carrier. The uplink carrier frequency will be related to the downlink carrier frequency by the ratio 221/240.

Table 6-2 lists some of the communication parameters for the CDH module.

Table 6-2. S-Band Telemetry, Tracking, and Command Parameters

Command Uplink

- Carrier frequency: 2050.0 MHz (assumption)
- Modulation: PCM/PSK/FM/PM
- Modulation indices: Command = 1.2 radian ±10 percent
  Ranging = 0.6 radian ±10 percent
- Bit rate: 2 kbits/sec
- Command modulution: PCM split-phase (mark)
- Command bit error rate: 10^{-6}

Telemetry Downlink

- Carrier frequency: 2226.2 MHz (assumption)
- Modulation: Mode 1: Real-time telemetry - PCM/PSK/PM
  512 kbits/sec medium telemetry - PCM/PM
  Mode 2: Real-time telemetry , PCM/PSK/PM
  Ranging: 500 kHz maximum
- Modulation indices: Mode 1: Real-time telemetry - 0.8 rad ±10%
  512 kbits/sec medium telemetry:
  1.1 radian ±10%
  Mode 2: Real-time telemetry - 1.3 rad ±10%
  Ranging: 0.9 radian ±10%
- Data rates: Modes 1 and 2: Real-time telemetry - 32 kbits/sec
  Mode 1 medium rate data: 512 kbits/sec
- Bit error rate: 10^{-6}

Tracking

- Ranging: Tone ranging with 500 kHz maximum frequency
- Range rate: Two-way range rate; uplink/downlink carrier ratio = 221/240

6.1.4.2 S-Band Telemetry, Tracking, and Command Link Calculations

This section presents the S-band link calculations for command, ranging and telemetry. The spacecraft communications and data handling systems are fully compatible with the NASA USB system. As is evident from Tables 6-3 and 6-4 a more than adequate performance margin exists for the three functions.

S-Band Uplink

Table 6-3 presents the link calculations which were performed for S-band uplink. The calculation was performed at 2050 MHz with an assumed ground station transmitter power level of 1 kw. This level is a typical value for the NASA STDN. The ground station antenna gain was taken as 43.0 dB, which is a typical value for the NASA 9-meter dish having a 50 percent efficiency. Assuming a spacecraft altitude of 716 km, the slant range to the spacecraft was found to be 2590 km for a 5-degree ground antenna elevation angle.

The spacecraft omni antenna gain was taken as -3.0 dBi over 95 percent of the sphere which is in effect, conservative since the combined patterns for the two omni antennas which will be used for EOS, typically provide -1.0 dBi coverage over 97 percent of the sphere. The spacecraft system equivalent noise temperature referred to the input to the receiver

6.1.5 Equipment Description

The communication and data handling equipment description is divided into two sections: communication equipment and data handling equipment. The communication equipment consists of the following components: diplexer, receiver transmitter/modulator, RF switch, baseband assembly, aft and forward omni. The data handling equipment consists of the following components: demodulator/decoder, bus controller, data interface units, on-board computer, and the central clock. (For the EOS-A baseline system, a high accuracy crystal oscillator with an oven is not necessary. The central clock is supplied by the bus controller crystal oscillator.)

Secondary power is supplied to all of the module components by a single converter unit. Off-the-shelf components with integrated

Table 6-3. Command Uplink Power Budget

Parameter	Nominal Value	Adverse Tolerance	Notes
Modulation format	PCM/PSK/ FM/PM	---	---
Frequency (MHz)	2050.0	0.0	---
Ground station transmitter power (dBm)	60.0	0.0	1 kw; "Spaceflight Tracking and Data Network User's Guide," STDN 101.1, p. 3-4
Ground station transmission losses (dB)	0.0	0.0	Assumed included in antenna gain
Ground station antenna gain (dB)	43.0	0.0	9-meter dish; RCP/LCP STDN User's Guide, STDN 101.1, p. 3-9
Polarization loss (dB)	0.0	0.0	Assumed included in antenna gain
Atmospheric attenuation at 5 deg elecation angle (dB)	0.3	0.1	Hogg and Mumford, "The Effective Noise Temperature of the Sky," The Microwave Journal, March 1960, p. 80
Space loss at 5 deg antenna elevation angle and 2590 km slant range (dB)	166.9	0.0	716 km circular orbit
Spacecraft antenna gain (dBi)	-3.0	0.0	95 percent spherical coverage
Spacecraft reception losses (dB)	5.1	0.2	Cabling = 0.3 dB; Diplexer = 1.5 dB; Hybrid combiner = 3.3 dB
Total received power at input to receiver (dBm)	-65.1	0.3	---
Spacecraft equivalent noise temperature referred to receiver input (°K)	2900.0	0.0	Assumes a spacecraft antenna temperature of 290°K with a noise figure of 10 dB referred to receiver input
Spacecraft reception system noise power spectral density (dBm/Hz)	-164.0	0.0	---
Received power to noise spectral density ratio (dB-Hz)	91.7	0.3	---
Carrier Performance			
Carrier modulation loss (dB)	4.3	1.0	Assumes 70 kHz command and subcarrier is phase-modulated onto the carrier at 1.2 radian ±10% simultaneously with tone ranging data at 0.6 radian ±10%
Received carrier-to-noise spectral density ratio (dB-Hz)	87.4	1.3	---
Carrier loop noise bandwidth (dB-Hz)	29.0	0.0	$2 B_{LO}$ = 800 Hz
Carrier-to-noise ratio (dB)	58.4	1.2	---
Carrier loop threshold (dB)	6.0	2.0	---
Carrier performance margin (dB)	52.4	3.2	---
Carrier performance margin less adverse tolerance (dB)	49.2	---	---
Command Performance (70 kHz subcarrier)			
Command subcarrier power-to-noise spectral density ratio (dB-Hz)	3.8	0.5	Assumes 70 kHz command and subcarrier is phase-modulated onto the carrier at 1.2 radian ±10% simultaneously with tone ranging data at 0.6 radian ±10%
Received subcarrier power-to-noise spectral density ratio (dB-Hz)	87.9	0.8	---

Table 6-3. Command Uplink Power Budget (Continued)

Parameter	Nominal Value	Adverse Tolerance	Notes
Discriminator FM improvement factor (dB)	6.7	0.0	$3\beta^2$. Assumes that command PSK data frequency modulates 70 kHz subcarrier with a modulation index of 1.25
Post-detection signal-to-noise spectral density ration(dB-Hz)	94.6	0.0	---
Detection noise bandwidth (dB-Hz)	33.0	0.0	2 kHz for 2 kbits/sec data
Command data energy-to-noise spectral density ratio (dB)	61.6	0.8	---
Theoretical energy-to-noise spectral density ratio required for BER = 10^{-6} (dB)	10.5	0.0	Coherent PSK detection
Degradation due to non-optimum detection (dB)	2.0	1.0	Assumed value
Command performance margin margin (dB)	49.1	1.8	---
Command performance margin less adverse tolerance (dB)	47.3	---	---

converters may use primary power. Primary power is supplied to the data interface units, which have internal power converters.

A detailed tradeoff analysis is contained in Appendix A, Sections 5.1.3 and 5.1.7.

6.1.5.1 Communications Equipment

This section describes the communication equipment portion of the communications and data handling module. All the equipment required to perform the telemetry, tracking, and command (TT&C) transmitter and receiver functions has been developed on previous programs so that no new development is needed for the EOS-A mission.

S-Band Omni Antennas (Forward and Aft)

Full antenna coverage is provided by two hemispherical coverage antennas which are hybrid-coupled to a single receiver. Each antenna is fed through a diplexer which permits simultaneous transmit and receive functions. A transfer switch is used to couple the transmitter with either antenna. Polarization diversity is used to eliminate antenna pattern interference. This is accomplished by using a left-hand circularly-polarized

antenna on the back side of the spacecraft and a right-hand circularly-polarized antenna on the front or earth-facing side of the spacecraft. To provide optimum coverage and minimum spacecraft blockage, the two antennas have slightly different beamwidths. The aft or back side antenna is boom-mounted and has a half-power beamwidth of 220 degrees. The earth-facing antenna is body-mounted and has a half-power beamwidth of 120 degrees. The pattern crossover occurs at the -1 dB point. Both antennas are the conical log spiral type having a VSWR less than 1.5:1. The 220 degree half-power beamwidth antenna was flown on the Defense Satellite Program spacecraft and the 120 degree half-power beamwidth antenna was flown on the Pioneer 10 and 11 spacecraft.

S-Band Diplexer

The transmit and receive functions are separated from the forward and aft antennas by diplexers. The diplexer design employs a six resonator bandpass filter in the receiver channel and an 11 resonator bandpass filter in the transmitter channel. The unit was developed for the Pioneer 10 and 11 spacecraft and is space-qualified.

RF Cables

The cabling of the various RF equipment can be implemented with a low-loss teflon spline dielectric semirigid coaxial cable. Where flexible cable is required, Type RG-142 is recommended. Both of these cables have been space-qualified.

S-Band Hybrid

The forward and aft antennas are connected to the receiver with an S-band four-port hybrid. A TEM mode unit using strip-line construction is available from Anaren Microwave Inc. and is recommended for this application.

S-Band Receiver

The uplink S-band command carrier is tracked and demodulated by a dual conversion phase lock receiver. The receiver design presented here is based on the current TRW Shuttle development program. A simplified functional block diagram is shown in Figure 6-5.

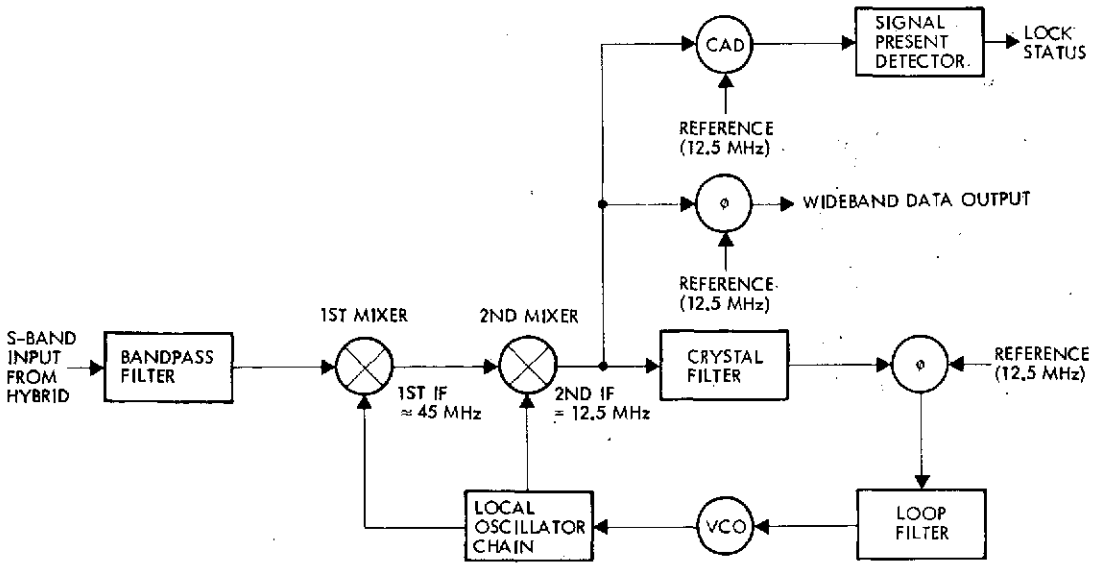

Figure 6-5. S-Band TT&C Receiver

As shown, the S-band signal from the diplexer is applied to a bandpass filter and first mixer where it is downconverted to IF.

The bandpass filter 3 dB bandwidth is 15 MHz which provides the required image frequency rejection. The particular filter used must be selected after the receiver USBS channel assignment has been made. The downconverted signal is amplified in the first IF (centered at 45 MHz) and heterodyned down in the second mixer to the second IF frequency of 12.5 MHz. After amplification in the second IF the signal is applied to the tracking loop phase detector (ϕ) through a narrowband crystal filter. The filter reduces the noise level at the phase detector input, thus minimizing the DC offset voltage at the output of the detector. The IF signal is also applied to a wideband phase detector for data detection and a coherent amplitude detector (CAD) for "signal present" detection.

The output of the loop phase detector (narrowband) is filtered in a second-order type integrating loop filter and applied to the carrier tracking VCO. The phase lock loop is formed by applying the VCO output to the multiplier chain which is used to drive the first and second mixers.

The signal is locked to the second IF frequency by applying a 12.5 MHz reference to the loop phase detector. A signal from the local

oscillator chain at X5 the VCO frequency is used to provide a coherent reference to drive the transmitter.

Receiver Mechanical Design. The receiver is fabricated with microminiature components on 14 alumina substrates using a reflow solder technique. The fourteen substrates are mounted in four shallow open-top machined modules. The modules are assembled in an opened top chassis that has a flush-mounted sheet metal cover with an RF gasket. was calculated at 2900°K for a 10 dB noise figure receiver and a 290°K reference temperature. The resulting worst-case performance margins were found to be 49.2 dB for the carrier and 47.3 dB for command. The command performance margin was calculated for a command bit error rate of 10^{-6}.

Finally, the probability of a false command execution was calculated to be 2.4×10^{-20} and the probability of a good command rejection was calculated at 7×10^{-6} over an input signal range from -112 dBm and above (see Appendix A, Section 5.1.1).

S-Band Downlink

Table 6-4 presents the link calculations which were performed for the S-band telemetry link. The calculation was performed at 2226.2 MHz for two telemetry modes. In mode 1, 32 kbit/sec real-time housekeeping and computer memory dump data is transmitted along with 512 kbit/sec medium rate user data. In mode 2, the 32 kbit/sec real-time data is transmitted with tone ranging data.

As seen from the table, a 2-watt transmitter is sufficient to telemeter the information in both modes to the ground station.

S-Band Transmitter

Downlink telemetry is provided by a 2-watt S-band transmitter coupled into the S-band omni by a diplexer. The transmitter generates a crystal-controlled carrier signal (noncoherent mode) or accepts a carrier from the receiver (coherent mode). Video information supplied by the baseband assembly unit is used to phase modulate the downlink carrier.

Table 6-4. Telemetry Downlink Power Budget

Parameter	Nominal Value	Adverse Tolerance	Notes
Modulation format	PCM/PSK, split-phase/ PM	---	---
Frequency (MHz)	2226.2	0.0	---
Spacecraft transmitter power (dBm)	33.0	0.0	2.0 watts
Spacecraft transmission losses (dB)	1.8	0.2	Cabling = 0.3 dB, RF transfer switch = 0.3 dB, Diplexer = 1.2 dB
Spacecraft antenna gain (dBi)	-3.0	0.0	95 percent spherical coverage
Space loss at 5 deg antenna elevation and 2590 km slant range (dB)	167.6	0.0	716 km circular orbit
Atmospheric attenuation at 5 deg elevation angle (dB0	0.3	0.1	Hogg and Mumford, "The Effective Noise Temperature of the Sky," The Microwave Journal, March 1960, p. 80
Polarization loss (dB)	0.0	0.0	Assumed included in antenna gain
Ground station antenna gain (dB)	44.0	0.0	9-meter dish. "Spaceflight Tracking and Data Network User's Guide," STDN 101.1, p. 3-9
Total received power (dBm)	-95.7	0.3	---
Ground station system noise temperature (°K)	166.0	0.0	Assumes a 150°K parametric amplifier noise temperature at zenith plus 16°K antenna temperature contribution at 5 deg elevation
Ground station system noise spectral density (dBm/Hz)	-176.4	0.0	---
Received power-to-noise spectral density ratio (dB-Hz)	80.7	0.3	---
Mode 1: 32 kbits/sec housekeeping and computer dump data plus 512 kbits/sec medium data rate user telemetry			
Carrier Performance			
Carrier modulation loss (dB)	8.3	2.5	Assumes 32 kbits/sec housekeeping and computer dump data split-phase modulates the 1.024 MHz subcarrier which in turn, phase modulates the carrier at 0.8 radian ±10%, The 512 kbit/sec data directly phase modulates the carrier at 1.1 radian ±10%.
Received carrier power-to-noise spectral density ratio (dB-Hz)	72.4	2.8	---
Carrier loop noise bandwidth (dB-Hz)	27.8	0.0	$2 B_{LO}$ = 600 Hz
Carrier-to-noise ratio (dB)	44.6	2.8	---
Carrier loop threshold (dB)	6.0	2.0	Assumed tolerance
Carrier performance margin (dB)	38.6	4.8	---
Carrier performance margin less adverse tolerance (dB)	33.8	---	---
32 kbit/sec Housekeeping Plus Computer Dump Telemetry Performance			
1.024 MHz subcarrier modulation loss (dB)	12.5	3.0	Assumes 32 kbit/sec housekeeping and computer dump data split-phase modulates the 1.024 MHz subcarrier which in turn phase modulates the carrier at 0.8 ±10% radian. The 512 kbit/sec data directly phase modulates the carrier at 1.1 radian ±10%

Table 6-4. Telemetry Downlink Power Budget (Continued)

Parameter	Nominal Value	Adverse Tolerance	Notes
Received data power-to-noise spectral density ratio (dB-Hz)	68.2	3.3	---
Detection bandwidth equivalent to bit rate (dB-Hz)	45.1	0.0	32 kHz for 32 kbits/sec
Received data energy-to-noise spectral density ratio (dB)	23.1	3.3	---
Theoretical energy-to-noise spectral density ratio required for 10^{-6} BER (dB)	10.5	0.0	Optimum detection of PSK
Degradation due to non-optimum detection (dB)	1.0	1.0	"Specification for a Manned Spaceflight MSTFP-3 PCM Decommutator System," NASA/GSFC, June 16, 1970, GSFC-S-8121P135, p. 6. Assumed tolerance.
32 kbits/sec telemetry performance margin (dB)	11.6	4.3	---
32 kbits/sec telemetry performance margin less adverse tolerance (dB)	7.33	---	---
512 kbit/sec Medium Rate User Telemetry Performance			
512 kbit/sec data modulation loss (dB)	2.5	0.9	Assumes 32 kbit/sec housekeeping and computer dump data split-phase modulates the 1.034 MHz subcarrier which in turn, phase modulates the carrier at 0.8 radian ±10%. The 512 kbit/sec data directly phase modulates the carrier at 1.1 radian ±10%
Received data power-to-noise spectral density ratio (dB-Hz)	77.2	1.2	---
Detection bandwidth equivalent to bit rate (dB-Hz)	57.1	0.0	512 kHz for 512 kbits/sec
Received data energy-to-noise spectral density ratio (dB)	22.1	1.2	---
Theoretical energy-to-noise spectral density ratio required for 10^{-6} BER (dB)	10.5	0.0	Optimum detection of PSK
Degradation due to non-optimum detection (dB)	1.0	1.0	"Specification for a Manned Spaceflight MSTFP-3 PCM Decommutator System," NASA/GSFC, June 16, 1970, GSFC-S-8121P135, p. 6. Assumed tolerance.
32 kbits/sec telemetry performance margin (dB)	10.6	2.2	---
32 kbits/sec telemetry performance margin less adverse tolerance (dB)	8.4	---	---
Mode 2: 32 kbits/sec housekeepong and computer dump data plus 500 kHz tone turnaround ranging			
Command Performance			
Carrier modulation loss (dB)	5.0	1.1	Assumes 32 kbit/sec telemetry data split-phase modulates the 1.024 MHz subcarrier which in turn, phase modulates the carrier at 1.3 radian ±10%. The 500 kHz range tone phase modulates the carrier at 0.9 radian ±10%
Received carrier power-to-noise spectral density ratio (dB-Hz)	75.7	1.4	---

Table 6-4. Telemetry Downlink Power Budget (Continued)

Parameter	Nominal Value	Adverse Tolerance	Notes
Carrier loop noise bandwidth (dB-Hz)	27.8	0.0	2 B_{LO} = 600 Hz
Carrier-to-noise ratio (dB)	47.9	1.4	---
Carrier loop threshold (dB)	6.0	2.0	Assumed
Carrier performance margin (dB)	41.9	3.4	---
Carrier performance margin less adverse tolerance (dB)	38.5	---	---
32 kbits/sec Housekeeping Plus Computer Dump Telemetry Data			
1.024 MHz subcarrier modulation loss (dB)	2.3	0.5	Assumes 32 kbit/sec telemetry data split-phase modulates the 1.024 MHz subcarrier which in turn, phase modulates the carrier at 1.3 radian ±10%. The 500 kHz range tone phase modulates the carrier at 0.9 radian ±10%
Received data power-to-noise spectral density ratio (dB-Hz)	78.4	0.8	---
Detection bandwidth equivalent to bit rate (dB-Hz)	45.1	0.0	32 kHz for 32 kbits/sec
Received data energy-to-noise spectral density ratio (dB)	33.3	0.8	---
Theoretical energy-to-noise spectral density ratio required for 10^{-6} BER (dB)	10.5	0.0	Optimum detection of PSK
Degradation due to non-optimum detection (dB)	1.0	1.0	"Specification for a Manned Spaceflight MSTFP-3 PCM Decommutator System," NASA/GSFC, June 16, 1970, GSFC-S-8121P135, p. 6. Assumed tolerance
32 kbit/sec telemetry performance margin (dB)	21.8	1.8	---
32 kbit/sec telemetry performance margin less adverse tolerance (dB)	20.0	---	---
500 kHz (Grarr) Ranging Performance			
500 kHz tone modulation loss (dB)	28.0	2.2	Assumes 32 kbit/sec telemetry data split-phase modulates the 1.024 MHz subcarrier which in turn, phase modulates the carrier at 1.3 radian ±10%. The 500 kHz range tone phase modulates the carrier at 0.9 radian ±10%
Received 500 kHz tone signal to noise spectral density ratio (dB)	52.7	2.4	---
Signal-to-noise ratio required for 5-meter RMS error due to thermal noise (dB)	32.0	0.0	1 Hz bandwidth
500 kHz tone ranging performance (dB)	20.7	2.4	---
500 kHz tone rangine performance less adverse tolerance (dB)	18.3	---	---

A simplified transmitter block diagram is shown in Figure 6-6. As shown, a reference signal at approximately 92 MHz is applied to a phase modulator. The reference is supplied by either a crystal oscillator or the receiver. The phase modulator output is used to drive a x24 multiplier chain which brings the signal up to S-band and increases the phase modulation index to the desired level. The S-band signal is then applied to a solid state power amplifier that supplies a 2-watt signal to the diplexer.

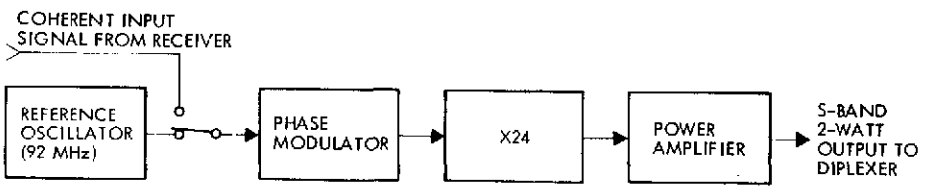

Figure 6-6. S-Band 2-Watt TT&C Transmitter

Transmitter Mechanical Design. The transmitter is fabricated with the same reflow solder microminiature technique described above for the receiver.

RF Switch

A coaxial switch is used to connect the transmitter to either the forward or aft omni antennas. The switch is a high-reliability unit that was used on Pioneer 10 and 11. It is manufactured by Teledyne Microwave.

6.1.5.2 Data Handling Equipment

The data handling equipment is illustrated in Figure 6-7 and described in the following paragraphs.

Demodulator/Decoder

The demodulator/decoder similified block diagram is shown in Figure 6-8. The unit is a modified version of the Particles and Fields and HEAO decoders with a redesign of the data detector and digital processor.

The demodulator/decoder has one input from the command receiver and one serial output to the bus controller. Command priority (direct

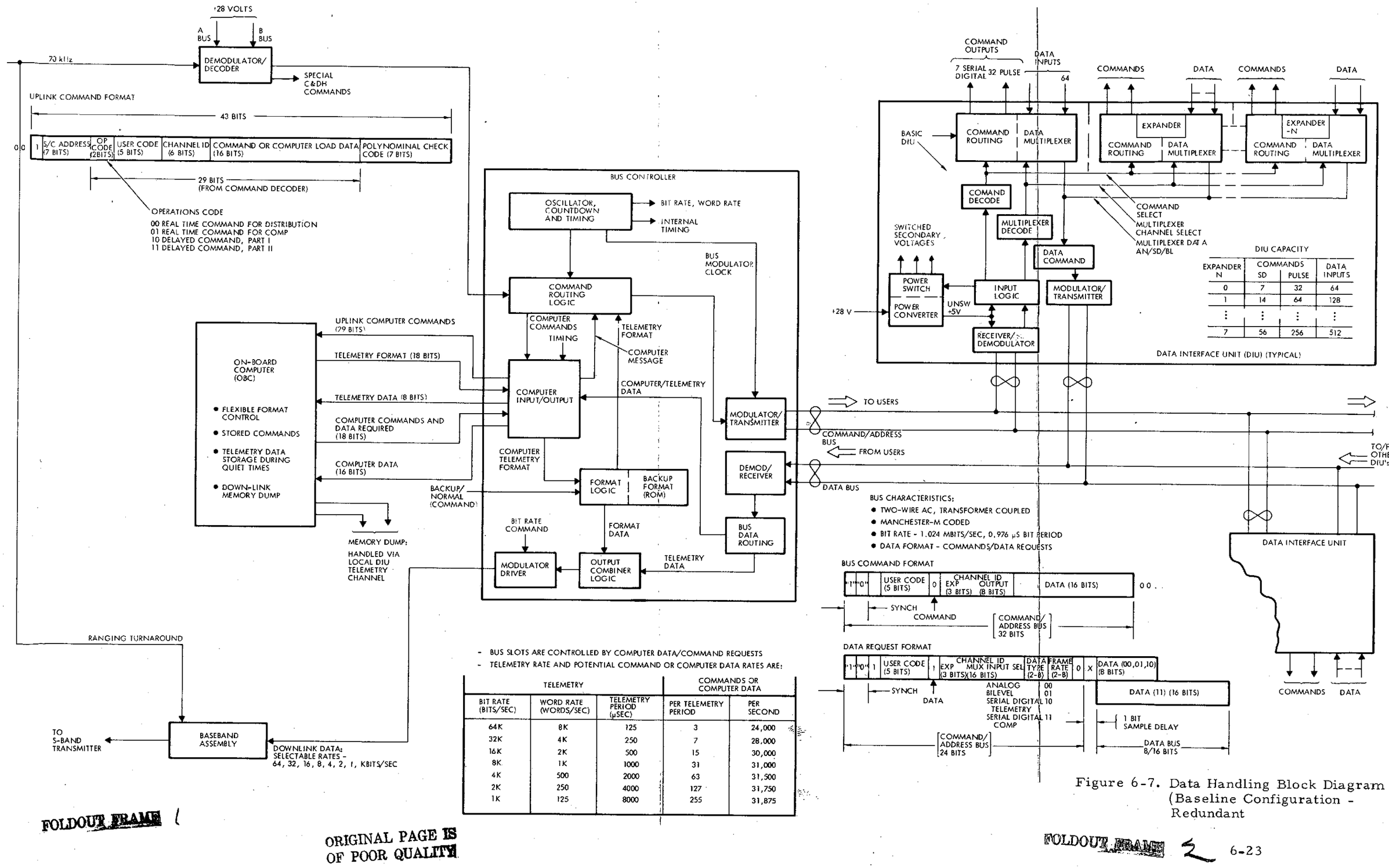

- BUS SLOTS ARE CONTROLLED BY COMPUTER DATA/COMMAND REQUESTS
- TELEMETRY RATE AND POTENTIAL COMMAND OR COMPUTER DATA RATES ARE:

TELEMETRY			COMMANDS OR COMPUTER DATA	
BIT RATE (BITS/SEC)	WORD RATE (WORDS/SEC)	TELEMETRY PERIOD (μSEC)	PER TELEMETRY PERIOD	PER SECOND
64K	8K	125	3	24,000
32K	4K	250	7	28,000
16K	2K	500	15	30,000
8K	1K	1000	31	31,000
4K	500	2000	63	31,500
2K	250	4000	127	31,750
1K	125	8000	255	31,875

Figure 6-7. Data Handling Block Diagram (Baseline Configuration - Redundant

FOLDOUT FRAME 1

ORIGINAL PAGE IS OF POOR QUALITY

FOLDOUT FRAME 2

data bus or computer stored) is established in the bus controller. A validate pulse at the end of the command word indicates recognition of the sync code, the decoder address, and the seven-bit polynomial check code (see Figure 6-8).

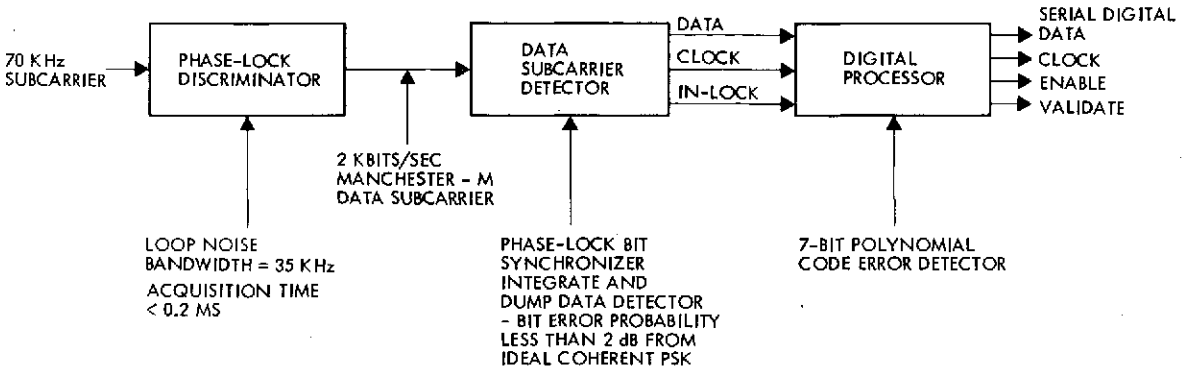

Figure 6-8. Baseline Command Decoder Simplified Block Diagram

Two special commands are decoded directly in the decoder giving discrete pulse outputs. The first command turns off computer power and the second puts the bus controller in the backup mode, using the internal ROM to generate the telemetry format.

Data Bus System

The data bus system configuration is shown in Figure 6-7, including its interface with the demodulator/decoder, the on-board computer (OBC), and the baseband assembly. The data bus system comprises the bus controller unit (BCU), the command/address bus, the data bus, and the remotely located data interface units (DIU).

Bus messages are controlled by uplink commands, computer generated instructions, or fixed backup telemetry format.

Figure 6-9 illustrates the 29-bit message format for the uplink commands received from the demodulator/decoder. The message has two parts:

1) Op code. Two bits identifying command type.
   - 00, 01 — Real time commands for bus users (00) or computer (01) to be executed directly.
   - 10, 11 — Delayed commands for the computer.

2) Command Message – 27 bits

Computer inputs will have computer designated format.

Real time commands have the following components:

- User ID – 5 bits identifying up to 32 different remote users.
- Channel ID – 6 bits identifying up to 56 serial digital commands and eight pulse command channels per user.
- Command Data – 16 bits of data giving serial digital magnitude or identifying one of 64 pulse commands within a channel.

In addition, special commands to control critical functions are decoded within the demodulator/decoder and separately provided to the BCU.

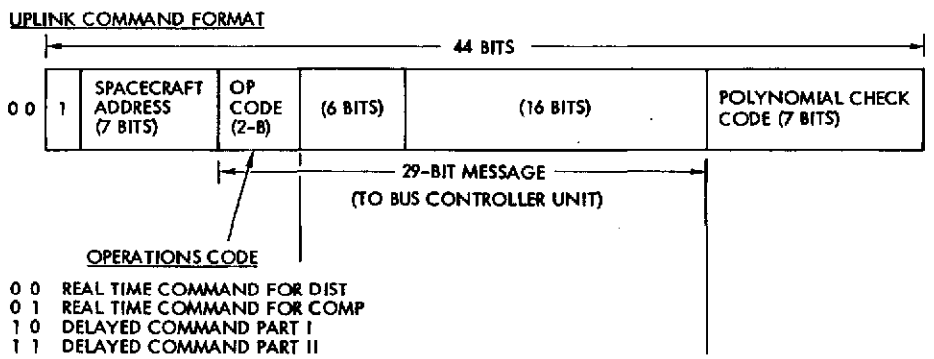

Figure 6-9. Command Format

The computer interface provides for transferral of uplink computer commands, computer generated telemetry formatting, computer requests for data, stored computer commands, and data for the computer. Computer memory dump can be made through a DIU telemetry channel under computer format control.

There are two user AC-coupled buses transmitting data from the BCU to the DIU's (command/address) or from the DIU's to the BCU (data). Each unilateral bus operates at 1.024 Mbit/sec.

Each of the DIU's provides commands and telemetry sampling as required by the using module. Figure 6-9 shows the expandable features of the DIU where the command and telemetry capability can be augmented by the addition of up to seven expanders per DIU. The using modules can

interface directly with the DIU or with signal conditioning for command pulse stretching, register buffering, or telemetry conditioning.

The telemetry data to be transmitted on the downlink is routed to the baseband assembly as NRZ data at a bit rate selectable between 1 and 64 kbit/sec.

Bus Formats

The format for the command/address derived from the uplink command is shown in Figure 6-9. Data bus messages are shown following the data request.

For the bus command format, a synchronous code and a bit to identify the message as a command are added to the 27-bit uplink command format to form the 32-bit command message, as shown in Figure 6-8.

Bus Characteristics. Operational bus characteristics are as follows:

- AC Coupling. A single twisted shielded pair shielded line is used in a balanced configuration using transformer coupling at the receivers and capacitor coupling at the transmitters. Transformer coupling at the receiver provides common mode rejection while maintaining transmission line balance. Isolation resistors in the transformer lines preclude transformer shorts from disabling the bus. Capacitive coupling at the transmitters provide low impedance coupling to the transmission line maintaining DC isolation.

- Manchester Coding. Manchester-M coding is used to maintain zero DC component on the line. Encoding is one cycle per bit. The message on the command/address line begins with the 4-bit sync code followed by the specific command or data request (see Figure 6-10).

- Bit Rate. A 1.024 Mbit/sec bit rate enables handling the maximum telemetry and command signals anticipated.

- Bus Time Slots. In Figure 6-7, the time slots for the command/address bus are shown related to the telemetry period. The slot assignments are determined by the telemetry bit rate selected and the computer controlled format, command list, and data requests. The table in Figure 6-7 shows the relationships of telemetry word rate and command or computer data rates to telemetry bit rate. An uplink real time bus command would override any message currently being processed.

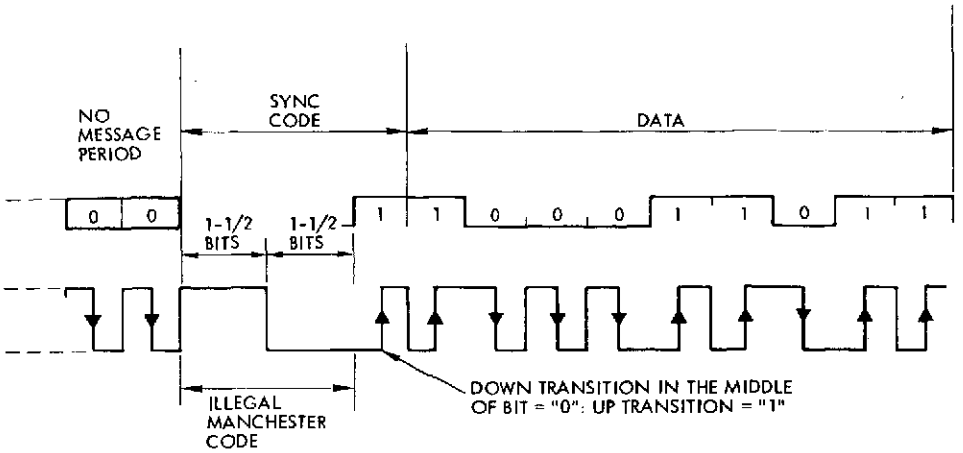

Figure 6-10. Typical Modulation Waveforms

On-Board Processor and Software

On-Board Processor. The key on-board processor (OBP) requirements are summarized below (refer to Appendix A, Section 5.1.4):

- Straightforward computer architecture
- 16-bit minimum word length
- Hardware multiply and divide
- Capability to implement double length arithmetic (32 bits minimum). Double length add 40 μsec, multiply 200 μsec.
- Good logical and conditional branch instructions
- Fast add time: 5 μsec minimum
- Direct memory access channels; expandable to 16
- Hardware protection against illegal write to memory; region selectable via software
- 16 interrupts; individually maskable
- 16K words of memory expandable to 64K in 8K increments
- Plated wire memory with capability for using semiconductors on future missions
- Cycle-by-cycle power switching of memory modules.

The Goddard AOP is selected for the baseline computer. This selection is based on three major criteria: 1) the AOP meets all of the

requirements listed above (none of the other candidates include two important features: "selectable write protect" and "cycle by cycle power switching"); 2) use of the AOP is planned for several future Goddard programs with similar applications; and 3) previous OAO-OBP flight experience has been satisfactory. The OBP is, in essence, the prototype AOP.

The selection of the AOP as the baseline is made independent of costs: the interfacing component, the bus controller will operate with any of the candidate computers, so the final selection can be made at any time. Also, normalized AOP costs, as shown in Table 6-5, are not final. Present estimates for the AOP central processor LSI chips indicate that substantial reductions from the Table 6-5 costs are possible. In production, AOP costs should be competitive with alternate OBC selections.

The simplest computer which can be devised and which will meet the requirements for the EOS missions will contain two 8K by 16-bit plated-wire memory modules. The memory will be expandable in 8K modules to a maximum capacity of 64K by 16 bits. Nonvolatility of the stored data in case of power failure is required.

The preference for plated-wire is a result of properties of its true nonvolatility and nondestructive readout (NDRO) combined with parameter stability over a wide temperature range. Plated-wire and its associated system parameters make it ideal for severe environmental, low wattage, and small volume conditions.

On-Board Software. The on-board software will be developed in keeping with the groundrules listed below. These groundrules stress straightforward software, easy to check out and modify, and an executive structure which can accommodate different missions without reprogramming. This approach is in keeping with the low-cost approach although it does increase the initial programming effort.

- Modularity. Develop functional elements independently prior to integration with executive
- Executive must be easy to modify and debug

Table 6-5. Characteristics of Candidate Computers

	Goddard AOP	Autonetics D216	CDC 469	Bendix BD-910
Add time (μsec)	4.0	2.0	2.4	2.0
Multiply time (μsec)	30	11	13	21
Word length	18	16	16	16
Memory capacity	64K	64K	32K	32K
DMA	Yes	Yes	No	Yes
Microprogrammable	No	Yes	No	Yes
Selectable write protect	Yes	No	No	No
No. of instructions	55	100	42	72
Interrupt levels	16	7	3	12
Cycle-by-cycle power switching	Yes	No	No	No
Double length add (hardware)	No	Yes	Yes	No
Double length multiply (hardware)	No	Yes	No	No
Weight (lb)	9	10	8	7.5
Power (watts)	10	65	23	22
Relative cost	4	1	1	0.8

- Executive must have well-defined behavior
  - Provide linkage between program elements
  - Satisfy subsystem data execution rate requirements
  - Control input/output
  - Provide rescheduling capability
- Capability for adding and modifying functions from ground

- Extensive ground simulation to check out program changes
- Ability to accommodate different missions without reprogramming executive
- Diagnostic routines executed both as scheduled application programs and during dead time
- Ability to handle stored commands
- Efficient coding concepts borrowed from structured programming

Storage estimates for the software modules which comprise the computer programs are shown in Table 6-6.

Table 6-6. Software Modules and Storage Estimates

Program	Instructions	Data
Executive		
Interrupt handlers	100	70
Input/output control	300	50
Telemetry control	100	500
Computer data control	100	250
Stored commands processing	150	1000
Data dump control	100	50
Application program scheduling	200	200
Application Programs		
Attitude control and determination	4700	1700
Thermal control	200	120
Power monitoring	50	20
Telemetry data storage	150	2000
Experiment control	150	100
Real time command processing	300	100
Self-test	350	50
Total	6950	6210

6.2 ATTITUDE DETERMINATION MODULE

The attitude determination module (ADM) houses the attitude control hardware that is used without change for all missions. The multimission module is applicable to a wide variety of orbits for both earth and inertial pointing. This universality is achieved using existing state-of-the-art components.

Table 6-7. Attitude Determination Module Equipment List (Minimum Redundancy)

Unit	Source	Program Derivation	Quantity	Unit Weight (lb)	Unit Size (in.)	Unit Power (watts)
Inertial reference unit	Bendix	IUE	3	7	8 x 10 x 6	8
Star tracker	Ball Bros.	SAS0C	3	11	5 x 6 x 12	5
Magnetometer	Schoenstedt	SESP 72-1	1	4	Sensor, 4 x 4 x 3 Electronics, 6 x 6 x 3	1
Sun sensor	TRW	HEAO	1	1	4 x 6 x 2	-
Transfer assembly	TRW	HEAO	2	13	6 x 8 x 11	16
Data interface unit	TRW	-	2	4	3.5 x 6 x 8	2.5
Power conditioning unit	TRW	HEAO	2	3	1.5 x 8 x 8	2.5
Star tracker shade	TRW	Pioneer F	3	2.5	9D x 21	-

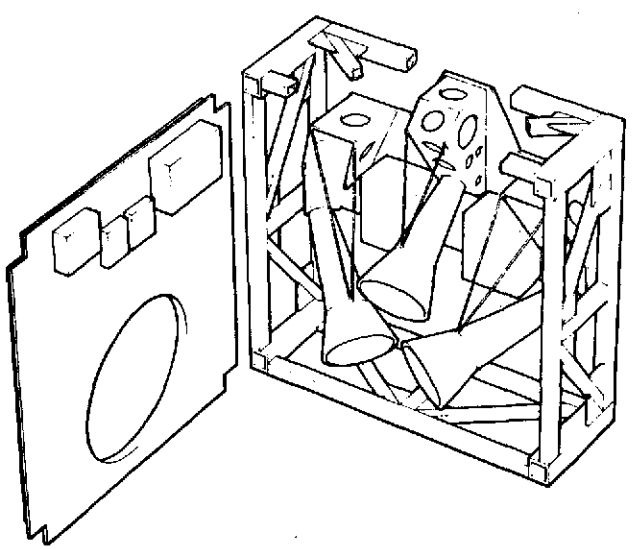

Figure 6-11.
Attitude Determination Module

The selected baseline equipment list for the EOS-A attitude determination module is shown in Table 6-7. The ADM applicable to use of either the Thor-Delta or Titan booster is shown in Figures 6-11 and 6-12. The level of redundancy shown eliminates single-point failures which would prevent entry into the safe mode or Shuttle resupply/retrieval. Section 3.7 describes, in general, the design for the ADM. Additional discussion of the EOS-A design selection is presented below.

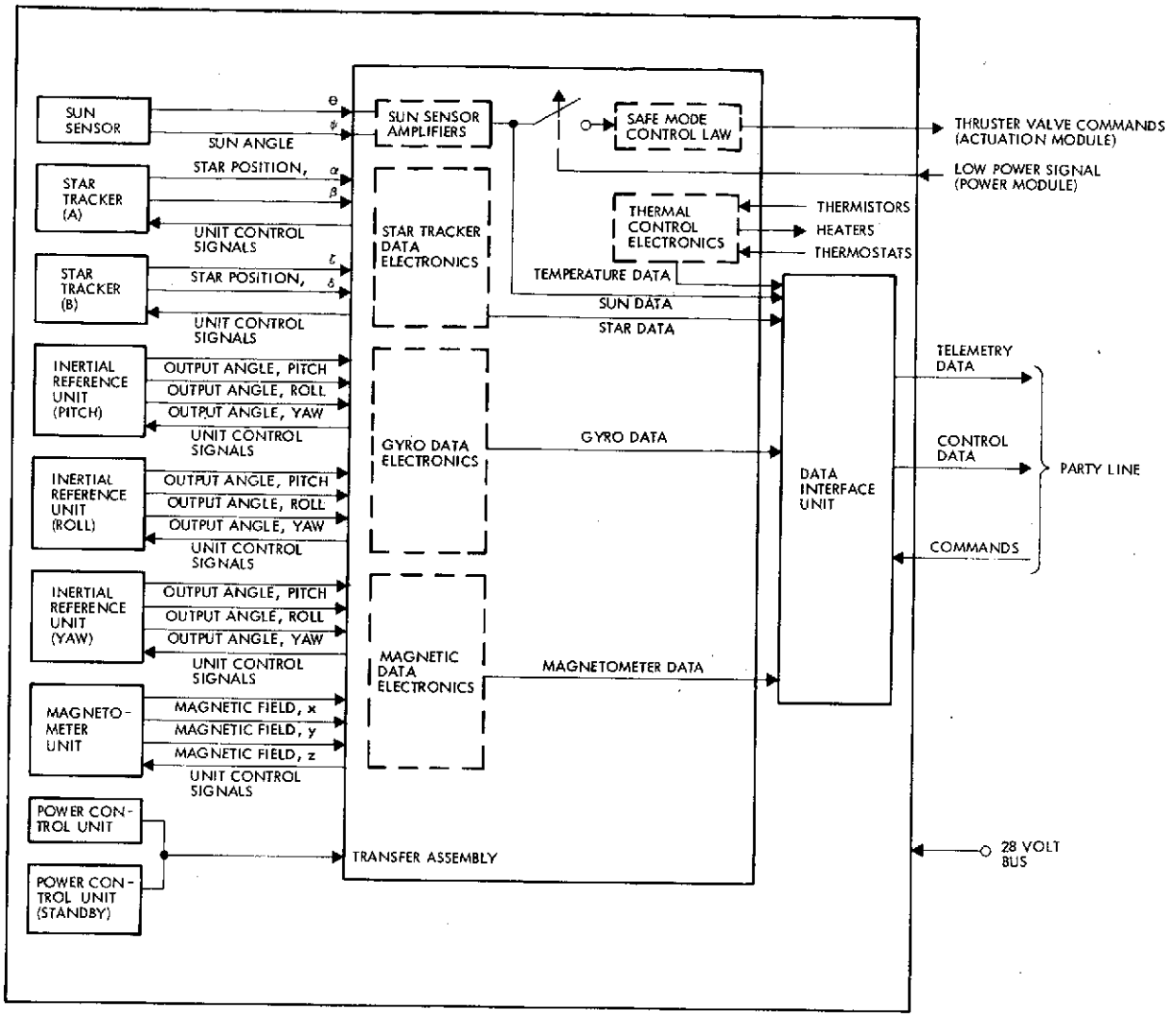

Figure 6-12. Attitude Determination Module Block Diagram

6.2.1 Inertial Reference Unit

Each inertial reference unit (IRU) contains a single-degree-of-freedom gas-bearing gyro (Bendix PM RIG-2000) and the associated support electronics developed for the IUE program. Gyro selection and redundancy concepts are discussed in Appendix A, Section 5.2. Pulsewidth-modulated binary capture loops are used to maintain the gyro pickoffs at null. The output of this pulse torque loop is a quantized series of binary pulses. In this design each pulse represents an angular increment of 0.1 arc-sec. These pulses are accumulated to provide integrated incremental attitude changes over a readout period.

6.2.2 Star Tracker Assembly

Star tracker assembly (STA) detail design and selection considerations are presented in Appendix A, Section 5.2. The star tracker selected for EOS-A is the Ball Brothers unit developed for SAS-C. A stray-light shade will be incorporated. Three STA's are installed with one out of the three providing standby redundancy.

The STA has an 8 x 8 degree square field of view. Its optical axis lies in a plane perpendicular to the scan axis such that spacecraft rotation provides star tracker scan motion. Target stars moving through the STA field of view are acquired and tracked at angular rates up to 0.4 deg/sec (0.6 deg/sec will be a design goal).

The repeatability on nonlinearity, distortion (pin cushion effect, fixed distortion), and gain variations in response to environmental changes (temperature, star color, star magnitude, and magnetic fields) will allow determination of a star's true angular position relative to the STA optical axis to within 10 arc-sec. This will be performed by applying correction factors determined during sensor manufacture and acceptance testing.

The STA major elements are an optical system with a protective bright object shutter, an image dissector with focus and deflection coils, signal processing electronics, and a bright object sensor provided as a part of the STA but mounted remotely from it. The 76 mm f/0.87 Super Farron lens (Farrand Optical Company) is space-qualified and spectrally corrected for optimum performance down to sixth magnitude star detection. The bright object sensor and shutter mechanism (located in the lens housing) protects the image dissector tube from excess energy. A bilevel logic signal becomes true and the shutter closes when a bright object comes within 35 degrees of the STA optical axis. The response time of the shutter is sufficiently small to provide protection at a 6 deg/sec spacecraft angular rate.

The type F4012RP image dissector tube (ITT, Inc.) is space-qualified and specifically designed for star tracker application. Uniformity and freedom from contamination are provided by separate fabrication and test of the photo cathode. An internal voltage divider for the dynode chain gives excellent long term gain stability.

A video processor receives the star threshold commands and develops a digital star presence signal and an analog star magnitude signal. A mode control logic places STA functional blocks into a search or track mode in response to either the star presence signal or a telemetered search command. Search scan and track scan generators provide waveforms for the X and Y deflection currents. When in the track mode, a demodulator converts the thresholded video signal into tracking loop error correction voltages. X and Y integrators produce the voltage inputs to the X and Y deflections current amplifiers. This keeps the track scan centered on the moving star image. Finally, the output amplifiers sample the deflection coil currents and provide filtered output voltages proportional to the X and Y angular star position.

A folded stray light shade (thermally isolated from the lens) provides 10^8 attenuation of sunlight or earthshine for angles outside 48 degrees of the STA optical axis. Conical in shape, the outer diameter is 9 inches and the overall shade length is 21 inches.

6.2.3 Magnetometer

A single triaxial fluxgate magnetometer is installed in the attitude determination module. The unit built by Schoenstedt Instruments for SESP 72-1 spacecraft has been selected for the EOS-A baseline design.

The magnetometer assembly employs three fluxgate magnetometers sharing a common excitation reference section, with remotely positioned sensors mounted at right angles to each other. Each sensor coil primary is excited by an oscillator which is divided successively by two flip-flops to obtain a fundamental square-wave whose frequency is exactly twice the fundamental. The fundamental waveform is filtered, amplified, and applied as a relatively pure sine wave to the primary windings of the sensor coils. Any DC magnetic field, such as the earth's, tends to bias the iron core of the sensor to a nonlinear region of the B-H curve, resulting in a distorted output waveform at the secondary winding. The distortion is essentially second harmonic components, which are amplified in a second harmonic bandpass amplifier. The amplified second harmonic is demodulated in a phase sensitive demodulator, amplified again and fed

back to the secondary winding as a DC current which counteracts the applied DC magnetic field. This negative feedback allows a high degree of linearity and stability of output, virtually independent of the magnetic properties of the sensor coil. The DC voltage is further filtered and buffered with another amplifier to provide outputs to telemetry in the standard 0 to ±5 volt format.

The magnetometer attitude assembly is capable of flux density measurements from ±0.5 gauss, to a resolution of 0.004 gauss and with stability and scale factor accuracy within ±1 percent of full scale. Selection of suitable oscillator frequency and filter characteristics allows sufficiently high frequency response (in excess of 50 Hz) for the required attitude determination accuracy.

6.2.4 Sun Sensor Assembly

A single internally redundant sun sensor assembly (SSA) is installed on the attitude determination module with optical axis in the -Z direction. A 2π steradian operating field of view is provided. The design is similar to units previously flown by TRW on other space programs.

The SSA contains two fine detectors, four coarse cell detectors, a circuit board, one connector, and the structure. Two fine detector modules are employed for redundancy. Each includes a silicon quad cell detector and a quartz block. One surface of the block has a mask that blocks the light over the total surface except over a small square region. Cell outputs are summed to obtain a sun presence indication. The outputs are differenced to develop a proportional error signal. At null, the light through the aperture illuminates all four quadrants of the quad cell equally, producing a zero difference signal. Differencing of the coarse cell outputs provides an error signal outside the 35 degree field of view of the fine detectors. The null accuracy of the SSA is 0.5 degree.

6.2.5 Transfer Assembly

The transfer assembly (TA) contains the special-purpose electronics for processing and buffering the attitude determination module sensor signals in a form suitable for input to the data interface unit. The TA also contains electronics for module thermal control and the control circuitry.

Two TA's are installed for EOS-A. One TA is powered with the second unit in standby redundancy.

The TA construction is based on "slices" containing multilayer printed circuit boards. The slices are then bolted together with interconnection cables to form the complete assembly.

6.2.6 Data Interface Unit

Two data interface units (DIU's) are installed in EOS-A. One of these units is standby redundant. The DIU is of standard EOS design and is described in Section 6.1.

6.2.7 Power Conditioning Unit

The power control unit (PCU) provides regulated DC power for the module. Two are installed in the attitude determination module, with one of these being standby redundant. The PCU is of standard design, as described in Section 6.4.

6.3 ACTUATION MODULE

The mission-peculiar attitude and orbit control equipment, consisting of wheels, torquers, a hydrazine orbit transfer/adjust propulsion system, and a cold gas nitrogen reaction control propulsion system, are integrated into the actuation module.

Two EOS-A actuation module designs are shown in Figure 6-13, one for Thor-Delta and one for Titan. The Thor-Delta version is installed from the bottom end of the spacecraft and cannot be removed in orbit. The Titan version is installed from the side of the spacecraft and can be resupplied in orbit. Tables 6-8 and 6-9 list the actuation module equipment and design parameters for EOS-A. Figure 6-14 is a functional block diagram of the actuation module.

6.3.1 Reaction Wheels

A reaction wheel assembly consists of a motor-driven inertia wheel contained within a sealed case. The assembly develops torques through reaction of the motor through the case and mounting structure. The major

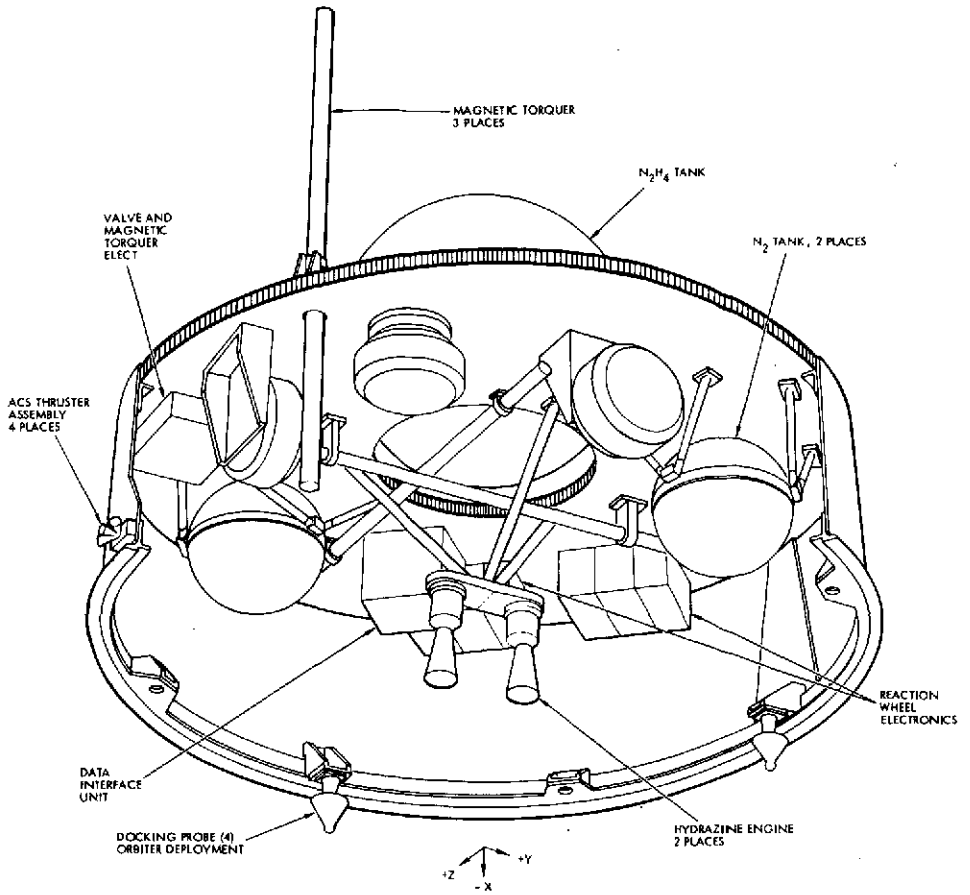

A) Thor-Delta (piping not shown)

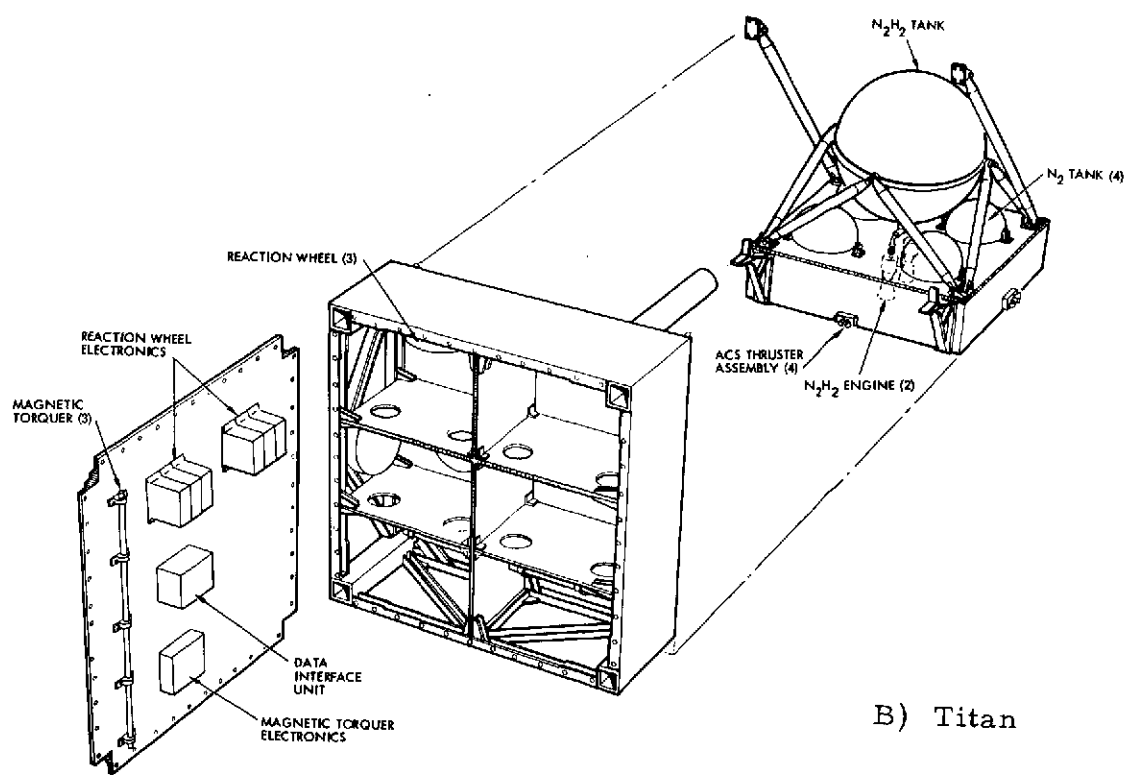

B) Titan

Figure 6-13. Actuations Module for the Thor-Delta and Titan

Table 6-8. Thor-Delta and Titan Actuation Module Hardware List

Item	Quantity	Total Weight (lb)	Total	Source
Thor-Delta				
N_2H_4 Tank	1	8.4	8.4	PSI
GN_2 Tank	2	11.25	22.5	PSI
Fill	2	0.5	1.0	TRW
Pressure Transducer	1	0.5	0.5	Statham
Filter	2	0.5	1.0	Wintec
Isolation Valves	6	0.6	3.6	HRM
Vent	1	0.6	0.6	HRM
Regulator	2	1.2	2.4	Sterer
N_2H_4 Thruster	2	0.6	1.2	TRW
GN_2 Thrusters	12	0.7	8.4	Sterer
Lines			5.0	TRW
			54.6	
GN_2			18.7	
N_2H_4			96.3	
			169.6	
Titan				
N_2H_4 Tank	1	35	35	PSI
GN_2 Tank	4	20.7	82.8	PSI
Fill	2	0.5	1.0	TRW
Pressure Transducer	1	0.5	0.5	Statham
Filter	3	0.5	1.5	Wintec
Isolation Valves	11	0.6	6.6	HRM
Regulators	4	1.2	4.8	Sterer
N_2H_4 Thrusters	2	3.5	7.0	TRW
GN_2 Thrusters	12	0.7	8.4	Sterer
Lines and Brackets			8.0	TRW
			155.6	
GN_2			68	
N_2H_4			866	
			1089.6	

C - 3

Table 6-9. Actuation Module Equipment List (Minimum Redundancy)

Unit	Source	Program Derivation	Quantity	Unit Weight (lb)	Unit Size (in.)	Unit Power (watts)
Reaction wheels*	Bendix	OGO	3	16.5	120 x 4.7	53 (peak)
Magnetic torquers*	TRW	SESP 72-1	3	8.7	1.20 x 40	0.5
Reaction wheel electronics	TRW	HEAO	3	4	6 x 8 x 3.5	12
Valve and magnetic torquer electronics	TRW	HEAO	1	1.9	6 x 8 x 1.6	3
Data interface unit	TRW	--	1	4	3.5 x 6 x 8	2.5
Reaction control and propulsion system	TRW	Refer to Section 3.8				

*Mission-peculiar units. Size shown is for EOS-A.

components are: case assembly, inertia wheel, bearings, bearing lubrication mechanism, motor, and tachometer. The characteristics of each are described briefly below.

Three wheels are installed in EOS-A, one along each of the three control axes. Reaction wheel performance requirements are evaluated in Appendix A, Section 5.2. For EOS-A, a Bendix reaction wheel flown on OGO has been selected. This wheel has the following performance:

- Momentum: 7.2 ft-lb-sec at 1,250 rpm
- Torque: 20 in-oz
- Power: 53 watts (peak)

For alternate missions (e.g., MSS payloads) launched on Thor-Delta, a smaller wheel could be used.

6.3.2 Magnetic Torquers

Three orthogonal magnetic torquers are installed in the actuation module. The electromagnetic torquer is basically a long cylindrical iron rod wrapped uniformly with a large number of turns of wire conductor.

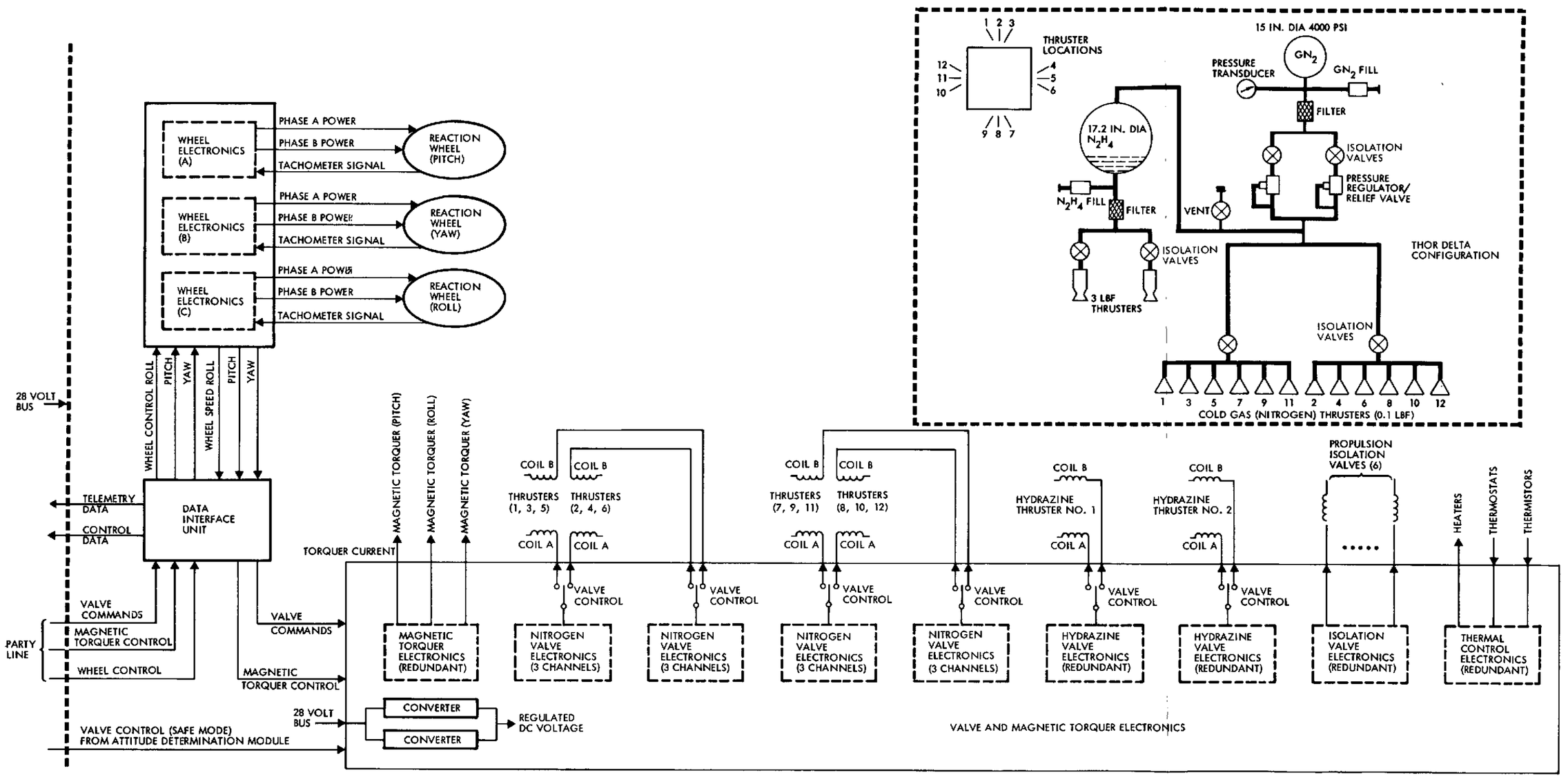

Figure 6-14. Actuation Module (Minimum Redundancy)

FOLDOUT FRAME 1

FOLDOUT FRAME 2

A magnetic field is produced in the rod by energizing the coil with direct current. The magnetic field produced in the electromagnet interacts with the ambient earth magnetic field to produce a torque for attitude control.

Design requirements are discussed in Appendix A, Section 5.2. The selected design for EOS-A is based on a unit provided by TRW for the SESP 72-1 spacecraft. The EOS design has the following characteristics:

- Magnetic field strength (linear): 120,000 pole-cm
- Power at 120,000 pole-cm: 0.5 watt
- Length: 40 inches
- Weight: 8.7 pounds
- Coil: 40,300 turns (Number 32 copper wire)
- Residual magnetism: <688 pole-cm
- Core material: Allegheny Ludlum electrical steel 4750.

6.3.3 Reaction Wheel Electronics Assembly (RWEA)

The EOS-A configuration incorporates a standby redundant pair of RWEA's for each of the three reaction wheel channels. The design is similar to that developed for the FLTSATCOM program.

The RWEA supplies two-phase power to the reaction wheel in response to a serial digital input signal. The wheel is started after the spacecraft is placed in orbit and activated in normal mode. The general approach to developing two-phase power for the reaction wheels is to first develop DC power proportional to the input control signal, then switch this power into two phases at 125 Hz.

The drive motor is a 125 Hz, two-phase, center-tapped AC induction motor. The output of the switching regulator filter is applied directly to the motor center taps and the ends of the motor windings are alternately switched to ground in a 90-degree, two-phase sequence to provide for either forward or reverse torquing. The power driver transistors are stud type required to deliver high peak currents. A path for inductive motor currents is provided by the reverse connected diode

across each power output transistor. The power amplifier driver stages are transformer coupled to a set of buffer drivers driven by the 125 Hz, two-phase logic. The buffer drivers and transformers provide variable current drive to the power amplifiers. The drive current to the transformers consists of two components; one fixed and the other proportional to the switching regulator output, and ensure adequate current drive to the output stage when operating a high output levels. Drive current can be reduced at lower outputs thus reducing base overdrive which in turn improves power efficiency and switching characteristics.

The RWEA base provides a direct heat sink for drive transistors and other significant power dissipating components as well as compartments for EMI filtering of incoming power, wheel drive outputs, and a small power converter. Associated circuitry is packaged on a circuit board located in this housing. The upper module is isolated from the base by a thermal panel/EMI barrier and contains control circuitry on two boards.

The unit is designed to maximize the mounting interface area in order to handle the maximum power dissipation during wheel unloading while maintaining component temperatures within their derated limits.

6.3.4 Valve and Magnetic Torquer Electronics

The EOS-A design incorporates a single internally redundant valve and magnetic torquer electronics which provide controlled power to the thruster valves, magnetic torquers, and module thermal control.

6.3.4.1 Magnetic Torquer Electronics

The electromagnet driver electronics generates a drive current (I_c) with the magnitude and polarity determined by the magnetic moment command. Two complete drivers are provided for each control axis. These two separate systems (per axis) are operated in an active/standby mode.

The principal design requirements established for the driver electronics was that coil current must be proportional to the magnetic moment command, and the driver circuit must operate efficiently.

After evaluating different circuit configurations which included linear power amplifiers and variable voltage DC/DC converters, it was found that a pulsed transistor bridge switch could best satisfy these design requirements.

6.3.4.2 Valve Drive Electronics

Each valve driver consists basically of a transistor switch which applies bus power (28 VDC) to a thruster solenoid valve coil. There is an individual valve driver circuit for each of the redundant solenoid valve coils. This redundancy configuration is shown in Figure 6-14.

6.3.4.3 Data Interface Unit (DIU)

The DIU is a standard EOS design used for processing signals for data bus transmission. This module contains two DIU's with one of these in standby redundancy.

6.3.5 Description of Baseline EOS-A Propulsion Configuration

The propulsion functions for the EOS-A Thor-Delta configuration include orbit adjust for drag makeup during the spacecraft operational phase, attitude control during the orbit adjust maneuvers, backup to the reaction wheels for spacecraft attitude control, and backup to the magnetic torquers for reaction wheel unloading. The propulsion system for the Titan configuration has these same functions plus the additional function of performing orbit transfer maneuvers to place the spacecraft into the operational orbit and to return the spacecraft to the Shuttle orbit.

Based on the tradeoff studies presented in Appendix A, Section 5.3, the basic system selected for both the Thor-Delta and Titan configurations consists of a cold gas (GN_2) system for providing the reaction control combined with a monopropellant hydrazine system for performing the orbit transfer and/or orbit adjust maneuvers. The two systems are similar in concept, differing primarily in the size of the tanks and the thrusters as related to the total impulse requirements of the spacecraft. Figures 6-15 and 6-16 show the schematic configurations and the tankage volumetric requirements for each configuration.

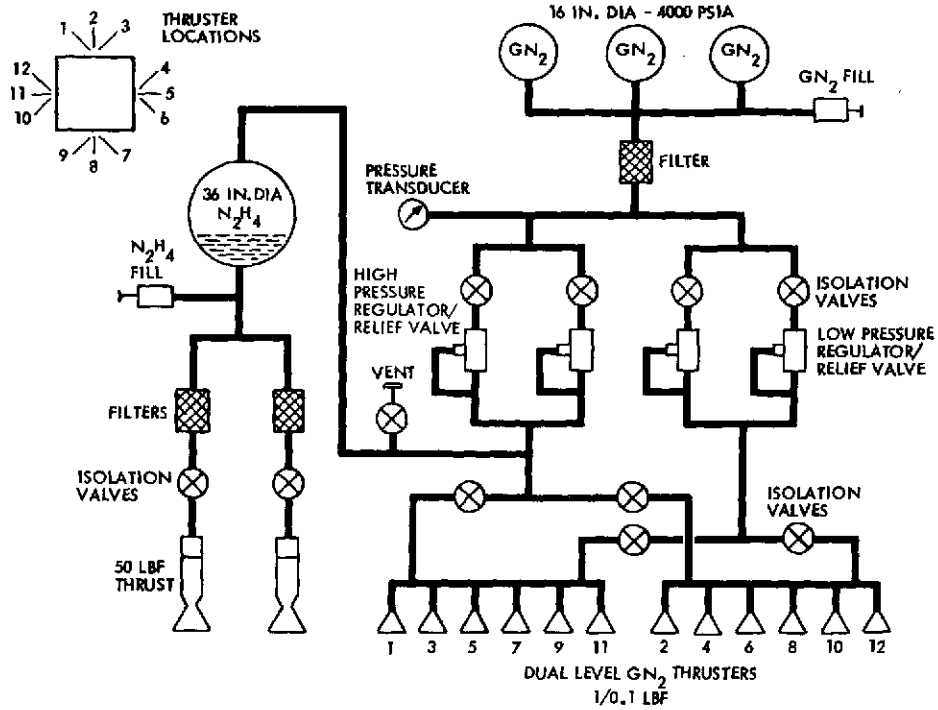

Figure 6-15. Orbit Transfer/Orbit Adjust - Bilevel RCS Configuration (Titan Configuration)

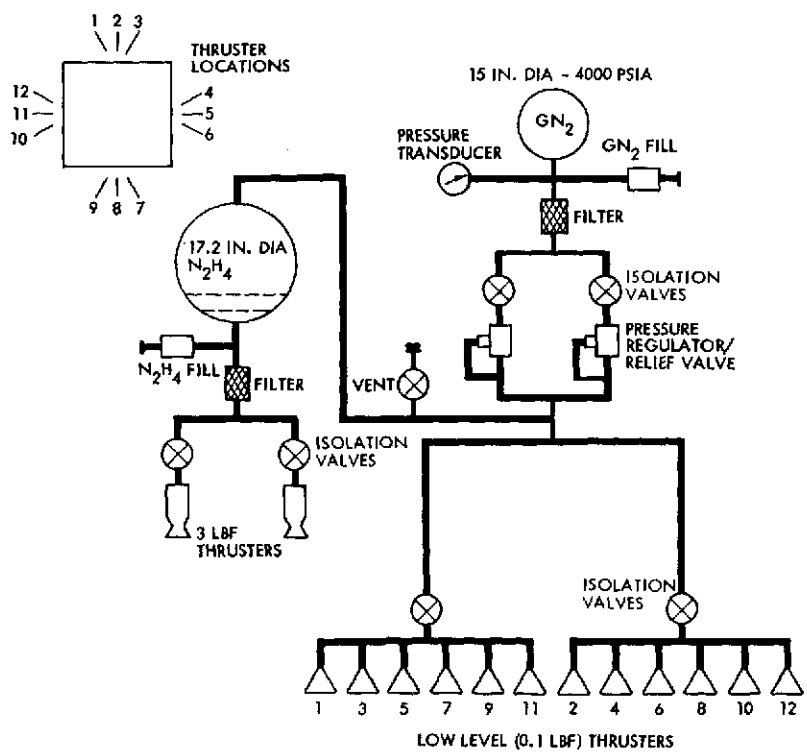

Figure 6-16. Orbit Adjust - Single-level RCS Configuration (Thor-Delta Configuration) (Minimum Redundancy removes 1 to 3 pound thruster)

The Titan orbit transfer/adjust system consists of a single 36-inch diameter spherical propellant tank, two 50 lbf thrust monopropellant hydrazine thrusters, two torque motor isolation valves, a fill valve, and two propellant filters. The propellant tank is pressurized from a line connected downstream of the high pressure regulators in the RCS. Pressure in the tank is maintained at 300 psia throughout the mission. Propellant orientation is maintained by a surface tension screen in the lower portion of the tank. The thruster consists of a torque motor latching solenoid valve, a shower-head injector, and a two-layer Shell 405 and HA3 catalyst bed encased in a Haynes 25 chamber/nozzle assembly. Each thruster is qualified for firing the full propellant load so that the system is protected against single-point failures at all points below the tank outlet where the system divides into two parallel legs. The isolation valves are identical to the thruster valves. The filters are high capacity 25 micron ansolute units with double dutch twill filtering elements.

The Thor-Delta orbit adjust system consists of a 17.2-inch diameter propellant tank, a fill valve, a filter, two isolation valves, and two 3 lb-ft thrusters. As in the Titan system the propellant tank is pressurized from a line connected downstream of the RCS pressure regulator. The tank pressure is also maintained at 300 psia and the propellant orientation is achieved by surface tension screens. A single filter was used in the system in place of the two units proposed for the Titan. The isolation valves are the same type torque motor latching solenoid as recommended for the Titan configuration only smaller in size. The 50 lb-ft thrusters used for the Titan configuration have been replaced by 3 pound thrusters. The thruster consists of a dual seat, dual coil direct-acting solenoid valve, a discrete spray injector, and a Shell 405 catalyst bed encased in a Haynes 25 chamber.

The reaction control system for the Titan configuration, as previously shown in Figure 6-15, consists of three gas storage tanks, a gas fill valve, a pressure transducer, a filter, a pair of high pressure regulators, a pair of low pressure regulators, six isolation valves, a vent valve, and 12 dual-level thrusters. The 12 dual level thrusters provide completely redundant control in all three axes at both thrust levels, as explained in Appendix A, Section 5.3. Redundant regulators protected by both

upstream isolation valves and integral relief valves are recommended to enhance reliability. The other components, tanks, filter, pressure transducer, and vent are sufficiently reliable (or in the case of the pressure transducer not critical to the system operation) as to not require redundant counter parts. The high-level thrust is used for attitude control during orbit transfer and orbit adjust maneuvers; the low-level thrust is used for attitude control backup, wheel unloading backup, and initial acquisition maneuvers.

The Thor-Delta reaction control system, as shown in Figure 6-16, is a more conventional single thrust level cold gas system. With the low thrust orbit adjust motors, high-level reaction control torques are not required. The thrusters and regulators are redundant for the nominal redundancy case, tanks and other components are not redundant.

6.4 POWER MODULE

6.4.1 Introduction

The power module contains electrical power subsystem primary power regulation, fault protection, and energy storage functions. Raw power is conducted to the power module from the solar array and drive module through four twisted pairs, as shown in Figure 6-17.

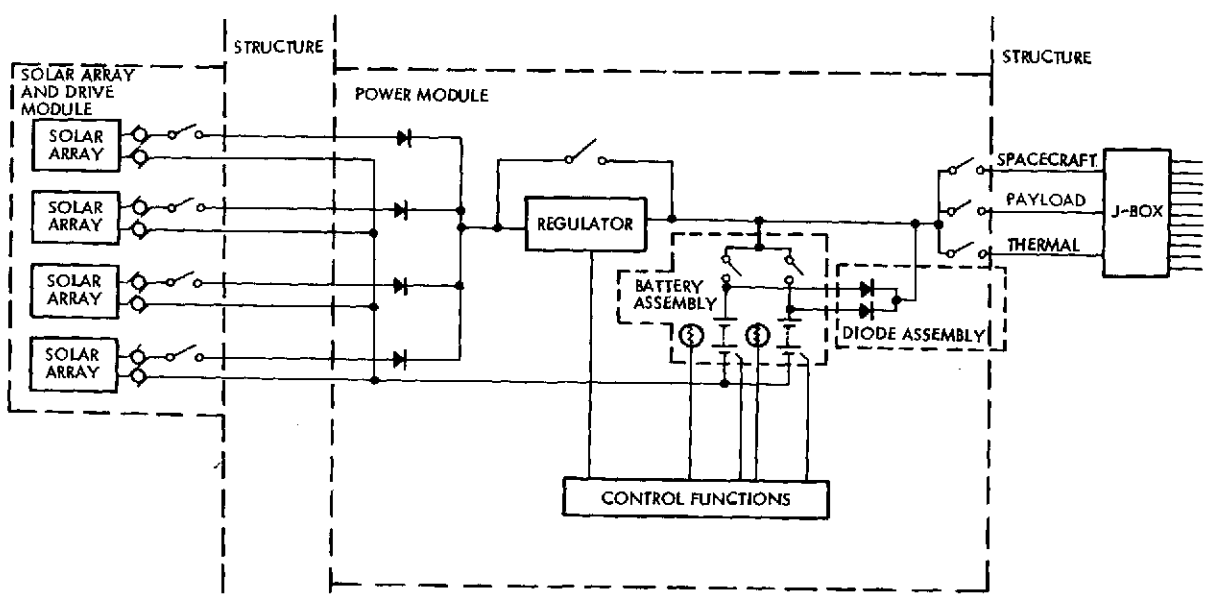

Figure 6-17. Power Module and Interface Block Diagram

Electrical isolation of the raw power buses is maintained by isolation diodes to prevent common point failure due to shorts in the raw power structure harness. Power flows through the power module to the loads via the spacecraft junction box and the structure harness. The central ground point for primary power is located in the power module. Spacecraft structure and module structure bonding is provided by conductors in the module interface connector. A detailed block diagram of the power module is shown in Figure 6-18. A perspective view of the power module is shown in Figure 6-19.

6.4.2 Detailed Description

The major elements of the power module are the data interface unit, power control unit, battery assembly, secondary power and bus protection assembly, diode assembly, and power disconnect assembly. The data interface unit is discussed in detail in Section 6.1.5.2

The primary function of the power control unit is to control the state of charge of the battery. The sequence of operation during one orbit consists of three charge/discharge regimes:

1) Eclipse. Power regulator is shorted, load power is provided by the battery.

2) Initial Sunlit Period. Power regulator is shorted; the solar array provides battery charge current and load power.

3) Final Sunlit Period. Power regulator is activated; the power from the solar array is reduced to that required by the load and battery taper charge.

During normal operation, the battery enable/disable switches and the power disconnect switches are in the closed state. The battery is connected directly to the main bus at all times and bus voltage is determined by discharge, charge, and taper charge terminal voltage.

During abnormal operation, the following conditions may exist:

- Payload power disconnect switches open to reduce load. Thermal bus disconnect will remain closed to prevent damage to modules, unless a short occurs on the thermal bus.
- One battery enable/disable switch open. This may occur if it is desired to charge one battery at a time due to battery overheating or a shorted cell. The battery diodes ensure that power can always be supplied to the bus from the batteries as needed.

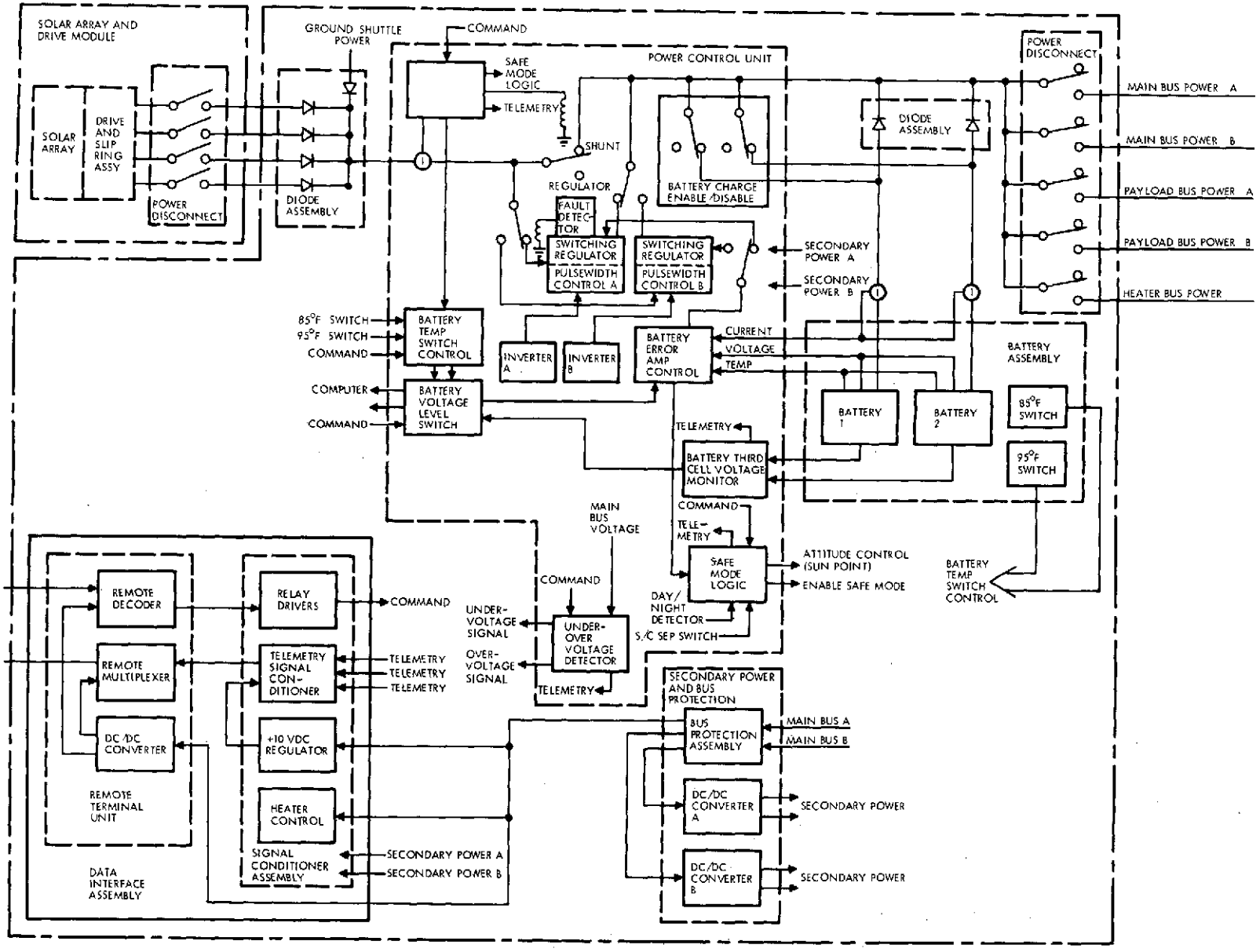

Figure 6-18. Electrical Power Module Block Diagram

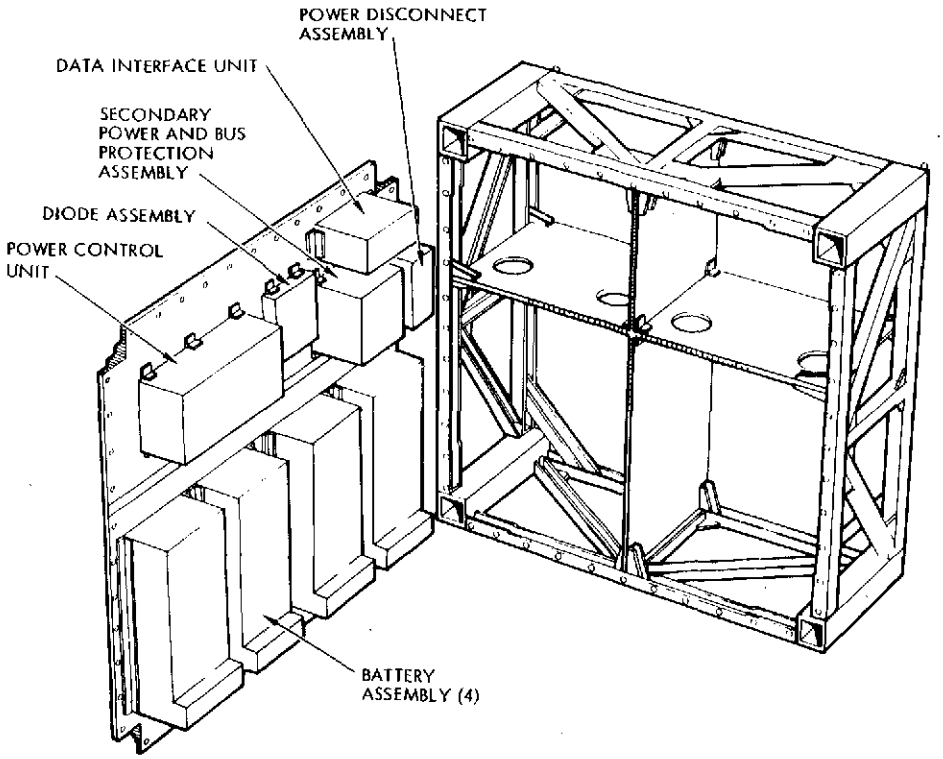

Figure 6-19. Perspective View of Power Module

A description of the functions of the major elements of the power module are discussed in the following paragraphs.

6.4.3 Power Control Unit

The power control unit provides main bus power control with a pulse-width modulation (PWM) buck regulator connected between the solar array and the main bus. Regulation control is normally based on a voltage temperature characteristic selected on ground command. Fault sensing circuitry controls redundant regulator switching and provides safe mode enable signals.

6.4.3.1 Main Bus Regulator

The PWM buck regulator (Figure 6-20) or nondissipative regulator function is performed by chopping input voltage with a solid-state switch and integrating the resulting waveform with the output filter inductance. The effect may be compared to a variable turns ratio transformer. The

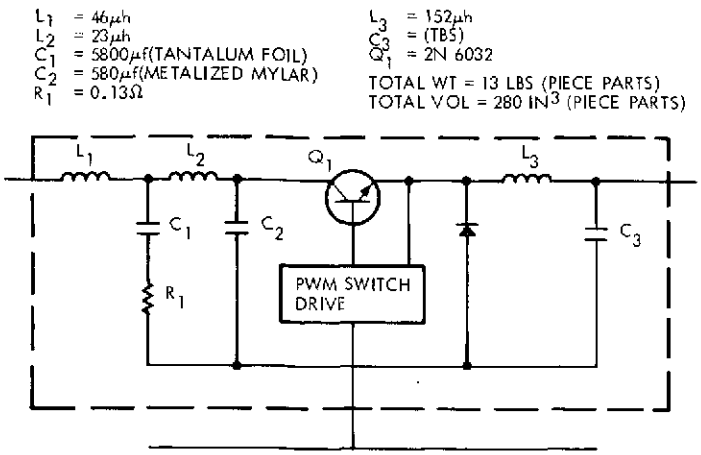

Figure 6-20. 1.0 kw Pulsewidth Modulator Regulator

low losses inherent in this design enable a single device to control considerably more power than a dissipative regulator. The filters are necessary for proper performance and are functions of voltage ratio, maximum and minimum power. A typical efficiency curve is illustrated in Figure 6-21 as a function of rated load. Peak power dissipation will occur at the moment the regulator is switched to initiate battery taper charge. Assuming a 1 kw array, peak dissipation of approximately 95 watts may be expected at that time. As the taper charge decreases, total load approaches approximately 50 percent of full load and dissipation will drop back to approximately 50 watts for the remainder of the sunlit period.

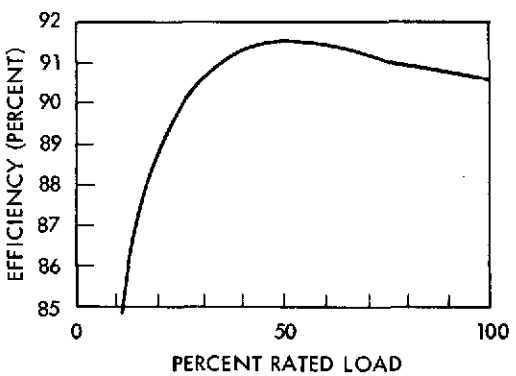

Figure 6-21. Typical Efficiency — PWM Regulator

The filter elements shown in Figure 6-20 are essential to the function of the regulator as well as maintaining ripple current within power subsystem and EMI specifications. The input filter design also restricts startup overshoot to approximately 30 percent of steady state values. Calculations are based on an optimized filter design program available at TRW. Transistor Q1 was selected on the basis of switching

performance and in the final design may consist of a matched pair operating in parallel to reduce maximum stress and improve reliability.

6.4.3.2 Regulator Control

The error signal which normally controls the PWM regulator is derived from a weighted sum of the outputs of the battery voltage and temperature transducers which is than compared with one of eight reference levels selected by ground command. The circuit configuration used to implement this function is illustrated in Figure 6-22.

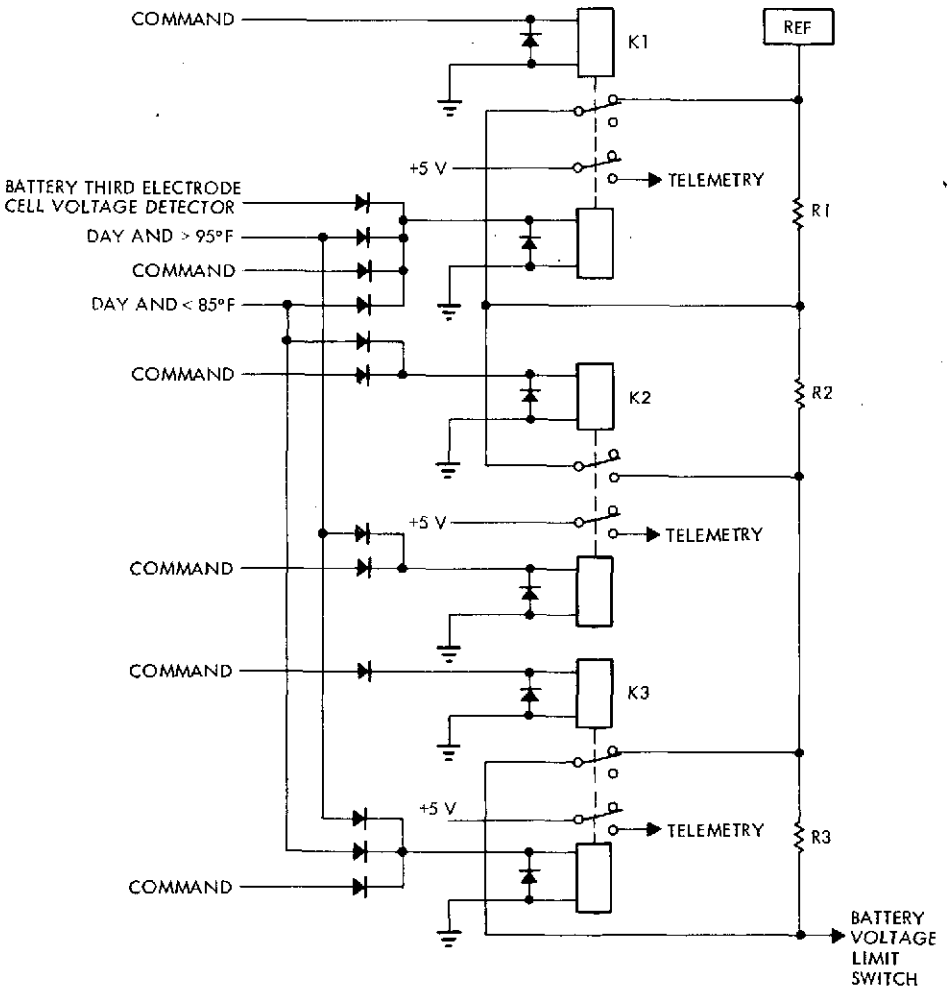

Figure 6-22. Battery Voltage Limit Switch

Developing the drive signal in this manner results in a regulator control characteristic, as illustrated in Figure 6-23. The battery voltage

limit (BVL) control may also be switched to the lowest level by battery temperatures in excess of 95°F or signal from the third electrode which indicate abnormal conditions. In the event battery temperature exceeds 95°F, the lowest BVL level is maintained until battery temperature drops below 85°F.

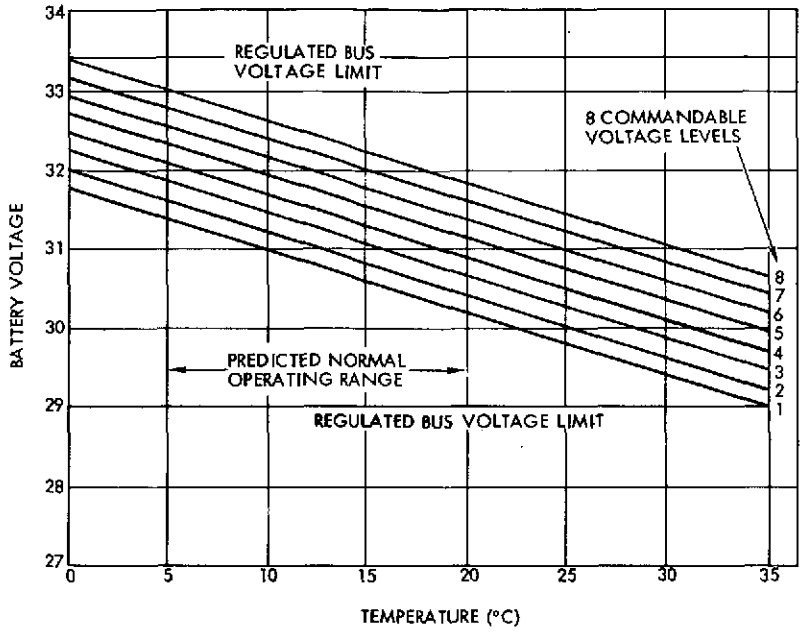

Figure 6-23. Battery Voltage Limit Curves

6.4.3.3 Fault Sensing and Isolation

The reliability of the PWM regulator is maintained by box redundancy. Operation of regulator A or B may be commanded from the ground or by overcurrent/undervoltage fault sensing circuitry. During eclipse and for the initial portion of the sunlit period of an orbit, the regulator is shorted out to permit the total array capability to provide load and battery charge power. The implementation of these functions is illustrated in Figure 6-24.

The battery third electrode voltage detector functional diagram is presented in Figure 6-25. The third electrode cell voltage of each battery is monitored continuously. This voltage is amplified and compared with a reference voltage by the operational amplifier circuit U1 or U2. If the

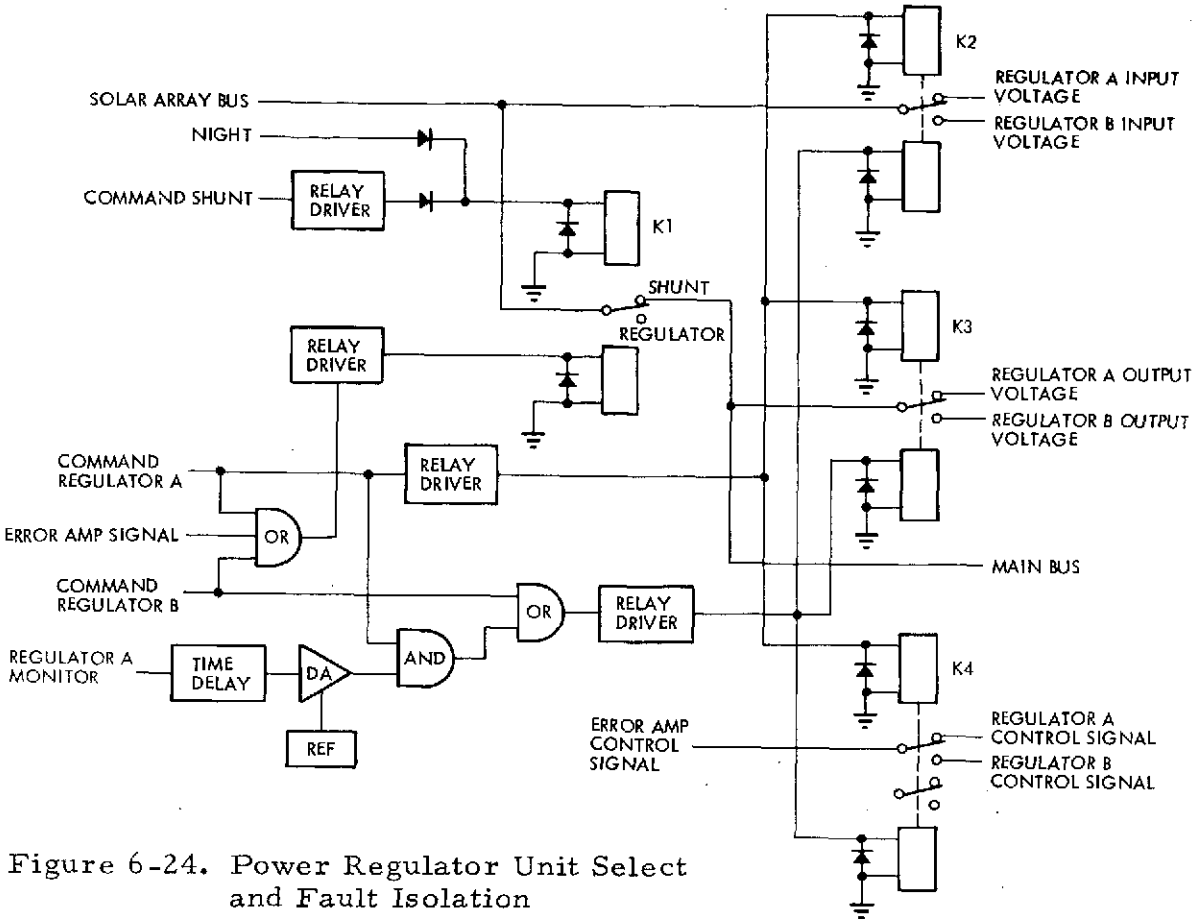

Figure 6-24. Power Regulator Unit Select and Fault Isolation

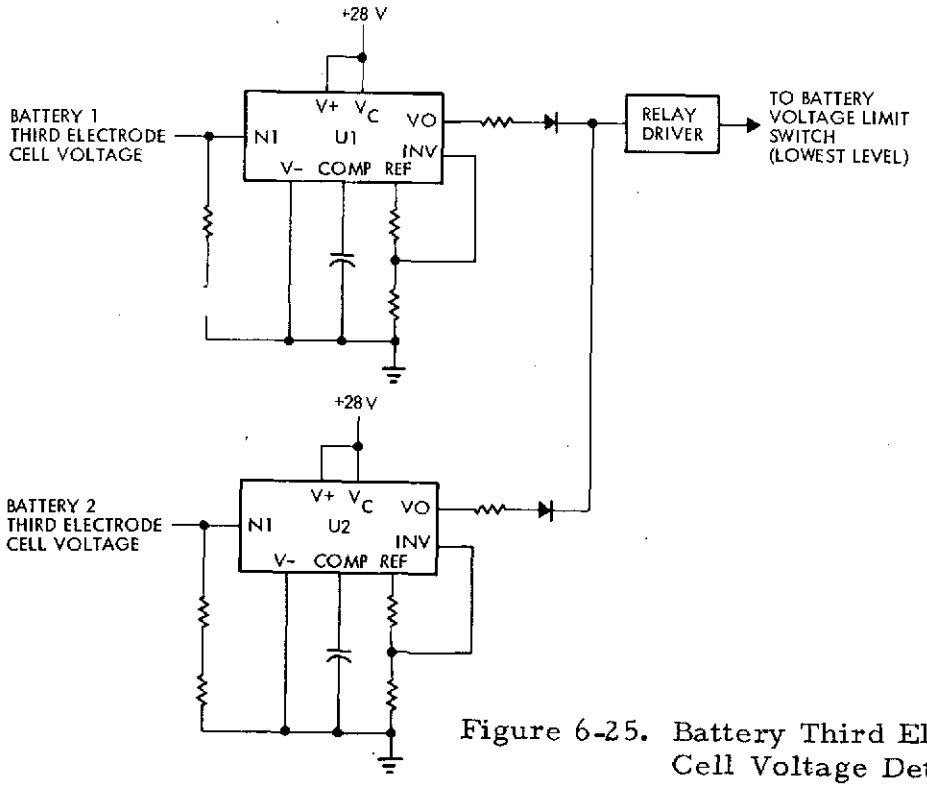

Figure 6-25. Battery Third Electrode Cell Voltage Detector

third electrode cell voltage of either battery increases beyond the preset reference, an output signal enables the relay driver circuit and places the battery voltage level switch to the lowest position. This fault sensor may be disabled by ground command.

Day/night detection is provided in this design by sensing solar array current. Battery discharge was discarded as an indication of eclipse due to the possibility of peak loads or transient faults producing a false indication. This signal provides the eclipse switching control of the regulator and a signal for the safe mode logic. Upon receipt of the safe mode signal the spacecraft is automatically oriented for maximum sun illumination of the solar array. Attitude control is by means of the sun sensor and the low level thrusters. Special-purpose safe mode attitude control electronics replace the on-board computer for attitude control and the gyros reaction wheels, and magnetic torquers are disabled. The safe mode provides a benign power and thermal regime which can be held for a long period of time during which the ground can provide failure diagnosis and corrective action, either via redundant hardware activation or Shuttle servicing. Return from the safe mode to normal control will be command initiated.

The power control safe mode logic block diagram is shown in Figure 6-26. These circuits are required to enable the attitude determination safe mode functions. This logic is provided to sense anomalous sun-pointing by monitoring battery charge control status and is activated if either of two conditions occur:

1) Loss of solar array current for a period exceeding the maximum eclipse time

2) Two consecutive sunlight periods without the batteries reaching the voltage limit.

The power control safe mode logic receives a signal from the day/night detector and starts a 45-minute timer. If the condition persists for 45 minutes and the logic circuit is enabled, the attitude control module safe mode functions will be enabled. If the day/night detector senses solar array current, the 45-minute timer will reset.

When the spacecraft enters eclipse, a signal from the day/night detector will set the state of the battery voltage limit sense circuit and

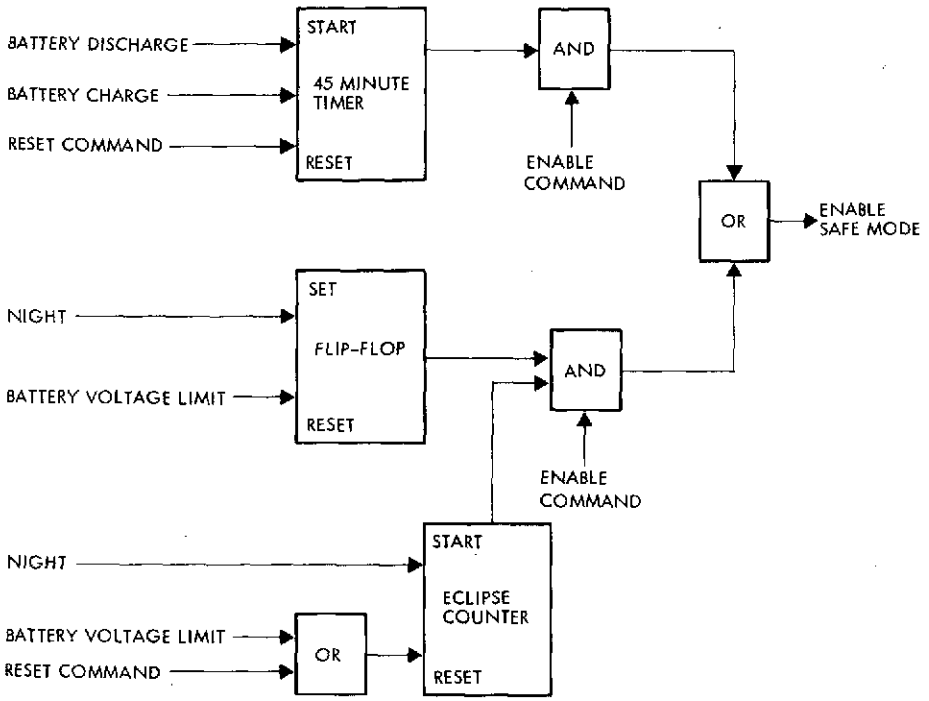

Figure 6-26. Power Control Safe Mode Logic

also start the two-stage eclipse counter circuit. If the batteries fail to attain sufficient charge by not reaching the battery voltage limit after two eclipse periods, the attitude control module safe mode functions will be enabled when the safe mode logic is enabled. If the batteries reach full charge, the battery voltage limit circuit will reset the logic and the eclipse counter. The eclipse counter can also be reset by ground command.

6.4.4 Battery Assembly

Two batteries are contained in the EOS-A power module. Their physical and performance characteristics are summarized in Table 6-10.

Each battery is equipped with one cell that contains a third electrode for the generation of a signal proportional to cell pressure. Each battery pack contains three temperature sensing circuits to provide a signal for BVLS charge control and signals for the high temperature BLV switches (85 and 95°F). The signal conditioning required for the temperature and pressure signals is performed within each battery assembly on printed

circuit boards. Each battery contains two electrical connectors; one is used for the monitoring of individual cell voltages during ground test sequences while the other contains all flight harness functions.

Table 6-10. EOS-A Battery Characteristics

Total battery system capacity (amp-hr)	80
Battery cell capacity (amp-hr)	40
Batteries per spacecraft	2
Cells per battery	22
Maximum depth of discharge (%)	15.2
Total delivered energy (watt-hr)	333.3
Weight per battery (lb)	104.5
Total battery weight (lb)	209.0

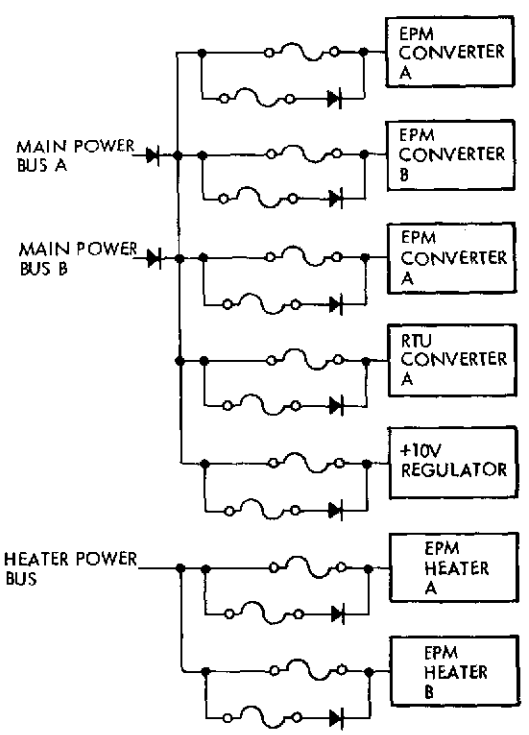

Figure 6-27.
Electrical Power Module Bus Protection Assembly

The secondary power and bus protection assembly provides the fault isolation components necessary to protect the spacecraft main power buses from load faults occurring within the electrical power module, and the DC/DC power converters necessary to generate the secondary power required by the electrical power module equipment.

A functional block diagram of the bus protection assembly is provided in Figure 6-27. Power is supplied to the bus protection assembly from main power buses A and B. These buses are connected together through series isolation diodes in the bus protection assembly. Power is distributed to each load through a fuse paralleled by a fuse and series diode fault isolation configuration.

As long as both fuses are functional the fuse with the diode in series will not conduct. Should the primary fuse fail, the fuse/diode path will carry the load current. The heater power bus is also supplied to the bus protection assembly and distributed to each heater load through a similar fuse configuration.

Redundant DC/DC power converters are provided to supply the secondary power required by the electral power module. Design of these units appear in Section 6.4.9.

6.4.5 Diode Assembly

Diodes are provided in the module for isolation of faults and battery power control. The solar array bus and the launch/shuttle umbilical bus are connected to the main bus through diodes to avert a single-point failure due to a short in the unregulated power harness. The availability of battery power to the main bus is ensured by diodes which are in parallel with the charge enable/disable switches. These switches may be operated in the event of a battery cell fault or abnormal temperature conditions.

6.4.6 Power Disconnect Assembly

The power disconnect assembly contains circuitry necessary to remove all input and output power from the module, and to automatically open individual lines in the event of a fault. Circuitry consists of relays that are controlled by external commands and that open automatically in the event excess current is flowing in the circuit. Each relay is a hermetically sealed magnetic latching relay with two sets of contacts. The main set of contacts (single-pole, double-throw, double-break) rated at 50 amperes and auxiliary contacts (single-pole, double-throw) rated at 5 amperes.

6.4.7 Power Converters

Power conversion in all basic modules is accomplished with one of two standard designs. One design yields a total power output of 40 watts and the other an output of 80 watts. Both deliver their power at ± 5 volts, ± 10 volts ± 15 volts or +28 volts. Each output is regulated to 5 percent over the range of input-voltage and load variations. Distribution of the

total available power between these voltages can vary between the modules by simple component substitution in the output circuits. Modules employing the 40 watt design are the CDH, electric power, and solar array drive. Modules employing the 80 watt design are the attitude determination and the wideband communicator. All designs are based on the block diagram in Figure 6-28.

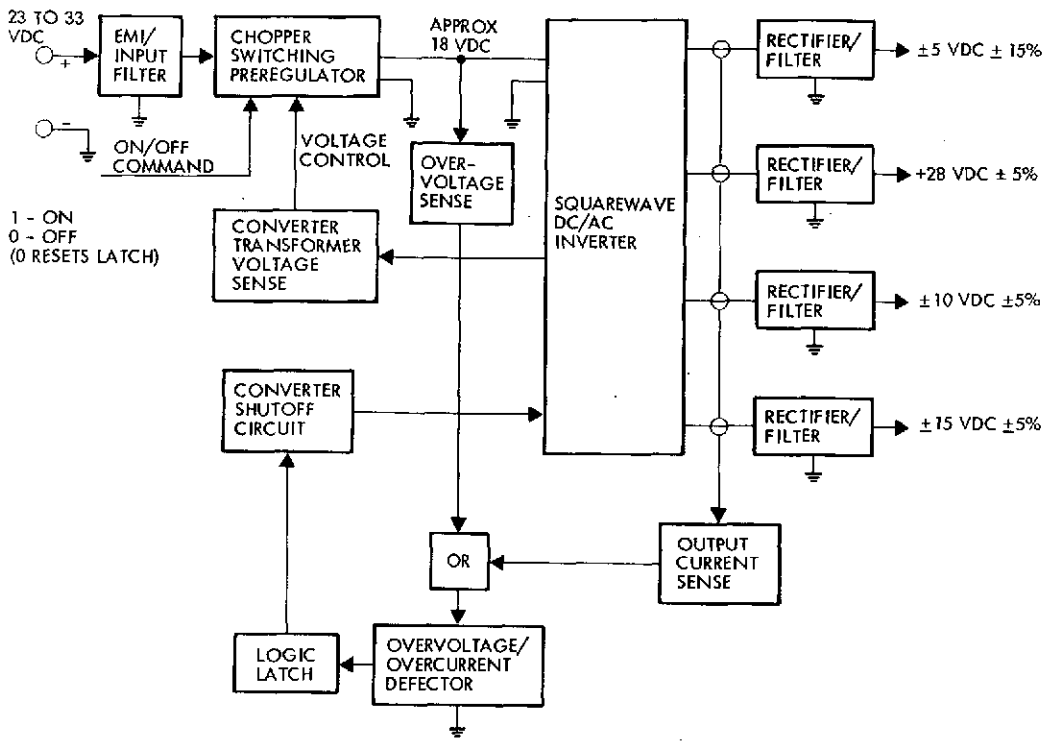

Figure 6-28. Secondary Power Converter

Relatively wide input voltage variations necessitate using the preregulator/squarewave inverter approach to meet the output voltage regulation requirements. Output voltage regulation is accomplished through sensing the magnetic flux in the inverter transformer and using the resultant voltage to control the preregulator output. The switching regulator uses a two loop feedback (AC and DC) control circuit technique to obtain optimum dynamic output regulation.

Converter output overcurrent and overvoltage protection are provided by sensing each output load with a current transformer and "or" gating these outputs with an overvoltage sense signal into a detector which

terminates power transistor switching when activated. A logic latch is used to prevent converter on/off oscillation during a sustained overload or overvoltage. The converter on/off command is an "1" or "0" state command with its return common to the input power return. During the "1" state command the converter is on unless the overload/overvoltage latch has been tripped. If so, the command state must be returned to 0 and then to 1 again to re-energize the converter. The squarewave inverter, rather than the preregulator, must be shut off during a potential overvoltage condition since shorting of the preregulator pass element could cause an unprotected output overvoltage.

6.5 ELECTRICAL INTEGRATION

Electrical integration of the EOS-A spacecraft design has been based on the use of data bus and on-board computer capability for intermodule communications. A simple backup function with a minimum number of hardlines ensures that the observatory can be retrieved or resupplied. Primary power for the subsystems is distributed on redundant pairs. The data bus consists of two pairs (four lines) to provide full duplex operation. A separate pair of lines provide power for the heaters in each module. The use of separate lines for the module heaters allows thermal maintenance during Shuttle servicing without powering the total spacecraft. Electrical integration tradeoffs performed during the study are included as part of Section 5.4, Appendix A.

6.5.1 Power Distribution

The primary power distribution design provides separate buses for the spacecraft and payload to allow individual control and reduce the impact of mission-to-mission changes in the harness. Redundant power buses eliminate the possibility of a short to structure causing complete loss of the primary power. Figure 6-29 shows the redundant primary power bus protection concept. The resettable circuit breakers open up a bus in the event of a short to structure, and the diodes in the user module ensure that the other bus is isolated and operable. Fuses provide isolation for load faults and are described in Section 3.4. The primary power buses for the subsystems and payload are controlled by

current sensing and magnetically-driven circuit breakers. The circuit breakers for the spacecraft subsystem power bus are interconnected so that if one circuit breaker opens the other will be commanded to close (whether it is closed or not). This assures that power to the spacecraft is uninterrupted.

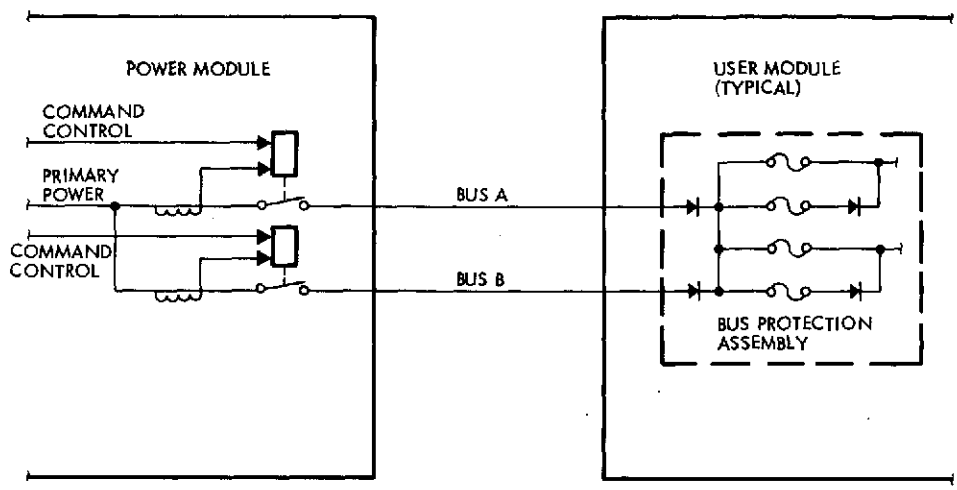

Figure 6-29. Redundant Primary Power Bus Protection Concept

The module heater power is distributed on a bus pair (two lines) to all subsystem and payload modules. The heater bus is fault-isolated in the bus protection assembly of each module and may be opened within the power module. A separate heater bus line eases servicing of the observatory by not requiring power on the main bus to maintain thermal control.

Structural heaters on the payload and subsystem structures are powered and controlled through the solar array and drive module. This location was selected because it more fully utilizes the DIU in this module.

Provisions are included for separately energizing the primary power bus, the module heater bus, and the structure heaters from the umbilical connector. Each bus is diode-isolated to eliminate the possibility of sneak current paths between the observatory and ground or Shuttle power sources.

6.5.2 Signal Distribution

Signal distribution within the observatory is almost exclusively accomplished on the full-duplex data bus interconnecting all modules. A few hardline signals are required to ensure retrievability of the observatory, and perform one-time-only functions. The data bus provides module-to-module communication, ground-to-module command, and module-to-ground telemetry. Two twisted, shielded pairs are used for the data bus function.

A single wire safe mode bus between all modules is used to put the observatory solar array in a sun-pointing mode in the event of anomalous behavior which could cause battery power depletion. Additional lines for safe mode control interconnect the attitude determination and actuation modules for valve control in the safe mode. Solar array drive control for sun-pointing is self-contained within the solar array and drive module. Additional hardlines interconnecting modules are listed in Table 6-11; umbilical interconnections are listed in Table 6-12.

Figure 6-30 provides the detailed interconnection information for each of the electrical interfaces discussed above and the electrical grounding configuration for a typical module, as discussed in Section 6.5.5.1.

6.5.3 Observatory Harness Configuration

The electrical interfaces within the observatory are interconnected by two major harness sections: the spacecraft harness and the payload harness. Figure 6-31 shows the selected harness concept.

The umbilical functions required for launch and resupply, as well as electrical interconnections for the spacecraft structure heaters, are included in the spacecraft harness section. Interconnection between the spacecraft and payload harness sections is made in a J-box located at the transition ring. Use of the J-box facilitates integration of the spacecraft and payload sections as separate assemblies and eases the task of modifying a harness. It also provides a convenient location for the ordnance control circuits needed for initial deployment of the antennas and

Table 6-11. Hardline Signal Interconnections

From	To	Number of Lines	Purpose
HRPI	Wideband communications	1	High rate (128 Mbit/sec) data
Telemetry	Wideband communications	1	High rate (128 Mbit/sec) data
Telemetry	Wideband communications	8	LCGS unbuffered data
Wideband communications	HRPI	1	MODS control
Wideband communications	Telemetry	1	MODS control
Solar array and drive	Hard-mounted J-box	14 (7 safe/arm) (7 fire)	Ordnance control and firing
Communication and data handling	Structure	Coax	Aft omni (deployed) RF output

Table 6-12. Umbilical Interconnections

From	To	Purpose
Communications data handling	Umbilical	Telemetry output
Communications data handling	Umbilical	Computer output
Umbilical	Communications data handling	Shuttle command input
Umbilical	Power	External power
Umbilical	Power	Load disconnect
Umbilical	Hard-mounted J-box	Module heaters
Umbilical	Solar array and drive	Array disconnect
Umbilical	Solar array and drive	Structure heaters

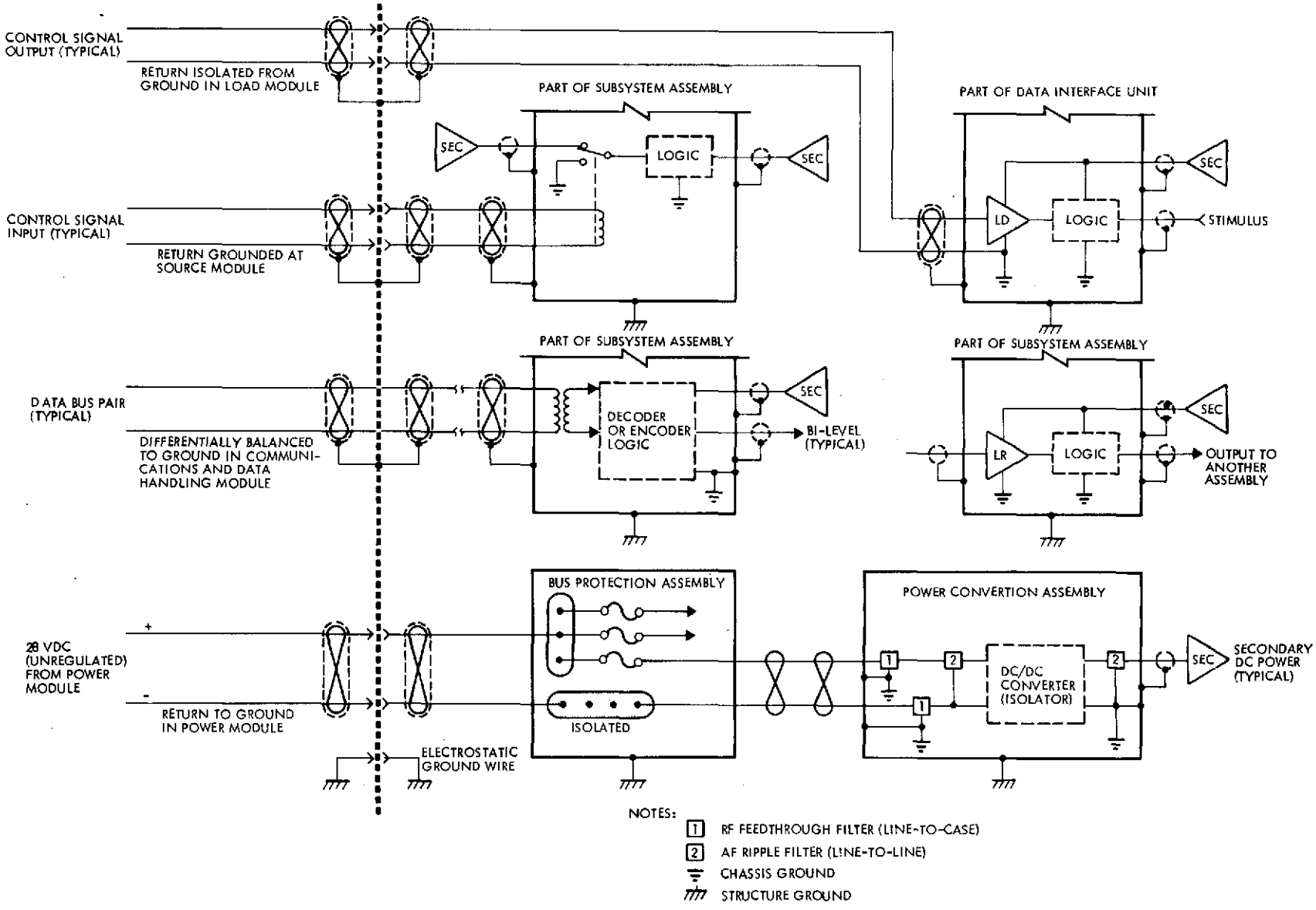

Figure 6-30. Detailed Module Electrical Interfaces

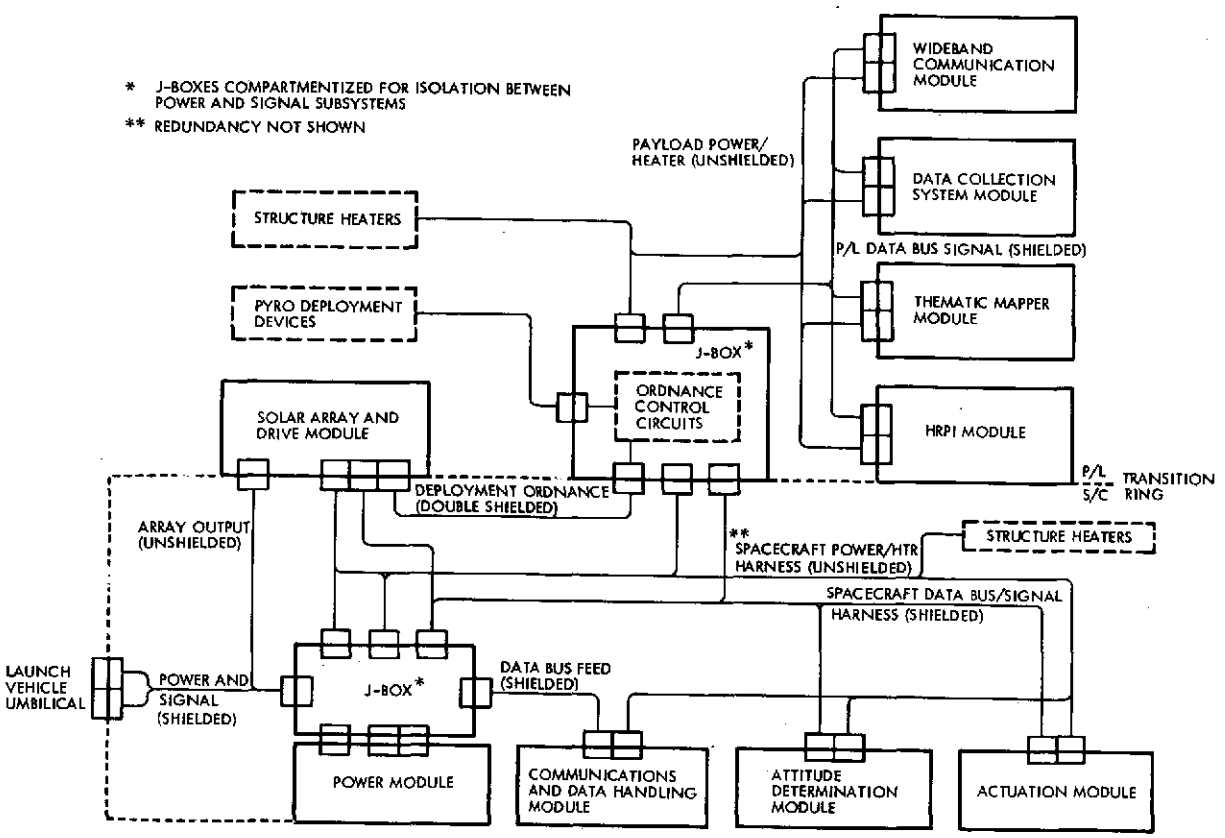

Figure 6-31. Wire Harness Concept

solar array. The payload harness section includes structural heater wiring required for the payload structure and the interconnections for the payload modules.

A J-box, located near the power module in the spacecraft structure, will be used for central distribution of the power and signal lines to the subsystem modules. This approach would allow removal of a harness for an individual module if necessary, and facilitate modifications or additions to intermodule wiring since only one module connector may be affected.

Each harness section is divided into power and signal subassemblies to minimize interaction. The ordnance harness for the pyrotechnic circuitry will be separated from, but run parallel to the other harnesses. The design is such that any harness subassembly (power or signal) may be reworked without major impact on the other subassemblies within the harness.

An examination of connector types suitable for the module-to-spacecraft interface indicates that types such as the Cannon DPK series may be used without modification. These are space-qualified connectors with the following characteristics:

- Rear insertable and removable contacts
- Available in many contact arrangements accommodating 18 to 161 contacts
- Contact sizes from 12 to 22 AWG
- Allows up to 0.060 misalignment
- Temperature range of -67 to + 392°F
- Meets all EMC requirements.

The connectors used on the J-boxes may be selected from the many flight-qualified available types, since it will not be necessary to disconnect these in-flight.

6.5.4 Module Harness Configuration

The harness interconnecting subassemblies within each module can be fabricated using standard techniques, but are designed so that assemblies and harnesses may be removed independently. Connectors used for the subassemblies within the modules can also be selected from flight-qualified types and will be standardized to minimize cost.

6.5.5 EMC Controls

The electromagnetic compatibility (EMC) control program for the EOS-A, discussed in Section 3.6, will be implemented as a portion of the electrical integration system. The design criteria and controls which will be imposed at the observatory and/or module levels, as applicable, are summarized in the following paragraphs and will be delineated in the subsystems specifications.

6.5.5.1 Electrical Systems Grounding

The primary DC power and party line data bus distribution subsystems will have single-point grounds. Single-point grounding will be employed for low-level analog sensor circuits and high current control

circuits. Subsystem circuitry wholly contained within a given module will, with some exceptions, employ multiple-point grounding using the module radiator panel and support structure as the ground reference plane and return path for secondary power and signal currents within the module. These grounding methods will:

- Prevent the injection of high level circulating currents into common structural elements
- Reduce the magnetic field sensitivity of low level sensor/amplifier circuits
- Allow for stable and efficient subsystems operation at high audio and radio frequencies.

Figure 6-30 represents the grounding scheme for a typical module.

6.5.5.2 Electrical Bonding

The electrical bonding configuration of the observatory will be designed to provide maximum electrical conductivity across all mechanical joints between metallic members except where DC or thermal isolation is a design requirement. In general, the standardized bonding provisions of MIL-B-5087, "Bonding, Electrical, and Lightning Protection for Aerospace Systems," will be implemented. Also, interfacing metals will be suitably treated with conductive protective coatings to prohibit the deterioration of electrical bond joints through electrolytic or galvanic action. The design goal of the electrical bonding configuration is to provide a low impedance, electrically continuous, homogeneous ground reference plane at the module level. This will result in a common, equi-potential ground reference for all electronic equipment within the module which, in conjuction with electrical circuit grounding controls, will ensure compatible operational performance.

6.5.5.3 Interconnect Wiring/Harness

The amplitudes of noise voltages and currents injected into the input terminals of a subsystem by functional operations in another subsystem through wire-to-wire coupling will be minimized by using shielded wires for all signal and control circuits between components within a module and between modules except for the primary DC power distribution subsystem

which will employ unshielded, twisted pairs. Wherever practical, power wiring will be physically separated from the shielded signal wire harness.

6.5.5.4 Unit Case Shielding

The cases of all units or equipment housing active electrical or electronic circuitry except communications receivers and transmitters will be designed, using standardized RF gasketing materials and techniques, to provide for a minimum of 40 dB attenuation of RF radiated fields. Communications equipment housing will be designed for a minimum of 60 dB shielding effectiveness.

6.5.5.5 Filtering

EMI filters will be required at all interfaces from the primary DC power subsystem to user power conversion units. These will be two-stage filters: 1) an input stage consisting of a high performance feedthrough, bulk-head-mounted filter in each power leg to reduce high frequency regulator switching noise voltages to acceptable levels; and 2) a line-to-line, "L" or double-L audio frequency ripple filter to reduce input line currents at the fundamental and lower order harmonic frequencies of the regulator. The line-to-chassis capacitance of the filter section will be minimized so as not to unduly degrade the beneficial effects of the wire twisting in the power harness.

The use of shielded interconnecting wire harnesses for all but primary DC power should eliminate or substantially reduce the need for EMI filtering at all other interfaces.

6.5.5.6 Specifications

The Space Shuttle program EMC specifications (NASA/JSC SL-E-0001 and SL-E-0002) have been selected as primary EMC control guideline documents for the EOS program. These specifications, which are adaptations of the more commonly known MIL-E-6051D and MIL-STD-461A/3, will be amended or modified as needed by the EMC Control Plan and an EMI/EMS Limits and Test Methods Specification. These two documents, to be prepared by the systems integration contractor, will be tailored to the specific needs and requirements of the EOS program.

6.5.5.7 Design Verification Test Program

A design verification test program will be structured in three phases. Successful test results in each phase will ensure that the fully integrated observatory will be functionally compatible in the operational mission environment. These three phases are:

1) Unit Level Engineering Tests. EMI survey tests at the unit level will be performed by the module subcontractor and/or unit suppliers. Only those conducted emission and susceptibility tests necessary to provide assurance that the module will be self-compatible, plus radiated tests to verify that the units and their associated wire harnesses provide adequate shielding, will be performed by the system contractor.

2) Module Level Qualification Tests. EMI qualification tests at the module interfaces in accordance with the applicable specifications will be performed by the module subcontractor on the first article qualification model to verify compliance with specification requirements.

3) System Level Compatibility Tests. EMC tests will be performed by the systems integration contractor on the qualification model observatory to verify that adequate EMC safety margins are achieved on the fully integrated system. After initial qualification at the module and system levels, acceptance tests and/or requalification of production modules will not be necessary.

6.6 SOLAR ARRAY AND DRIVE MODULE

The module contains the following elements:

- Solar array
- Solar array drive and slip rings
- Solar array drive electronics (redundant)
- Power converter (redundant) for the solar array drive electronics
- Data interface unit (DIU)
- Bus protection assembly
- Power disconnect assembly.

A block digram and a mechanical drawing of the solar array and drive module is shown in Figures 6-32 and 6-33. Solar array power is

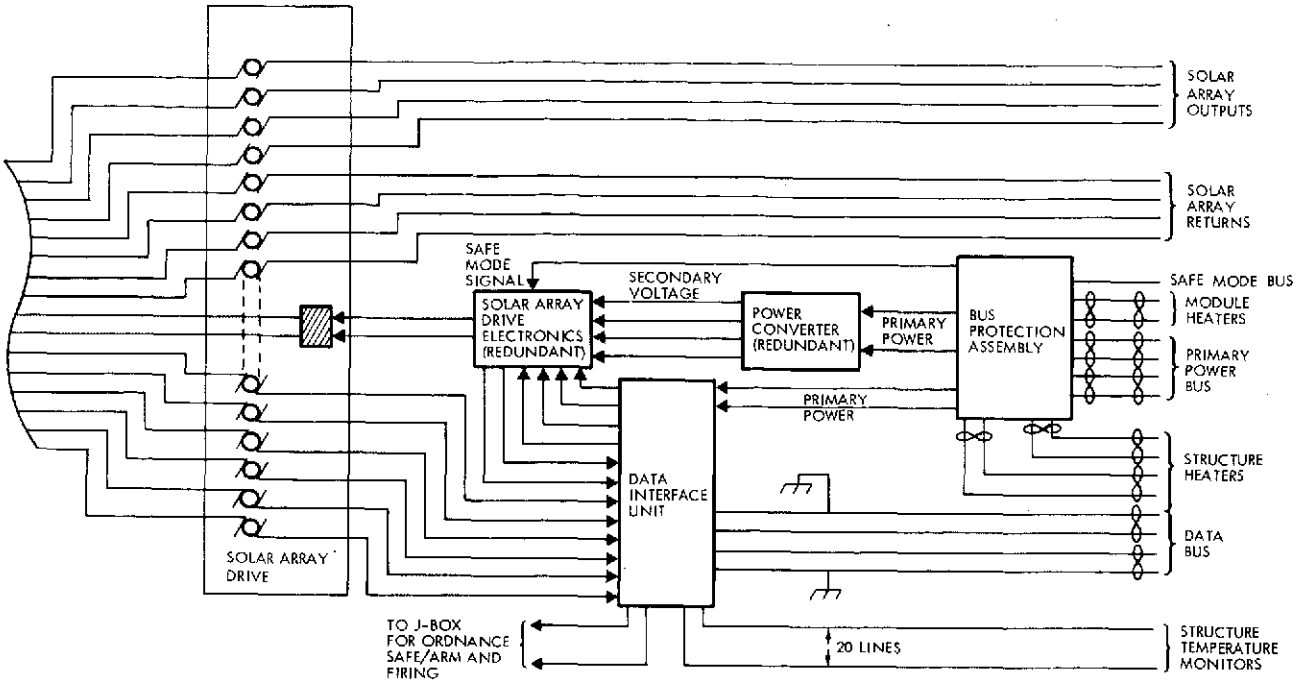

Figure 6-32. Solar Array and Drive Module Block Diagram

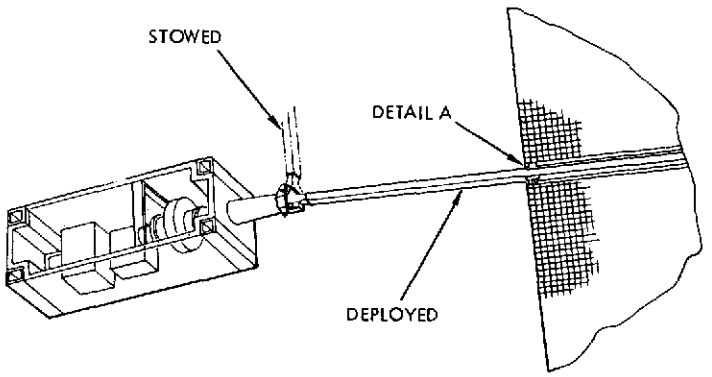

Figure 6-33. Solar Array and Drive Module Perspective

transmitted through the subarray drive assembly and the power disconnect assembly to the power module. The solar array is electrically divided into four sections. Each section delivers power to the drive interface by means of a power line and a return line. Thus, the array drive contains eight slip ring assemblies designed for power handling. In addition there are seven slip ring assemblies for solar array temperature telemetry signals. The slip ring assemblies each contain redundant

brushes for maximum reliability. Solar array and drive module tradeoffs are discussed in Appendix A, Section 5.4.

The power disconnect assembly contains contactors for each power line. Their function is to disconnect the solar array from the electrical distribution system in the event of retrieval of the spacecraft from orbit by the Shuttle. The contactors can be opened only by a command transmitted through the Shuttle umbilical connector.

Electrical power required for the operation of the solar array drive, drive electronics and power converter, power for all other electronic functions within the module is derived from the primary power bus which originates in the power module. The primary power bus is protected from component malfunction within the solar array and drive module by the bus protection assembly which is similar to those located in each of the other modules.

6.6.1 Solar Cell Array

The basic building block used to construct various EOS solar cell arrays is a honeycomb sub-panel upon which solar cells are bonded in a flat lay-down configuration. This construction has been qualified by TRW for the five-year geostationary-altitude USN/USAF FLTSATCOM solar array.

The EOS solar array is constructed of a number of panels which fold together for stowage during launch. The panels in turn are each composed of a group which is identical for both Titan and Thor-Delta configurations. Table 6-13 describes the physical characteristics of the sub-panels and panels for the two versions of the EOS-A spacecraft.

Table 6-14 summarizes the design factors used to determine the solar array size. Table 6-15 summarizes the performance capabilities of the EOS-A solar array.

The solar array power margin shown in Table 6-15 can be considered equivalent to a particular angle of off-normal solar incidence. For the case of the 11:00 a.m. orbit the 12-watt margin is equivalent to a ±8.8 degree angle measured from the solar panel normal with the solar array

Table 6-13. EOS-A Solar Array Physical Characteristics*

Characteristic	Thor-Delta	Titan, Shuttle
Sub-Panel		
Number of strings	Two groups of 98 cells in series by 3 in parallel	
Area	28.8 x 30 in. = 6.0 ft^2	
Array		
Total number of cells	14,112	
Number of sub-panels	24	
Number of sub-panels/panel	6	12
Number of panels/spacecraft	4	2
Total array area, ft^2	144	

Solar Cells	Solar Cell Coverslides
• Silicon N-on-P, gridded, SiO coated	• 7940 fused silica
• 1 to 3 ohm-cm base resistivity	• 0.012 cm thick
• 2 x 4 x 0.0356 cm	• MgF_2 antireflective coating
• Fully soldered titanium silver contacts	• Blue reflective coating
• 11.0% average, 10.2% minimum efficiency at 28°C, one solar constant AMZ	• Cut-on at 50% transmission at 0.400 ±0.015 micron

* See Figures 4-1 and 4-2 for Titan and Thor/Delta solar array configurations.

hinge set to 15 degrees. In orbit, the actual variation will not exceed ±4 degrees. Similarly, the margin obtained in the twilight orbit mission is equivalent to a ±46.5 degree angle of incidence, with the solar array hinge set to 90 degrees. The actual variation in orbit is within ±20 degrees.

6.6.2 Solar Array Drive

The solar array drive mechanism is a modification of the TRW-developed COMSAT drive (Figure 6-34). The drive mechanism incorporates the following elements:

- Two pancake AC synchronous motors (standby redundant)
- Harmonic drive gear reduction (200:1)
- Slip ring assembly (redundant brushes)
- Redundant shaft position potentiometers.

Table 6-14. EOS-A Solar Array Sizing Factors

2-Year Sizing Factors	
• Glassing and assembly	0.965
• Measurement factor: solar panels against standard cell	1.000
• Calibration factor: calibration of balloon and secondary standards	1.000
• Temperature cycling degradation	0.980
• UV degradation of coverslides	0.991
• Micrometeorite degradation	1.000
• Radiation degradation due to charged particles	
I_{SC}	0.968
I_{MP}	0.916
V_{MP}	0.970
V_{OC}	0.961
• Uncertainty Allowance	0.992
• Temperature coefficients	
I_{SC}, %/°C	0.9399
V_{OC}, V/°C	-0.2195
Maximum Array Temperature	
• 717 km (387 NM), 98.4 deg. inclination, 1100 AM equitorial crossing	73°C (equinox) 82°C (solstice)

Table 6-15. EOS-A Solar Array Performance Characteristics

Requirements/Capability	11:00 a.m. Orbit Capability (watts)	Twilight Orbit Capability (watts)
Solar Array Power Capability*		
• 0 years	1149.3	1080.4
• 2 years	999.5	900.8
Load Power Requirements		
• Average load power	552.0	552
• Battery charge power	319.0	42.5
• Distribution harness loss	18.5	11.9
• Contingency	55.2	55.2
Total Spacecraft Load	944.7	661.6
Load Power Capability		
• 2-year solar array power*	999.5	906.8
• Array harness and fault isolation diode loss	43.4	39.2
Total Load Capability	956.1	861.6
Solar Array Margin	11.4	200.0

* Normal solar incidence

The motor is operated synchronously with low frequency sine wave excitation in order to provide a "continuous" motion of the array shaft at the angular rate required to track the sun. Motor control is open loop and array position is initialized occasionally by ground command in a slew mode to correct accumulated sun pointing error. The selected drive mechanism design provides the advantages of high torsional and transverse stiffness and smooth operation which minimizes perturbation of spacecraft attitude due to array motion.

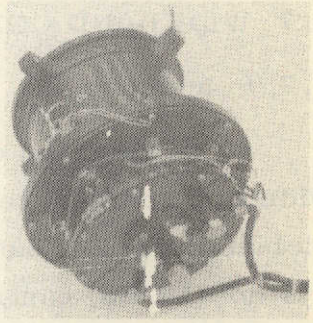

- DRIVE TORQUE: 31 FT-LB
- WEIGHT: 9.7 LB
- POWER: 2.8 WATTS
- SIZE: 6.3 DIA x 7.5 LENGTH

Figure 6-34. EOS-A Solar Array Drive

The drive mechanism incorporates a self-contained slip ring assembly containing four pairs of power circuits rated at 20 amperes each. Seven signal circuits are also provided. The reliability feature of parallel combinations of rings is enhanced by incorporating two brushes per ring. The nominal composition of the brushes is 12 percent MoS_2, 3 percent graphite, and 85 percent silver. The rings are coin silver.

Except for the slip rings which use a dry lubricant, the drive components will be lubricated with BRAY NPT-4 oil which has been flight proven on numerous spacecraft programs (OGO, NIMBUS/ERTS, DSCS-II). The oil is stored in several replenishment reservoirs (Nylasint). Sufficient oil is provided for an estimated lubricant life in excess of 100 years.

The EOS-A solar array and drive module incorporates a separate drive electronics unit for each of the two redundant array drive mechanism motors. The unused motor/drive electronics channel is in a standby condition. The drive electronics unit generates the low frequency sine/cosine excitation for synchronous operation of the drive motor. The frequency of the motor excitation is selected to produce the correct array drive angular rate for a particular mission. The AC voltage is generated by dividing a high frequency clock signal by a variable modulo frequency divider that may be programmed by ground command.

6.7 WIDEBAND COMMUNICATION MODULE

6.7.1 Introduction

The wideband communications module (WBCM) contains the complete wideband communication system (WBCS). The components of the WBDHS include the speed buffer (LCGS) and the multi-megabit operational data system (MODS) controller. The speed buffer accepts 8-line parallel data at 120 Mbit/sec (15 Mbit/sec each line) from the TM module and selects and reformats the data at 20 Mbit/sec for transmission to the low cost ground station (LCGS). The MODS controller controls and operates the MODS which consists of a high-speed PCM encoder and formatter contained in each instrument package.

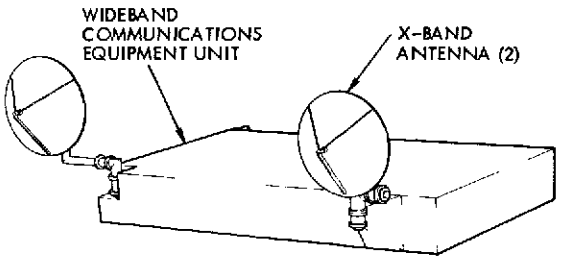

Figure 6-35.
Wideband Communications
Module Perspective

The WBCS perspective drawing and block diagram shown in Figures 6-35 and 6-36 consists of two quadriphase modulators, power amplifiers, transmission filters, and X-band antennas. This system accepts the 20 Mbit/sec data from the speed buffer and two 120 Mbit/sec data streams from the thematic mapper and HRPI modules. The data is modulated and transmitted to the LCGS and the STDN main ground stations, respectively. WBCM tradeoffs are discussed in Appendix A, Section 4.6.5.

6.7.2 System Summary

6.7.2.1 Data Handling System Overview

The mission instruments typically output many parallel channels of analog data (e.g., the Te TM has a 100-channel output). This data is telemetered by PCM encoding and time division multiplexing. The WBDHS performs the encoding and multiplexing functions outputing a serial digital data stream to the transmitter modulators. When required, the DHS may also edit, reformat, compress, or encode the data.

For the EOS-A baseline system, the PCM encoding is accomplished in each of the instrument modules by conventional methods; an analog multiplexer system connected to all of the instrument sensors analyzes the analog data for PCM encoding by a high-speed A/D converter. The serial digital data stream modulates the wideband transmitter or is operated on by the speed buffer (LCGS). The MODS controller controls and times the PCM encoder operation.

Sample rates and encoding accuracy are specified by the instruments and required reconstruction quality. For the EOS-A baseline system, the sample rate is 15 Mbit/sec with an output data rate of 120 Mbit/sec for each of the instruments (Te TM and HRPI). This data rate includes oversampling and instrument "fly-back" time. No speed buffering (or coding, data compression or editing) is necessary. Addition of these functions

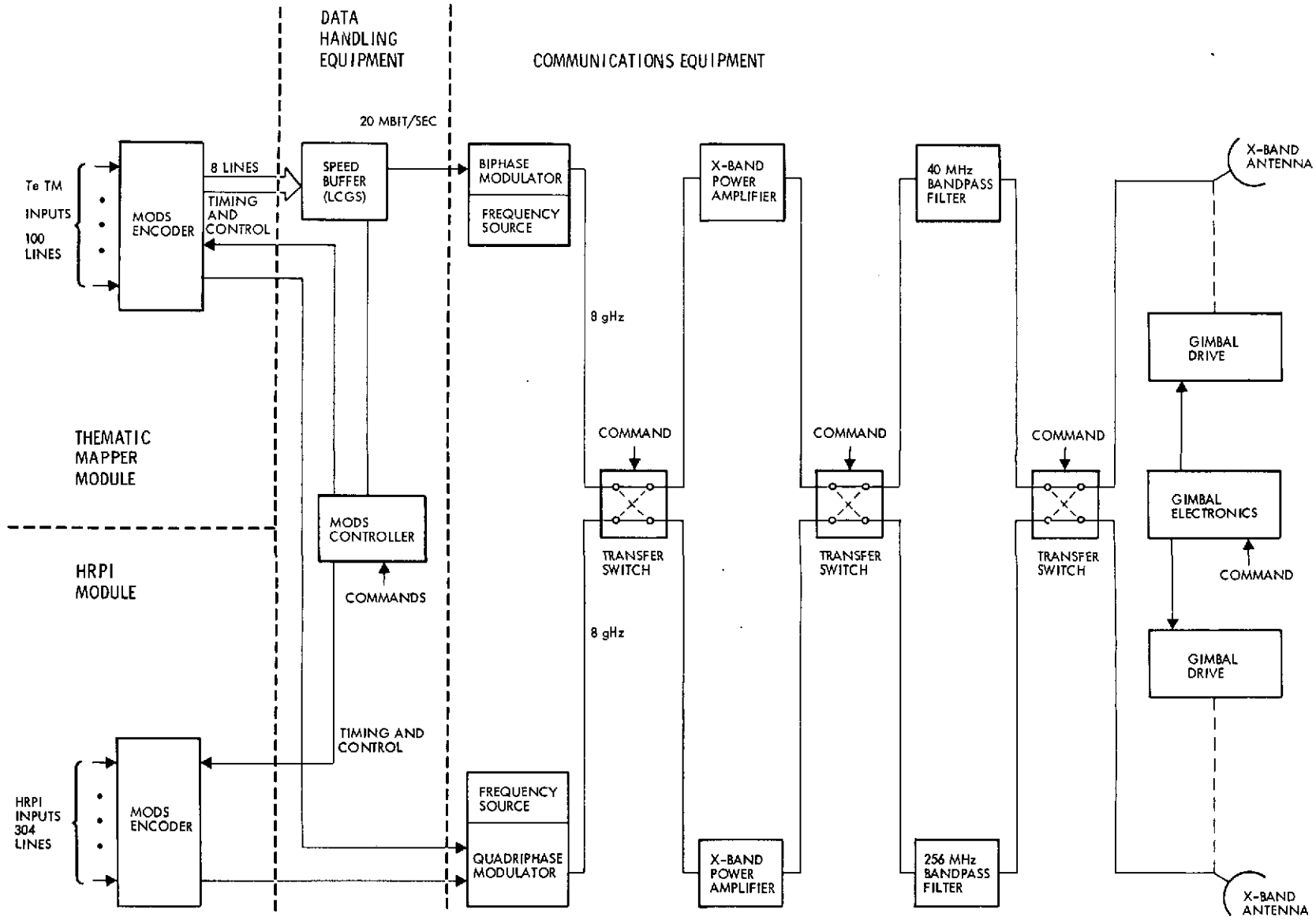

Figure 6-36. EOS-A Wideband Communications Block Diagram.

could only result in reduction of transmitter power or antenna diameter; these are presently 1/2 watt and 24-inches, respectively, so a slight reduction will be more than offset by additional component weight and power required for the speed buffering or coding, etc.

The LCGS requires a substantially lower data rate; 20 Mbit/sec as well as an edited format. The edited format for the Te TM is as follows:

- One color, full swath (normal = seven colors)
- Two colors, 1/2 swath
- Four colors, 1/4 swath
- Seven colors, 90 meters (1/9) resolution.

The speed buffer (LCGS) accomplishes this editing function as well as that of reformatting to line sequential.

6.7.2.2 Wideband Communication System Overview

The WBCS consists of modulators, amplifiers, antennas, and associated equipment required to transmit the two X-band signals. The data rates received from the WBDHS are 20 Mbit/sec for the medium-rate data and 120 Mbit/sec on two lines for the high-rate data. The medium-rate data is transmitted to the LCGS and the high-rate data is transmitted to the STDN main station.

The power amplifiers and the X-band antennas for the 20 and 250 Mbit/sec channels are identical. Transfer switches are included (as shown on Figure 6-36) so that either power amplifier and antenna may be used for either of the two signals. The transfer switches are relatively simple low-cost devices. Thus, the reliability of the system is increased with little or no design penalty.

6.7.3 Requirements Versus Capabilities

The requirements and capabilities for EOS-A WBCM are summarized in tabular form in Table 6-16.

6.7.4 Wideband Communication System Performance

6.7.4.1 RF Link Analysis

The modulation formats considered for the 20 Mbit/sec channel were BPSK and FSK. The power spectrum of FSK (discontinuous phase) has

Table 6-16. Requirements vs. Capabilities for EOS-A Wideband Communications Module and Data Handling

Requirement	Reference	Capability
Communications Equipment		
Transmit 240 Mbits/sec data to NASA STDN main ground station with P(E) 10^{-5} at X-band	EOS-410-06, GSFC, September 7, 1973	QPSK signal with modified ground station antennas achieves 6.5 dB margin
Transmit 20 Mbits/sec data to LCGS with P(E) 10^{-5} at X-band	EOS-410-06, GSFC, September 7, 1973	BPSK signal with 5-foot diameter antenna ground station achieves 6.6 dB margin
Power flux density at earth not to exceed U.S. government limits: • 140 dBw/m^2/4 kHz (zenith) • 150 dBw/m^2/4 kHz (horizon)	"Radio Frequency Allocations for Space and Satellite Requirements," GSFC, June 15, 1973	Transmitter power of 0.5 watt (EIRP = 25 dBw) for both channels satisfies PFD requirement
Data Handling Equipment		
Control a PCM encoder that encodes 100 channels analog data from the Te thematic mapper and 304 channels of analog data from the HRPI, including frame synchronization and housekeeping data. Output data rate is 120 Mbits/sec from each instrument	EOS-410-02, "Specifications for EOS System Definition Studies," GSFC, September 13, 1973	Controller is programmed by read only memory (ROM). Change in encoder channels or format requires additional multipliers for the Te thematic mapper and a ROM change in the controller – no HRPI change
Edit and reformat the data from the Tc thematic mapper PCM encoder reducing the output data rate from 128 to 20 Mbits/sec. Data editing is performed as follows: • One color full swath (normal, seven colors) • Two color one-half swath • Four colors, one-quarter swath • Seven colors, 90 meter resolution (normal, 30 meters)	EOS-410-02, "Specifications for EOS System Definition Studies," GSFC, September 13, 1973	Speed buffer (LCGS) performs this function. ROM control allows some additional flexibility

impulses at the carrier frequencies which contain half the total power. Thus, the PFD of PSK is 67 dB greater than BPSK at 20 Mbit/sec. Also, FSK requires 3.8 dB more total power than BPSK to achieve a 10^{-5} bit error rate. Therefore, BPSK is the best choice in terms of the PFD requirement and the efficiency of transmitter power.

QPSK and MSK modulation formats were considered for the 240 Mbit/sec channel. In terms of power loss, MSK has about a 0.4 dB advantage over QPSK, as shown in Figure 6-37. MSK appears to have a

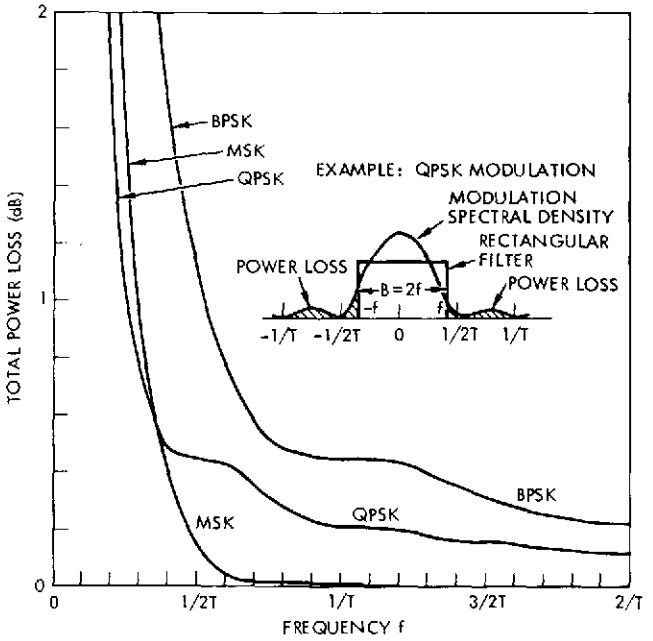

Figure 6-37. Power Loss Curves

slight advantage over QPSK in a narrow bandwidth. However, the total degradation (power loss, intersymbol interference, etc.) for QPSK at the bit rate bandwidth (240 MHz) is only about 1 dB, as shown in Figure 6-38. Thus, there is no compelling reason to use MSK in this system rather than QPSK.

Transmission filter bandwidths of 40 to 250 MHz for the medium- and high-rate data, respectively, give about 1 dB degradation, as shown in Figure 6-38. Increasing the filter bandwidth (to 1.3 times the bit rate, for example) would provide less than 0.5 dB improvements, as shown on Figure 6-38. Thus, the transmission filters are adequate for the 375 MHz bandwidth.

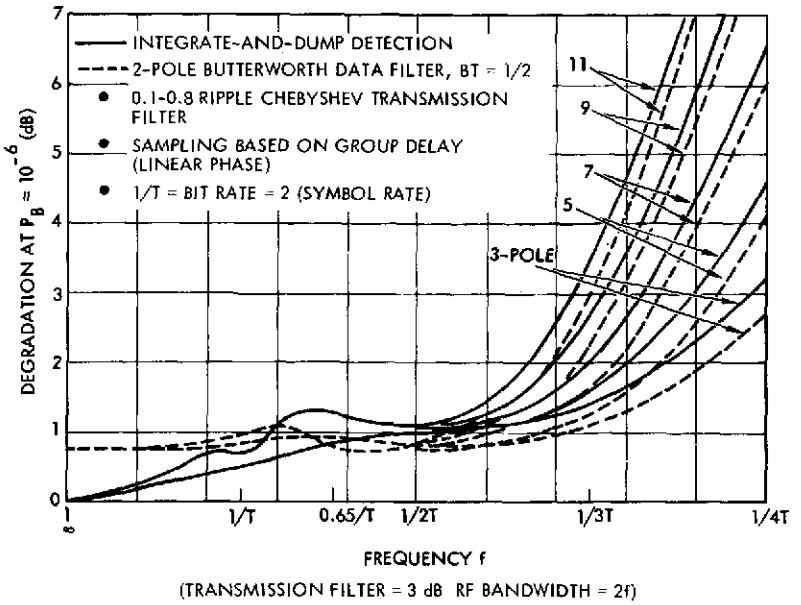

Figure 6-38. Degradation Due to Transmission Filtering vs. Filter Cut-off Frequency f for QPSK

The RF link analysis of the WBCS is summarized in Table 6-17. Notice that the high- and medium-rate signals have the same EIRP. This enables power amplifier switching between signals in case of a failure. The link analysis shows that signal power is adequate for both signals.

Table 6-17. RF Link Analysis Summary

	240 Mbit/sec	20 Mbit/sec
EIRP	25.0 dBw	25.0 dBw
Net path loss*	-128.1 dB	-138.1 dB
Received power, P_s	-103.1 dBw	-113.1 dBw
Bit rate	84.1 dB-Hz	73.0 dB-Hz
E_b	-187.2 dBw/Hz	-186.1 dBw/Hz
Noise Density, N_o	-206.2 dBw/Hz	-205.2 dBw/Hz
E_b/N_o	19.0 dB	19.1 dB
E_b/N_o at $P(E) = 10^{-5}$**	12.5 dB	12.5 dB
Margin	6.5 dB	6.6 dB

*Includes antenna gain

**Includes implementation margin

6.7.4.2 Power Flux Density Analysis

Maximum allowable power flux density on the surface of the earth (Table 6-16) places upper limits on spacecraft EIRP. To ensure compliance with PFD requirements, the RF link analyses were repeated with all tolerances on budget entries selected to maximize the PFD. The results are summarized in Table 6-18 which shows that for the design EIRP both links are within the PFD requirements.

6.7.4.3 Impact on Future Missions on System Configuration

At geostationary altitude, the SEOS would require 24 dB more transmitter power to achieve the same received signal level. This implies about 50 ~ 100 watt TWT's.

The EOS-A-prime requires about twice the data rate. This implies modification of the high-rate data channel at X-band to increase the

Table 6-18. Power Flux Density Analysis Summary

	240 Mbit/sec	20 Mbit/sec
PFD limit ($dBw/m^2/4$ kHz)	-140	-140
Net loss	-173.1	-165.1
Maximum EIRP	33.2 dBw	25.1 dBw
Design EIRP	25.0 dBw	25.0 dBw
Margin	8.2 dB	0.1 dB

transmission filter bandwidth if the bandwidth becomes available at X-band. Otherwise, higher-order modulation can be used. For example, octaphase modulation will essentially double the data rate in the same bandwidth.

6.7.5 Wideband Communications Equipment Description

The wideband communications equipment is listed in Table 6-19. The equipment is divided into two major sections: the digital data handling equipment and the communication equipment. Components contained within the module but technically described in other sections are the data interface unit (Section 6.1) and the power converter (Section 6.4).

Table 6-19. EOS-A Wideband Communications and Data Handling Module Equipment List

Component	No. Required	Size (in)	Weight Each (lb)	Peak Power (watt)	Low Power (watt)	Secondary Power	Comments
Communications Equipment							
X-Band Antenna	2	24-inch dish	2.0	0	--	--	
Gimbal Drive	2	6.4 x 7.1 x 13.6	14.2	5.6	0.3	--	
Gimbal Electronics	2	5.7 x 7.7 x 11.5	6.3	3.5	0.3	--	
RF Transfer Switch	3	2.5 x 1.4 x 1.4	0.4	1.0	0	--	
Bandpass Filter - 40 MHz	1	0.7 x 0.4 x 2	0.1	0	0	--	
Bandpass Filter - 240 MHz	1	0.7 x 0.4 x 2	0.1	0	0	--	
X-Band Power Amplifier, 0.5W	2	6 x 6 x 1.5	2.0	7.0	7.0	X	
X-Band Modulator	2	8 x 8 x 3	3.6	10.0	10.0	X	
Waveguide Sections	TBD	N/A	N/A	0	0	--	
Data Handling Equipment							
MODS Controller	1	6 x 8 x 2	3.0	5.0	5.0	X	
Speed Buffer (LCGS)	1	12 x 8 x 16	20.0	40.0	40.0	X	
Data Interface Unit (DIU)	1	6 x 8 x 1	1.2	0.2	0.1	X	
Power Converter	1	6 x 8 x 2	5.0	80.0	70.0	--	Total secondary power = 62W

Secondary power is supplied to all components with a single power converter. Off-the-shelf components with self-contained converters may use primary power. The data interface unit handles all the module command and telemetry requirements. In general, it does not handle communication between components within the module.

The wideband communications data handling equipment is illustrated in Figure 6-36.

X-Band Power Amplifier

Both downlink wideband systems require 1/2 watt X-band power amplifiers. TRW recommends the use of solid-state Impatt diodes for this application. Space-qualified diodes are currently available that can be used in a three-stage amplifier design integrated with a multiport circulator to provide directivity between the RF input and output.

Bandpass Filters

A low-loss bandpass filter is required at the output of each 1/2 watt X-band amplifier to restrict the transmitted signal energy to a narrow frequency band. A 5-pole 0.1 dB ripple Chebyschev design has been selected for both the 20 and 240 Mbit/sec links. The filter response and design was predicted with the aid of a complex computer-aided design technique developed by TRW. The result is a fixed tuned design which does not require a costly alignment procedure during manufacturing. Both filters can be fabricated from waveguide.

X-Band High-Gain Antennas

A pair of high-gain steerable antennas is used for the wideband downlink transmissions. In operation, one antenna transmits the 20 Mbit/sec signal while the other is used for the 240 Mbit/sec link. Each antenna is a 2-foot diameter right-hand circularly-polarized parabolic dish providing a gain of 31.5 dBi. The design for the EOS-A mission was scaled from the high-gain S-band antenna used on the Defense Satellite Program. This antenna was constructed from aluminum honeycomb sandwiched between two fiberglass facesheets.

X-Band Transfer Switch

The wideband power amplifiers and antennas are cross-strapped by using transfer switches. The switch is the conventional four-port rotor type using curved waveguide to opposite ports.

Gimbal Drive and Electronics (Figure 6-39)

Drive Mechanism. Each X-band antenna is gimballed in two orthogonal axes by a geared mechanism using a stepper motor drive for each axis. The mechanism is the flight-proven two-axis antenna positioner on DSCS-II. This unit employs a permanent magnet stepper motor driving through two stages of gearing. The first stage is a harmonic type gear reducer. A multi-speed resolver on the output shaft which drives the antenna provides an indication of the output shaft position. Lubration of the gears is accomplished by using a fluid lubricant stored in sintered nylon reservoirs. Each axis of the antenna positioner is limited in angular travel. A cable wrapup carries the electrical signals of shaft position directly from the rotor to the output connector, thereby eliminating the use of brushes.

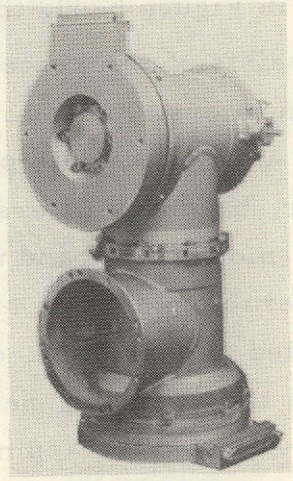

- STEP SIZE: 0.0315 DEG
- POWER: 5.6 WATTS AT SLEW
- SLEW SPEED: 1.5 DEG/SEC
- DRIVE TORQUE: 13.0 FT-LB
- SIZE: 6.4 x 7.1 x 13.6 IN.
- WEIGHT: 14.2 LB

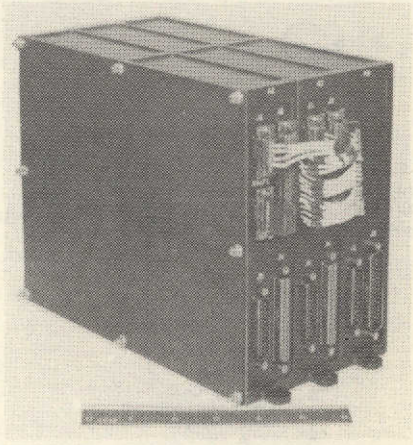

- SIZE: 5.5 x 7.7 x 11.5 IN.
- WEIGHT: 6.3 LB
- POWER: 3.5 WATTS AT SLEW
- GIMBAL READOUT ACCURACY: 0.03 DEG

Figure 6-39. Antenna Gimbal Drive and Electronics

Gimbal Drive Electronics. The gimbal electronics assembly contains two identical gimbal control subassemblies and a resolver electronics subassembly, which provide redundant control of two antenna biax drive assemblies. Each gimbal control subassembly (GCS) is capable of stepwise driving four antenna gimbal stepper motors, one at a time, in response to input commands from the on-board computer. The signal inputs are in the form of a digital code and include a:

- Motor address, selecting the gimbal motor to be stepped
- Sign bit, identifying the direction of motor rotation
- Step pulse for each step of the addressed motor.

The command inputs from the on-board computer result in outputs which control four bifilar wound DC step motors.

The resolver electronics subassembly contains three synchronous demodulators which process a X36 speed sine, X36 speed cosine, and X1 speed sine outputs of each of four identical resolvers.

6.7.5.1 Wideband Communication Equipment

This section describes the communication equipment portion of the wideband communication module. As shown in Figure 6-40, the equipment consists of reference frequency generators, X-band modulators, 1/2-watt solid-state power amplifier, bandpass filters, two gimbal-mounted X-band narrowbeam steerable antennas, and the associated gimbal drive electronics and the switching necessary to affect cross-strapping of the power amplifiers and antennas.

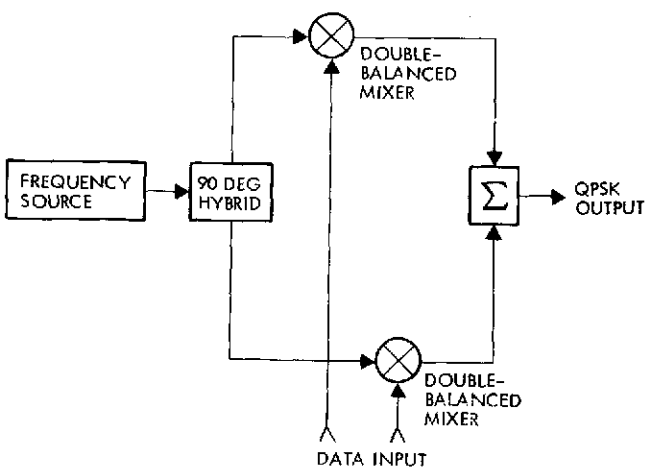

Figure 6-40. Direct Modulation Design

X-Band Modulators

A pair of wideband modulators is used to generate the X-band downlink RF signals. One modulator is used for the 20 Mbit/sec biphase data while

the other is used to produce the 240 Mbit/sec quadriphase signal from a pair of 120 Mbit/sec data streams. A single modulator design is employed which is capable of operating in either the low bit rate biphase or high bit rate quadriphase modes.

Of the various techniques available for achieving X-band modulation, TRW recommends the direct method using double-balanced mixers. This design is shown in Figure 6-40, where an X-band reference frequency is split into two 90 degree components in a quadrature hybrid. The quadrature components, along with the digital data, are applied to a pair of double-balanced mixers which function as suppressed carrier biphase modulators. A quadriphase modulated signal is formed by applying independent data streams to the mixers and summing the mixer outputs. Biphase modulation is produced by driving both mixers with the same data.

Frequency Source

Two X-band reference frequency sources are required to drive the direct X-band modulators. One source supplies a frequency at 8.050 gHz for the 20 Mbit/sec system while the other drives the mixer st 8.235 gHz for the 240 Mbit/sec system. Both sources are identical in design and are driven b y two crystal oscillators which differ slightly in frequency. The source design employs direct multiplication (by 96) of the crystal frequency. The multiplication is performed in several steps using transistors for frequencies up to S-band and a x4 S- to X-band varactor multiplier in the final stage.

6.7.5.2 Wideband Digital Data Handling Equipment

A simplified block diagram of the data handling equipment is shown in Figure 6-41. The multi-megabit operational data system (MODS) encoders are located in the instrument modules, and the MODS controller and speed buffer (LCGS) are located in the wideband communications module. For the sake of clarity, this discussion will consider the wideband data handling system as one function regardless of the modular location.

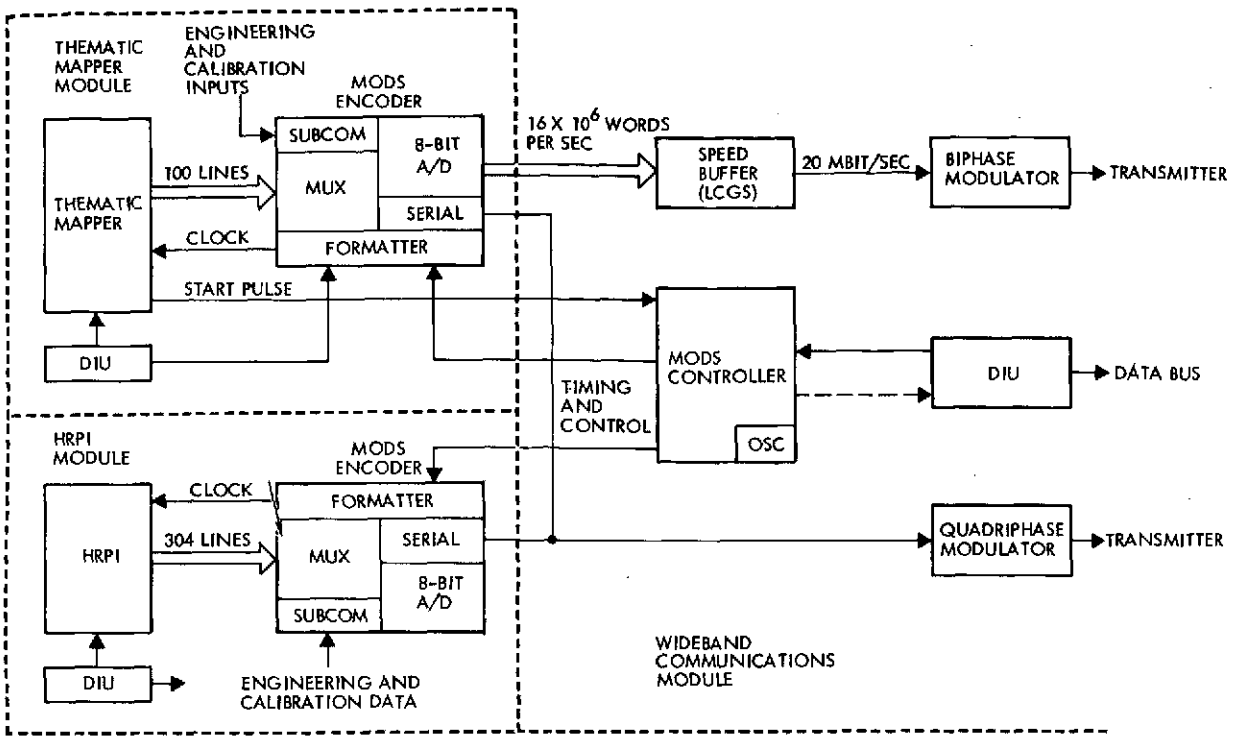

Figure 6-41. Wideband Data Handling Equipment

MODS Components

The MODS components are functionally identical to the multi-megabit operational multiplexer system (MOMS) components. The MODS nomenclature is used to stress the importance of modular design for this component group.

The EOS-A MODS system consists of three components:

1) High speed A/D converters (encoders), each located with their respective instruments

2) The thematic mapper and HRPI

3) The MODS controller which is located in the wideband communications module.

Locations of the two encoders with the instruments is obvious; the interface with the thematic mapper and the encoders requires 100 analog data lines and the HRPI/encoder interface requires 304 lines. With the encoders located next to the instruments, these lines can be made short, minimizing noise pickup, obviating AC coupling and reducing weight. The

thematic mapper encoder requires an eight-line output interface to the speed buffer and each instrument requires just a single line output to the quadriphase modulator in the wideband communications module.

It is expected that the encoder integration will be handled by the instrument manufacturer. This procedure will allow proper test of special-purpose circuits such as the Te thematic mapper variable delay scan start (described further in Appendix A), as well as the overall test of a complex interface.

The MODS components are functionally identical to the multi-megabit operational multiplexer system (MOMS) components. Study of future EOS requirements indicated that the wideband data handling system could be designed with modular components so that one design will fit all missions as well as all instruments. Special-purpose signal conditioning boards/slices (a part of the component) will probably be necessary in many instances, but the major portion of the system will require only firmware changes in the controlling read only memories (ROM's) to be adapted to different instruments. This is the fundamental difference between the recommended baseline system (MODS) and the proposal baseline system (MOMS).

The MODS nomenclature is used to stress the importance of modular design for this component group.

Modularization is achieved as follows:

1) Standard boards/slices are designed. These sections are combined to perform the desired functions. Figure 6-42 shows how these boards/slices are combined for the baseline system (Te TM and HRPI).

2) ROM's or PROM's are used to program minor and major frame events to the following quantization levels (see Figure 6-43):

Major Frame Timing:	12 bits (4096) The major frame may be quantized in as many as 4096 minor frame groups
Minor Frame Timing:	9 bits (512) The minor frame may be quantized in as many as 512 word groups

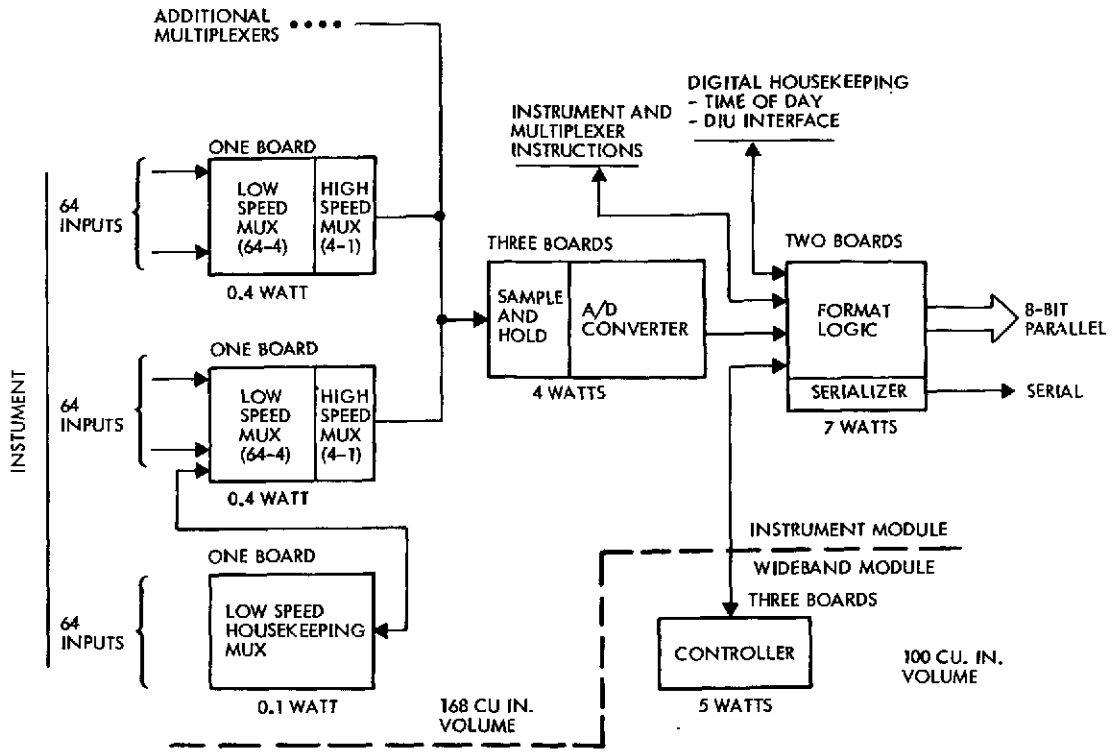

Figure 6-42. MODS Conditioning

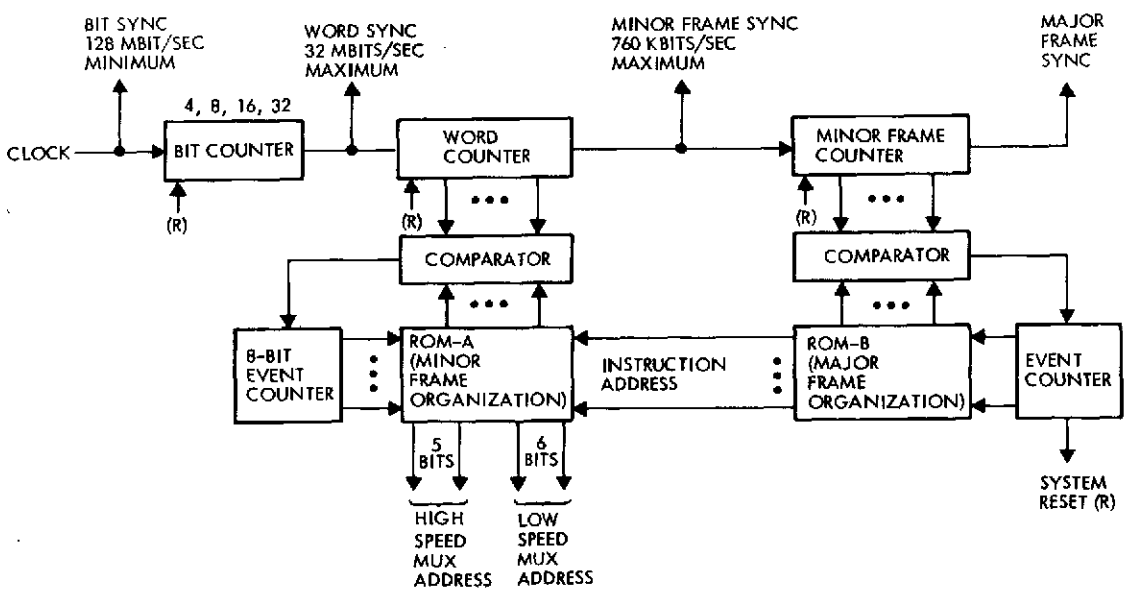

Figure 6-43. Micro-controller for the High-Speed Multiplexer

Word Timing:	Word lengths of 4, 8, 16 and 32 are selectable
Maximum Address Selection:	11 bits (2048) 2048 data addresses may be selected (the high speed multiplexer is addressed with 5 bits and the low speed with 6 bits).

EOS-A Format

For EOS-A, identical data rates for the two instruments are recommended. As discussed in Section 6.8.2, the two data channels are quadriphase modulated on the wideband downlink carrier. This requires identical bit rates or a known harmonic relationship. Equal rates are achieved in EOS-A by oversampling the HRPI and providing a header sequence similar to that used in the Te thematic mapper.

The formats for the thematic mapper and HRPI are shown in Figures 6-44 and 6-45, respectively. The major frame length for the thematic mapper is 8.9×10^6 bits, whereas the HRPI is 0.186×10^6 bits. No frame synchronization is provided at the minor frame level.*

Speed Buffer (LCGS)

The data rate to the LCGS from the Te TM must be reduced from 120 Mbit/sec to approximately 20 Mbits/sec. This data reduction is achieved by selectively editing the data so that approximately 1/6 of the original data is transferred. To provide a continuous 20 Mbit/sec data stream to the transmitter modulator, the edited data must be speed buffered. A secondary function of the speed buffer is that of reformatting

*The necessity for minor frame synchronization is determined by the expected slippage in the HDDT tape recorder bit synchronizer. The recommended baseline tape recorder system (Ampex-2042) specifies a bit error rate of less than 10^{-6}. This rate includes all effects from tape dropouts and bit slippage. With the optimum synchronization scheme used by Ampex (phase-lock bit synchronization with matched data filters) an actual phasing slip or loss of a clock pulse should occur orders of magnitude less than tape dropouts. Frame synchronization at the beginning of the major frame only greatly simplifies the synchronization circuitry with no appreciable signal degradation.

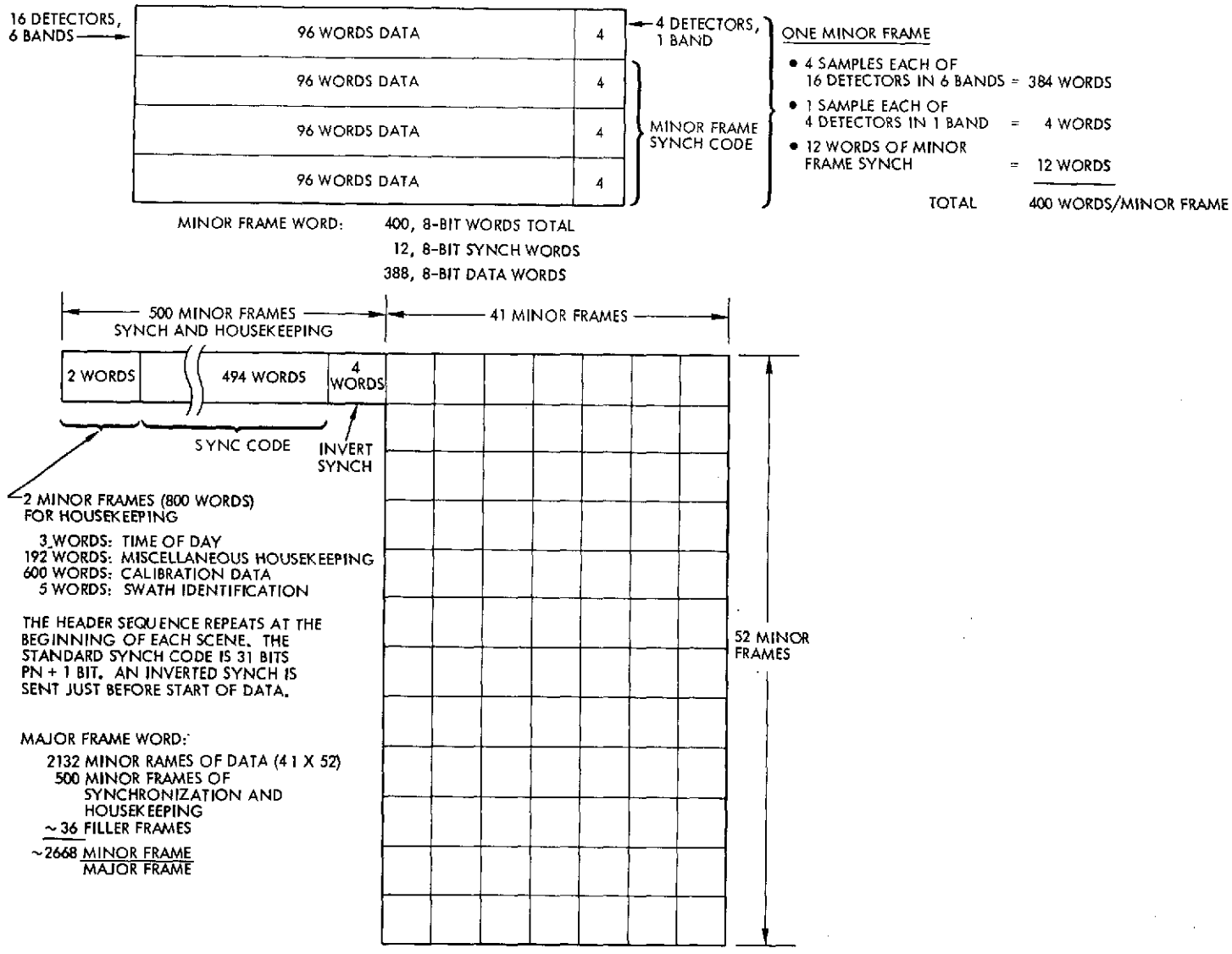

Figure 6-44. EOS-A Wideband Data System CDPF Data Format — Thematic Mapper

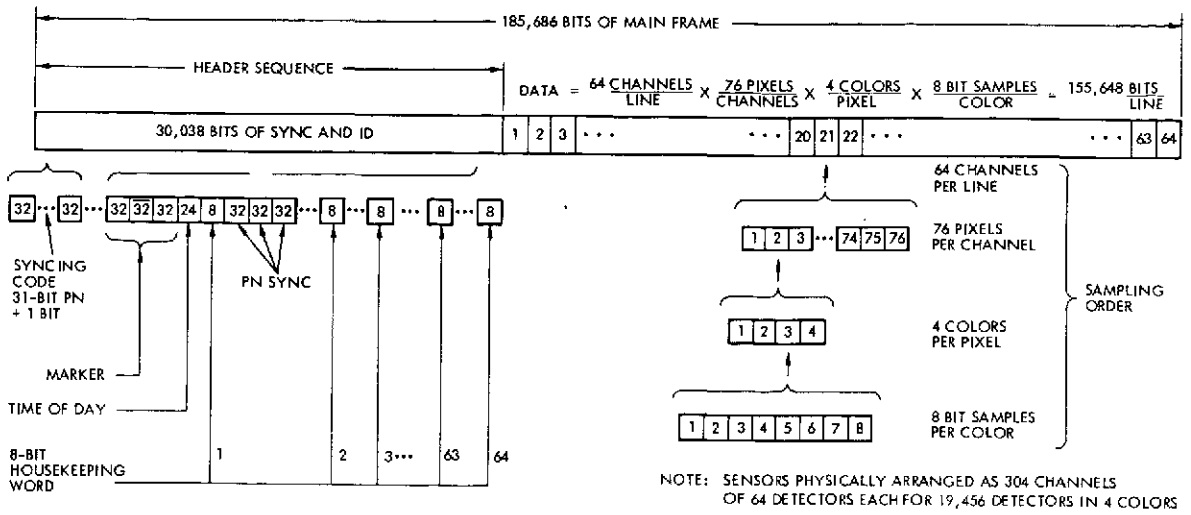

Figure 6-45. Wideband Data System CDPF - HRPI

the data so that it can be handled directly by a cathode ray tube or other picture-producing equipment. Reformatting is necessary because the data is normally transmitted in pixel or column sequential order rather than live sequential order.

The speed buffer is constructed in two major sections: the line stripper and formatter. The line stripper edits 120 Mbit/sec data to reduce the average data rate to 20 Mbits/sec, and the formatter speed buffers and reformats the data to line sequential. Figure 6-46 shows how the data is received from the MODS encoder; complete minor frames (columns) are received in numerical sequence, frame 1 first, frame 8538 last. The pixels, which comprise the frame, are also received in numerical sequence. The reformatter must change the order of transmission so that pixel row 1 is first transmitted, then row 2, etc. In other words, the first pixel of each minor frame is transmitted first, then second, etc.

The line stripper edits the data before reformatting. The baseline design provides for four possible editing options:

1) All data from one band (out of seven possible), full swath

2) Two bands for one-half swath

3) Four bands for one-quarter swath

4) Seven bands, reduced resolution (90 meters)

Equipment Design

A block diagram of the speed buffer is shown in Figure 6-47. The editing instruction to the line stripper is received by ground command through the DIU. The reformatting instructions are contained in the format memory ROM. Editing changes from the baseline can be made by changing the format memory ROM and adding (or subtracting) data memory slices/boards.

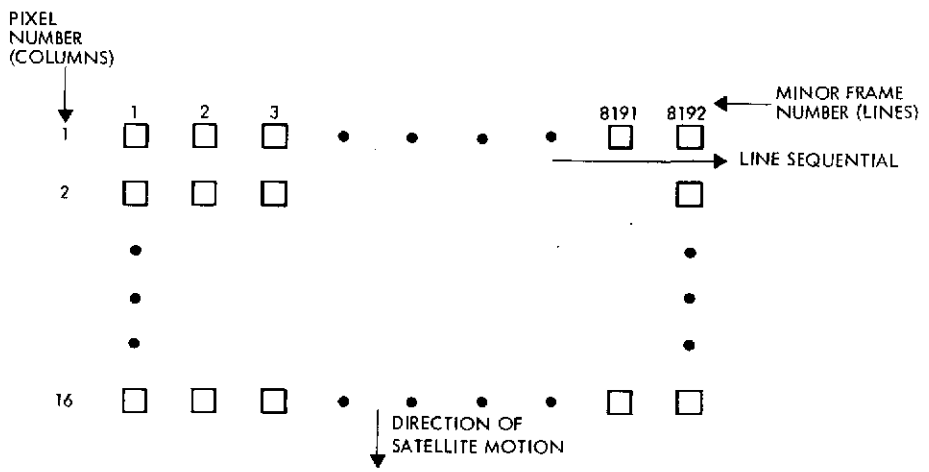

Figure 6-46. Speed Buffer Data Format (One Swath)

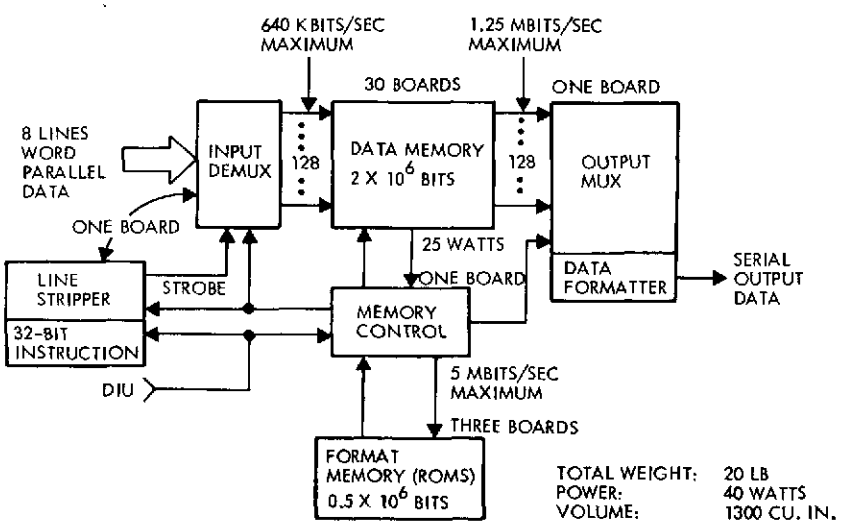

Figure 6-47. Speed Buffer (LCGS) Partitioning (includes a line stripper and formatting)

The data memory for reformatting uses N-MOS technology. The memory is contained on 30.6 x 8-inch boards and requires 25 watts of power. The entire speed buffer weighs 20 pounds and requires 40 watts of power (active). Modular design as well as ROM control means that future missions and other instruments may very well use the same equipment with no design modification.

Personnel requirements do not change appreciably from ERTS to EOS. Additional EOS tasks, such as HDDT handling and laser beam recorder operation, are offset by deletion of the electron beam recorder system and the manual RCP interaction and intermediate film processing of ERTS. Operational costs are dominated by the cost of tape media. A considerable savings in operational cost can be obtained if holographic storage replaces HDDT archiving and output product generator input (>$1M). However, the holographic storage system requires significant development effort, and as such has not been included in the baseline.

6.8 SPACECRAFT STRUCTURE AND MECHANISMS

The spacecraft, that part of the observatory from the transition ring aft, is comprised of a structure and group of subsystem modules. The solar array module, located just forward of the transition ring, is also a spacecraft module. The mechanisms release, separate, and deploy various spacecraft and payload devices.

6.8.1 Spacecraft Structure

This study analyzed two EOS-A baseline structural configurations: the Titan (Figure 6-48) and the Thor-Delta (Figure 6-49). Preliminary stress and modal analyses have been performed on each configuration to confirm that design requirements and/or goals have been met and that the structural weight allocated and reported in Section 4.5 is accurate.

This section describes the following:

- Structural design requirements and philosophy for both the Titan and Thor-Delta configurations
- Structural descriptions of each configuration
- Results of structural analyses performed on each of the two baseline configurations.

Each configuration is discussed separately and is identified as either Titan or Thor-Delta.

The EOS-A baseline structures use aluminum as the primary structural material. In local areas, titanium and/or fiberglass is used for thermal isolation since the thermal conductivity of these materials is significantly less than aluminum.

Two joining methods were considered: welding and mechanical fasteners. The differences in costs of the two methods are negligible. However, strength, structure weight, and distortion considerations for both the Thor-Delta or Titan configurations eliminated welding as an overall acceptable joining technique. Aluminum allow 6061, the best candidate material for a welded structure, in the as-welded condition has a yield strength of approximately 16,000 psi compared to the T6 condition where F_{ty} = 35,000 psi. Since the structures are large and require many close tolerance fits and alignments, distortions associated with welding and stress relief are undesirable. Machining critical surfaces after welding and stress relief is expensive. Welding fixtures and assembly fixtures have the same relative cost and complexity therefore mechanical fastening was selected as the preferred joining method on the basis of overall cost efficiency. Higher strength alloys can also be used to provide additional weight margin if required, as long as the structure is riveted or bolted.

6.8.1.1 Design Requirements and Philosophy

Requirements

Structure design requirements for the spacecraft are specified in terms of load factors associated with various flight events. For preliminary structural analyses, these loads are identified by the launch vehicle contractors based on past launch and flight experience with payloads of similar weight and stiffness. Table 6-20 is a list of limit load factors recommended for the various tabulated flight events for four candidate launch vehicles including Shuttle. Limit load is defined as the maximum anticipated flight load expected for the event shown. As the table indicates, the Shuttle loads are small relative to Thor-Delta or Titan loads, which therefore govern the strength requirements for the baseline spacecraft designs.

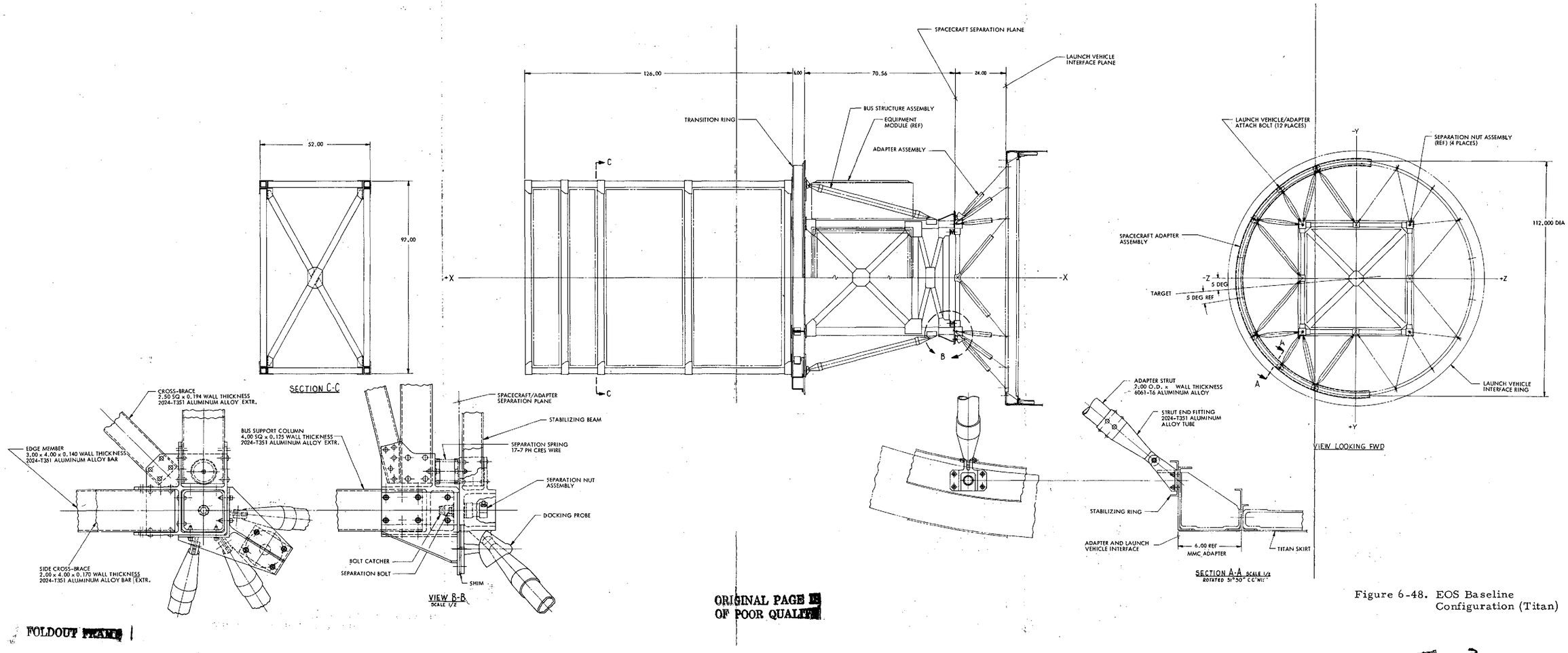

Figure 6-48. EOS Baseline Configuration (Titan)

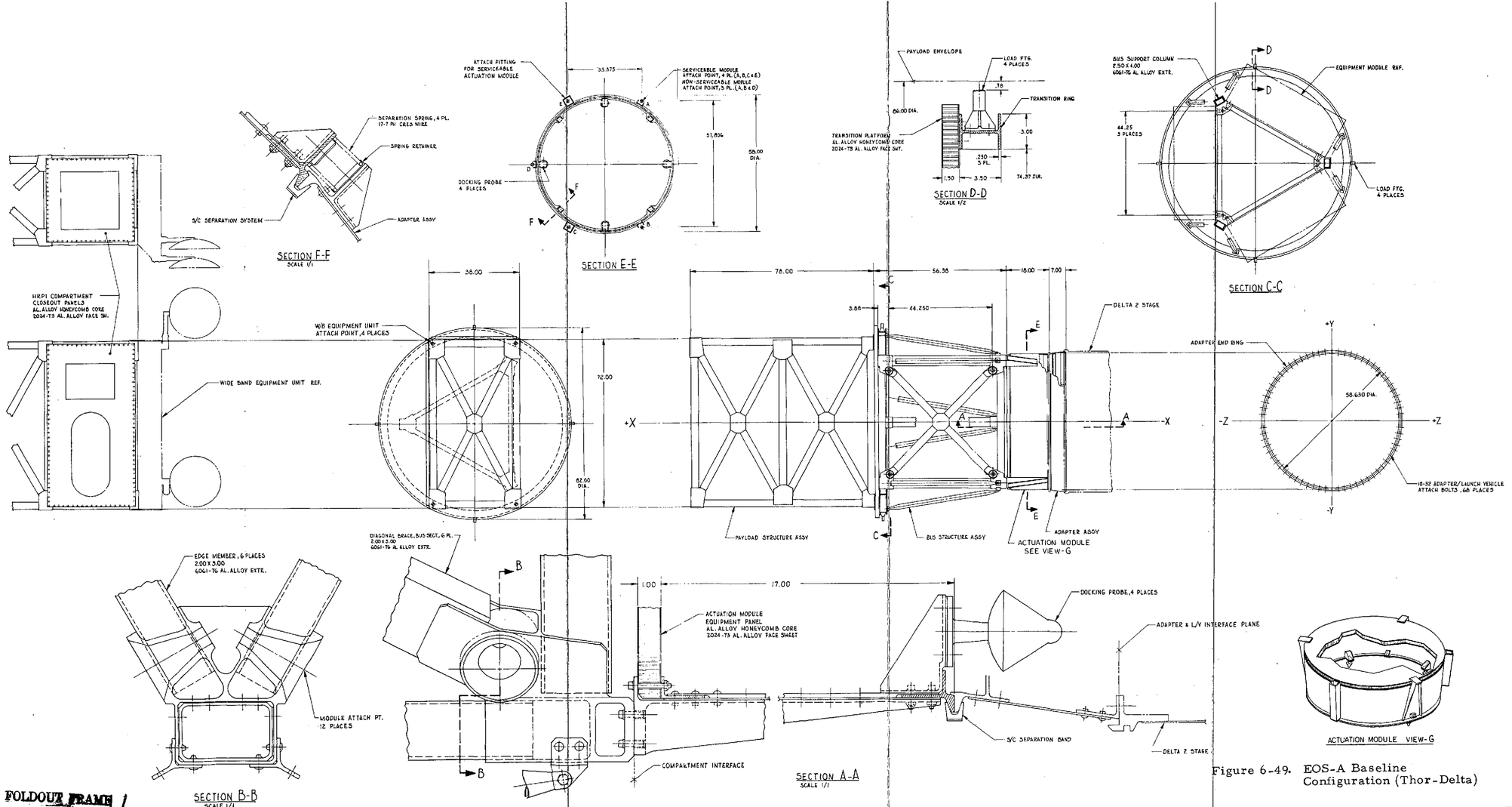

Figure 6-49. EOS-A Baseline Configuration (Thor-Delta)

FOLDOUT FRAME 1

FOLDOUT FRAME 2

FOLDOUT FRAME 3

Table 6-20. Maximum Expected Flight Loads *+ (g's)

Flight Event	Shuttle			Thor-Delta 2910			Titan IIIB 5,000 lb Spacecraft			Titan IIID 15,000 lb Spacecraft		
	X	Y	Z	X	Y	Z	X	Y	Z	X	Y	Z
Liftoff	-2.3	±0.3	-0.8	-2.9 +1.0	±2.0	±2.0	-2.3 +1.0	±2.0	±2.0	-2.5 +1.0	±2.5	±2.0
High or maximum dynamic pressure	-2.0	±0.5	±0.6									
Booster or Stage I burnout	-3.3	±0.2	-0.4	-12.3 -4.0	±0.65	±0.65	-8.2 +2.5	±1.5	±1.5	-7.6 +2.5	±1.5	±1.5
Orbiter or Stage II burnout	-3.3	±0.2	-0.75				-10.8 +2.0	±1.5	±1.5	-6.7 +2.0	±1.0	±1.0
Shuttle space operations	-0.2 0.1	±0.1	±0.1									
Entry and descent	+1.6 -0.25	±1.5	+3.0 -1.0									
Landing and braking	±1.5	±1.5	+2.5									
Crash**	+9 -1.5	±1.5	4.5 -2.0									

+Each triad of X, Y, Z loads is applied simultaneously.

*X, Y, Z refer to Shuttle axes.

**Crash loads are ultimate and used only for satellite support fitting design.

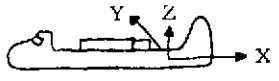

The yield and ultimate safety factors below were used for preliminary structural analysis and are recommended for use on EOS-A. The yield factor of 1.5 and ultimate factor of 1.88 are 50 percent greater than the currently used unmanned spacecraft factors of 1.0 for yield and 1.25 for ultimate. This additional margin provides several advantages as discussed in the following section on Design Philosophy.

Load	Safety Factor
Limit	1.00
Yield	1.50
Ultimate	1.88

Because of requirements for relatively small thermal distortions (discussed in Section 6.9), and instrument pointing accuracy, the total spacecraft and payload structure will be controlled to maintain a constant temperature close to ambient ($70^{\circ}F$). Therefore, temperature effects (material property changes and/or thermal stresses) do not impose any design requirements on the spacecraft structure except with regard to the pointing accuracy discussed later.

In the deployed configuration, all hinges and joints must have zero "slop" to assure that the observatory behaves linearly as it undergoes low amplitude vibration. This is required for fine pointing and accurate attitude determination.

Design Philosophy

In most past spacecraft programs structural weight has been minimized to allow the largest possible spacecraft payload. For large spacecraft, this design approach results in spacecraft bending modes low enough in frequency to couple with booster modes. Thus, analysis of structural responses of the booster/spacecraft combination has been required to establish spacecraft structural loads and deflections. To verify the spacecraft structural analytical model used in these analyses, modal survey tests have often been conducted on structural model spacecraft. The loads resulting from the combined booster/spacecraft analysis have then been applied statically to the structural model. This design

approach is used routinely on Titan payloads and is advisable for the larger Thor-Delta payloads which cannot easily comply with minimum frequency requirements.

For EOS, this process has been re-examined in light of the opportunity to employ more structural weight in order to reduce cost. It has been concluded that the structural weight penalty required to stiffen the structure enough to eliminate combined booster/spacecraft loads analysis is excessive and would seriously compromise the payloads of booster-launched EOS missions. Consequently, an intermediate approach has been adopted to minimize, but not eliminate, structural analysis and test. The key ingredients of this approach are as follows:

1) A yield factor of 1.5 and an ultimate factor of 1.88 above maximum expected flight loads will be used in the design. These factors are 50 percent greater than the usual values of 1.0 and 1.25 and provide the following advantages:

   - Small design changes can be incorporated without major reanalysis and test
   - Uncertainties in load paths, local flexibility in joints, and damping are less important
   - Substantial growth potential is possible without redesign of hardware by reduction to conventional safety factors if required
   - Dynamic (sinusoidal) testing to near limit load becomes more feasible.

2) The number of bending modes below 50Hz (i.e., in the range of booster frequencies) will be minimized. This simplifies analysis by permitting less detailed models and allows for less costly modal frequency measurement techniques. Specific design features incorporated for this purpose include: 1) stiffening all modules to maintain minimum frequencies above 50 Hz, and 2) incorporating pin-pullers to support the front faces of the two upper refurbishable payload modules during Titan launches.

3) Low-level sinusoidal base excitation in three axes will be used to identify primary structural frequencies and obtain a qualitative description of mode shape. If required, the analytical model can be altered after the sine tests to correct for frequency errors. In any event, only analytically predicted mode shapes will be used in loads analysis. The use of less costly sinusoidal tests in lieu of a modal survey is justifiable when a limited number of modes having rather simple shapes are expected.

4) Sinusoidal vibration testing to levels below yield, but generally at or above limit load, will be used to verify structural adequacy. Such a test is relatively inexpensive, particularly when combined with the low-level sweeps, but has the disadvantage of not testing all structural elements uniformly. The 50 percent overdesign in the structure permits overtest in some members while others are tested at or near limit loads.

The net result of these design and test goals for EOS-A are to: 1) minimize the need for detailed analytical loads prediction through the use of generour margins of safety, and 2) replace the costs of static and modal survey testing with those of three-axis sinusoidal base excitation tests.

6.8.1.2 Structural Description

Each of the baseline structural configurations consists of two major sections: 1) the primary structure (rectangular or triangular box-type structure), and 2) the equipment models. The primary structures for the two configurations are significantly different and are described separately. The modules are basically common in structural configuration (48 x 48 x 18 inch box) and are consequently described only once. The different and unique propulsion module is described separately by reference to a drawing layout.

Primary Structure (Titan Configuration)

The primary spacecraft structure for the Titan configuration is shown in Figure 6-48 and consists of three major subassemblies:

1) Cross-braced square cross-section four-legged truss structure centered on the observatory longitudinal axis and extending from the aft adapter to the plane of the transition ring

2) Transition ring and cross-beams located nominally in the plane of the transition ring, with load fittings for Shuttle compatibility

3) Eight diagonal outrigger struts extending aft from the transition ring to the separation plane at the aft end of the spacecraft raft box structure.

Assembly of all the elements into the all-up aluminum spacecraft structure is done with mechanical fasteners.

The box structure has four square tube longerons (one at each corner) which serve as the major load carrying and stiffening members

of the structure. They carry the axial loads directly to the aft adapter through the separation pads and also act as the caps of the cross-braced beams to transfer primary bending loads. This structure has two bays with the upper one matching the height (48 inches) of the side-mounted subsystem modules and the lower accommodating the aft-end mounted propulsion module and providing interface with the adapter. Corner gussets with integral fittings at each corner of the upper bay pickup the mating module attachment fittings which transfer their loads into the primary structure at these locations. Thus, the module-to-structure mechanical interface occurs at these typical four corner locations. The firm hard interface desired structurally conflicts with a low-conductivity interface desired thermally to minimize thermal distortions. The compromise and means of meeting both requirements is discussed in Section 6.9 where thermal distortion considerations are evaluated. The diagonal cross-braces for transferring shear loads are attached directly to these corner gusset female fittings so that module loads are transferred directly into primary structural members (horizontal, vertical, or diagonal) at these points.

The transition ring and its in-plane cross-beams provide an effective lead redistribution bulkhead between the spacecraft and payload. To transfer loads from the payload through to the spacecraft the outrigger struts must be included to make the bulkhead structurally efficient. The four spacecraft primary longerons and eight outriggers intercept the plane of the transition ring outside the pattern of longerons which outline the payload primary structure. Thus, the redistribution is necessary except for that part of the load which transfers directly from the payload longerons into the outrigger directly beneath it at the ring. In addition to acting as a redistribution bulkhead type structure, it is used as the support frame in the Shuttle. The ring mounts three load fittings (located on the basis of four) for mating to Shuttle and provides the cantilevered support of the spacecraft aft and the payload forward of this ring.

The diagonal outrigger struts combine with the transition ring to provide a direct longitudinal load path from the payload longerons to the aft adapter. The struts also act as sway braces for the spacecraft primary structure relative to the transition ring.

Primary Structure (Thor-Delta Configuration)

The primary Thor-Delta configuration spacecraft structure is shown in Figure 6-49 and consists of four major subassemblies:

1) Equilateral triangular main frame outlined by three longerons projecting aft from the plane of the transition ring

2) Aft stiffened cylindrical shell structure which mounts the forward section of the separation joint

3) An I-section transition ring and sandwich bulkhead in the plane of the ring, plus load fittings for Shuttle compatibility

4) Six struts joining the transition ring to the forward end of the aft cylindrical shell structure.

The triangular main frame uses the three rectangular tubular longerons to transfer the axial loads through the spacecraft to the aft stiffened cylindrical shell. The longerons are joined top and bottom with closeout tubular frame members and diagonal cross-braces provide shear resistance by completing the truss frame.

The forward end of the longerons intercepts the bulkhead in the plane of the transition ring. The bulkhead and ring serve as load redistribution members between the payload section and the spacecraft section of the observatory.

At the aft end, the three longerons are faired into the cylindrical skirt to help more uniformly distribute the loads into the separation ring at the aft end of the skirt. The stiffened cylindrical shell (skirt) mounts the support frames for the propulsion tankage, thus transferring these loads directly to the separation plane. The upper mating half of the separation ring will provide the aft closure ring for the cylindrical shell at the separation plane. The forward end of the cylindrical shell will be ring stiffened with fittings spaced around the ring for attaching the tank support struts and/or frames.

The Delta design has provisions for the actuation module to be space-serviceable by the addition of the attach mechanisms. The structure includes a beam to pick up two of the four actuation module attach points for the serviceable case only (Figure 6-50). The baseline is not

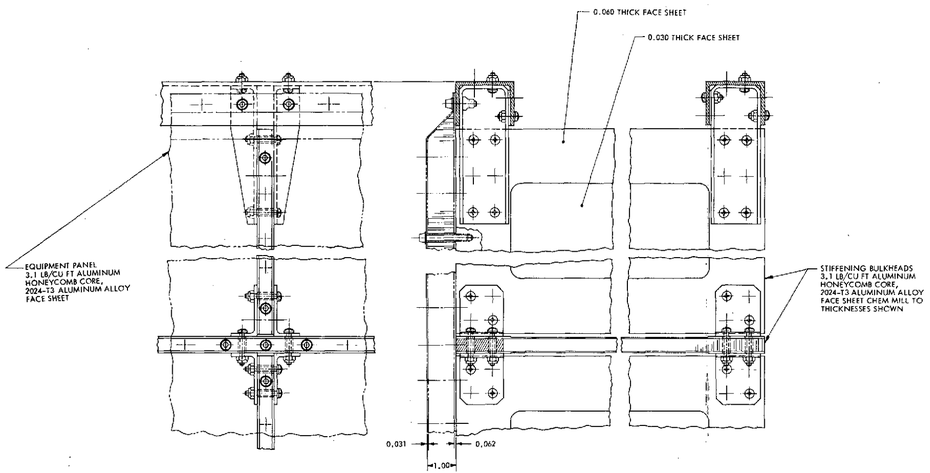

SECTION A-A
SCALE 1/1

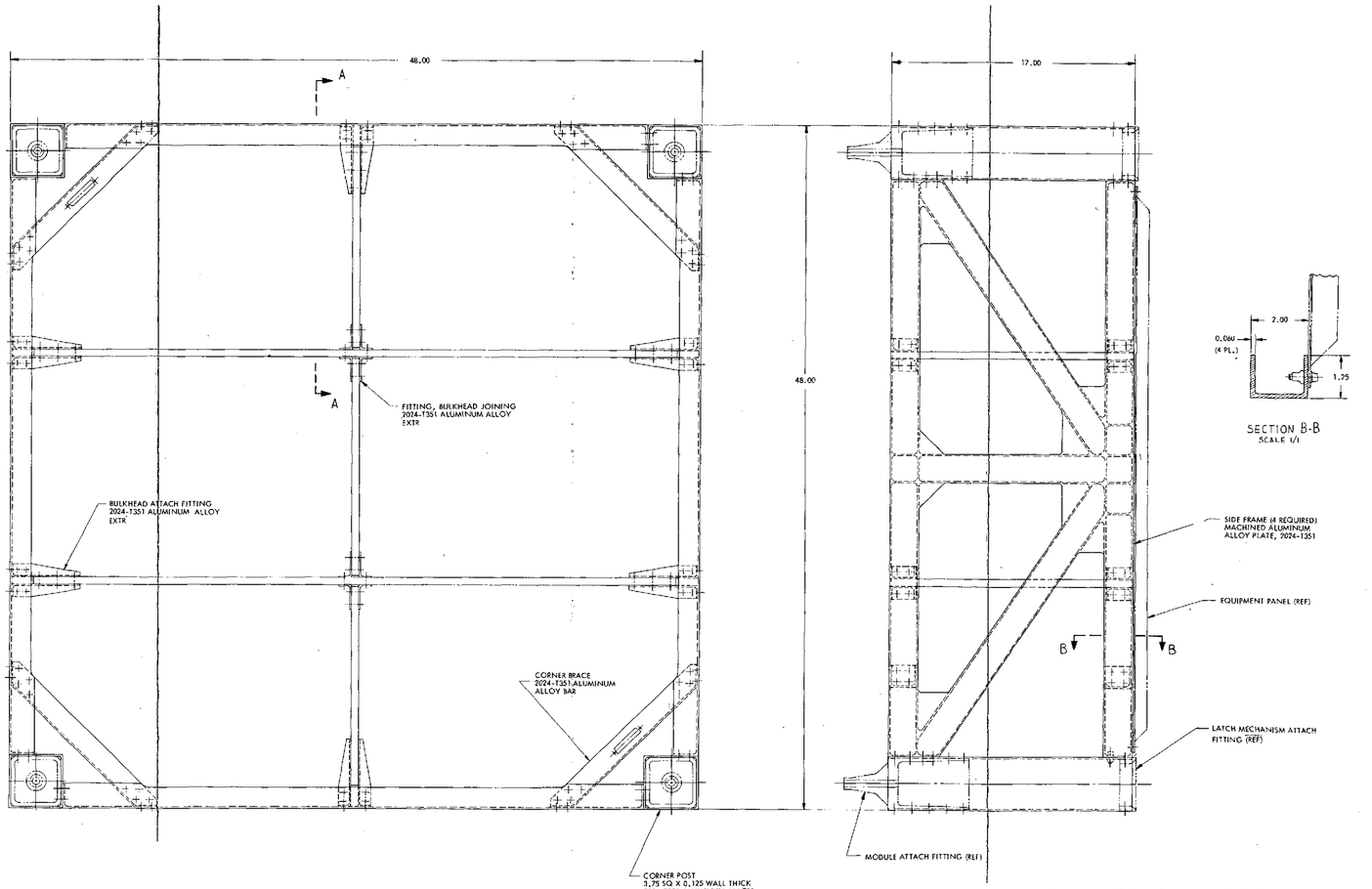

Figure 6-50. Power Module Structural Configuration

FOLDOUT FRAME 1

FOLDOUT FRAME 2

FOLDOUT FRAME 3

space-serviceable because of the limited Delta payload capability, but serviceability can be incorporated with minimum change to structure on module.

Six canted struts provide a direct load path from six points on the transition ring to the aft end of the three longerons at sta 18.0. They provide lateral as well as axial strength and stiffness support to the transition ring and the bulkhead and beams in the plane of this ring.

Subsystem Modules

The EOS-A baseline spacecraft has five modules. Three are very similar structurally (Figure 6-50). The power module includes stiffening shear webs to support the outboard radiator panel. The other two similar module structures (for communications and data handling and for attitude determination) are configured to accommodate the specific equipment in these modules. The actuation module for Titan consists of a module assembly identical to the three common modules, plus hydrazine and nitrogen systems. The Thor-Delta actuation module has the same components but is configured to occupy the triangular volume within the spacecraft structure plus a cylindrical volume at the aft end.

The basic spacecraft modules for the Titan and Thor-Delta (48 x 48 x 18 inches) are identical in design except that the attachment fitting for the Titan is included for serviceability, Bolts are used for the Thor-Delta configuration since the Delta ordinarily cannot launch serviceable observations (Section 4.5), but provisions are included for in-orbit exchange; only the attachment mechanisms must replace the bolts.

Each module structure is 48 x 48 x 18 inches deep and consists of:

- Four square tubes at corners for mounting the latching mechanism
- Four identical numerically-controlled machined side frames (one each side and top and bottom)
- Equipment mounting/radiator sandwich panels on outboard surface
- Corner braces
- Internal bulkheads as required for individual equipment complements.

Since the modules are cantilevered from the four corners at the inboard face of the module, the square tubes provide the primary load path from the outboard equipment platform to the latch mechanism. The cross-braced frames reinforce the corner tubes by feeding the equipment panel loads into them via the diagonals. Once the frames and tubes are assembled, the module becomes a four-sided box with the sandwich equipment panel as a lid.

The corner braces reinforce the inboard plane stiffness of the module against shear deflection. The sandwich bulkheads, positioned for specific module equipment layout, provides intermediate support to the equipment mounting panel. Primarily, these supports are required to provide an adequate frequency (goal of >50 Hz) for the sandwich equipment panel as well as the total module.

Each of the similar modules has the same primary structural elements and transfers the loads in the same manner. The power module was used for sizing and analysis because it has the highest equipment weight. The other modules are structurally adequate because they carry less weight.

Both configurations use the same basic structural concept and mounting technique for the actuation modules. Special support structure to accommodate the mounting of tanks and associated thrusters is shown in Figure 6-51.

The solar array module, which includes the solar array drive assembly and associated equipment is located above the transition ring because of the location of the array itself. This module is attached to the rear payload primary structure using the same module attachment mechanisms as the other subsystem modules.

The solar array is a multiple panel configuration with conventional aluminum sandwich substrates (aluminum facesheets, aluminum honeycomb core). The substrates are supported by aluminum edge members and crossbraces to which the hinge and constraint lugs are attached. This design concept is similar to previous deployable arrays such as used on FLTSATCOM.

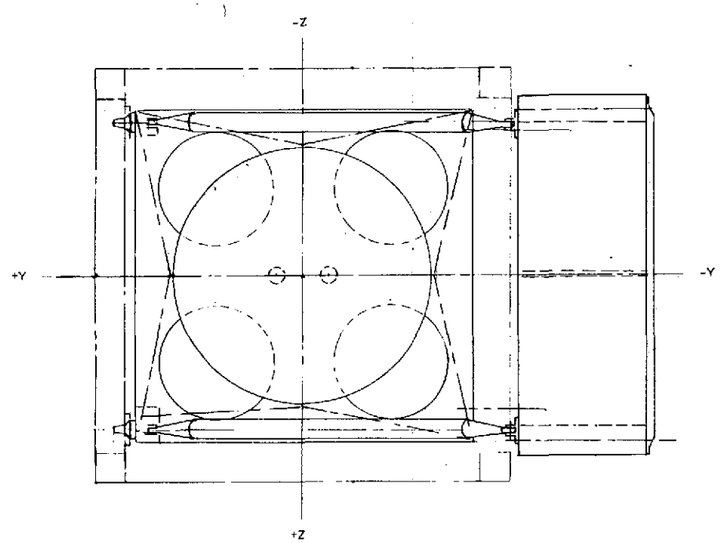

MODULE
REMOVAL
DIRECTION

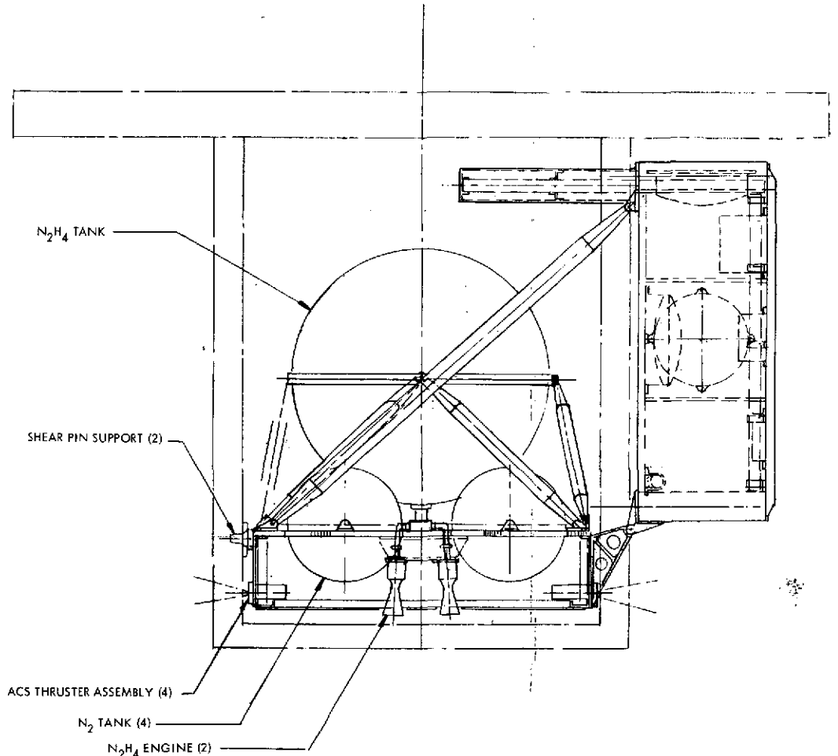

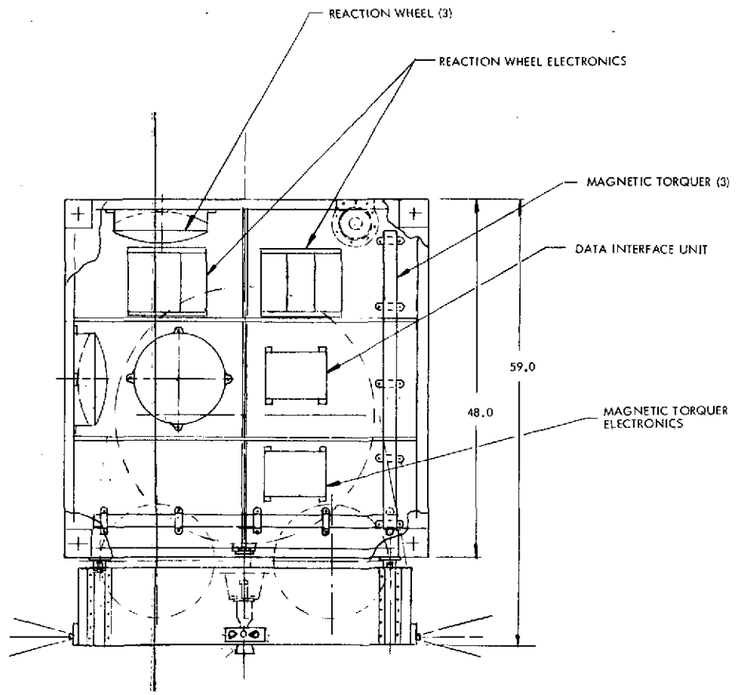

Figure 6-51. Propulsion Module Structural Configuration (Titan Baseline)

6.8.1.3 Structural Analyses

Stiffness and stress analyses were performed for both the primary spacecraft structures and the representative module structure for both Titan and Thor-Delta configurations. Analytical models for the total observatories (spacecraft and payload) were generated and used for both the modal and stress analyses of the spacecraft structures. Schematic models are plotted by machine as shown in Figures 6-52 for the Titan configuration and Figure 6-53 for the Thor-Delta.

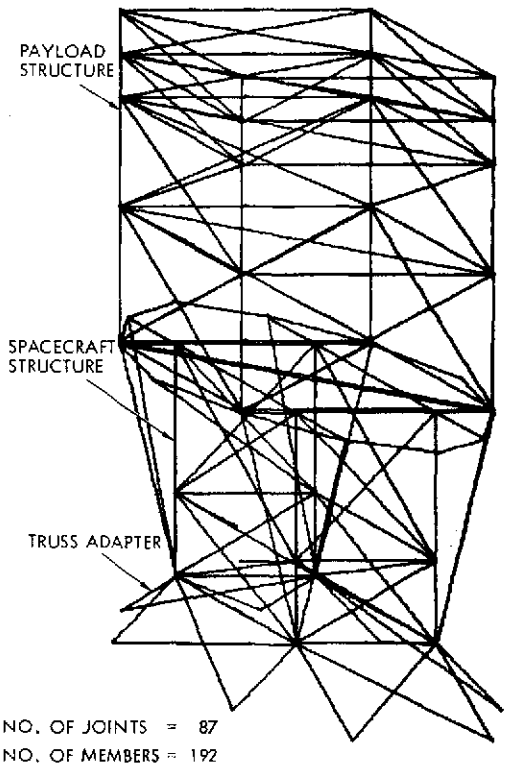

Figure 6-52.
Analytical Model of Titan Observatory Configuration

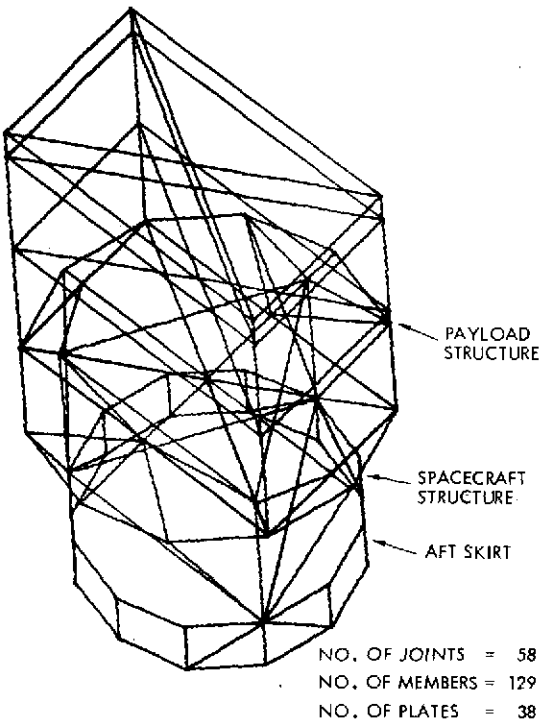

Figure 6-53.
Analytical Model of Thor-Delta Observatory Configuration

An analytical model of the power system module (Figure 6-54) was also generated and similarly used for dynamic and static analysis of the representative spacecraft module.

Modal Analysis (Spacecraft and Payload)

Analytical structural dynamic models of EOS-A in the launch configuration were generated for Titan and Thor-Delta launches. The

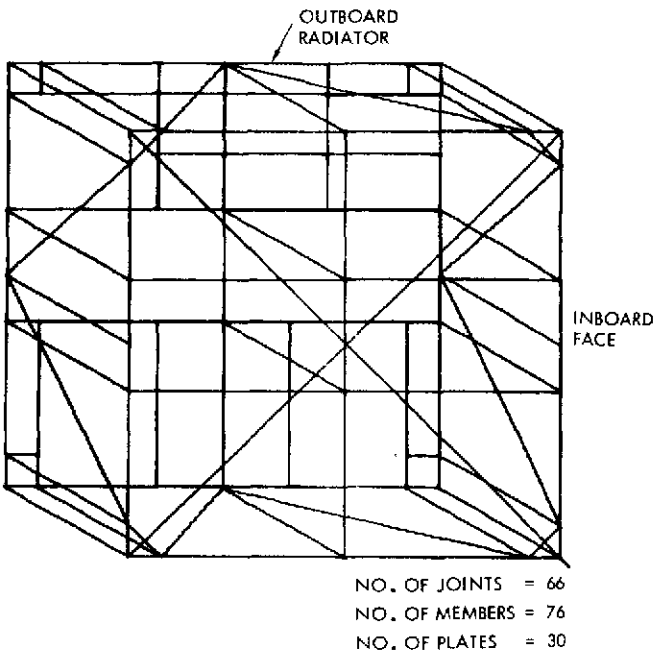

Figure 6-54. Analytical Model of Power Equipment Module

weights of the model were 5000 and 2500 pounds, respectively. Both models were assumed to be supported by conventional aft-end adapters.

A disadvantage of the aft-end support is that the fundamental bending frequencies of the observatory are low enough to couple with primary booster modes. The designs have therefore been stiffened to obtain reasonable bending frequencies, although some coupling is still to be expected. On the Titan version, member sizes were traded off against structural frequency to obtain adequate stiffness with minimum weight penalty. Table 6-21 summarizes this tradeoff. The conclusion is that a minimum bending frequency of about 7 Hz can be obtained at a reasonable weight. Added stiffening above this point is of little benefit. Table 6-21 also indicates that a 15 Hz lateral bending frequency can be obtained using a transition ring support; however, the structural weight required for this support is excessive. Table 6-22 lists primary structural frequencies of the Titan-launched design.

A similar analysis was performed for the Thor-Delta configuration. Here a minimum bending frequency of nearly 10 Hz was obtained. Mode descriptions and frequencies are listed in Table 6-23. Mode shapes for both spacecraft are presented in Section 5.6.1 of Appendix A.

The power module structure was sized to produce a minimum frequency greater than 50 Hz. The frame members are common for all spacecraft modules. The power module supports the heaviest equipment and contains stiffening shear webs which support the outboard radiator panel to which the equipment is mounted. This design produces a minimum frequency of 51.5 Hz. Other spacecraft modules will have higher minimum frequencies because of supporting lighter weight equipment.

Table 6-21. EOS Observatory Titan Configuration Stiffness Sensitivity Study

Structural Member Cross-Sectional Area ($in.^2$)**							Frequency (Hz)		
Adapter		Spacecraft		Payload					
Legs	X-Members	Longerons	X-Members	Longerons	Vertical X-Members	Horizontal X-Members	Y	Z	Torsion
3.0	0.33	1.94	0.33	1.44	0.33	1.44	5.76	7.09	8.98
2.4	1.44	1.94	1.94	1.44	0.33	1.44	7.24*	9.12	12.5
2.4	1.44	1.94	1.94	1.44	1.44	1.44	8.08	9.82	14.5
Rigid		1.94	1.94	1.44	1.44	1.44	9.12	12.0	15.7
Rigid support at transition ring		1.94	1.94	1.44	1.44	1.44	15.3	23.1	31.6

*Baseline configuration

**All members are adequate as regards strength

Table 6-22. Description of Observatory Modes - Titan Serviceable Version (5000 pounds)

Mode	Frequency (Hz)	Description
1	7.25	Lateral (Y)/torsion
2	9.12	Lateral (Z)
3	12.6	Torsion/lateral (Y)
4	27.5	2nd lateral (Y)
5	30.7	2nd lateral (Z)
6	36.9	Lateral
7	39.1	Lateral
8	41.7	Fundamental axial
9	50.7	Axial/lateral
10	53.0	Lateral

Table 6-23. Description of Observatory Modes — Thor-Delta Non-serviceable Version (2500 pounds)

Mode	Frequency (Hz)	Description
1	9.6	Lateral (Z)
2	13.2	Lateral (Y)
3	16.2	Torsion
4	25.0	Lateral (Z)
5	37.2	Lateral (Y)
6	39.8	Axial

Stress Analyses

Preliminary stress analyses of the primary spacecraft structure for the Titan and Thor-Delta configurations and the power module were performed to confirm the structural integrity of the EOS-A baseline design. The analytical models shown in Figures 6-52, 6-53, and 6-54 were used for the structure and module analyses.

The critical load condition, assuming the Titan IIIB as the launch vehicle, was the Stage I or II burnout with an axial limit load of 10.8 g's and a lateral load of 1.5 g's. For Thor-Delta, the corresponding limit loads are 12.3 and 2.0 g's.

A summary of the minimum margins of safety for the major elements of the spacecraft and module are shown in Table 6-24.

Table 6-24. Summary of Minimum Margins of Safety

Member Description	Element Configuration	Critical Failure Mode	Margin of Safety
a) Titan Spacecraft Configuration			
Primary longeron	4 x 4 x 0.125 in. square tube	Crippling	0.39
Cross-diagonals	4 x 4 x 0.125 in. square tube	Crippling	2.14
Outrigger struts	3 x 3 x 0.12 in. square tube	Crippling	1.19
Horizontal frames	4 x 4 x 0.125 in. square tube	Crippling	0.73
Transition ring	Hat section	Crippling	2.80
b) Thor-Delta Spacecraft Configuration			
Primary longeron	3 x 3 x 0.11 in. square tube	Crippling	1.11
Cross-diagonals	2 x 3 x 0.05 in. rectangular tube	Crippling	0.96
Lower frame	2 x 3 x 0.14 in. rectangular tube	Column	1.96
Upper frame	2 x 3 x 0.14 in. rectangular tube	Column	1.71
Lower skirt ring	Separation ring (single)	Compressive yield	Large*
Upper skirt ring	1 x 2 x 0.090 in. angle	Crippling	0.26
Transition ring	3 x 3.5 x 0.25 in. channel	Compressive yield	1.27
Outrigger struts	2 in. O.D. x 0.125 in. tubing	Column	1.03
Frame & transition ring	3 x 3 x 0.12 in. square tube	Crippling	1.30
Skirt diagonals	2 x 2 x 0.17 in. square tube	Crippling	2.89
Aft skirt cylinder	31.5 in. radius x 0.060 in. thick	Buckling	0.09
Sandwich platform	1-1/2 in. core x 0.050 in. f/s	Facesheet wrinkling	2.57
c) Power Module Structure			
Corner tube	3.75 x 3.75 x 0.10 in. square tube	Crippling	Large*
Frame longeron	2 x 1 x 0.06 in. lipped channel	Crippling	0.07
Frame diagonal	2 x 1 x 0.06 in. channel	Crippling	0.09
Radiator panel	0.94 in. core x 0.03 in. f/s	Facesheet wrinkling	Large
Internal shear panel	0.45 in. core x 0.05 in. f/s	Compressive yield	Large

* > 3.00 (300 percent)

6.8.2 Mechanisms

6.8.2.1 Module Attachment

In addition to the basic considerations outlined in Section 3.2 for a module fixation approach, we have configured a module attachment scheme, illustrated in Figure 6-55 along with the elements integral to each observatory module. The SPMS will provide the driving mechanisms which

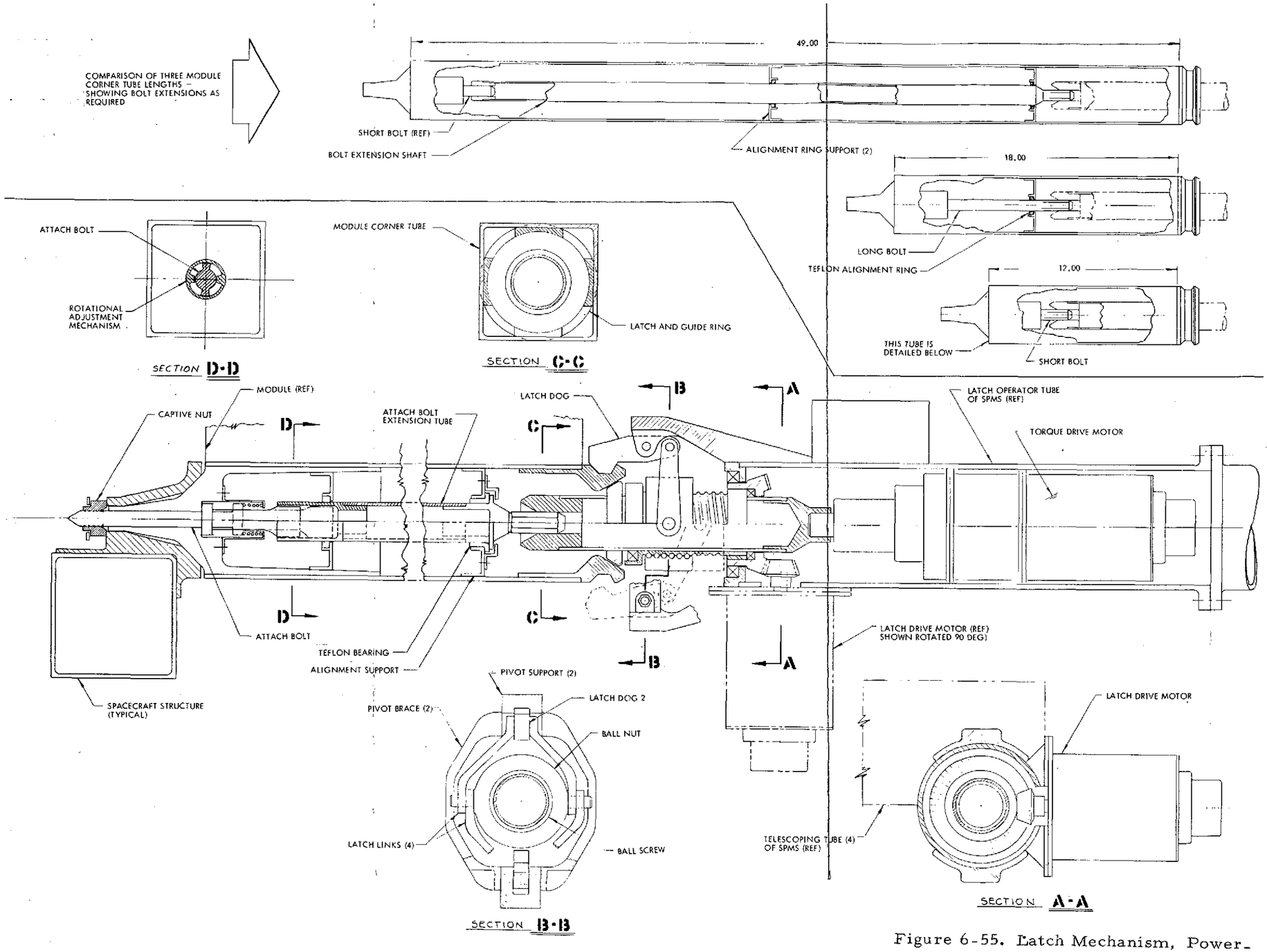

Figure 6-55. Latch Mechanism, Power-Driven EOS MEM/Module Interface

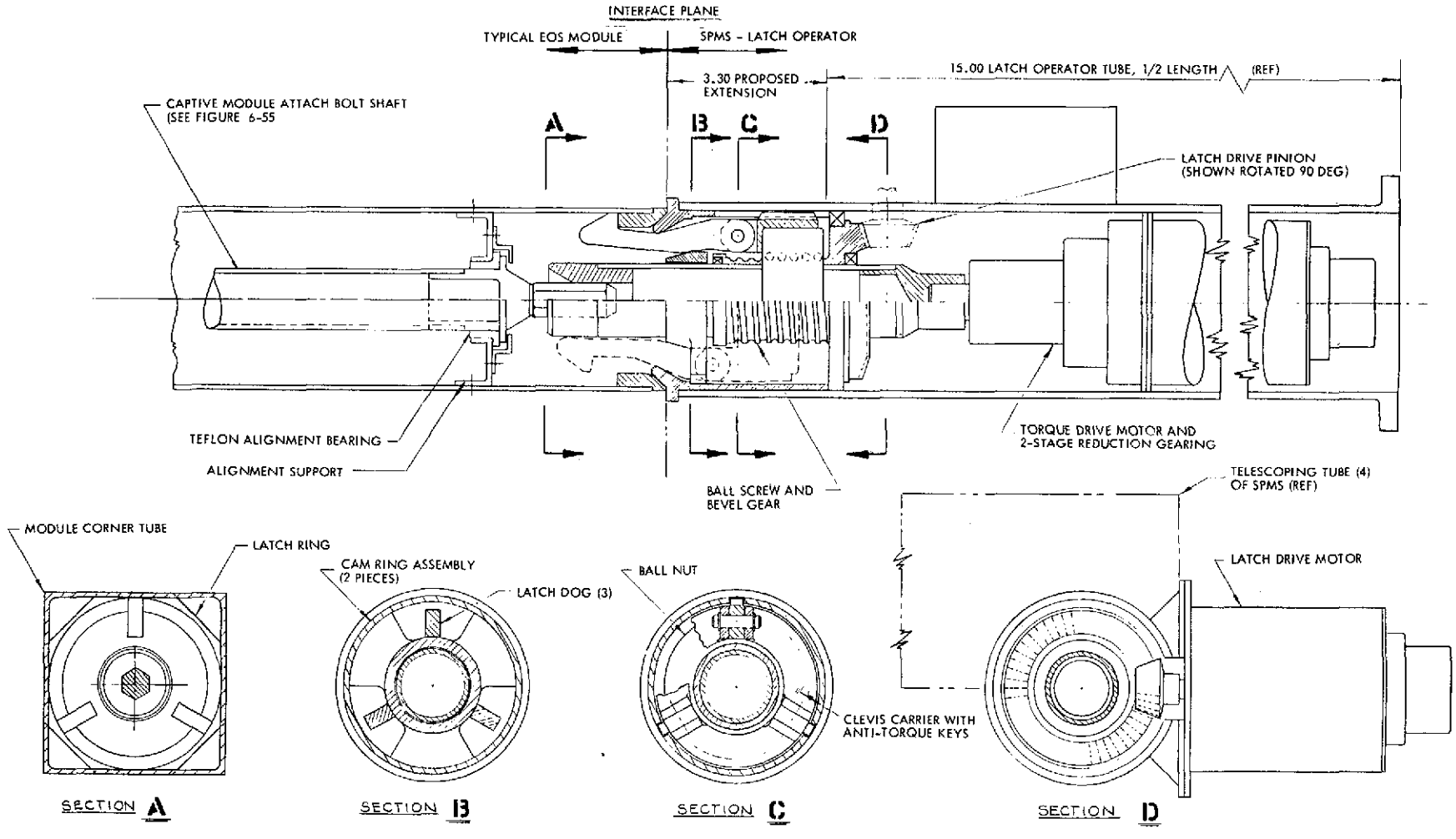

Figure 6-56. Latch Mechanism, Power-Driven Internal Concept

interface with the observatory modules; the mechanism illustrated in this section is our concept of a cost-effective device that meets its requirements and constraints.

Each module corner is equipped with an attachment bolt and extension tube, to bring the interface between SPMS and module to within 3 inches of the module outboard surface (i.e., SPMS side). The extension tube transfers the torque to install or remove a module to the attachment bolt which is at the inboard surface.

The SPMS has two functions: 1) to grapple the module in order to move it from one location to another, and 2) to provide a means of torquing each module attachment bolt for module removal or installation.

Two grappling schemes are illustrated in Figure 6-55 and 6-56. The first shows external dogs driven by a ball screw which engage mating surfaces at each corner of the module. The latter is a similar mechanism but engages internal surfaces which are within the module dimensional envelope; this is the preferred scheme. A separate motor and gear drive is used for grappling.

Torquing of the attachment bolt is by a similar motor and gear drive as shown in the figures. Both grappling and torquing functions may be performed by a single motor and gear drive; such details should be left to the SPMS contractor.

The extension tube incorporates a joint capable of a maximum of 1/6 revolution free motion, in order to allow the SPMS torque drive to be aligned with the driven attachment bolt, as shown in Figure 6-55. It would probably be more cost effective to incorporate this joint on the SPMS side of the interface.

A module removal and insertion sequence is as follows:

1) The SPMS approaches the module, with its end effectors poised to enter the corners of the module. The end effectors have previously been positioned to conform to the dimensions of the module being exchanged; the docking adapter of the

FSS supports the observatory with respect to the SPMS in a known relationship. *

As the SPMS and effectors contact the module, only tolerance buildups between SPMS and observatory have to be accounted for; mating surfaces have conical faces (Figure 6-56 and 6-57) and it is assumed there is sufficient lateral flexibility in the SPMS arms to provide for any misalignments.

2) As contact occurs between SPMS and module, the ball screw drives are initiated, enabling the dogs to complete the grappling. The cam shapes of the mating parts provides snug contact. At the same time the torque driver mates with the extension tube, and the latter's rotational joint permits driving and driven sockets to be mated.

3) After the grappling motor torque rise indicates that grappling is completed, the bolt torquing motors are initiated, to break free the attachment bolts at each corner. When the bolts are loose as indicated by a drop in motor torque, the SPMS is free to pull the module free of the structure. To do this it must exert sufficient force to overcome the connector mating force; an alternate version of this mechanism could provide the connector demating force as part of the attachment bolt torquing motion.

4) The SPMS can now move the module away from the structure and into the storage magazine, or from the magazine to the observatory.

5) To install a module, the opposite procedure is followed. When the module is in position, as indicated by a suitable sensory technique in the SPMS, the torque motors are rotated clockwise commencing the attachment sequence. After initial engagement of the threads, continued rotation provides the electrical connector mating force. When the motors reach a predetermined torque, the module has been securely bolted to the observatory structure and the exchange is complete.

The SPMS and FSS are described in the following reports:

Shuttle/Typical Payload Interface Study, Final Report; Space Division, North American Rockwell Report SD 72-SA-0194, 30 October 1972, Contract NAS5-23093.

Design Definition Studies of Special Purpose Manipulator System for Earth Observatory Satellites, SPAR/DSMA Report R. 592, January 1974, prepared for Goddard Space Flight Center.

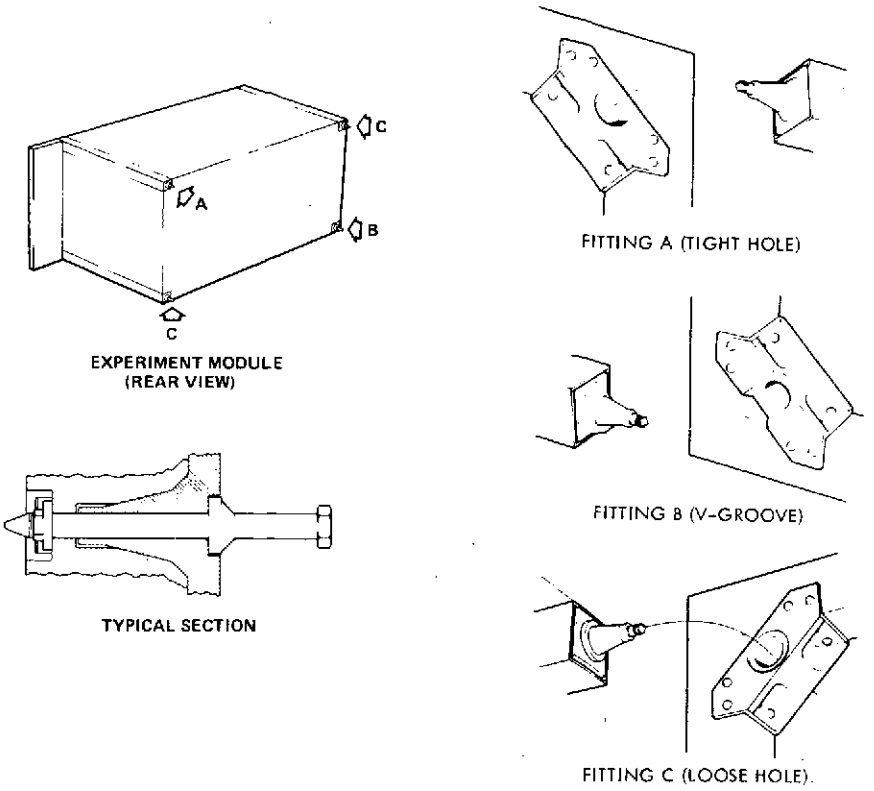

Figure 6-57. Tailoring of Attachment Fairing for Selective Constraint

The absolute location of the male probe on the module to female socket on the structure is determined by the beveled shoulder seating interface (Figure 6-57). This interface can be tailored to provide either positive location in three coordinates, two or one depending on the location on the module. Generally a module will have four latches with location constraints as discussed in Section 3.2 to open fabrication tolerances and assure no binding during module insertion. The module is not assumed in the structural analysis to contribute stiffness or strength to the observatory structure (or conversely, the structure to the module). However, once a module is bolted in place it does contribute significantly in this respect, providing additional design margin, since its attachment bolts are adequately preloaded to prevent slip during the launch environment. By torquing the attachment bolts to 140 ft-lb, a load capability of nearly twice that required under worst case launch condition analysis (~4000 lb) is established, assuming a conservative 0.35 friction coefficient. It is important that the observatory structure and module be

near operational temperatures before mating to avoid residual stress buildup after attachment and normalization.

An alternate approach, structurally decoupling the module from the observatory structure by means of flexures or lightly preloaded slip joints, was also investigated. However, since critical elements such as sensors will be structurally decoupled from the module internally, it was decided to firmly attach the modules simplifying the design and analysis of the observatory.

The Titan actuation module will be required to have positive location at all four corners due to the protrusion of its tankage into the center section of the spacecraft structure. By using the actuation module structure to provide support to the spacecraft structure, a significant weight penalty is avoided. This will require tighter fabrication tolerances for only this one module. For the Thor-Delta configuration the actuation module does not provide spacecraft support; for Thor-Delta launches, with the aft adapter, launch loads go through the actuation module. For transision ring support of the observatory, which applies when the Thor-Delta configuration is Titan or Shuttle-launched, the actuation module supports only its own mass.

It should be noted that the latch mechanisms may be able to be operated with the SAMS manipulator fitted with a special end effector capable of supplying the required torque. This allows greater overall flexibility and a backup mode of operation.

6.8.2.2 Solar Array Deployment/Retention Mechanisms

Retention of the solar array panels (and the wideband communication and omni antennas) will be accomplished conventionally with pyrotechnic devices (Shuttle-approved ordnance). Initial deployment will be made with spring-driven hinges and pivots. Referring to Figures 4-1 and 4-2, the boom hinge will initiate unfolding of the panels upon reaching a latched position. The Delta configuration will require three boom hinges for more compact storage due to its confined fairing. In this case, a cable will maintain the proper angular relationship of the hinged joints during deployment. Figure 6-58 shows the deployment sequence for the Delta spacecraft solar array.

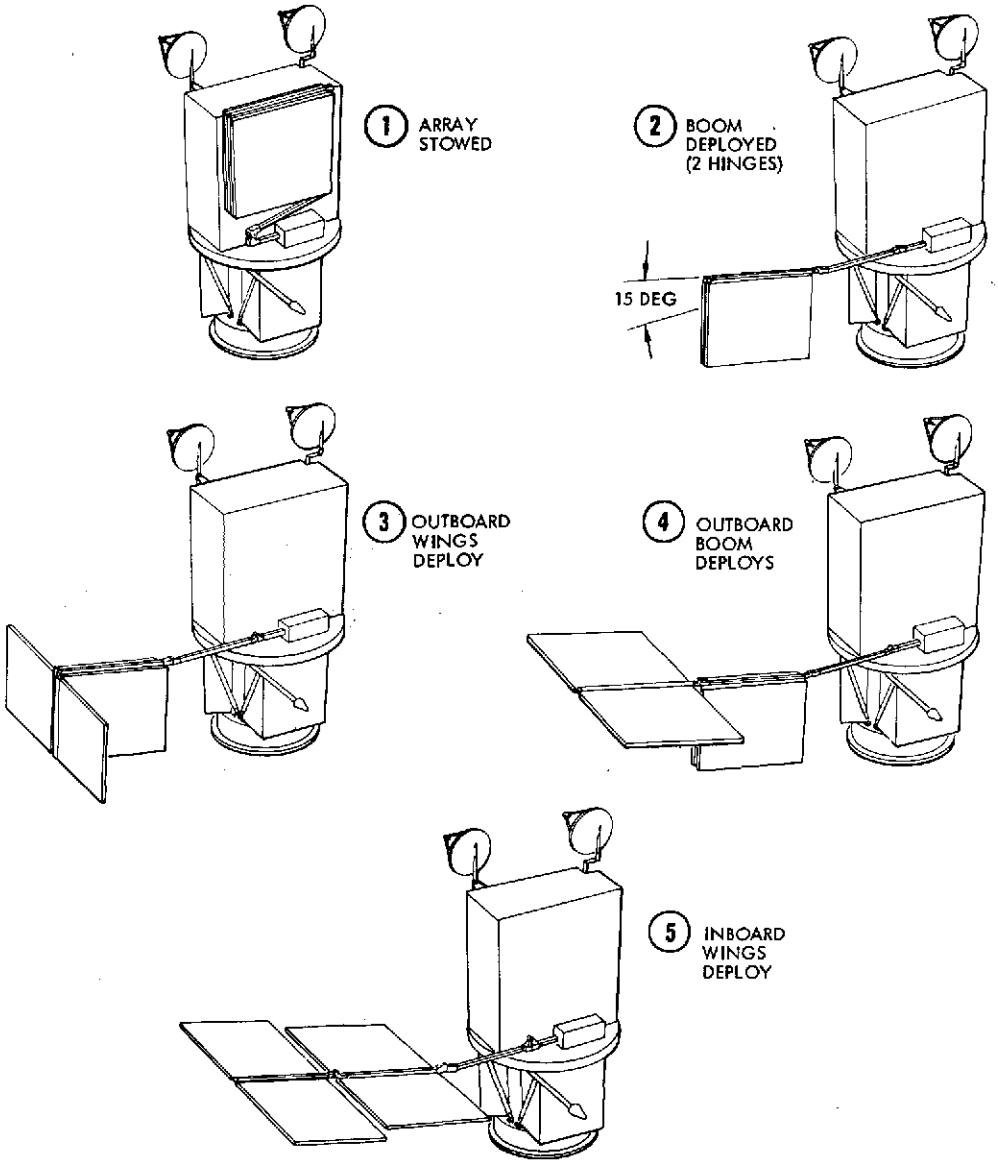

Figure 6-58. Solar Array Deployment Sequence (Thor-Delta)

Variations of a spring-actuated hinge used on the FLTSATCOM satellite (pictured in Figure 6-59) will be used. This hinge in unique in that no dampers are necessary because of its programmable spring torque. By properly configuring a cam over which lies the spring tensioned deployment cable, a controlled and variable torque versus angle is provided. This predominantly alleviates the temperature dependence and other difficulties associated with dampers. A zero-slop spring catch firmly locks the hinge in the open position to assure structural linearity.

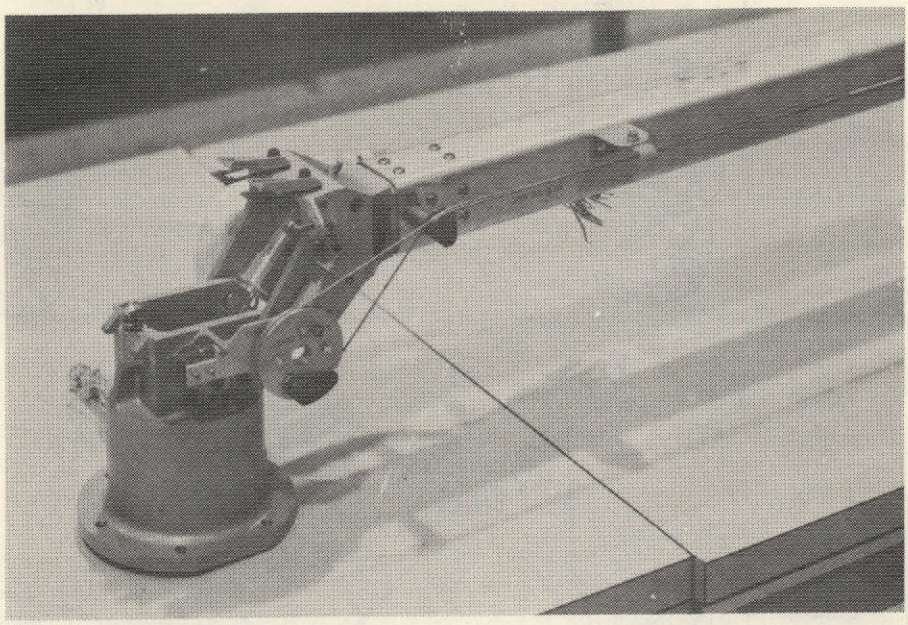

Figure 6-59. Spring-Actuated Hinge

For retracting the array (and omni boom) permitting observatory refurbishment or retrieval, the SAMS manipulator will be used. Each hinge catch will have a suitable over-center lever attached to facilitate disablement by SAMS. The array is sequentially retracted by SAMS to the stowed position, where over-center clamps secure the stowed array to the observatory structure for retrieval.

6.9 PAYLOAD STRUCTURE

The payload structure is that part of the observatory forward of the transition ring which mounts the experiments and the communications equipment (see Figures 6-48 and 6-49).

6.9.1 Design Requirements and Philosophy

The structural loads and stiffness requirements for the payload are the same as those for the spacecraft which are shown and discussed in Section 6.8.1.1 of this report so are not repeated here.

In addition to these requirements there is a pointing accuracy requirement for the two payload experiments, the thematic mapper, and the HRPI. These requirements are shown in Table 6-25 as an allowable

Table 6-25. Allowable Pointing Tolerance and Drift Rates (Thermal/Structural)

Axis	Allowable Angular Uncertainty* (arc-sec)	Allowable Drift Rate (arc-sec/hr)
Roll**	30	32.4
Pitch**	30	32.4
Yaw	120	144.0

*Angles measured relative to the attitude sensors on the spacecraft (attitude determination module)

**Assumes a nominal 386 nautical mile orbital altitude.

Note: Reference Appendix A, Section 5.2.7 for pointing accuracy budget allocation

"thermal/structural" pointing tolerance and a "drift rate". Both of these values have been derived from a total error budget such that these are the values specifically allocated for distorting of the observatory structure during orbital operational flight. The distortion is caused by the thermal gradients within the structure generated either by the external or internal environment associated with the observatory at any given time.

The distortion of interest is that occuring between the attitude determination sensors in the spacecraft and the earth viewing sensors in the payload. The calculation of the distortions is discussed later in Section 6.9.3.3 and the thermal control techniques proposed to maintain these distortions within the budgeted limits are discussed in Section 6.10.

6.9.2 Structural Description

There are two baseline structure configurations considered and discussed herein. The Thor-Delta configuration is smaller in all dimensions than the Titan configuration and is nonserviceable.

6.9.2.1 Structural Description (Titan Configuration)

The baseline payload structure for the Titan configuration consists of a rectangular cross braced frame type primary structure with open front bays for inserting the payload modules (four modules). The structure is much like a rectangular dresser with the experiment modules being the drawers (see Figure 6-48).

The primary structure consists of four square tubes acting as continuous longerons forward from the transition ring to the wideband communication module at the forward end of the payload stack. There are three bays plus the open top to accommodate a total of four serviceable modules. A rectangular square tube frame outlines the base of each module. These frames are cross-braced to maintain these planes rectangular to help minimize torsional flexibility. The two sides and rear face of each is braced with cross-diagonals to build an effective truss-frame capable of providing adequate bending stiffness to the structure.

6.9.2.2 Structural Description (Thor-Delta Configuration)

The baseline payload structure for the Thor-Delta configuration is a simple rectangular two-bay box, as shown in Figure 6-49. Square tubes at the corners act as primary longerons with similar horizontal tubes outlining the box at the bottom of each bay. The wideband communication equipment unit actually mounts to the top of the upper bay frame.

Each bay has a sandwich base mounting plate and is enclosed on all four sides with truss structure. Experiment radiators protrude between truss members. Appropriate brackets, trusses, beams, etc., will be required internal to the outer structure to mount individual experiment packages and to provide the necessary load paths and constraints for launch and flight operation.

Both external and internal insulation plus heater controls will be used for controlling thermal distortions within the payload structure as discussed later in Section 6.10.

The forward side of each bay (nadir direction) is open to permit insertion and retraction of modules and also provides thermal separation

of these module radiating surfaces from the primary structure on this surface. This helps to minimize thermal distortion so that required pointing accuracies can be met but also induces a reduced bending and torsional stiffness relative to a closed or cross-braced face.

The module attachment female fittings are positioned in the four corners of the rear face of the structure where vertical, horizontal, and diagonal strut members join to provide direct load paths from the attachment directly into the primary structure in any direction. Location of the attachments on the rear face helps thermally since this area can be more readily protected and/or controlled from local temperature variations which occur more easily on the forward surfaces near the radiators.

The frame and cross braces below the lower module bay tie across the transition ring and also intercept the four aft spacecraft longerons and outrigger struts. Thus, the payload and spacecraft structure are joined directly in the plane of the transition ring.

The payload modules themselves are similar in basic construction to the equipment modules discussed in Section 6.8 except that the gross dimensions vary according to the internally mounted experiments. Figure 6-50 shows a representative equipment module structure with the four attachment fittings in the corners of the aft face. The detailed structural arrangement of any given module will be tailored to the individual experiment, its method of support, pointing requirement, thermal considerations, etc.

6.9.3 Structural Analyses

Both a stress and distortion analysis of the payload structure was performed. The modal analysis of the payload structure was performed in conjunction with the spacecraft and is reported for the total observatory in Section 6.8.1.3.

The distortion analysis reported herein also included the entire observatory since it is not meaningful to evaluate only the payload when the relative distortions of significance occur between the attitude determination sensors on the spacecraft and the experiment sensors on the thematic mapper HRPI located in the payload section.

6.9.3.1 Stress Analysis

Preliminary stress analyses of the EOS-A baseline payload structure were performed in conjunction with the overall observatory by using analytical model(s) as described in Section 6.8.1.3 and shown in Figures 6-52 and 6-53. The models are the same as used for the modal analysis and as such confirmed that the structural design does meet the strength requirements as specified in Section 6.8.1.1.

A summary of the minimum margins of safety for the major structural elements of the baseline payloads are shown in Table 6-26 a and b. The table lists the element description, type of member, critical failure mode, and margin of safety. As in the case of the spacecraft structure, the margins are all relatively high indicating the structure to be stiffness rather than strength critical.

Table 6-26. Summary of Minimum Margins of Safety

Member Description	Element Configuration (square tube - in.)	Critical Failure Mode	Margin of Safety
a) Payload Section of Titan Configuration			
Primary longerons	3 x 3 x 0.12	Crippling	0.26
Horizontal frames	3 x 3 x 0.12	Crippling	Large*
Cross-diagonals	3 x 3 x 0.12	Crippling	Large
Horizontal cross braces	3 x 3 x 0.12	Crippling	Large
b) Payload Section of Thor-Delta Configuration			
Primary longerons	3 x 3 x 0.080	Crippling	0.53
Horizontal frames	3 x 3 x 0.060	Crippling	1.10
Cross-diagonals	3 x 3 x 0.040	Crippling	Large
Horizontal cross braces	3 x 3 x 0.020	Crippling	1.04

*>3.00 (300 percent)

6.9.3.2 Distortion Analysis

The thermal distortion analysis used the same observatory analytical model as was used for the modal and stress analyses for the Titan configuration and is shown computer plotted in Figure 6-52. In

this case, temperature distributions throughout the structure as determined by a thermal analysis described in Section 6.10, were used as the effective loading on the structure. The temperature gradients across the structure produce linear, bending, and/or torsional distortions, depending on the specific temperature distribution at any given time. Since the design requirements (Section 6.9.1) specify both an angular pointing tolerance and a drift rate, three time-sequenced temperature distribution cases were analyzed. Plotting these three distortions in terms of pointing angle off-true permits computing the rate of change between two adjacent time points, thus indicating a drift rate (assumed linear between computer points).

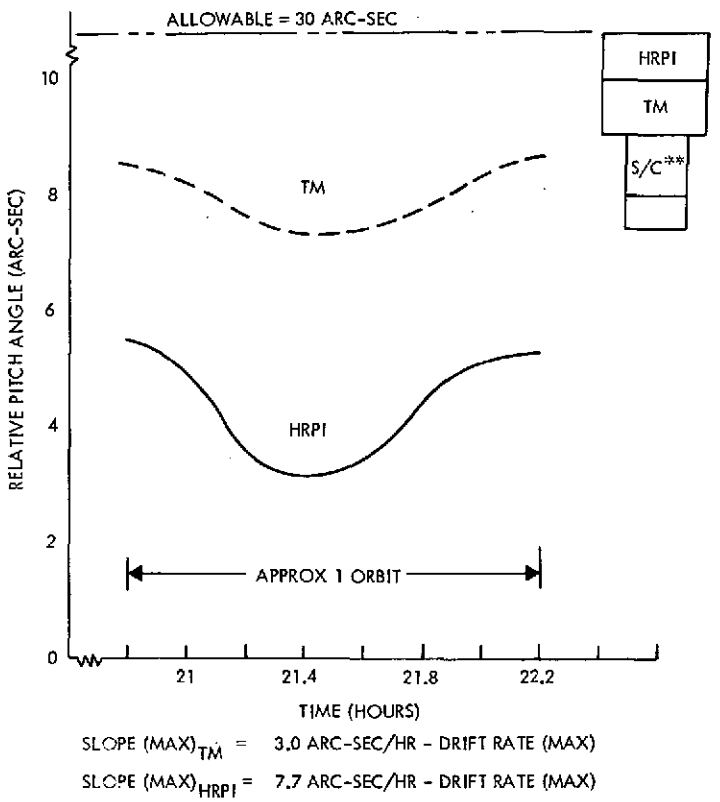

*ROLL ANGLE UNCERTAINTY MAXIMUM = 2.6 ARC-SEC
**S/C = SPACECRAFT (LOCATION OF ATTITUDE DETERMINATION MODULE)

Figure 6-60. Pitch Angle Uncertainty* (Thermal/Structural)

Figure 6-60 shows a plot of the computed pitch angle relative to neutral for each of the two experiment compartments at three sequential

flight times. The pitch angle, the most sensitive axis, is well within the allowable tolerance and the drift rate also is less than budgeted. Therefore, it is concluded that the thermal control technique proposed and discussed in Section 6.10 can adequately keep the necessary experiment pointing accuracy relative to the thermal/structural part of the overall distortion allocation. In fact, since the curves in Figure 6-61 closely approximate a sine wave, the absolute uncertainty could be further reduced by biasing the pointing relative to the HRPL. This could be done by shifting the relative pitch angle zero line up to the currently shown 6 arc-sec line on Figure 6-60 via a calibration. It is to be noted that the relative pitch angle shown in the figure is that of each instrument relative to the attitude determination module nominal pointing direction with the total structure initially assumed at 70°F. (See Appendix A, Section 5.6.2 for specific calculations.)

6.10 THERMAL CONTROL

The overall EOS thermal control system consists of both structure and module thermal designs, each constrained by module/structure interface requirements. The presentation follows this division.

6.10.1 Design Requirements

General design requirements that have guided the thermal control system design are presented in Table 6-27. These requirements pertain to both Thor-Delta and Titan designs with the exception that Thor-Delta modules/sensors need not be resupplied. Many requirements are not subsystem compatible; for example, mechanical interfaces must satisfy thermal isolation but yet provide structural integrity. Some specific thermal requirements are listed in Table 6-28 with references, if applicable, to specific tradeoffs in Appendix A of this report.

In arriving at the proposed thermal design, we have considered the use of louvers and heat pipes as well as heaters. These tradeoffs are discussed in Appendix A, Book 2, Section 5.6.2. Our design has also been aimed at minimizing thermal/vacuum testing. This has been accomplished through the use of computer control of module heaters and by allowing sufficient power margin to handle contingencies.

Thermal margin at TRW usually refers to the power excess or deficiency required to drive a unit to its thermal bounds, rather than the difference between anticipated and tolerable temperatures. In this sense, calculations alone can be used to verify thermal design (as opposed to thermal vacuum testing) if the thermal power handling capabilities of the system exceed any combination of likely contingencies. This can always be accomplished within our concept at some price for extra power and/or extra radiating surface.

Each of the standard modules has a potential surface radiating area of ab out 16 square feet, while calculations discussed in Appendix A, Section 5. 6. 2 show that 2. 5 square feet is the largest area required. to hold any of the modules cooler than maximum permissible temperature. Thus, capability for extra area is inherent in our design. On the other hand, little expense is incurred in providing an excess power handling capability in heaters, control circuits, or computer software so that the excess cost is largely in the solar array and electric power modules. At $400 per watt (orbital average) for power, even doubling the required heater power from the baseline design would increase the cost by only $60,000; a very favorable tradeoff compared to thermal vacuum testing. Finally, the ability to fine tune the thermal design on-orbit through software changes, combined with the arguments above, ensures that adequate operation can definitely be achieved without prelaunch thermal vacuum verification.

6.10.2 Baseline Structure Thermal Control Design

6.10.2.1 General Design Description

Structure as defined here refers to both payload and spacecraft structures with each TCS consisting of multilayer insulation (MLI) and several independently-controlled heaters. Outside layer of MLI is aluminized Kapton.

Table 6-27. General EOS-A Observatory System Thermal Design Requirements and Functions

- Thermally decouple modules/sensors from payload/subsystem structures to:
  - Allow independent module thermal design
  - Permit module interchangeability
  - Prevent significant module impact on structural thermal distortion
  - Allow on-orbit module replacement
- Provide design flexibility and growth margin to accommodate:
  - A wide range of experiments
  - Various near-earth missions
- Limit structural temperature gradient and fluctuations to preserve structural alignment by satisfying thermal distortion pointing allocation
- Provide for module replacement in orbit (for Titan launch vehicle but not for Thor-Delta) to permit module replacement via Shuttle
- Minimum total program cost but with reasonable risk factors

Table 6-28. Specific EOS-A Observatory System Thermal Design Requirements

- Accommodate environmental conditions for the following orbits:
  - Circular, sun-synchronous

    Altitude (h) = 300 to 900 nmi (with corresponding inclination range from 97.7 to 103.1 degrees)
  - Node/sun phasing from 6 a.m. to 6 p.m.
  - Reference orbit (h = 386 nmi, i = 98.4 degrees and 11 a.m. phasing of node to sun line)
- Provide module/structure isolation as required by the mechanical/temperature method used by TCS. Isolation specifics are discussed in Appendix A, Section 5.5
- Provide thermal control that maintains structural thermal distortion within pointing allocation. (Thermal distortion pointing allocation has an uncertainty compontnt of 30 arc-sec between in-orbit calibration points, and a rate of change allocation not to exceed 0.01 deg/hour.)
- Provide module thermal control that meets component acceptance limits and module/structure interface heat flow requirements
- Thermal control elements (coatings, insulation, baffles, dynamically-controlled heaters, etc.) satisfy performance requirements with a mission life of 3 years

a - 4

Structure provides support for modules and sensors with the attachment method particularly significant in structural temperature control because of thermoelastic pointing requirements. Thermal distortion pointing allocation has both an uncertainty component and a rate of change allocation, as indicated in Table 6-28. Accommodation of this alignment requirement is a coupled structural-thermal consideration involving a number of interacting factors affecting performance. Important factors are listed in Table 6-29.

Table 6-29. Structure TCS Performance Factors, Control Parameters and Methods

1) Performance Factors	Variability Considerations
• External environment - Solar - Albedo (earth reflected solar) - Earth emission	• Orbit - Altitude - Node/sun phasing
• Induced environment - Module/structure interface - Payload structure/transition ring interface - Heat leaks	• Interface - Conductive interface resistance - Temperature gradient across interface - Radiative interchange
2) Control Parameters	
• Temperature level • Temperature distribution • Temperature fluctuations	• Temperature level, distribution, fluctuations function of control methods
3) Control Methods	
• High efficiency multilayer insulation to temper natural (external) and radiative (internal) environments	• Effective emittance (or equivalent conductance) range
• Module/structure thermal interface control with temperatire gradient mechanical control	• Interface - Resistance range - Temperature gradient range
• Heater circuits to control temperature level, distribution and fluctuations	• Number and placement of heaters • Type of heater control - Thermostatic - Computer - Electronic switching - Ground command • Temperature level

Both payload and subsystem structures are individually studied by exercising multi-node math models for various combinations of performance factors, control parameters, and methods as identifies in Table 6-29. Study details are presented in Appendix A, Section 5. 5, with important investigative results summarized in Table 6-30. Property values used in the study were selected from the passive elements and properties listed in Appendix A, Section 5.5. These results indicate that multilayer insulation blankets satisfactorily attenuates effects of external environment, that 1-watt per module attachment point heat flow can be readily accommodated, and that on-off type of heater control with appreciable temperature dead-band induces significant structural thermal transients relative to those induced by either the external environment or the module/structure interface heat flow. Heater-induced thermal transients result in significant themoelastic distortion. As a result, a number of control methods were examined to minimize or eliminate these thermal transients but with reasonable cost penalty as a guide. Heater placement and number were also part of the investigation. Heater-induced thermal transients can be minimized by reducing the temperature control dead-band or eliminated by having constant power heater circuits. The temperature dead-band can be reduced by using either computer-control or electronic switching. A constant power heater circuit requires either voltage regulation or computer-control with electronic switching since the bus voltage swings from 26 to 32 volts. Several types of control methods were examined. If thermostats are used, a reasonable structural temperature control with reasonable risk factors will require about 36 independent heater circuits. If a power-level control method is used, as few as nine independent heater circuits will provide results equal to or better than thermostats. Thermal distortion analysis, as reported in Section 6. 9, indicates that thermo-elastic distortion with the power level control method is significantly less than the allowable pointing allocation.

The power level control can be either by voltage regulation or by electronic switching with computer control but computer control provides more flexibility, margin and less risk because of in-flight adjustment capabilities than either thermostats or voltage regulation. Although computer control has a slight cost penalty, this method is preferred and recommended.

Table 6-30. Study Summary of Structural Thermal Control Modules

Elements	Design Characteristics
1. Multilayer Insulation	Configuration/characteristics • Sandwiches structure (including transition ring) • Outside layer is aluminized kapton • Effective emittance, (E^*) =0.01
2. Heater Circuits	
2.1 Power Requirements	• 64 watts to maintain orbital average temperature of 70°F
2.2 Number of Circuits	• Variable, from 9 to 36 circuits depending upon control method
2.3 Control Methods	
2.3.1 No Heaters • Cost =$0	Performance • Not satisfactory Comments • Large uncertainty and risk • No positive control with temperature level governed by natural and induced environments • Interface heat flow much greater than the desired one-watt per attachment
2.3.2 Temperature-Controlled Thermostatic • 9 circuits • 36 circuits • Cost, $1K/circuit • Dead-band = 10°F (minimum)	Performance • 9 circuits: marginal • 36 circuits: satisfactory Comments • Reasonal risk for 36-circuit design • Heater-induced thermal transients • No in-flight adjustments • Preflight temperature setting
2.3.3 Power Level Control	
(1) Unregulated • Preflight power setting • Cost, <$10K (9 circuits)	Performance • Not studied but expected to be unsatisfactory Comments • In-flight power level variation of 50 percent due to swinging bus voltage of 26 to 32 volts
(2) Regulated • Preflight power setting • Cost, > $50K (9 circuits)	Performance • Satisfactory Comments • Reasonable risk • No heater induced transients • No in-flight adjustments • Number of circuits, nine
(3) Computer with electronic switching • Power slicing method prevents heater-induced transients	Performance • Satisfactory Comments • Small risk • Software (simple or sophisticated) • In-flight adjustment of power level, temperature level, etc. • Number of circuits, nine
3. Module/Structure Attachment	Effective conductive resistance • >5 of -hr/BTU

6.10.2.2 Specifics of Structure Thermal Design

A summary of the structure baseline thermal design is presented in Table 6-31 which is used in conjunction with Figures 6-61 and 6-62. These thermal control features were based on weighing heavily performance and minimum cost factors with reasonable margin, reliability, and growth.

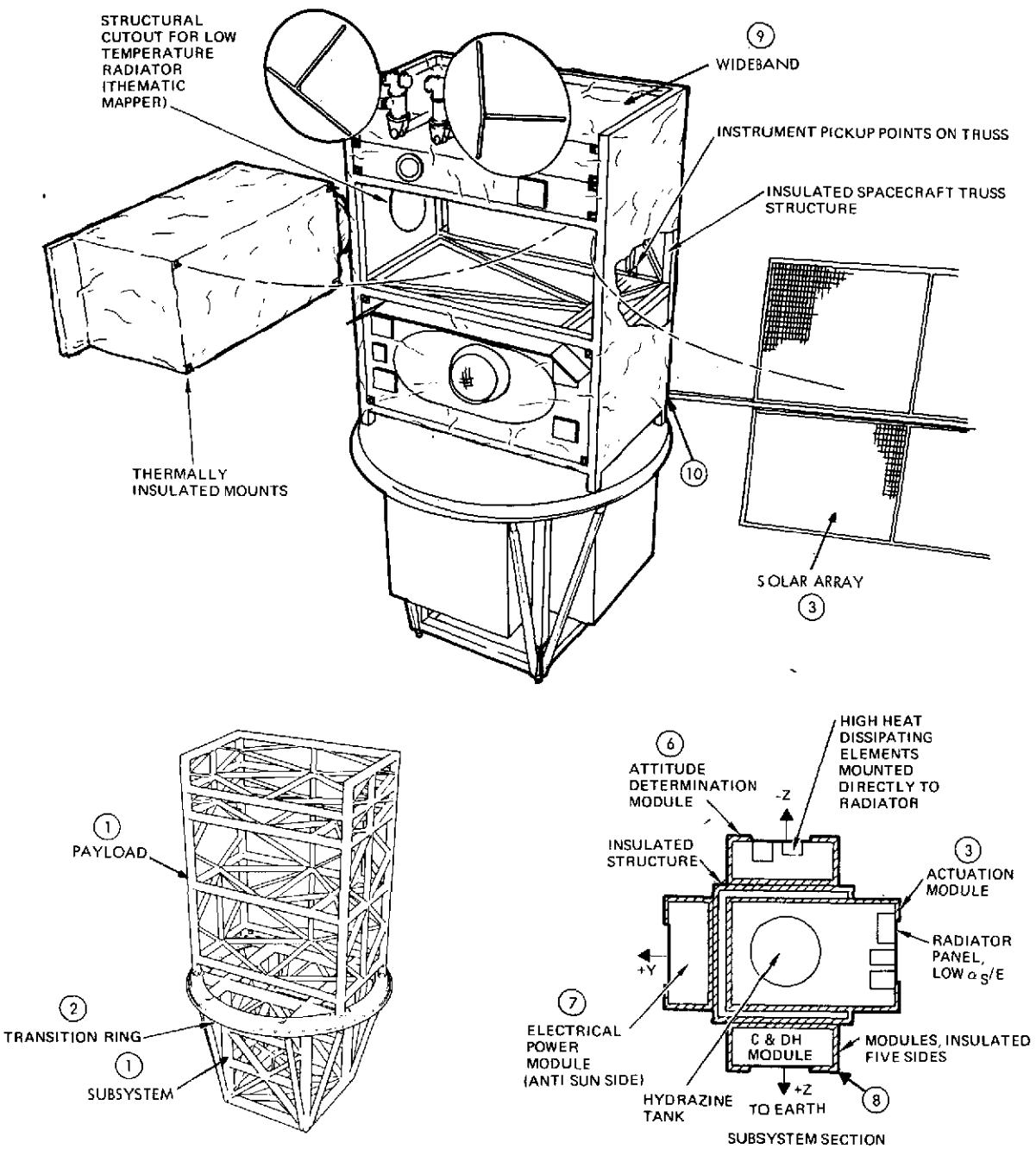

Figure 6-61. Observatory Thermal Features

Table 6-31. EOS-A Baseline Thermal Design Description and Function

ID No. 1 (Refer to Figure 6-62 and 6-63	Component/Thermal Control Elements	Baseline Description	Function
(1)	Structural frame		
	• Insulation sandwiches	• Thermal insulation, ≈20 layers 1/4 mil aluminum Mylar filler sheets, 2-mil aluminum Mylar, inner sheet, 3-mil aluminum kapton, outer sheet	• Insulation, temper natural environmental effects
	• Independent heater circuits	• Independently-controlled heaters – Computer/electronic switching – 9 circuits – Strip-type heaters cemented directly to surface	• Maintain structural frame temperature, limit temperature gradient, limit temperature fluctuations
(2)	Transition ring (same as structural frame)	Same as structural frame	Same as structural frame
(3)	Solar array substrate		
	• Thermal coating	• Thermal coating, S-13G LO white paint	• Coating, minimize solar array temperatures and low outgassing absorbed albedo heating
(4)	Module/structure interface		
	• Isolation	• Isolation, low conductance attachments (i.e., small contact area, low thermal conductivity material)	• Limit module/structure interface heat flow
	• Temperature gradient control	• Temperature control, control of structure and module temperature swings	• Limit module/structure interface heat flow
All modules	All modules		
	• Radiator coating	• Radiator coating, silvered teflon	• Maximize radiator heat rejection, stable solar absorptivity, reasonable cost
	• Insulation	• Insulation, > 10 layers 1/4-mil aluminum Mylar filler sheets, 2-mil aluminum Mylar inner and outer sheets	• Insulation, minimize module/structure radiative interactions, temper environmental heating
	• Independent heater circuits	• Heater circuits – Thermostatic-controlled – Strip-type heaters cemented directly to surface – 4 thermostats per circuit	• Limit module temperature excursions, positive control to account for uncertainties
(5)	Actuation (including propulsion) module		
	• Radiator area (-Y face)	• Radiator area = 2.32 ft^2	• Reference orbit, T = 70°F
	• Heater circuit	• Heater power requirement = 22.5 watts	• Minimum risk, orbital average
(6)	Attitude determination		
	• Radiator area (-Z face)	• Radiator area = 1.93 ft^2	• Reference orbit, T = 70°F
	• Heater circuit	• Heater power requirements = 7.7 watts	• Minimum risk, orbital average
(7)	Electrical power		
	• Radiator area (+Y face)	• Radiator area = 4.0 ft^2	• Reference orbit, T = 50°F for batteries and 70°F for remainder
	• Heater circuit	• Heater power = 16.2 watts	• Minimum risk, orbital average
(8)	Communications and data handling		
	• Radiator area (+Z face)	• Radiator area = 2.49 ft^2	• Reference orbit, T = 70°F
	• Heater circuit	• Heater power = 7.7 watts	• Minimum risk, orbital average
(9)	Wideband		
	• Radiator area (+Z face)	• Radiator area = 2.32 ft^2	• Reference orbit, T = 70°F
	• Heater circuit	• Heater power = 14.2 watts	• Minimum risk, orbital average
(10)	Solar array and drive		
	• Radiator area (-Z face)	• Radiator area = .21	• Reference orbit, T = 70°F
	• Heater circuit	• Heater power = 1.3 watts	• Minimum risk, orbital average

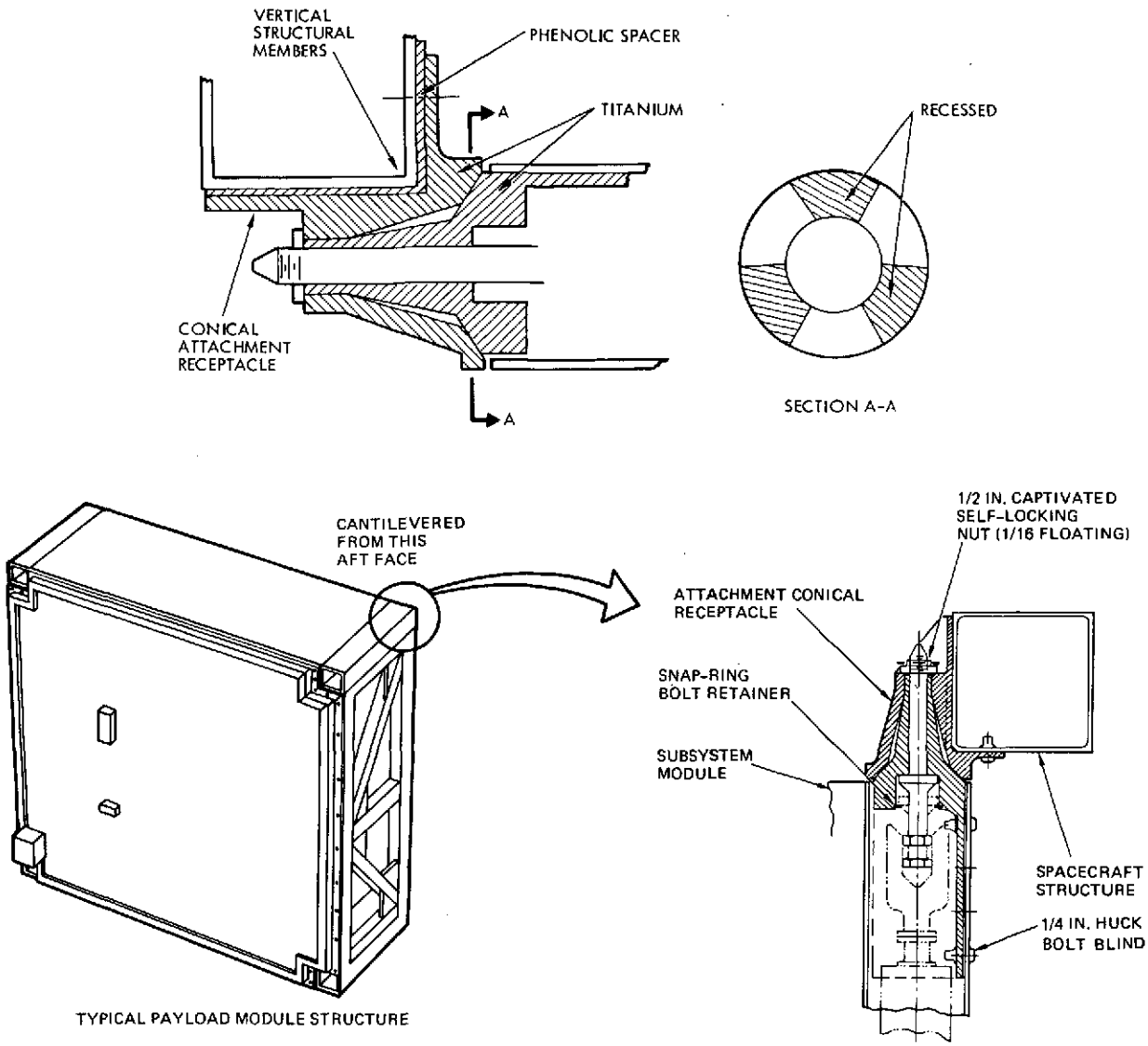

Figure 6-62. Module Thermal Features

Structure heater power requirements are functions of temperature, external environmental conditions, and multilayer insulation characteristics. For an on-orbit average set point of 70°F, which corresponds to the module orbit average set point, approximately 64 watts are required, as shown in Table 6-32. Performance summary is presented in Appendix A, Section 5.5.

6.10.3 Baseline Module Thermal Control Design

6.10.3.1 General Design Description

Each spacecraft module and sensor has its own independent thermal control system and each is thermally isolated, as well as possible, from

Table 6-32. Module Structure Heater Power Requirements

Module/Structure	Reference Orbit – Small Risk					6 a.m. Orbit
	Radiator Area[1] (ft^2)	Orbit[2] Average (watts)	Duty Cycle	Maximum Power	Higher Risk Average (watts)	Orbit Average (watts)
Modules						
Wideband communication	2.32	14.2	(3)	Twice	6	18.2
Attitude determination	1.93	7.7	(3)	Orbit	3	18.2
Command and data handling	2.49	7.7	(3)	Average	3	12.7
Electrical power	4.0	23.9	Orbital	Power	19.2	24.9
Actuation (including propulsion)	1.82	22.5	Orbital	Requirements	17.8	18.2
Solar array and drive	.21	1.3	(3)		1.3	1.3
Total module power		77.3			50.3	93.5
Structure						
(Payload and subsystem) (structural members uniformly heated)		64			50.0	64.0
Total (module/structure)		141.3			100.3	157.5

[1]Radiator sizing based on effective emittance (E^*) of MLT = .005 and no heat leaks

[2]Heat leaks through multilayer insulation based on $E^* = .01$ and $T_{module} = 60^\circ F$

[3]Will not be activated if heat loss and leak estimates are accurate

[4]Average structural temperature is $70^\circ F$.

the spacecraft structure and other modules/sensors. The thermal design, shown in Figure 6-61 consists of multilayer insulation blankets over all surfaces, except for those areas used as radiators. Silvered teflon was selected for the radiator area because it has a low α_s/ϵ, a very stable solar absorptivity and is relatively inexpensive. In all cases, the radiator area is applied only to the outboard face of the module with distribution of radiator areas tailored to minimize temperature gradients in equipment platforms. In general, that producing equipment is located on the outboard panel, as illustrated in Figure 6-62. Thus, heat generated by electronic boxes is conducted through the platform and rejected to space by the radiators.

The size of each radiator was selected to maintain an orbit-average temperature of $70^\circ F$, based on nominal external environments and nominal operating duty cycles. Thus, passively-controlled modules would have a mean temperature of $70^\circ F$; mean temperature variation due to uncertainties in the heating environment, optical properties of thermal control surfaces; heat dissipations by electronics, etc., is about $10^\circ F$.

Passive thermal control satisfies equipment temperature requirements (level and excursions) but is inadequate to maintain orbital average

temperature level for the range of near-earth orbits. A near-constant orbital average temperature is desired to limit interface temperature gradients as part of structural thermal distortion control. The baseline design uses thermostatic-controlled heaters with a turn-on temperature of 60°F to minimize heat leaks from spacecraft structure; these heaters provide positive control which accounts for thermal design uncertainties, allows for considerable growth margin that is only subject to heater power restriction and radiator area, and minimizes design risks.

Details of each module thermal design are presented in Appendix A, Section 5.5. Design approach and resulting performance of all modules, except actuation (includes propulsion) and electrical power, are similar. The radiator area was sized for the 11:00 a.m. reference orbit and for orbital-average module heat dissipation. Typical average platform temperature oscillations are about ±3°F. Thermal design of the electrical power module was tailored to accommodate pecularities of the batteries; thermal design of the actuation module had to account for dissipationless conditions in the propulsion components.

Tradeoff studies involving thermal control schemes, module interchangeability, and costs were made. These tradeoffs are reported in Appendix A, Section 5.5.

6.10.3.2 Specifics of Module Thermal Design

A summary of each module thermal design is presented in Table 6-30. These thermal control features were tailored to the specific spacecraft location, module requirement, orbit conditions, and minimal cost objectives. It should be noted that heater power requirements are affected significantly by the need to limit module orbit-average temperature variations. A major impact on heater requirements is accommodation of heat leaks (through insulation and others) which are subject to large uncertainties; this is detailed in Appendix A, Section 5.5. For a minimal risk design, total module heater power requirement is 77.3 watts (Table 6-32).

6.10.4 Module/Sensor to Structure Interface

6.10.4.1 General Design Description

Each module and sensor is attached to the spacecraft structure with four fittings, one at each corner of the inboard side. A design objective

is restriction of this interface heat flow to a reasonable level of less than 1 watt per attachment point. This goal is achieved by controlling structure/module temperatures with heaters and by mechanical design of attachment fittings to provide a reasonably high resistance. Design goal is a resistance of >10 Hr-^{0}F/BTU but spacecraft thermal control system is based on a value of 5 Hr-$^{\circ}$F/BTU, which can be attained with use of titanium fittings, minimal contact area, and fiberglass isolation, as discussed in Appendix A, Section 5.5 and illustrated in Figure 6-63.

Fluctuation of the module temperature is attenuated considerably by the time constant effect between the attachment and radiator with the result that temperature swing and rate of change at the attachment point is small. Details are reported in Appendix A, Section 5.5.

6.10.5 Comment on Titan and Thor-Delta Configuration Thermal Designs

Basically, thermal design of the Titan and Thor-Delta configurations are the same except for details since modularity has been applied to both. Design differences are due to: 1) the resupply requirement for Titan and not for Thor-Delta, and 2) the square-shaped Titan subsystem structure versus the triangular Thor-Delta subsystem structure.

Both configurations will employ computer-controlled heaters on structure which is blanketed with multilayer insulation. Modules will use thermostatically-controlled heaters with appropriately sized radiators and multilayer insulation. Module design differences between Titan and Thor-Delta are reported in Appendix A, Section 5.5. Since the Thor-Delta configuration needs to be resupplied and thus the insulation custom installed, heat leak uncertainty should be significantly less than the Titan configuration.

6.10.6 Summary

The thermal control system with passive elements coupled with active heater circuits represents a cost-effective method with reasonable margin, minimal risk, and large growth potential (assuming necessary heater power is available). Heater power requirements for this approach for a small risk and a higher risk design are indicated in the heater power summary of Table 6-32.

7. EOS-A BASELINE INTEGRATION AND TEST CONCEPT

The baseline integration and test concept planned for EOS-A is a progressive departure from the conventional approach. It is aimed at producing the lowest-cost test program consistent with the required confidence levels, and it is guided by the objectives of the modularity concepts. In general, the baseline concept calls for extensive qualification testing to validate the modular design parameters and limited acceptance testing at the spacecraft and observatory level. In this way, cost savings over the conventional approach are realized over a large number of observatories and mission applications. An overview of the EOS-A baseline and the conventional test program is given in Table 7-1.

The lowest-cost integration and test concept for EOS-A is based upon a single contractor performing the integration and test functions for both modules and observatory. In fact, one test laboratory and the same personnel within that contractor should provide an integrated effort for the integration and test operations and the ground support equipment (GSE). The following cost advantages are realized from this approach.

- The EOS-A test program can be better optimized to reduce redundant testing between the module and observatory levels.
- One set of EGSE and MGSE can be used to support both the module and observatory test operations. Common equipment can be shared between modules to reduce the total quantity needed for the overall project.
- Start-up and familiarization costs are virtually eliminated for the observatory integration and test operations.
- Since there is a great deal of similarity between the module and observatory functional performance tests, significant savings in the plans and procedures can be achieved.

Figures 7-1 and 7-2 depict the lowest-cost integration and test flows for the EOS-A pilot and flight models. As an innovative cost saving feature for flight EOS acceptance, a burn-in test has been substituted for the conventional thermal vacuum test. The burn-in operation has been employed effectively on two military projects at TRW Systems.

Table 7-1. Overview of EOS Baseline and Conventional Test Programs

	EOS Baseline	Conventional
Qualification		
Component (unit)	Functional Random vibration (3 axes) Thermal vacuum EMI/EMS (1)	Functional Sine and random vibration (3 axes) Thermal vacuum or solar simulation Shock EMI/EMS
Subsystem (module)	Functional Acoustics Thermal vacuum EMI/EMS	Functional (2) Thermal (2)
Spacecraft	Payload interface checks	Functional Payload interface checks
Observatory	Functional Low frequency sine vibration (3 axes) Acoustics Ordnance firing shock Thermal vacuum Electromagnetic compatibility	Functional Sine and random vibration (3 axes) Modal survey Acoustics Ordnance firing shock Solar simulation and/or thermal vacuum Electromagnetic compatibility Static load
Acceptance		
Component (unit)	Functional Random vibration (3 axes) Thermal vacuum	Functional Sine and random vibration (3 axes) Thermal vacuum
Subsystem (module)	Functional Acoustics (4) Burn-in (4)	Functional
Spacecraft	None	Functional Payload interface tests
Observatory	Functional (5) Acoustics (5) Burn-in (5)	Functional Acoustics or vibration Thermal vacuum Burn-in (6)

NOTES:
(1) Engineering data only
(2) Large integrated payloads only
(3) Limited
(4) Refurbish items only
(5) Complete observatory launch
(6) Special cases (i.e., storage, launch delay, or suspected infant failure)

Appendix A, Sections 6.1 and 6.2 present the following supporting data for the EOS-A baseline:

- Qualification test matrix
- Acceptance test matrix
- EOS-A assembly, integration, and test for qualification
- EOS-A assembly, integration, and test for acceptance

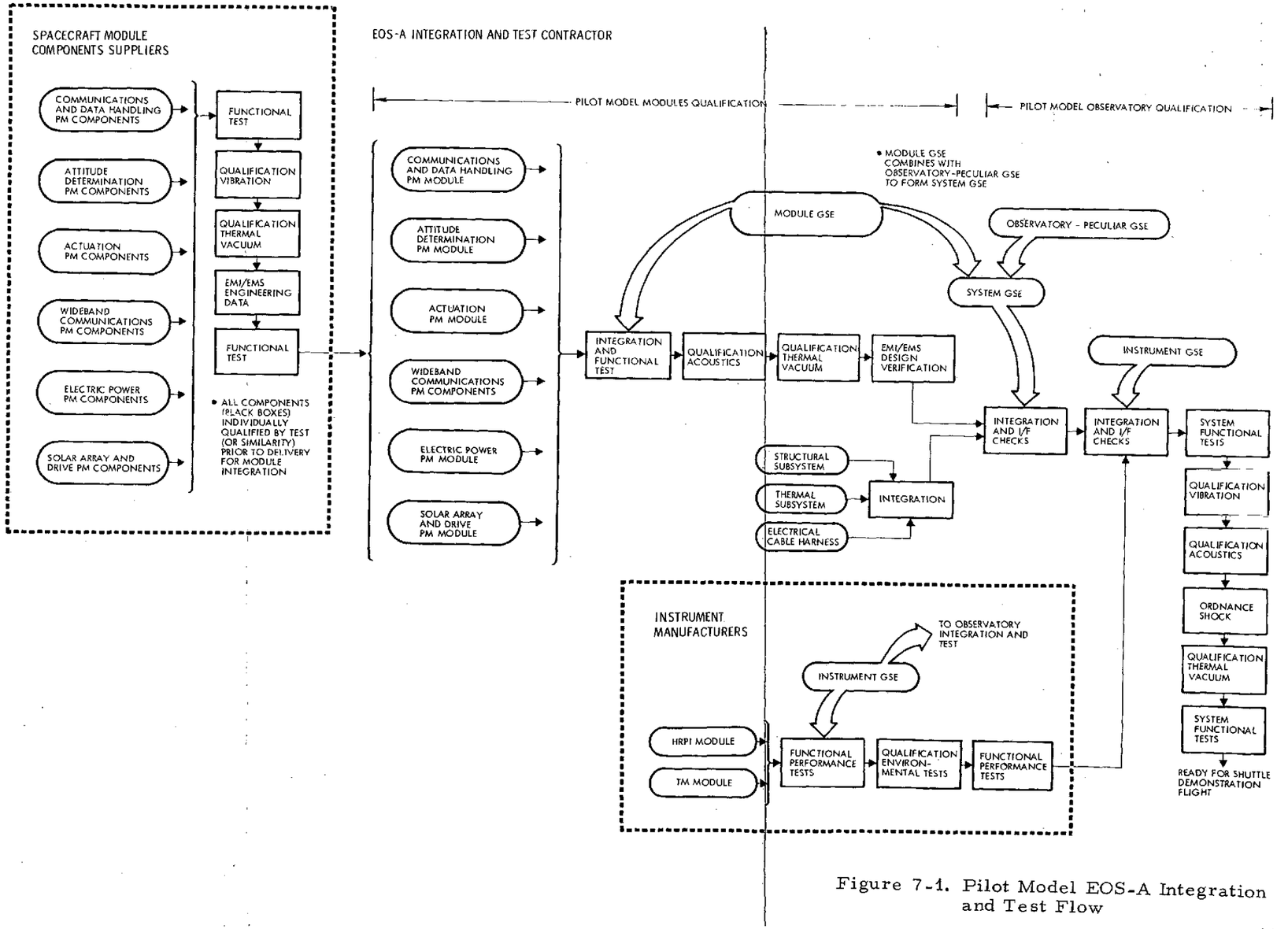

Figure 7-1. Pilot Model EOS-A Integration and Test Flow

FOLDOUT FRAME 1

FOLDOUT FRAME 2

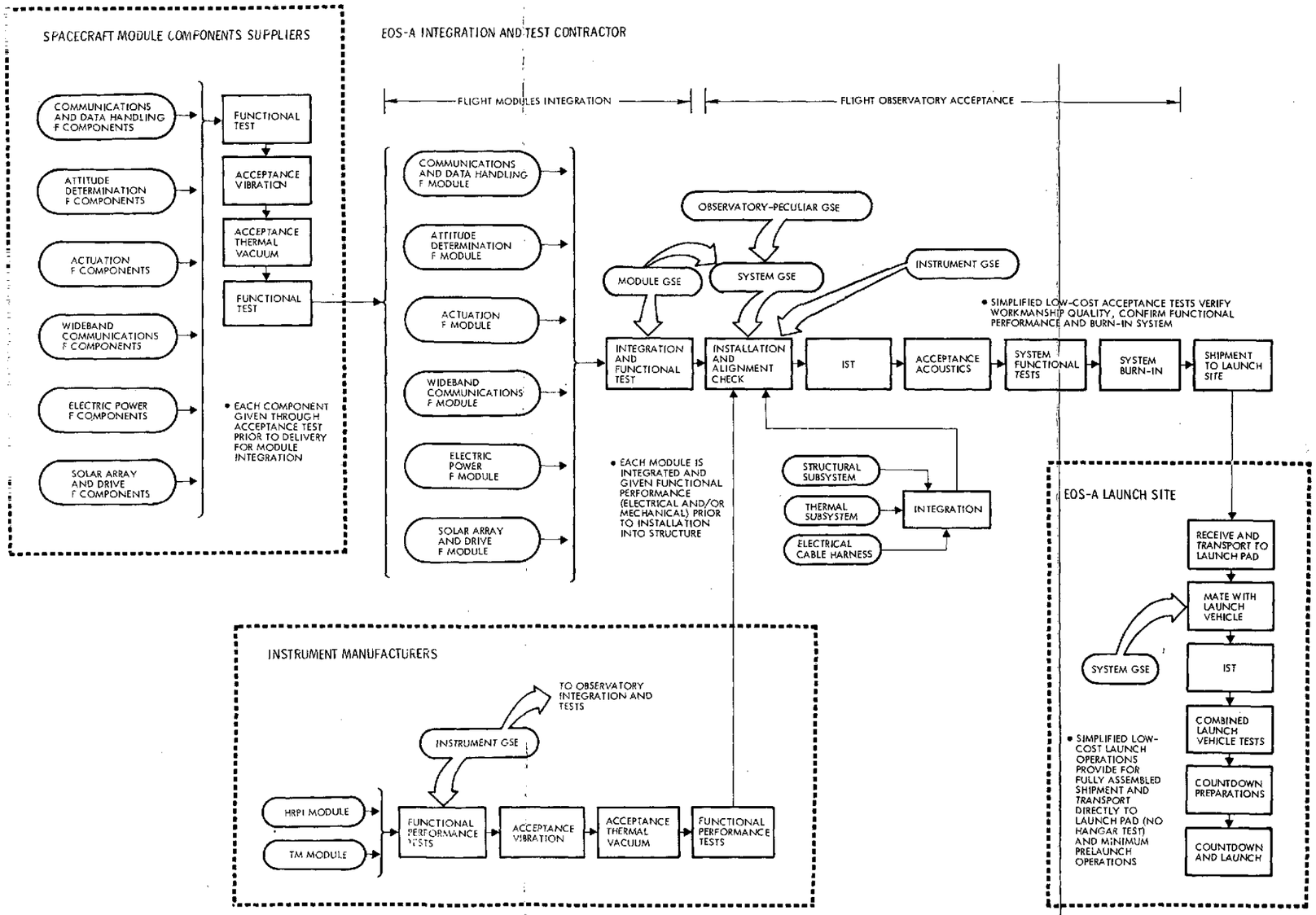

Figure 7-2. Flight EOS-A Integration, Test, and Launch Operations Flow

The conventional NASA test program was assumed for the instruments and included in the overall instrument costs.

7.1 QUALIFICATION

A basic philosophy of the baseline concept is that extensive component level testing (black box or unit) is fundamental to the lowest-cost test program. To reduce the impact of failures and retest at higher stages of assembly, the baseline approach plans to screen out faults at the lowest level of assembly.

A second critical driver in the qualification test program is the philosophy that the most important design parameters to validate are the module interfaces. The margins for each interface (thermal, mechanical and electrical) must be determined to assure repeatable system performance and permit flexibility in module applications over a variety of missions.

Component qualification tests include:

- Functional. Performance parameters, electrical and/or mechanical, are measured before and after the environmental tests.
- Random Vibration. Each component will be subjected to a random vibration from 20 to 2000 Hz in all three axes while electrically powered in the maximum normal load condition. Performance will be continuously monitored to detect failures (either hard or trends).
- Thermal Vacuum. Thermally cycle the component beyond expected orbital temperatures while at an orbital vacuum condition. The component is operating continuously and detailed performance parameters are measured at each temperature extreme.
- Electromagnetic Interference (EMI) and Susceptibility (EMS). Engineering EMI and EMS data are measured to provide diagnostic information for the module EMI/EMS qualification.

Module qualification tests include:

- Functional. Performance parameters, electrical and/or mechanical, and electrical interface characteristics are measured before and after the environmental tests.
- Acoustics. Acoustics testing will be performed with the module mounted in a receptacle which provides acoustic shielding similar to the observatory structure. The module will be heavily

instrumented to verify design adequacy of interconnections (electrical and mechanical) between the module and other observatory elements. The test data will be used to confirm estimates of the vibration environment for components mounted on radiators and establish procedures for acceptance testing. The module will be electrically powered and continuously monitored via the data bus to detect failures and out-of-tolerance performance trends. The solar array will be excluded from this test.

- Thermal Vacuum. The objectives of the subsystem module thermal qualification test are to determine: 1) maximum and minimum operating temperatures for the subsystem module for worst-case environments and operating duty cycles, 2) temperature levels and temperature variations of the module adjacent to the interface fittings, and 3) heater power requirements for cold case conditions.

  The test will be conducted in a thermal-vacuum chamber with liquid nitrogen cold walls. The subsystem module will be mounted on a fixture simulating the spacecraft frame. The properties of this fixture shall permit its temperature to be held constant at any level between 0 and 100°F.

  A heating source for the radiators will approximate the absorbed flux of the external environment. This can be done with electrical heaters, infrared lamps, or other techniques where the absorbed heating can be determined accurately.

  The test conditions are summarized below:

Test	External Heating	Operating Duty Cycle	Spacecraft Frame Temperature	Purpose
Nominal conditions	Nominal (SS)	Nominal	70°F	Determine nominal temperatures of module
Hot case	Maximum (SS)	Maximum DC	100°F	Verify maximum module temperatures
Cold case	Minimum (SS)	Minimum DC	40°F	Verify minimum module temperatures and heater power usage
Orbital transients	Maximum (TR)	Maximum DC	70°F	Verify module temperature fluctuations, particularly near the interface

  The module EGSE will be connected to the flight interface and test connectors. After thermal stabilization at each temperature level:

- Power bus and data bus will be tested in excess of their operational limits to determine design margins and compliance with the interface specification
- Detailed performance data will be measured to determine subsystem specification values.
- Thermistor/heater control and calibration will be determined.

- EMI and EMS. EMI measurements will determine the levels radiated on each module electrical interface and verify there is adequate design margin to assure non-interference with other modules. EMS measurements will verify that each module has adequate susceptibility margin to prevent performance degradation resulting from other module allowable radiation levels.

Spacecraft segment qualification tests include:

- Payload Interface Checks. As each instrument is integrated, interface signal characteristics will be measured to verify design margins and compatible operation with the spacecraft data bus and power bus.

Observatory qualification tests include:

- Functional. System performance parameters will be measured before and after the environmental tests. The functional tests consist of: 1) integrated system test (IST), 2) detailed subsystem tests, 3) detailed instrument tests, 4) power load determination (before only), 5) deployment tests, 6) alignments determination, 7) leak test and 8) solar array illumination. In addition, weight and center of gravity design is measured.

- Low-Frequency Sine Vibration. The observatory will be subjected to sine vibration at levels less than 1.1 x limit load over the range of 5 to 100 Hz in all three axes. The observatory will be heavily instrumented to verify the analytical model used for loads prediction and design adequacy of primary and secondary structure and module connections. The observatory will be electrically powered in the launch mode. RF telemetry data will be monitored continuously to verify the electrical system performance and design adequacy of the electrical interconnections between modules.

- Acoustics. The observatory will be subjected to an acoustics test while mounted vertically on an integration and test pedestal. Extensive instrumentation will be used to: 1) verify design adequacy of the solar array and other non-module components, 2) confirm estimates of the vibration environment for components mounted on walls other than radiators, and 3) confirm adequacy of the module receptacle used for module-level acoustics test. The observatory will be electrically powered in the maximum normal load condition and continuously monitored via the RF telemetry link to detect performance degradation.

- Shock. All ordnance (separation system, pin pullers on the array, antennas and module supports) will be fired to verify design adequacy of all observatory components. The observatory will be electrically powered in the appropriate mode during the firing. RF telemetry will be monitored to detect performance degradation.

- Thermal Vacuum. The observatory thermal control test has the basic objectives to evaluate the modular testing concept and the thermal control system. Evaluation of modular testing requires correlation of system and module test results. Evaluation of the thermal control system entails the following: 1) structure thermal control, 2) module/structure interaction, and 3) required heater power.

  The thermal vacuum test will be conducted in a thermal vacuum environmental chamber with an LN_2 cold wall. The -Z side will be irradiated with a heat source that can be accurately defined (solar simulation will not be necessary). The +Z side will face the cold wall; no attempt will be made to simulate the external energy input (earth emission, albedo, and solar). This test method will allow an accurate thermal definition of the chamber environment. The test conditions will include a cooldown phase to evaluate heat leaks, a steady state phase to evaluate heater requirements and a transient phase to evaluate interface interactions.

  Throughout the test, detailed temperature data will be measured to verify the thermal analytical model. Design adequacy of the thermal insulation, heater control and thermistor placement will be determined. In addition, thermistor calibration and methods for thermal evaluation and control by the ground station will be analyzed. At each thermally-stabilized level, integrated systems test and sensor (ADM and instrument) aliveness tests will be performed. Telemetry data will be monitored continuously to verify design margins of all subsystems.

- Electromagnetic Compability. Noise levels will be measured on critical signals (including interfaces) utilizing the module test connectors. This will verify module design adequacy and validate the EMI/EMS interface criteria established for module-level qualification.

7.2 ACCEPTANCE

The basic philosophy of the baseline concept for acceptance is "streamlined testing" to produce the lowest-cost test program which verifies the workmanship quality. This approach requires extensive environmental testing at the component level and fundamental workmanship tests at the module and observatory levels.

Component acceptance tests include:

- Functional. Performance parameters, electrical and/or mechanical, are measured before and after the environmental tests.

- Random Vibration. Each component will be subjected to a random vibration from 20 to 2000 Hz in all three axes while electrically powered in the maximum normal load condition. Performance will be continuously monitored to detect failures (either hard or trends).

- Thermal Vacuum. Each component will be subjected to extended thermal cycling at orbital vacuum. This test will stress the components repeatedly to uncover the workmanship problems. The component will be operating continuously and detailed performance measured at each temperature extreme.

Module acceptance tests include:

- Functional. Electrical and/or mechanical performance and interfaces are verified to assure compliance with the controlling specifications.

- Acoustics. An acoustics test at the module level will be performed only for refurbishment. The module will be mounted in a receptacle which provides acoustic shielding similar to the observatory. The module is lightly instrumented on the front face. The module will be electrically powered in the maximum normal load condition. Performance and interfaces will be monitored to verify assembly and interconnections workmanship.

- Burn-in. A burn-in test at the module level will be performed only for refurbishment. This test will be a continuous operation of the module over a 15-day period of time. Thermal cycling will be created via variations in primary power and heater demands introduced by commanded configuration changes. All modes of operation planned for the mission will be verified, detailed module performance parameters will be measured and electrical interface characteristics will be verified.

Observatory acceptance tests include:

- Functional. System performance parameters will be measured before and after the acoustics tests. In the interest of lowest-cost with little project risk, the pre-acoustics tests are limited to module alignment checks and an IST. To provide the required confidence level prior to shipment for launch, the final tests include: 1) IST, 2) detailed subsystem tests, 3) detailed instrument tests, 4) alignments determination, 5) deployment torque-theta tests, 6) leak test, and 7) solar array illumination.

- Acoustics. The observatory will be subjected to an acoustics test while mounted vertically on an integration and test pedestal. Module faces will be lightly instrumented. The observatory will be electrically powered in the maximum normal load condition and continuously monitored via the RF telemetry link to detect performance anomalies and failure trends.

- Burn-in. The observatory will be operated continuously over a 15-day period of time to assure detection of all infant failures and performance degradation. Thermal cyling will be created via variations in primary power and heater demands introduced by commanded configuration changes. All modes of operation planned for the mission will be exercised and all system-level electrical performance will be verified.

8. EOS-A BASELINE GROUND SUPPORT EQUIPMENT

8.1 ELECTRICAL GROUND SUPPORT EQUIPMENT

The lowest-cost approach was selected for the baseline EGSE concept. This approach provides a single set of EGSE located in a single test complex to be used for both module and observatory testing.

Each module has a corresponding subset. For module testing, these subsets are combined with a data/power bus simulator, as shown in Figure 8-1. There are two types of simulators required for the common data bus: 1) user – to simulate the remote terminals, and 2) source – to simulate the communications and data handling controller. Figure 8-2 depicts the concepts for these two simulators. The lowest-cost and simplest approach was selected here – one which does not require a computer and related software costs. Manual controls and visual displays are employed and provide a versatile and flexible means for module testing. Similarly, two types of simulators are needed for the common power bus: 1) user – to simulate the bus load, and 2) source – to simulate the bus power supply.

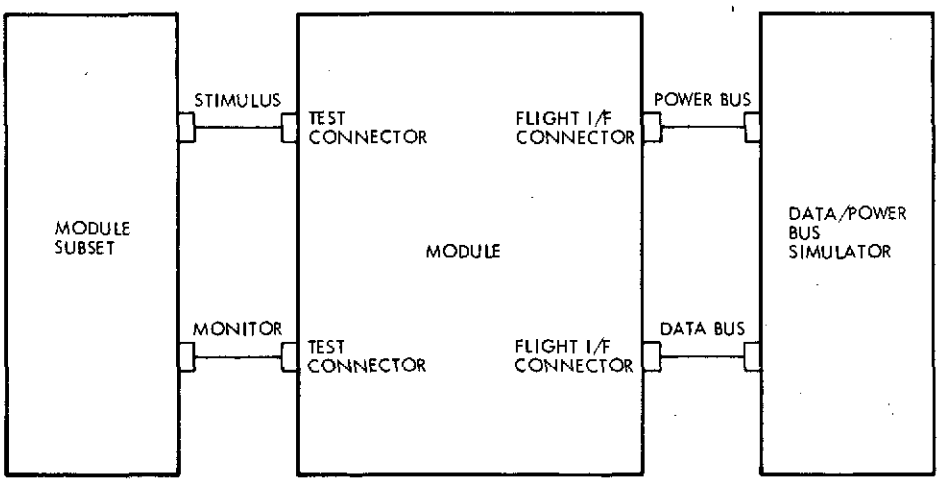

Figure 8-1. Module Test Concept

For observatory system-level testing, the module subsets are supplemented with automatic data processing equipment (ADPE), as shown in Figure 8-3. Because of the large quantity of test data and commands

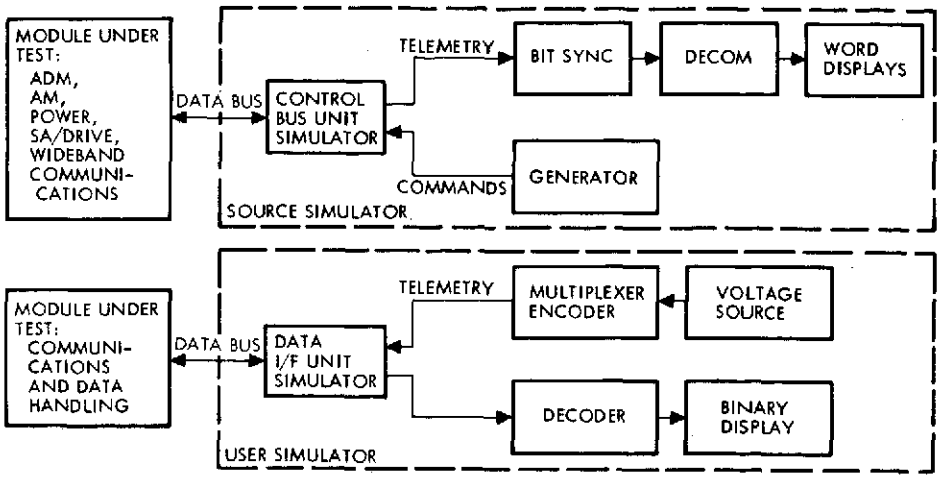

Figure 8-2. Data Bus Simulators

required for observatory testing, a computer system and tape recorder are incorporated into the system test set.

One each of the following electrical ground support equipment is required for the EOS-A baseline:

- Communications and data handling subset
- Attitude determination subset
- Actuation subset
- Electric power subset
- Solar array and drive subset
- Wideband communications subset
- Data bus user simulator
- Data bus source simulator
- Power bus user simulator
- Power bus source simulator
- Automatic data processing equipment.

A definition of performance requirements and equipment descriptions follows.

Communications and Data Handling Subset

1) Performance Requirements

- Simultaneously generate the two spacecraft uplink signals with command and ranging modulation
- Receive and demodulate, alternately, the two spacecraft downlink signals containing telemetry and ranging information

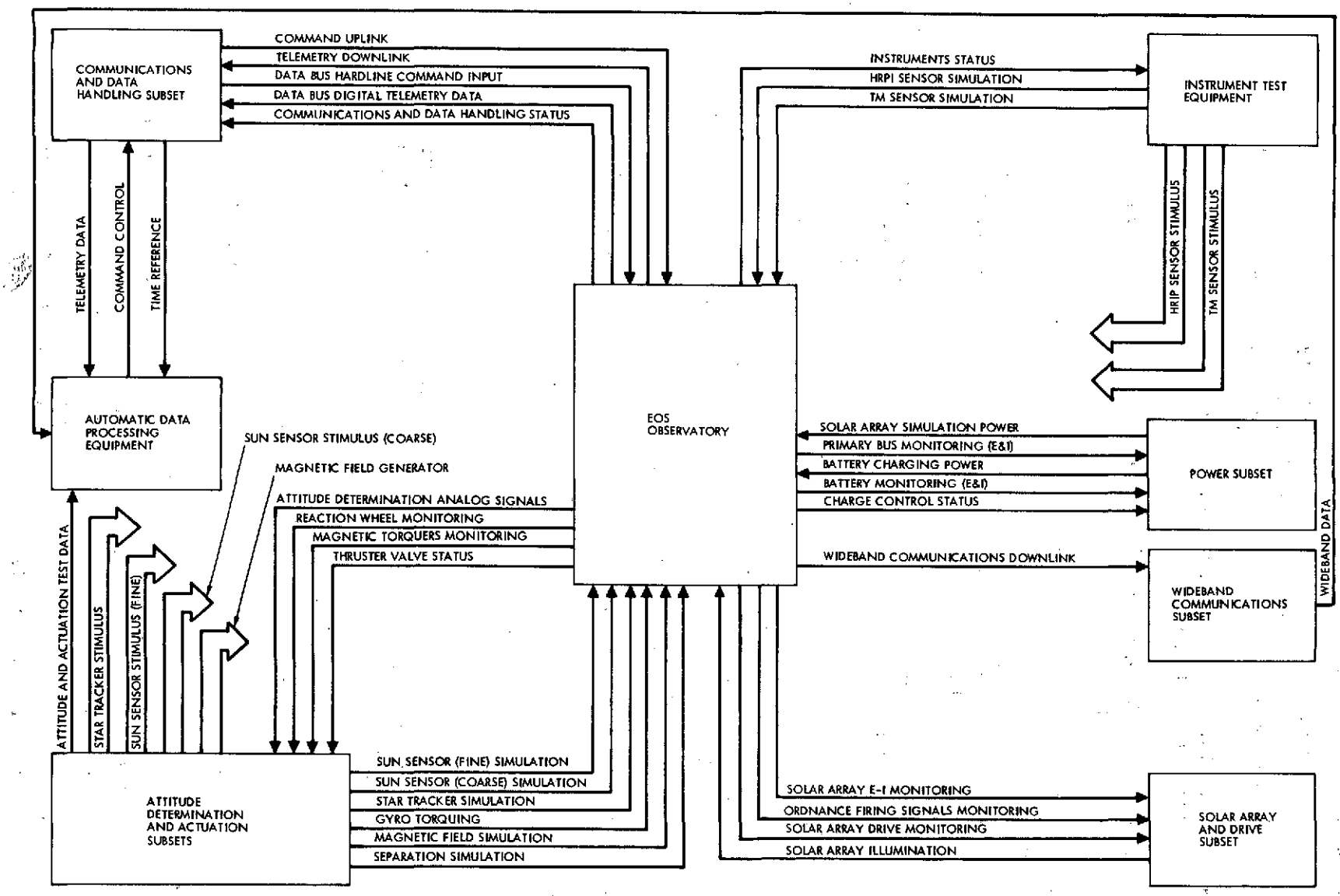

Figure 8-3. System Test Set Concept

- Evaluate the subsystem RF characteristics

Sensitivity	Spectral purity
Power level	Modulation density
Frequency	Range tone time delay

- Demodulate, bit synchronize, and decommutate the PCM/PSK real-time telemetry
- Display selected telemetry words in both a binary and decimal format
- Format telemetry data for input to the computer for processing
- Provide telemetry simulation for software checkout and console self-test
- Provide magnetic tape recording of the downlink telemetry data (PCM/PSK demodulated) stream, and time-code data
- Provide time-correlation for the ADPE and recording equipment
- Encode commands in the PCM/PSK/FM uplink command format under either manual or computer control
- Printout of on-board computer memory (via telemetry link)
- Input to on-board computer memory (via command link)
- Measure conditioned power, clock, etc.

2) Description

- RF Console

S-band transmitter	Range tone time delay unit
S-band receiver	Console power control unit
Modulation index meter	RF interface control unit

- Instrumentation Console

Power meter	Oscilloscope
Counter	Spectrum analyzer
DVM	Console power control unit

- Digital Console

Command generator	Time code generator/translator
PCM bit synchronizer	PSK modulator
PCM decommutator	PSK demodulator
PCM simulator	Oscilloscope
Counter	Console power control unit
Word selector/display	

- Magnetic Tape Recorder Console (Analog)
- Mini Computer Console

  CPU, 16 K core
  Digital input/output (4)

- Computer Peripherals

  Keyboard/printer
  Paper tape reader/punch
  Cathode ray tube display

Attitude Determination Subset

1) Performance Requirements

- Provide stimuli to the ADM sensor assemblies
- Provide appropriate precision simulated sensor outputs
- Provide time varying simulated sensor output signals (sinusoids, ramps, or pulsed outputs)
- Provide monitoring for ADM status
- Provide duration and period measurement capability for pulsed signals
- Provide voltage measurement capability for ADM hardline and test set signals
- Provide capability to permanently record in oscillographic form selected groupings of ADM hardline and test set signals
- Provide patching and switch selection of ADM hardline and test set signals to recording/measurement equipment

2) Description

- Sensor Stimulator Units

  Star tracker optical stimulator
  Coarse sun sensor optical stimulator
  Fine sun sensor optical stimulator
  Magnetic field generator

- ADM Test Console

  Sensor simulator unit
  Stimulator control unit
  Patch panel
  Visicorder
  Console power control unit

Actuation Subset

1) Performance Requirements

- Monitor reaction wheel speed
- Monitor thruster drive signals
- Monitor wheel drive signals from ADM
- Monitor valve drive signals from ADM
- Monitor magnetic torquer current
- Monitor regulated voltage
- Monitor conditioned telemetry signals
- Monitor isolation valve position status
- Record (oscillographic form) selected actuation module test signals.

2) Description

- Actuation Module Test Console

Thruster monitor panel	Patch panel
Visicorder	Console power control unit

Electrical Power Subset

1) Performance Requirements

- Provide solar array simulation power
- Provide battery charge power for independent charging of each of the batteries
- Provide hardline monitor of power subsystem parameters
- Provide external battery control and simulation functions

2) Description

- Electric Power Test Console

Solar array simulator
EOS power control and monitor
Battery reconditioning unit
DVM, voltage monitor
DVM, current monitor
Console power control unit

Solar Array and Drive Subset

1) Performance Requirements

- Provide simulated power control unit load
- Illuminate solar array with simulated solar light flashes

- Monitor solar array output voltage and current
- Monitor solar array position signal
- Monitor solar array drive signals
- Display ordnance bus status
- Determine that spacecraft firing circuit remains energized for the required time duration
- Determine that the firing current applied to the ordnance device is greater than the minimum for sure fire
- Continuously monitor the firing circuit for the ordnance no-fire current level
- Operate front panel lights for each circuit that indicates: no-fire, fire, or clear
- Simulate heater loads
- Simulate temperature sensor signals

2) Description

- Solar Array Test Console

  Power control unit load simulator
  Console power control unit
  Ordnance fire/no-fire detectors (one for each device)
  Visual display of ordnance bus arm/safe status
  Ordnance load simulator

- Solar Array Illumination Equipment

  Solar flash unit
  EI monitor panel

- Heater simulator

Automatic Data Processing Equipment

1) Performance Requirements

- Automated command control
- Process and display telemetry data
- Time-correlate all processed telemetry data and commands
- Process and display attitude and actuation hardline test data
- Process and display wideband instrument data

2) Description

- Computer Hardware

  CPU
  Core memory (64K words)
  Disc memory (491K words)

Digital input/outputs (5) (80 bits total)
Analog input/outputs (6)

- Peripherals

  Magnetic tape recorder (digital)
  Cathode ray tube display (2)
  Line printer (1100 lines/minute)
  Card reader
  Card punch
  Keyboard/printer

Wideband Communications Subset

1) Performance Requirements

- Receive two downlinks
- Demodulate, bit synchronize, and decommutate data streams
- Display selected data in both binary and decimal form
- Provide tape recording of both data streams
- Format the data for input to the ADPE computer
- Simulate thematic mapper and HRPI data outputs

2) Description

- Wideband R F Console

  X-band receiver
  Mod index meter
  RF interface control unit
  Console power control unit

- Wideband Digital Console

  Bit synchronizer
  Demodulator
  Data simulator

- Tape Recorder

Data Bus User Simulator

1) Performance Requirements

- Simulate data interface unit
- Simulate remote decoders
- Simulate remote multiplexers

2) Description

- Data interface unit simulator
- Remote decoder simulator
- Remote multiplexer simulator

- Command display
- Telemetry voltage sources
- Power control unit

Data Bus Source Simulator

1) Performance Requirements

- Simulate control bus unit
- Display telemetry data

2) Description

- Control bus simulator
- Telemetry bit synchronizer
- Telemetry decommutator
- Telemetry word display
- Command generator

Power Bus User Simulator

1) Performance Requirements

- Simulate power bus load

2) Description

- Variable resistive network

Power Bus Source Simulator

1) Performance Requirements

- Simulate power bus voltage and current
- Overvoltage/overcurrent protection

2) Description

- Variable power supply
- Fault protection circuits

8.2 MECHANICAL GROUND SUPPORT EQUIPMENT

The baseline MGSE consists of module, spacecraft segment, payload segment, and observatory handling and test support equipment. Based on the supporting analyses and tradeoffs in Appendix A, Section 6.3, the following complement of equipment has been selected.

	Quantity
• Ground Handling Equipment	
Module dolly* type A	2
Module dolly* type B	4
Module dolly* type C	2
Module dolly* type D	2
Module dolly* type E	1
Module sling* type A	1
Module sling* type B	1
Module sling* type C	1
Module sling* type D	1
Module sling* type E	1
Module installation fixture* type A	1
Module installation fixture* type B	1
Module installation fixture* type C	1
Module installation fixture* type D	1
Module installation fixture* type E	1
Solar array handling frame	2
Solar array dolly	2
Solar array sling	1
Solar array protective covers	1 set
Spacecraft segment integration and test pedestal	1
Payload segment integration and test pedestal	1
Observatory rotation fixture	1
Observatory sling	1
Spacecraft segment sling	1
Payload segment sling	1
Vertical work stand	1
• Test fixtures	
Observatory vibration fixture	1
Observatory thermal vacuum fixture	1
Observatory shock test fixture	1
Observatory weight and CG fixture	1
Solar array deployment fixture	1
Antenna deployment fixture	1

*As a function of module configuration.

	Quantity
• Ordnance Checkout Equipment	
Resistance measurement unit	1
Adapter cables	1 set
• Leak Test Equipment	
Leak detector	1
Test enclosure	1
Adapter ducts	1 set
• Propellant and Pressurant Loading Equipment	
Loading unit	1
Lines and fittings	1 set
• Alignment equipment	
Theodolites	3
Reference targets	1 set
• Observatory Shipping Container	
Container	1
Instrumentation	1 set

9. EOS-A BASELINE GROUND DATA MANAGEMENT DESIGN

9.1 LOW-COST GROUND STATION

The low-cost ground station (LCGS) concept makes earth observation data available to users in a timely manner in a format which allows processing to their unique needs. The concept requires the implementation of an RF equipment subsystem for acquiring sensor data over an X-band link and an image processing subsystem to produce output products. There are two primary considerations in the design of these subsystems: 1) sufficient detail in the design to allow analysis and tradeoffs to be performed on the EOS-A spacecraft for impact on its technical approach and cost data, and 2) a design approach which allows low-cost implementation. The baseline design successfully addresses both of these considerations.

The baseline design consists of two basic configurations: the direct display design and the record and process design. Each of the two designs require the same acquisition equipment and operational interface characteristic between the user and NASA. The difference between the two designs is the approach to the image processing subsystem. The direct display design produces only film output products, recording them in real-time, and is the lowest-cost system. The record and process design records the data and then processes the image data using a minicomputer-based system; it produces a range of output products tailored to the needs of the user and has output data quality commensurate with the central data processing facility (CDPF) product. Figure 9-1 summarizes the functional aspects of each design.

The operational characteristics of the LCGS and the NASA/LCGS interface will be discussed first; then each of the three subsystems acquisition, direct display, and record and process) will be discussed. The last subject to be considered is system engineering and integration.

9.1.1 Operational Characteristics

Only thematic mapper sensor data is transmitted to the LCGS. The baseline orbit yields a 17-day cycle for this data coverage. The LCGS can acquire up to 10 scenes in one pass. Pass requests for the LCGS are

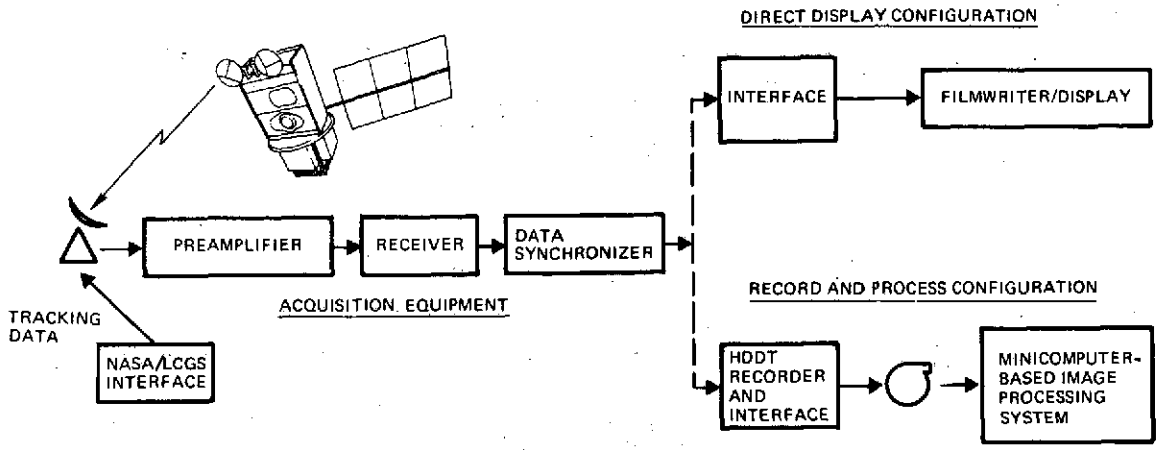

Figure 9-1. LCGS Functional Block Diagram

sent to the CDPF one cycle prior to the desired pass date. The CDPF automatically processes these standing orders and serves as the interface between the LCGS and the control center. Priorities are established at this point for conflicting pass requests through arbitration by the EOS project office. The processed requests are delivered to the control center for scheduling the pass assignments. The control center generates tracking data for the LCGS antenna system and image correction process; these data are transmitted to the LCGS facility using computer data link technology on the same day as the LCGS pass coverage.

The concept is that the principal NASA/LCGS interface is implemented within the CDPF; the control center only interacts with the LCGS to satisfy operational pass requirements. The CDPF provides LCGS support for siting and equipment calibration; it also provides any requested technical information within the purview of NASA. It is anticipated that an extension of the present ERTS Data Service Laboratory can provide the necessary administrative niche for these services.

The thematic mapper sensor data is edited on-board the spacecraft to reduce the downlink data rate from 120 to 20 Mbits/sec. In order to accomplish this data reduction, a number of LCGS thematic mapper compaction alternatives were suggested by NASA/GSFC. During investigation of these alternatives, it was assumed that all error correction processes and sensor edit options which do not significantly impact the spacecraft

cost would be implemented on-board the spacecraft. Using the philosophy, it was determined that all the thematic mapper compaction alternatives could be implemented. Table 9-1 presents a summary of the thematic mapper sensor data options available to the LCGS user.

Table 9-1. LCGS Thematic Mapper Compaction Alternative

Option	Swath-width (km)	Bands	Ground Resolution (M)
1	185 (full)	Any 1	30
2	90 (1/2 full)	Any 2	30
3	45 (1/4 full)	Any 4	30
4	185 (full)	All	120

During the course of this investigation, a preprocessing scheme was proposed for the reduced resolution alternative, option 4. If this scheme were implemented, additional data processing options could be made available. This option could provide any linear combination of up to nine pieces of data, e.g., an output consisting of the principal components of a combination of bands. The details of this proposed option are discussed in Appendix A, Attachment A, of Section 4.6.4.

The quality of the LCGS output products differs for the two baseline designs. Radiometric calibration of the LCGS sensor data will be performed on-board insuring the same potential radiometric accuracy for both designs. The direct display design will only produce a film output product. Therefore, the radiometric accuracy of its output product will be intrinsically less than the digital products of the record and process design. Furthermore, the direct display design will not perform any geometric corrections on the data. The film output product, then, will have a geometric accuracy dictated by the inherent accuracy of the transmitted sensor data and will be equivalent to the accuracy of the uncorrected HDDT output product of the CDPF. The record and process design is configured so that it has the capability of producing output products with

geometric accuracy equal to the quality of those produced in the CDPF. To summarize, the output data geometric quality specifications for the direct display and record and process designs will be determined by those used for the geometrically uncorrected and corrected output products of the CDPF, respectively.

9.1.2 Acquisition Equipment

The acquisition equipment block diagram is shown in Figure 9-2. This system is contained in both designs and its function is to acquire the X-band downlink containing the edited thematic mapper sensor data. The most expensive component of this subsystem is the antenna system which consists of an antenna, pedestal, feed, and control electronics. It was determined that programmed tracking could satisfy the pointing requirements. This allows a relatively low-cost implementation for the antenna system. An existing pedestal design is used which is driven by a punched paper tape. The information would be prepared by the control center and punched at the LCGS using a telephone link and computer technology. Because of the narrow beamwidth that is required, this design approach is the most cost-effective solution.

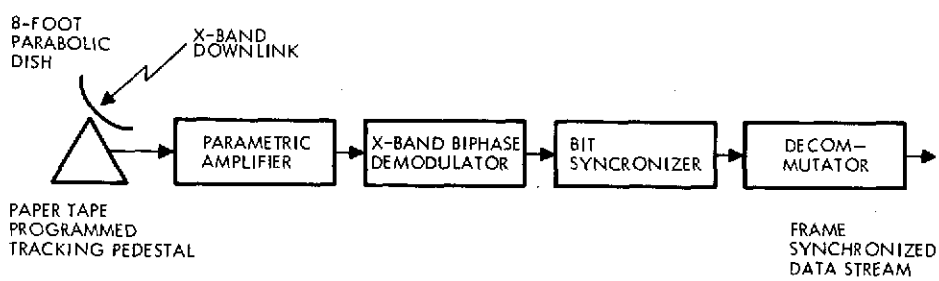

Figure 9-2. Acquisition Equipment Subsystem

An uncooled parametric amplifier is used for the X-band preamplifier. Again, this is the most cost-effective solution to satisfying the S/N ratio requirements for the communication link. The receiver is an X-band biphase demodulator. The modulation technique used for the downlink allows the use of this relatively inexpensive technology. The bit synchronizer and decommutator complete the subsystem components. These components are an extension of the technology used for the ERTS demultiplexing equipment.

9.1.3 Direct Display

The output of the RF equipment subsystem is a frame synchronized data stream. The direct display subsystem uses this data stream to produce an output film product. Cathode ray tube and electron and laser beam recorder technologies were investigated for their applicability to the direct display hardware implementation. Electron beam recorders were excluded because of their high recurring costs (~$200K). Laser beam recorders have a higher nonrecurring cost than cathode ray tube devices, and a comparable recurring cost. The nonrecurring cost for the laser beam recorders is necessary to achieve low recurring cost and provide an interface to the RF equipment, whereas the nonrecurring cost for the cathode ray tube approach is necessary to satisfy performance requirements. Because of this technical risk and the fact that the cathode ray tube technology cannot present all bands of option 4, laser beam recorder technology is recommended as the best overall cost/performance approach for implementing the direct display subsystem.

The data stream is buffered, line-by-line, and then recorded on film using a continuous 9-1/2-inch film transport. The data is band interleaved, i.e., line one of band one, then line one of band two, etc. The same line is scanned across the film, one band at a time, then the next scan presents the next sensor line. A maximum resolution of 8192 pixels per scan is required for the first three options, but the reduced resolution option requires 17,070 pixels for a laser scan line because of the seven bands. This is less than the 20,000 pixels attainable across a 9-1/2-inch film format for scanning mirror laser technology and is used to size the filmwriter resolution. Appendix A, Section 7.13 presents more details of this technology.

9.1.4 Record and Process

If additional data products, rather than just film or geometric accuracy equivalent to the CDPF product is required, then it is necessary to record the sensor data and provide additional processing. TRW's experience with precision processing of ERTS data on its minicomputer-based signal processing facility allows the design of a minimal cost record

and process configuration. The cost is minimal in the sense that it can provide output products with data quality equivalent to those produced by the CDPF. Figure 9-3 shows the configuration and its output products.

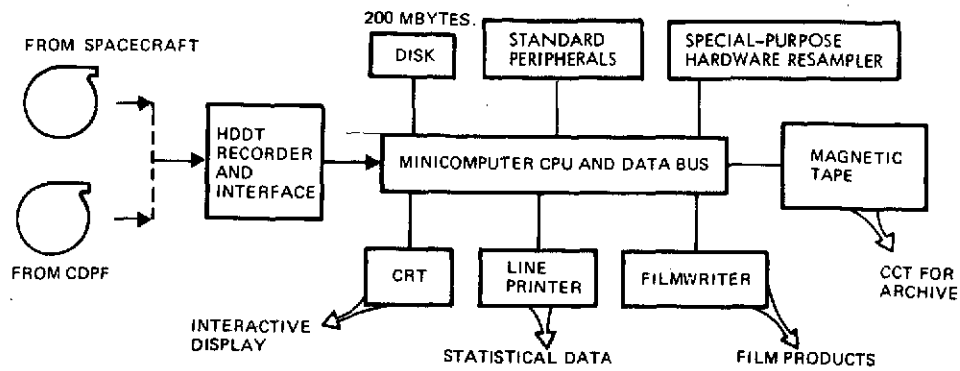

Figure 9-3. LCGS Minimal Cost Record and Process Configuration

The technology used for the high density digital tape recording at the CDPF is also used as the input tape recorder for the LCGS. This not only allows a cost-effective approach to acquiring the LCGS input tape recorder, but also yields a tape format interface between the CDPF and LCGS. Option 1 of the compaction alternatives provides a means, with no additional cost in hardware or software, whereby band-separated data can be transferred directly to the LCGS by the CDPF to compensate for uncollected scenes. Appendix A, Section 7.14 describes the scheme. It provides the LCGS user with an input source for HRPI and more thematic mapper data. This capability greatly enhances the LCGS concept.

It is noted that there is a special-purpose hardware component in the record and process configuration. The component is essentially a microprocessor for implementing high-order image processing algorithms and is entirely optional. It psorives increased throughput, a desirable feature if the high density digital tapes from the CDPF are processed.

The image processing functional flow is identical to that of the CDPF with two exceptions: 1) radiometric calibration is not required, and 2) the predicted ephemeris provided with the control center tracking data is used for the distortion estimation process. The lack of more

precise ephemeris data results in a greater registration control point search region, but two registration control points per scene will be sufficient to remove the bias errors and estimate the attitude errors. Appendix A, Section 5.2.7 discusses this problem in detail.

9.1.5 System Engineering and Integration

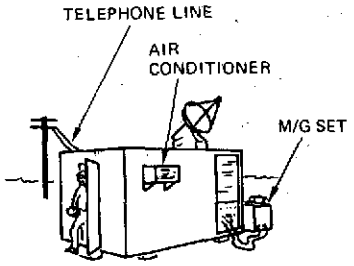

Figure 9-4. LCGS Facilities Configuration

It is anticipated that the location of the LCGS user will determine the form of the actual LCGS facility configuration. This configuration will then determine the system engineering and integration requirements beyond the hardware/software needs of the two baseline designs. Nevertheless, both designs are configured in a portable shelter facility which is complete with power generation equipment, air conditioning, and heating. Figure 9-4 shows a typical implementation.

This design allows easy relocation of the ground station site without expensive built-in transportation features. It yields a reasonable estimate for the cost of such facilities as well as providing potential LCGS users with complete cost estimates for implementing the total LCGS concept.

9.2 OPERATIONAL CONTROL CENTER

Our basic approach to a design concept and a cost estimate for an EOS control center was to lean heavily on the on-going ERTS operation and the existing hardware and software in the ERTS control center. This permitted our proposing to use virtually all of the ERTS hardware and much of the software. However, EOS poses a set of problems that were beyond those of ERTS:

- The EOS control center must support missions in varying orbital altitudes and orbital planes
- It must support missions with a wide variety of payloads
- It must support missions up to 15 years in the future and for which detailed definition or OPS concepts do not exist.

These future uncertainties made it imperative that we establish a design concept that had an adequate performance margin, that could be readily and logically expanded if required, and one that permitted configuration flexibility and equipment redundancy. Although it was mandatory that we make maximum use of ERTS hardware and software, our design concept still had to consider the possible use of new state of the art equipment that would, over the life of the EOS program, prove to be cost-effective.

Even a cursory analysis conclusively showed that there was no cost-effective alternative to making maximum use of the existing ERTS software, which in turn dictated the use of xerox equipment for any required expansion of control center capability.

The ERTS software design concept was followed quite closely resulting in five programs:

- Communication processing
- Online data processing
- Offline data processing
- Mission scheduling and support
- Command generation.

The principal design impact was in the scheduling programs which virtually required a complete redesign to support the optimum scheduling of the high resolution pointable imager (HRPI). Analysis further indicated a fairly significant rewrite of the command generation, validation, and verification programs. The assembly language programs for the Sigma 3 processors required recoding to Fortran IV to run on 32-bit machines. Our design/cost tradeoffs for the low-cost ground stations dictated the generation of station pointing angle information to be transmitted to these stations. This was a relatively trivial requirement, but one that had to be accommodated.

We made assumptions as to the design and adequacy of ERTS software documentation which resulted in an estimated requirement for the development of approximately 70K new or modified instructions.

Our design concept for the baseline system had certain salient proposed features:

- Replace the existing decommutators with programmable units which would permit very quick reaction support of missions with different telemetry formats.
- Remove the online Sigma 3 preprocessors to improve system reliability.
- Install a Xerox 550 processor to support all online functions of communications processing; display generation; and command generation, validation, and verification. This is a proven, production machine that can run most of the existing ERTS software, interface with certain of the ERTS peripherals and provide the principal future advantages of increased reliability, increased input/output bandwidth, and faster memory cycle time.
- Use the existing Sigma 5 processor as an offline processor to principally support the probable increase in mission scheduling that would result from either multiple operations or various complex payloads.
- Configure the system so that the Sigma 5 and its principal peripherals can be cross-switched to provide an online backup to the 550 processor.
- Provide a paper type generation capability.
- Provide redundant RAD's and discs.
- Use three existing ERTS control room consoles as is for operations supervisor, command controller, and online analyst.
- Modify the ERTS M&O console to support the EOS configuration.

Figure 9-5 presents the design concept of the EOS control center baseline system to the individual equipment level.

In this baseline design concept the equipment listed in Table 9-2 was required to replace or supplement existing ERTS control center equipment.

A design concept was also provided and costed that would permit expansion of the baseline system to support simultaneous multiple operations. The salient features of this concept were:

- Providing a second xerox processor (RAD and disc) paralleling the baseline system configured to be completely cross-switchable between PCM decommutators, processors, and peripherals

- Modifying two existing ERTS analyst consoles with EOS command capability
- Moving the Sigma 5 processor and its peripherals completely offline to support mission scheduling or other offline functions.

Table 9-2. Control Center New Equipment

Xerox Model No.	Quantity	Description
8275	1	4-byte interface
8264	6	Port expansion
7236	1	Extended width interface
8261	1	8K memory
8262	1	8K memory addition
4501	1	Xerox 550
4525	2	External interrupts
4561	2	16K memory, 2 ports
4562	3	16K memory increment
4570	1	Direct input/output interface
4580	1	Input/output cluster
4581	2	MIOP
4582	1	Input/output adapter
4591	1	KSR 35 keyboard printer
4566	4	Two-port memory expansion
3340	1	Magnitude tape controller
3345	2	Add-on tape drive
3465	1	Line printer
3211	2	Rotating storage container
3215	1	RAD storage unit
3243	2	Cartridge disc drive
3246	2	Disc cartridge
7071	1	Paper tape control
7072	1	Paper tape reader
7073	1	Paper tape punch
1126A	2	PCM decommutator
TM536	2	Switch

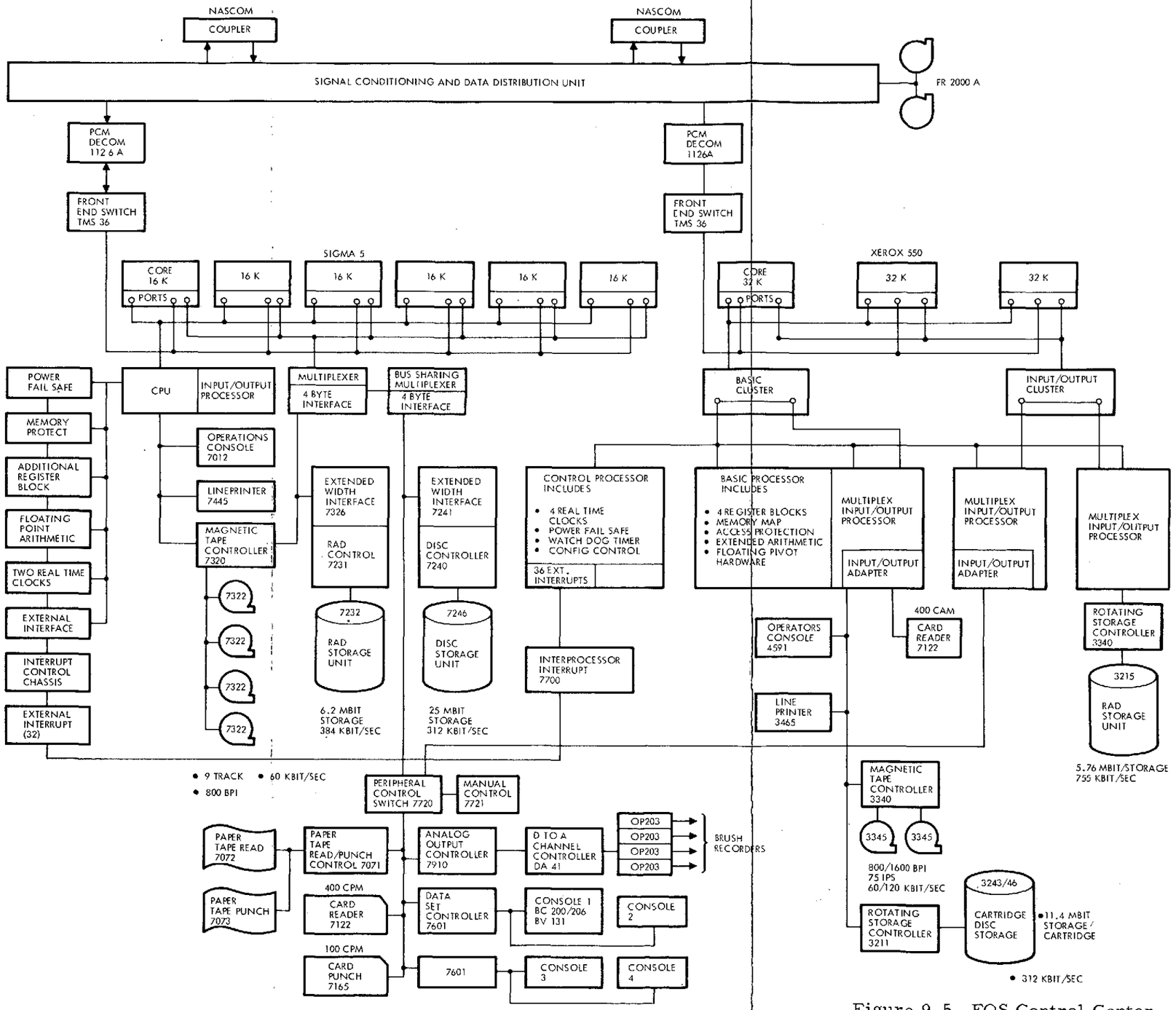

Figure 9-5. EOS Control Center Design Concept

FOLDOUT FRAME

No software changes from the baseline design were considered necessary to support this expanded configuration.

Figure 9-6 delineates this multi-operations control center concept down to the individual equipment level.

The design concept to support multi-satellite operations required additional equipment above the baseline design (Table 9-3).

Table 9-3. Multi-operations Control Center Additional Equipment

Xerox Model No.	Quantity	Description
4501	1	Xerox 550 CPU
4525	2	Extender interrupts
4561	1	16K memory 2 ports
4562	1	16K memory increment
4570	1	Direct input/output interface
4580	1	Input/output cluster
4581	3	MIOP
4582	1	Input/output adapter
4591	1	KSR 35 keyboard printer
4566	4	Two-port memory expansion
3340	1	Magnetic tape controller
3345	6	Add-on tape drive
3211	2	Rotating storage unit
3215	1	RAD storage units
3243	2	Cartridge disc drives
3246	2	Cartridge discs
7720	2	Peripheral switch
7722	4	Bus extender
OP203	5	Interface to recorders
FR2000A	2	Analog recorders
	4	8-channel brush recorders and aplifiers
	1	Event recorder

9.3 BASELINE CENTRAL DATA PROCESSING FACILITY DESIGN

This section presents a baseline functional and hardware design for the CDPF structures to fulfill the requirements for accuracy, formats, throughput and ease of access to EOS thematic mapper and HRPI data. This baseline design has been structured in sufficient detail to allow accurate performance and cost estimation and to provide a reference for which the relative cost and performance impacts of alternative EOS system design and tradeoffs can be assessed. Supporting analyses and tradeoff studies to justify throughput/performance predictions and hardware selection, costing, and reliability are presented in Appendix A, Sections 7.9 and 7.10. The hardware design presented is not a final, optimized design for the CDPF, but is instead a conservative cost versus performance estimation model. The design is predicated on the following criteria:

- Low cost – necessary for viability of entire program
- High throughput – two 120 Mbit/sec sensors
- Maximum accuracy – geometric and radiometric correction
- Modular growth capability – adaptability to higher data rates and new mission sensors
- Data reliability – minimization of data loss and errors
- Operational tractability – minimization of manual interaction
- Technical risk and development requirements – use of existing technology with minimal development
- Flexibility – ease of modification of algorithms and processing mix.

Data processing requirements and interfaces are discussed in Appendix A, Section 7.11 to justify the baseline CDPF functional structure. Sizing and timing of the CDPF functions are presented to justify the CDPF processing hardware complement selected. Principal hardware and software tradeoff areas are discussed, and hardware costing estimated are provided.

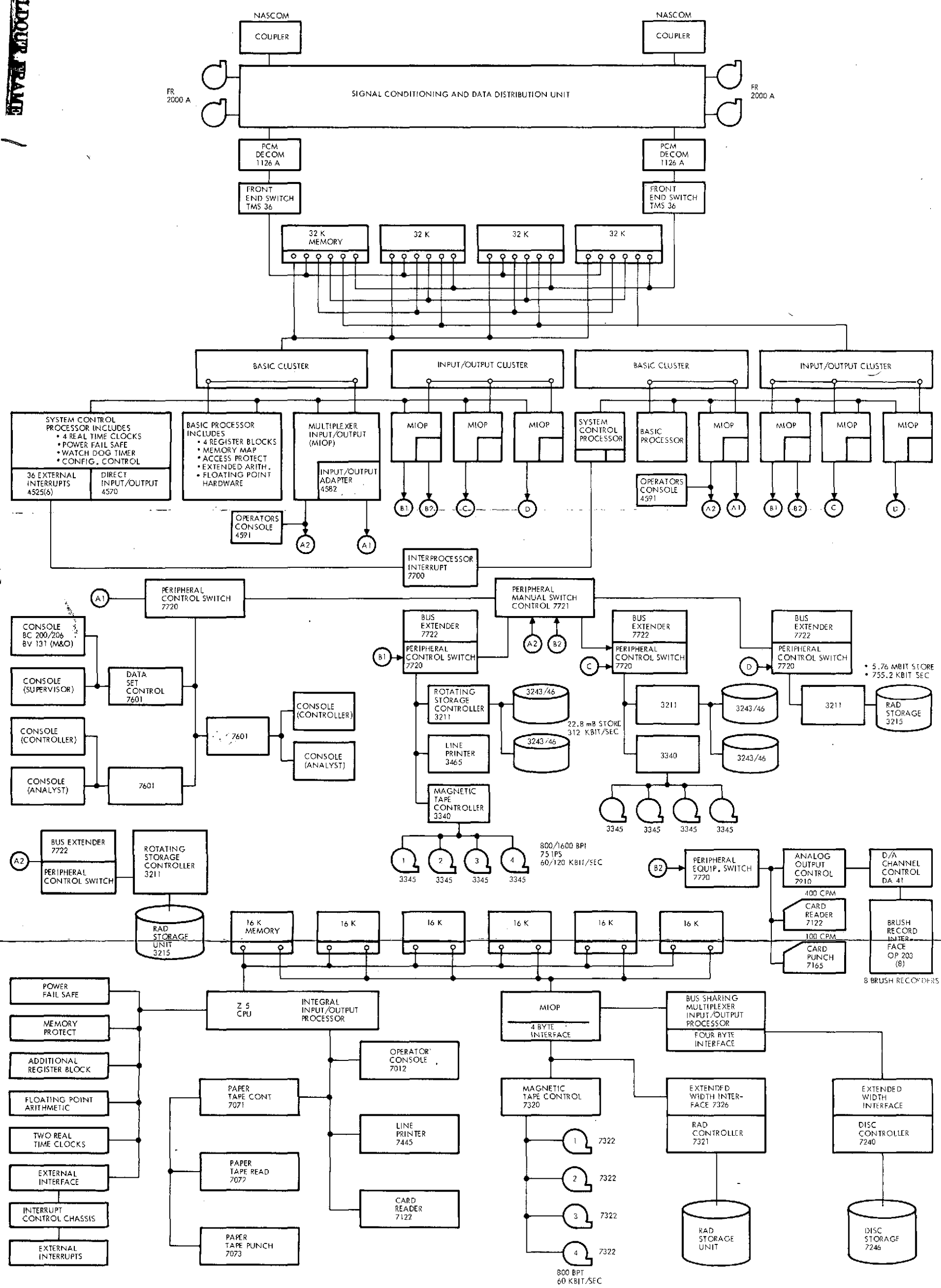

Figure 9-6. EOS Control Center Multiple Operations Design Concept

The cost-driving elements of the system are shown to be the input and output data reformatting operations in the image processing system, with the image correction subsystem handled easily in special-purpose hardware. The information management and photo processing systems draw heavily on existing ERTS capabilities for lowest cost.

The design philosophy of the CDPF includes:

- Use of existing hardware/software where applicable
- Construction of two critical throughput algorithms in special-purpose hardware, with the remainder of the image processing system in software for flexibility
- Structuring of all image processing functions except distortion estimation as parallel input/output processes.

All-special-hardware systems were avoided due to difficulty in changing algorithms, etc., to meet changing EOS requirements. Similarly, image reformatting or distortion correction using sufficiently accurate algorithms is intractable in all software-implemented systems.

9.3.1 User Requirements

User data quality requirements (see Table 9-4) are discussed in Appendix A, Section 7.9, and are driven by registration accuracy requirements of $\pm 1/4$ pixel maximum geometric error, preservation of sensor resolution capability through high-order correction algorithms and data format requirements differing from the sensor formats and between users. Digital correction of the data in the CDPF is required to meet these requirements. Data throughput requirements are extremely high, corresponding to over a million megabits of image data per day in several output formats and media. Data loads shown in Table 9-5 are used for design of a baseline CDPF system and are discussed in more detail in Appendix A, Section 7-11. User access to the data is required in the form of data storage, cataloging, and retrieval systems; LCGS support for ephemerides and mission scheduling; and processed data dissemination. It is assumed that all data processing capabilities will be available in the CDPF at the worst-case throughputs mentioned above in order to supply NASA investigators with EOS data for the entire United States. For reduction of CDPF cost, other users will access the data through the EROS Data Center of

Table 9-4. EOS User Data Requirements

End Use of Data Product	Resolution Requirement	Geometric Precision	Geodetic Control	Spectral Registration	Radiometric Fidelity	Principal Output Media	Special Processing	Tape Format**
Spectral signature classification	Moderate-high (10 to 30M)	Low	Low	High (~0.1 pixel)	High	Film/digital tape		Band interleaved
Change detection	Moderate-high (10 to 30M)	Very high (~1/4 pixel)	Moderate-low	Low	Moderate	Film/digital tape	Intensity normalization/registration	Band separated/interleaved
Mapping	Moderate-high (1 to 2 pixels)	High* national map accuracy standards	High* national map accuracy standards	Low	Low	Film	GCP's	Band separated
Mensuration	Moderate-high (1 to 2 pixels)	High (~1 pixel)	Moderate-low	Low	Low	Film/digital tape		Band separated
Terrain patterns	Moderate-high	Moderate-low	Moderate-low	Low	Moderate	Film		Band separated

*Depends on scale.

**Some users may request band interleaved or separated tape formats independent of end use of product.

Table 9-5. EOS CDPF Baseline Data Loading

Produce	Data Volume	No. of Data Users	No. of Formats
HDDT (uncorrected)	10^{10} to 10^{12} bits/day	2 to 10	---
HDDT (corrected)	10^{-10} to 10^{12} bits/day	2 to 10	---
CCT (corrected)	10^{9} to 10^{10} bits/day	10 to 100	1 to 5
Black and white positive/negative*	20 to 200 scenes/day	5 to 50	1 to 3***
Black and white prints		5 to 10	1 to 3***
Color positive/ negative**	10 to 100 scenes/day	2 to 20	1 to 3***
Color prints		2 to 10	1 to 3***

*First generation product — 241 mm (9.5 inch)
**Second generation product — 241 mm (9.5 inch)
***Enlargement to standard map scales.

the Department of the Interior or through low-cost ground stations or regional evaluation centers, thus offloading the CDPF.

An indirect user requirement is for low cost of the ground system, since cost-effectiveness is crucial to survival of the entire program. This requirement is addressed through use of existing capabilities (ERTS hardware and software, EROS Data Center, ERTS foreign ground stations), use of moderate-scale computers aided by hard-wired algorithms to render the image correction essentially input/output-limited, minimization of manual interaction in the processing to reduce operational costs, and utilization of standardized processing modules with easy adaptability to future EOS missions.

9.3.2 CDPF Functions and Interfaces

The CDPF receives wideband sensor data from three receiving stations in the form of wideband tape recorders. Auxiliary spacecraft

and calibration data are supplied by the NASA Orbit Determination Group and the control center. The CDPF processes and transmits user and LCGS requests for coverage to the control center mission planning function, and transmits output film and magnetic tape products to NASA investigators and to the EROS data center for dissemination to other users. The CDPF also provides a 70-day archive of tape and film products for NASA use. Deep archiving (>70 days) is relegated to EROS. Interfaces to the baseline CDPF are shown in Figure 9-7.

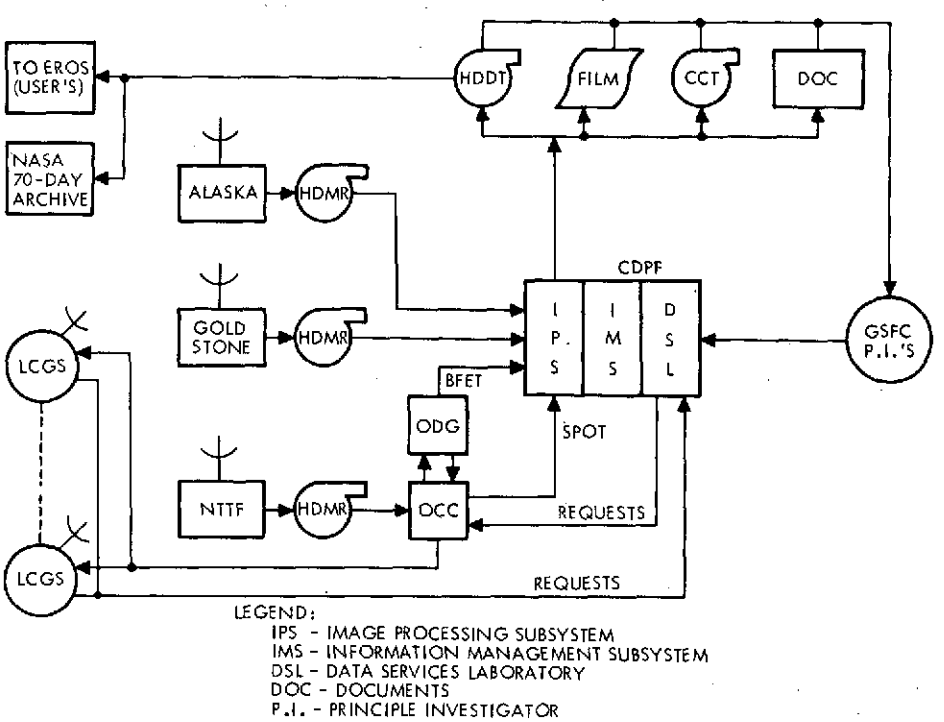

Figure 9-7. Baseline Ground Data Handling System Interfaces

The CDPF functional structure can be further broken down as shown in Figure 9-8. The CDPF is composed of three operating subsystems:

1) Data Services Laboratory (DSL)

2) Information Management System (IMS)

3) Image Processing System (IPS).

The DSL includes the management interface, user services, 70-day archiving, photographic production, and output product dissemination

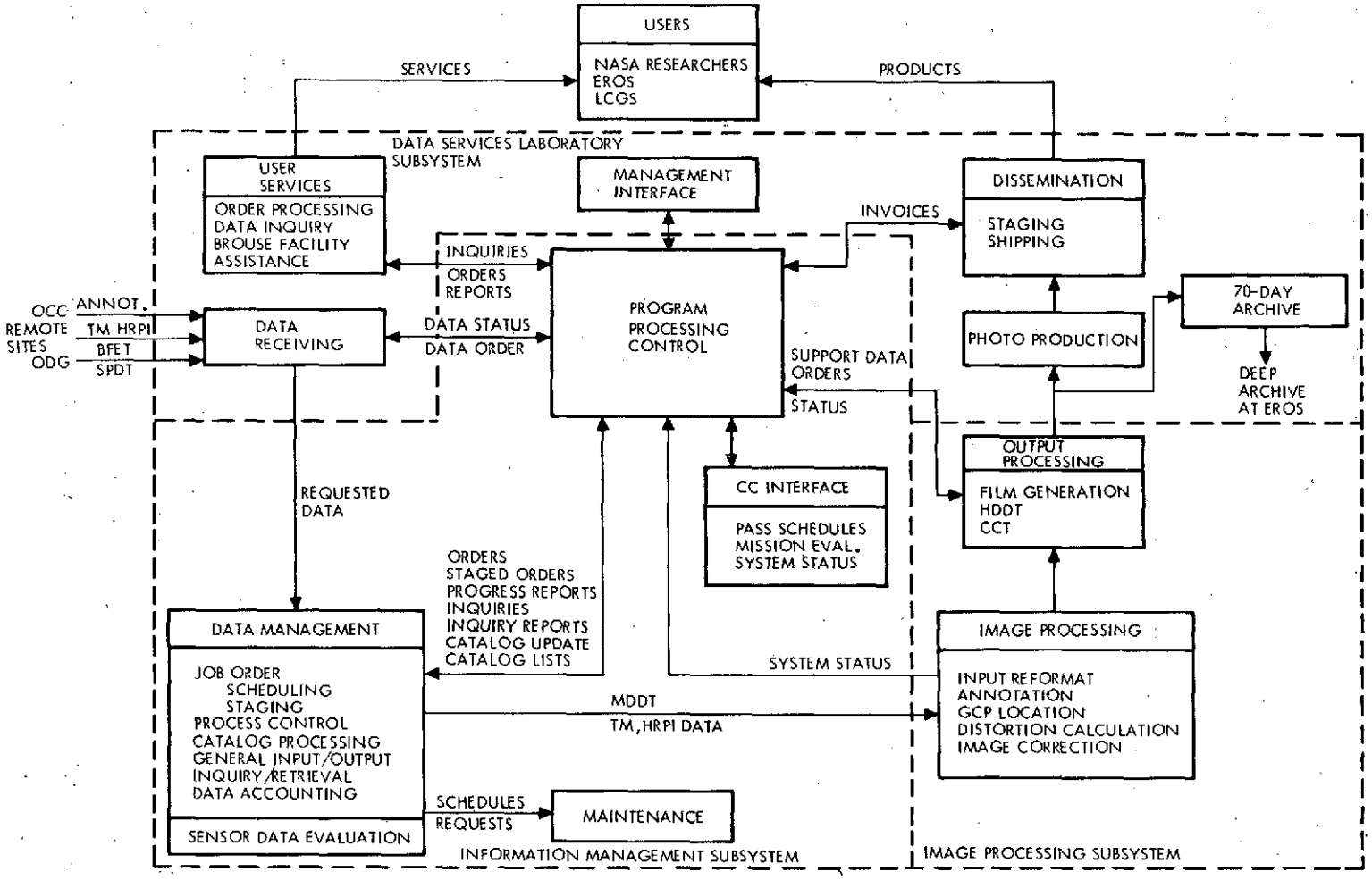

Figure 9-8. Central Data Processing Facility Functional Structure

and represents the user interface to the EOS data. The IMS includes the control center interface, the data management system, and processing control and represents the monitoring and control functions for internal CDPF data handling. The IPS includes the image correction and formatting functions and the output product generation. Commonality with existing ERTS functions is stressed, with the IPS being the primary development area for EOS.

9.3.3 Information Management System and Data Services Laboratory

The CDPF functions can be grouped into those which interact directly with the sensor data and those which do not. Most of the IMS and DSL (except for photo production and shipping) do not, dealing instead with summary characteristics of the data, such as catalogs and data routings. The existing ERTS IMS and DSL functions perform the same tasks as those required for EOS for approximately the same coverage, cycle time, and orbit. Data load increase is in the number of spectral bands and number of picture elements per scene, not in the number of scenes. Offloading of the CDPF user interface volume to EROS provides the same or lower expected loading on the DSL as experienced in ERTS. Coverage requests in ERTS are for on-board tape recorder scheduling, while for EOS scheduling is required for HRPI and LCGS coverage requiring a slightly greater requirement for mission planning. The mission planning function is contained within the control center with the DSL interfacing user coverage requests to the control center. Software functions for the IMS and DSL are discussed in more detail in Appendix A, Section 7.8.

The current ERTS NASA data processing facility (NDPF) system was used as a baseline from which the EOS IMS/DSL software configuration was established. Most of the major information management functions and some of the computational subsystem functions are retained, but augmented/modified as required to meet EOS requirements. Figure 9-9 shows an NDPF software overview with modification and replacement requirements designated.

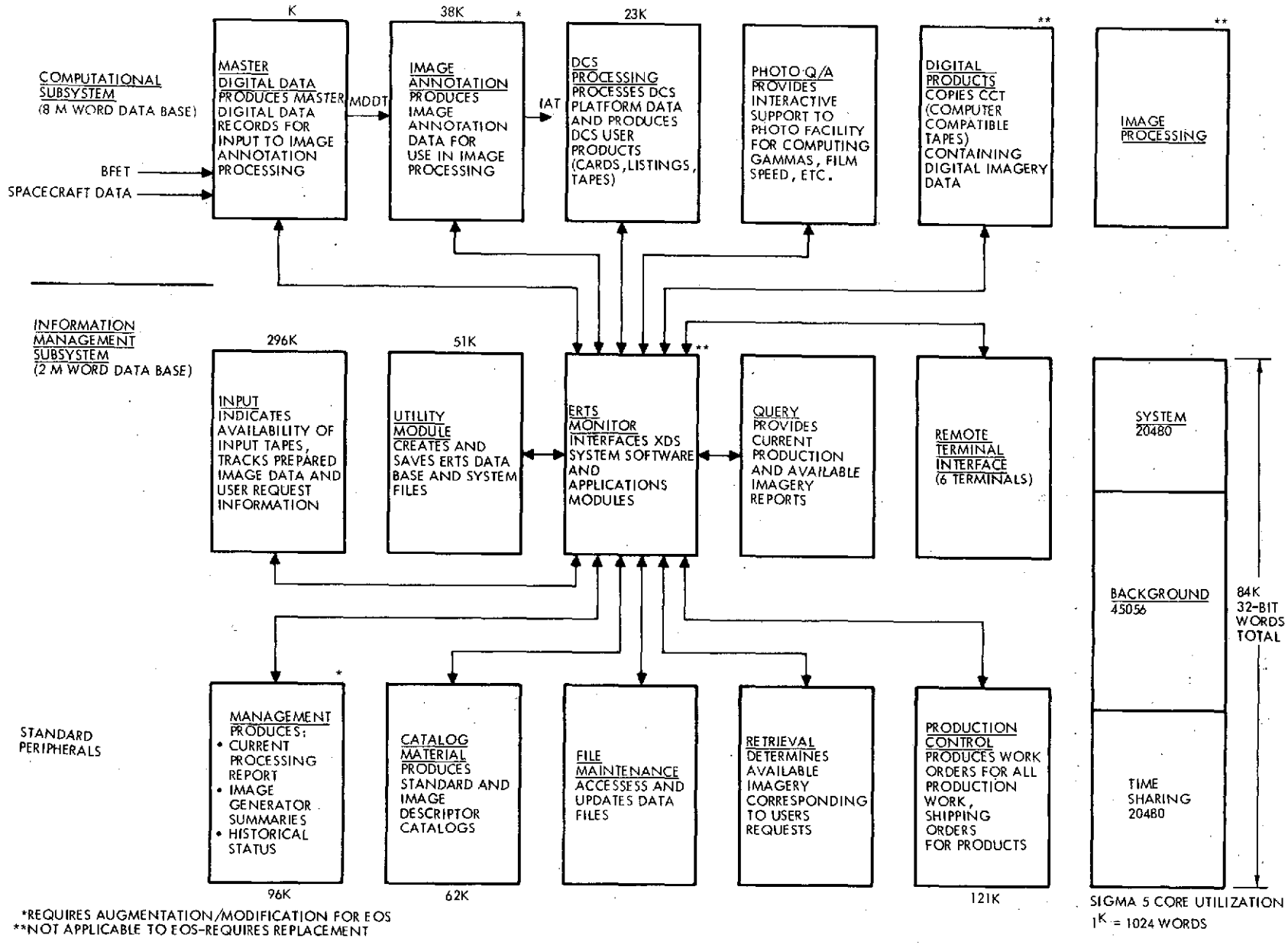

Figure 9-9. NASA Data Processing Facility System Overview

The current NDPF functions are performed on a single XDS Sigma 5 computer with 84K memory, three disk drive units, and 10 tape drive units. The photo production facility is sized to produce 860 MSS scenes/ week and 860 RBV scenes/week with 36,000 positive/negative transparencies for each. The electron beam recorder is not considered applicable due to the increased performance requirements of EOS, but the photo production facility is considerable applicable. Section 7.7, Appendix A lists EOS-applicable components of the ERTS information management hardware and photo production equipment. Replacement hardware cost is approximately $1.6M and must be weighed against increased operational costs due to the age of the equipment.

The baseline DSL/IMS uses the existing Sigma 5 hardware with added core memory, all applicable ERTS IMS software, and the ERTS photo production facility. The Sigma 5 is lightly loaded for EOS DSL/IMS software functions and rates. New hardware components such as the laser beam recorders and high density digital tape generation equipment are summarized in Section 9.3.5 under image processing output product generation and are discussed in more detail in Appendix A, Section 7.11. Software modifications include process control replacement, DCS processing replacement, and upgrading of image annotation processing for the different orbit and sensors and of the management interface for added process monitoring and trace-back capability.

9.3.4 Image Processing System

The image processing system (IPS) of the CDPF is required to perform the following functions:

- Reformatting of input sensor data tapes into line-sequential, pixel-ordered, band-interleaved-by-line, computer-compatible format and extraction of correction data
- Measurement of radiometric and geometric errors in the data using calibration data and measurements and registration control points
- Image correction of the thematic mapper and HRPI data for the measured errors and to desired map or reference image coordinates

- Generation of user output products, including all corrected and uncorrected high density digital tape and computer-compatible tape products and master copies of film products
- Generation and maintenance of the registration control point library
- Generation and maintenance of the sensor calibration data base.

The baseline functional IPS structure is shown in Figure 9-10 and is composed of four major functional subsystems:

1) Data reformatting and error measurement data extraction
2) Image error calculation
3) Image correction
4) Output product generation.

The algorithms used for error measurement and correction are discussed in detail in Appendix A, Section 7.9. Implementation is summarized in the following subsections. The basic design philosophy includes utilization of hard-wired algorithms in two critical areas with the remainder of the system in computer software to provide needed flexibility.

9.3.4.1 Data Reformatting and Error Measurement and Data Extraction

The data reformatting process converts the wideband recorder data from sensor line-parallel, pixel-scrambled, band-interleaved-by-pixel multiplexed serial data into sensor line-sequential, pixel-ordered, band-interleaved-by-line data in 32-bit parallel format for interface to the image correction system. This process relies heavily on special-purpose hardware buffers in the wideband recorder-to-computer interface for the demultiplexing and line buffering.

The error measurement data extraction function performs the image processing system prepass setup and the first-pass playback of the sensor data for registration control points (RCP) and calibration data extraction. The prepass setup phase generated control tables for use by the RCP and calibration data extraction hardware. The tables designate line and pixel numbers for RCP search regions based on apriori system calibration and measurement data (e.g., ephemeris, attitude, alignment, scan profile)

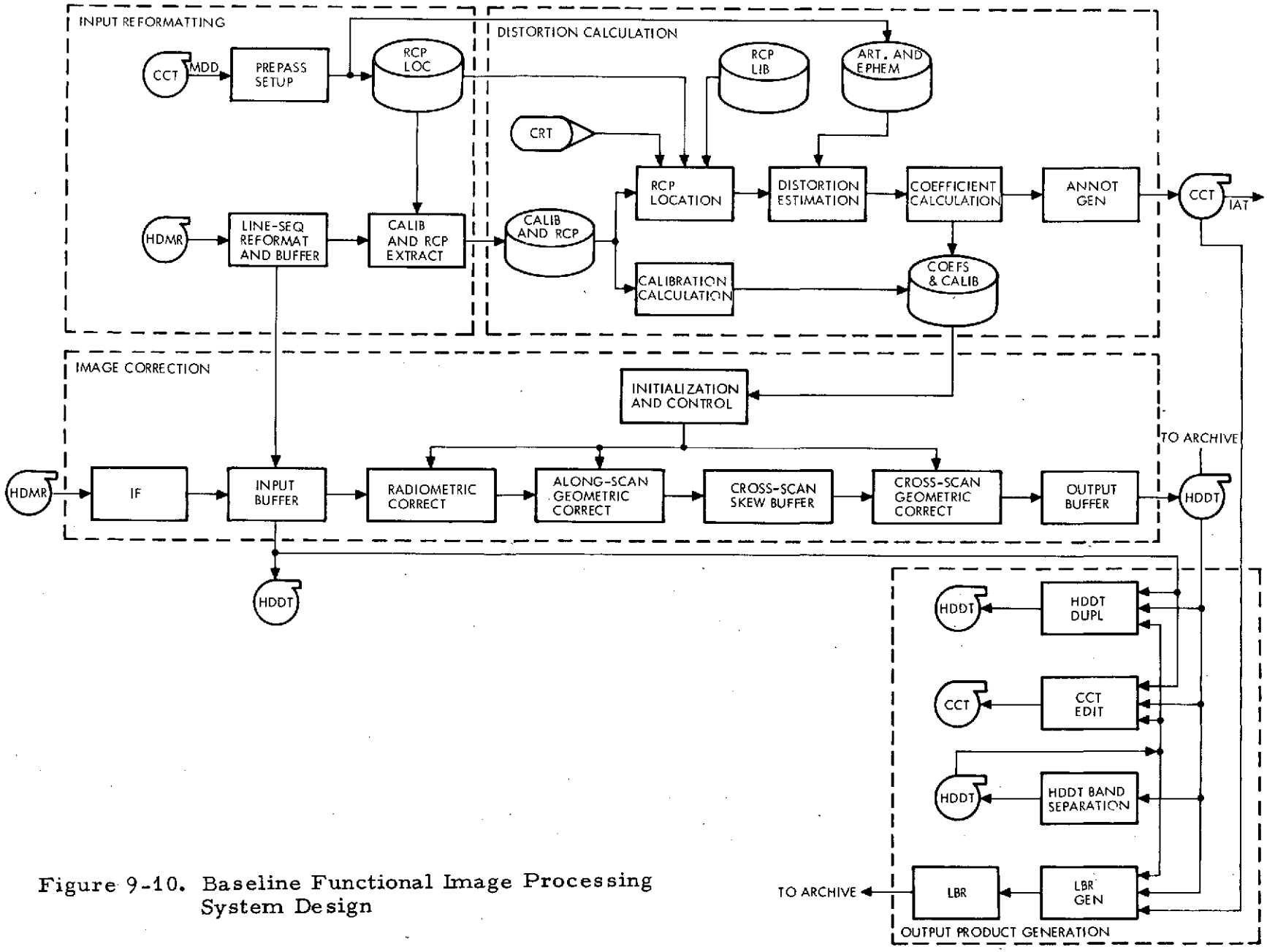

Figure 9-10. Baseline Functional Image Processing System Design

obtained from the control center and the information management system. Upon completion of the prepass setup phase, the thematic mapper and HRPI raw sensors data tapes are played through to extract the radiometric calibration measurement data and the RCP search areas for the entire pass. As the serial data stream is produced by the high-density multitrack recorder (HDMR) subsystem, the RCP search regions and calibration data are stripped out, buffered, and placed in temporary direct access files for later use by the distortion calculation function.

9.3.4.2 Distortion Calculation

The distortion calculation subsystem processes input data from the error measurement data extraction process and the master digital data tape to produce an error correction file. This file contains sufficient information to correct the sensor images and produce annotated output products. The file is stored on a cartridge disc pack and stored with the HDMR pass tape of each sensor.

The distortion calculation function has five major tasks: 1) RCP location, 2) detector calibration, 3) error estimation, 4) distortion coefficient calculation, and 5) annotation generation. Secondary tasks include maintenance of the RCP and calibration data library.

The RCP location phase consists of processing RCP search areas stripped from the raw data tape by the error measurement data extraction function. These areas are analyzed automatically for the precise location of the specified RCP within the scene. If the automatic RCP location processing fails with the preselected number of RCP's within a scene or their alternates, the operator may intervene to resolve the difficulty. The operator may select a new set of RCP's to avoid local cloud cover not predicted by the meteorological planning information. The reference RCP'c are stored in the RCP library, within a 100 MB disc file. The results of the RCP location process are passed to the error estimation phase.

The detector calibration data processing for each sensor depends on the time in the data base update cycle. If the data base for a particular sensor is due for update, the calibration data is processed completely and

used to update the detector calibration data base for that sensor. If no update is required, the data are scanned for limit violations, compressed and placed in the header file on the uncorrected data tapes.

The error estimation task calculates the sensor pointing vector as a function of time, using best-fit ephemeris and RCP location measurements. A sequential estimator is used to estimate the sensor pass dynamics. The updated pointing information is passed to the distortion coefficient calculation process. This process determines the image correction parameters necessary to map the distorted input sensor data into the corrected output coordinate system used for generating output products.

Annotation files are constructed for each pass/scene to supply data identification and labeling. These data will include data generated during processing of the image data such as frame time and number and nadir point as well as special annotation provided by the information management system.

The header data and annotation files, including the calibration data and correction coefficients, are placed on the cartridge disc pack. This pack contains the error correction and image annotation files, and is stored with the HDMR tape until image correction processing takes place. It provides sufficient information to correct the sensor data. The information on the disc pack also provides annotation and control for generation of the output products.

9.3.4.3 Image Corrections

The image correction function performs a second pass on the thematic mapper and HRPI raw data tapes. The data is corrected for radiometric calibration errors and processed along and across scan to remove geometric errors. The first two output products are output from this function. Corrected and uncorrected images are produced on high density digital tape (HDDT).

The image correction is under control of a process control task whose primary function is to provide data management functions to the various steps in the image correction process. These data management functions include control of the HDMR subsystem including the hardware

line reformatter, routing of the radiometric calibration data, management of the distortion correction coefficients used by the geometric correction hardware and control of the HDDT generation for primary output products.

The raw sensor data are received from the HDMR subsystem as a frame synchronized serial bit stream. This bit stream is decommutated via a special hardware line reformatter according to the basic format of the sensor, HRPI, or thematic mapper, and the desired data output format. The resultant line sequential, band interleaved data are buffered and distributed to the along-scan correction hardware and an HDDT system for the generation of uncorrected image tapes.

The along-scan correction hardware performs radiometric calibration of the input data using calibration data supplied from the calibration data base. The calibrated data are next corrected in the along-scan direction using the distortion coefficients from the distortion calculation function. The output of the along-scan corrector is placed into a large core skew buffer for use by the cross-scan correction hardware.

The along-scan corrected data are read from the skew buffer by the cross-scan correction hardware as sequential input lines to produce continuous, corrected output lines. The output of the cross-scan hardware is passed directly to the output HDDT system to create the corrected image tapes.

9.3.4.4 Output Product Generation

The output product generation function services the user product requests in response to planning data provided by the information management system. This function provides the user the output of the image correction function in the form most useful to his needs.

The primary input media are the HDDT's containing band-interleaved, corrected, or uncorrected image data. These HDDT's may be copied one to one, edited or reprocessed into band separated format. Computer-compatible tapes may be generated to support users having low data volume requirements.

User film products are normally generated from band-separated, corrected HDDT's via the system laser beam recorder. However, special processing and/or editing may be performed on small volumes of custom film products.

9.3.5 Image Processing System Hardware Baseline

The hardware design concept for the image processing system is based on the high throughput capacity of special-purpose hardware for the image data processing tasks and the flexible input/output and control capabilities found in the medium-scale 32-bit class of general-purpose computers. The design further emphasizes the isolation of high volume data paths by use of multiported memories with separate direct memory access for each process and direct data buses between high bandwidth processes that require only process control functions from the central processing unit.

The principal functions of the image processing system are divided into three processing subsystems: image correction; estimation, formatting, and film generation; and formatting and tape generation. Each of these subsystems is supported by a single medium-scale 32-bit computer.

The Xerox 550 system was chosen to be the basic building block for the subsystem implementation. This medium-speed machine, 0.35 Mips, offers the computational capacity necessary for each of the functions while offering the input/output flexibility and memory structure of a much larger system. This flexibility is essential to support the extensive use of special-purpose hardware in the baseline design.

9.3.5.1 Error Correction Subsystem

The error correction subsystem is allocated the function of performing the image correction on the thematic mapper and HRPI raw data and generating the primary output product, i.e., corrected HDDT's. The error correction subsystem is based on a single Xerox 550 central processing unit (CPU), 176K 32-bit words of main memory, a set of support peripherals and the special-purpose hardware necessary to support the thematic mapper and HRPI image correction streams. A summary of the

baseline hardware configuration for the image correction subsystem is shown in Figure 9-11.

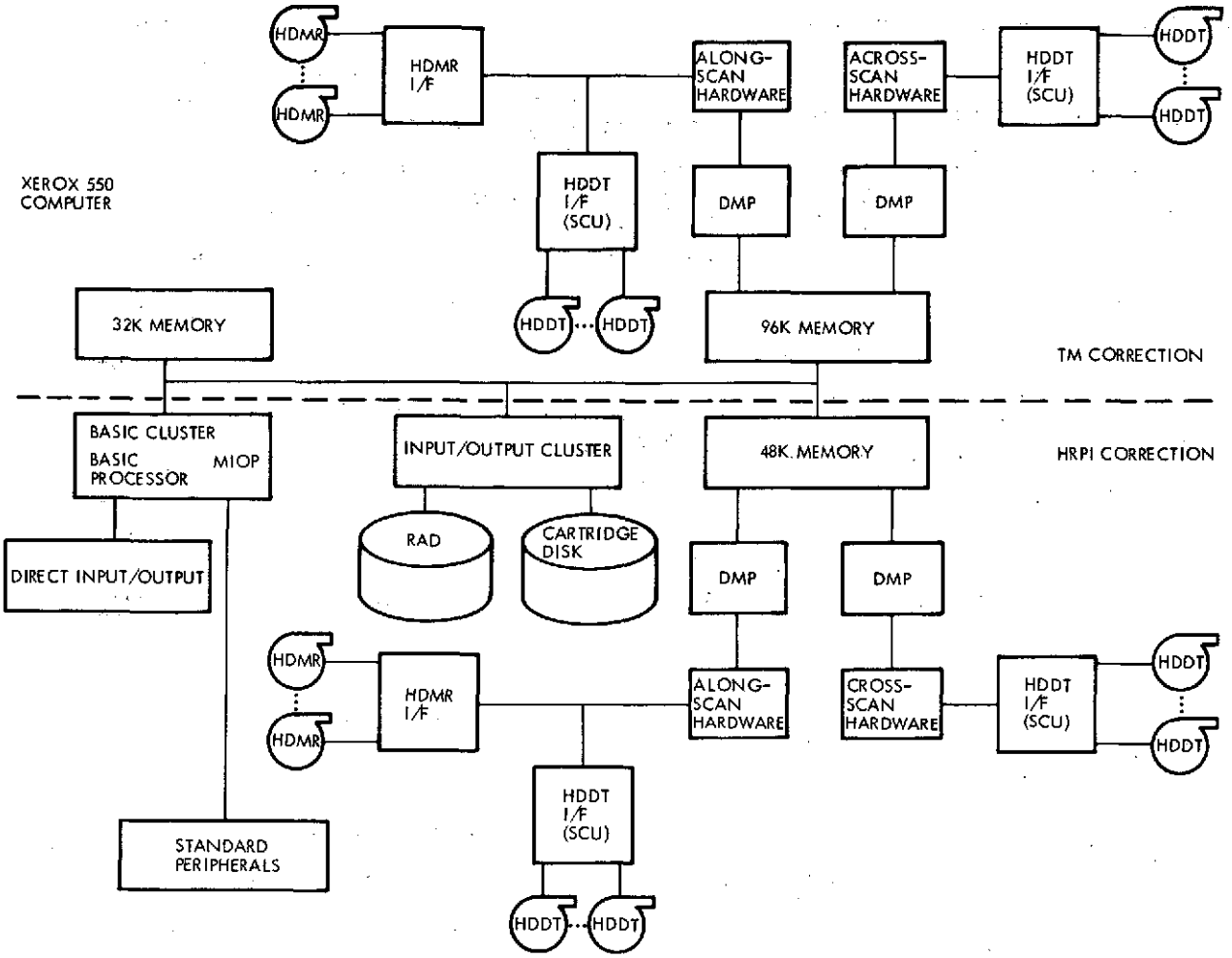

Figure 9-11. Error Correction Subsystem Hardware Complement

The basic Xerox 550 system with 32K of memory is used to support the process control for the two image correction chains. The throughput required is quite low with an average rate of less than 0.15 MIPS required to support the process control functions. This is well within the 0.35 MIPS capacity of the Xerox 550.

There are two separate image correction chains. One each for the thematic mapper and HRPI. Each image correction chain consists of a HDMR system interface, a hardware line reformatter, along- and cross-scan correction hardware, a segment of 32-bit main memory and a pair

of HDDT systems. The magnetic tape systems have only control interfaces to the Xerox 550 system for this configuration. All data flow is via direct data buses between the magnetic tape systems and the special-purpose hardware. The large core across-scan skew buffers are configured as part of the Xerox 550 system. However, this core is normally not used by the CPU except as a means of loading the large radiometric calibration constant arrays into the along-scan correction hardware. The normal use of these core modules is via dedicated memory ports and direct memory access controllers to the thematic mapper and HRPI image correction chains. The assignment of separate ports to the CPU modules and each of the image processors allows interference free use of the memory as separate buffers but still allows access by the main CPU if necessary.

The distortion correction coefficients, calibration data, and annotation data are passed to the error correction subsystem via cartridge disc packs. One cartridge is generated for each HDMR tape by the formatting subsystem.

9.3.5.2 Estimation, Formatting, and Film Generation Subsystem

The estimation, formatting, and film generation subsystem is allocated the error measurement data extraction, distortion calculation, and film output product generation functions. This configuration is supported by a single Xerox 550 CPU with 128K words of 32-bit main memory, standard peripherals, and the special-purpose hardware required to support the HDMR and HDDT systems. A summary of the formatting subsystem hardware configuration is shown in Figure 9-12.

The computational workload on this system is modest. The major tasks of prepass setup, RCP extraction and processing, distortion estimation, and calibration data management require less than 0.10 Mps capacity for a two-shift operation at the system loading specified in Appendix A, Section 7.11. The data base maintenance tasks for calibration data and the RCP library are low throughput tasks once the initial data base is established.

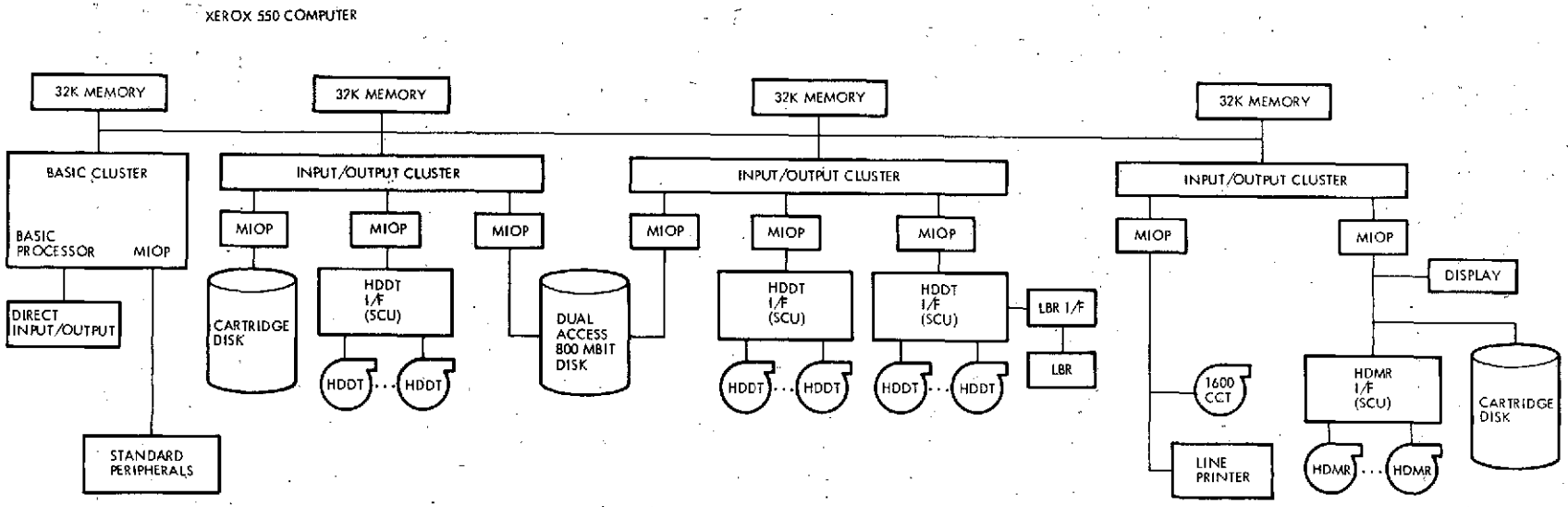

Figure 9-12. Estimation, Formatting, and Film Generation Subsystem Hardware Complement

These tasks also would not normally be run during first-pass processing since they would compete with the RCP processing for the display system. The remaining tasks are basically input/output-related and are limited by the available permutations of peripherals to accomplish low volume output generation.

The system memory configuration was sized to support the basic system software, pass one application software, and adequate input/output buffers to allow output product generation during pass one.

The first-pass processing of the sensor raw data tape is supported by the interface to the RCP extraction hardware and HDMR subsystem. This is the primary hardware interface for this function.

The RCP processing and distortion estimation processing are supported by the display system, 100 Mbytes of direct access for the RCP library and a cartridge disc system for distortion correction coefficients and calibration data.

The output product generation tasks, except computer-compatible tape duplication, involve the use of an HDDT either as an input and/or output medium. The HDDT systems have two independent data interfaces: one high rate port for use with the laser beam recorder and other HDDT's, and a separate multiplex input/output processor interface for providing a maximum data rate of 750 Kbytes/sec into the CPU memory. The control interface is via the direct input/output lines. An HDDT-to-HDDT tape duplication operation, then, would only involve the control interface and the data flowing directly between the tape controllers. High data rate laser beam recorder operation would use the high-speed bus from the HDDT controller although an image could be sent to the laser beam recorder from the main memory and/or large disc store via the multiplex input/output processor interface.

The generation of band-separated images and special editing of the image data tapes is supported by the use of the 1000 Mbyte disc system. This disc system is also provided with dual data paths to allow scene-by-scene processing at throughput rates approaching the average bandwidth of the discs.

9.3.5.3 Formatting and Tape Generation Subsystem

The formatting and tape generation subsystem is allocated the function of performing the output product formatting and generating the output tape. This configuration is supported by a single Xerox 550 CPU with 128K words of 32-bit words of main memory, standard peripherals, and a dual density 1600/6250 bpi high performance tape system. A summary of this hardware configuration is shown in Figure 9-13.

The computational workload on this system is also modest. The major band-separated task and generation of user requested CCT require less than 0.10 MIPS capacity for a two-shift operation. The generation of band-separated images is again supported by the 1000 Mbyte disk system in the same manner as the previous subsystem. This addition capability is necessary to satisfy the throughput requirement for a first-generation film product of each image. User requested computer-compatible tapes may be generated at either 1600 or 6250 bpi via the dual density tape system. Editing may be done to or from the 1000 Mbyte disk system.

9.3.6 Operational Considerations

Sizing and timing analyses are presented in Appendix A, Section 7.11 to justify the conservation of the above hardware design in performing the image processing at the required throughputs. Summary capability is 50 thematic mapper scenes and 200 HRPI scenes per 12-hour work day, including multiple HDDT copy, computer-compatible tape and positive-negative film masters of every scene, i.e., enough to allow complete United States coverage every 17 days in a two-shift-per-day operation, regardless of cloud cover. Estimated operational production timeline is shown in Figure 9-14, giving corrected data turnaround within one spacecraft pass of when it is collected.

Manual interaction in the image correction process is kept to a minimum, i.e., RCP library maintenance and tape mounts, etc. Initial entry of RCP's into the system is performed manually, with later utilization of RCP data (location) being under software control (with provision for manual editing). The low number of RCP's required per pass render this a one-man-or-less task. The sheer quantity of data, however, translates

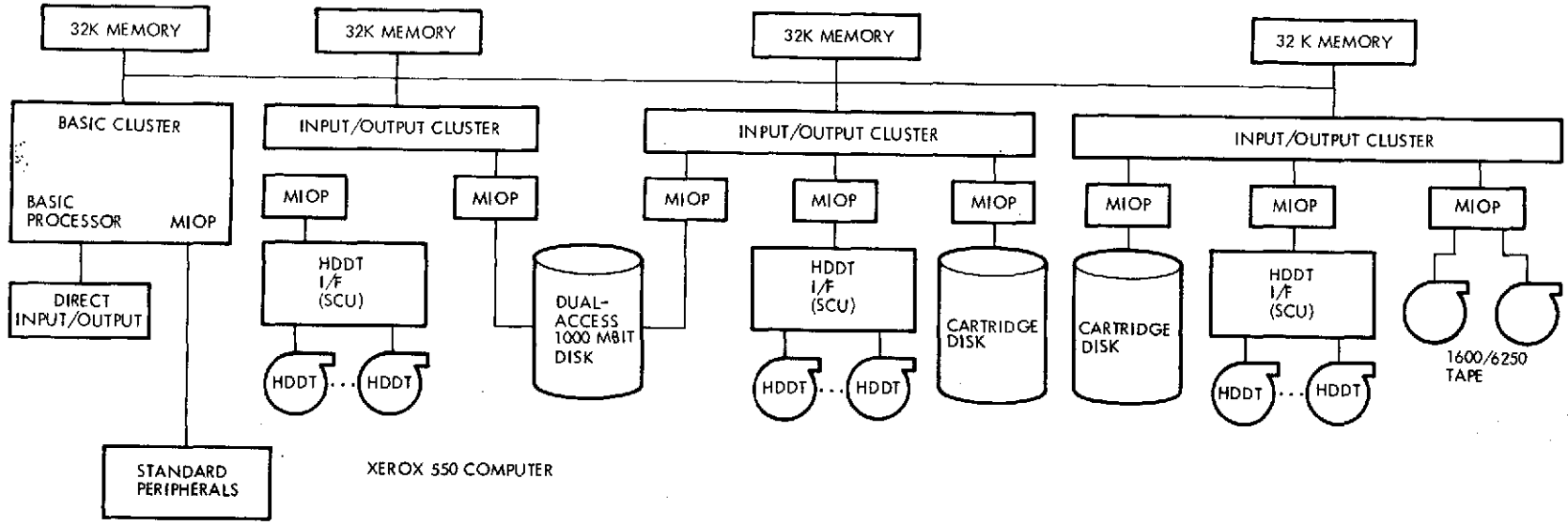

Figure 9-13. Formatting and Tape Generation Subsystem Hardware Complement

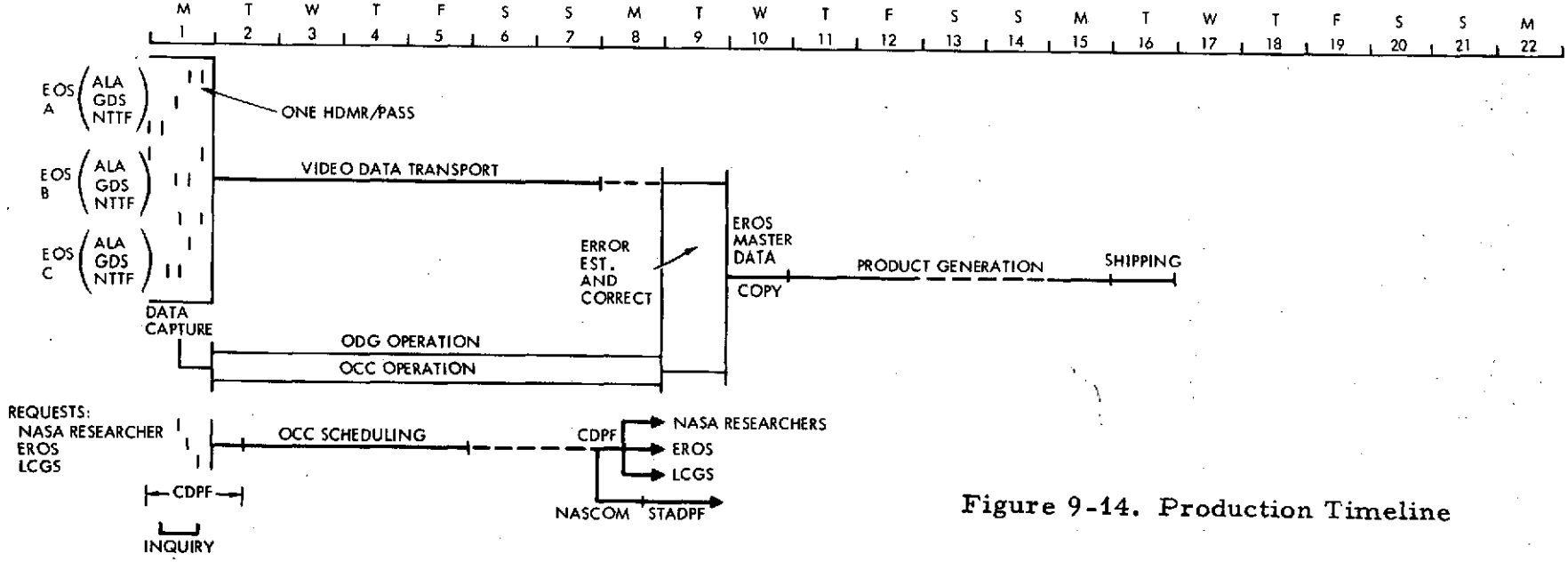

Figure 9-14. Production Timeline

into a large number of tape mounts/dismounts. For a worst-case United States coverage example, a total of 20 wideband tape replacements, 132 HDDT replacements, and 96 computer-compatible tape replacements (total of 248 reel replacements) per day, or an average 5.2 replacements/hour for each of four data handlers during a 12-hour processing day.

10. COST EVALUATION

Design/cost tradeoffs are an important aspect of obtaining an effective EOS program. Such comparisons have been or are being conducted at four distinct levels:

1) Subsystem design/cost tradeoffs. Selection of the best unit-level implementation in models, where this selection impacts only the module in question.

2) Spacecraft design/cost tradeoffs. Tradeoffs conducted at the spacecraft level (including unit-level tradeoffs which have a spacecraft level impact), where these choices do not impact other system elements such as ground data handling.

3) System level design/cost tradeoffs. Top-level tradeoffs where more than one system element is involved (e.g., launch vehicle selection, orbit selection, and instrument selection).

4) Mission-life-cycle cost tradeoffs. Design tradeoffs whose full impact can only be evaluated over a period of years involving many flights (e.g., the cost savings due to an orbit repair and a retrieval and the use of existing designs versus higher nonrecurring but lower recurring costs).*

10.1 COSTING APPROACH

Conduct of a heavily interactive cost tradeoff evaluation as implied at the system level requires a tool that will expedite the mechanical process involved. For this study, a computerized cost model was developed and used to perform the cost tradeoffs presented below. This computer program consists of two elements:

1) Equipment catalog

2) Configuration model.

The equipment catalog is a coded data base from which a specified satellite configuration can be assembled using the configuration model as

*A major system-level tradeoff is in the Shuttle application approach (Report 6), which concerns mission-cycle costs.

a driver. Data entered in the catalog includes a part and option number, the nonrecurring and recurring cost of the item, whether the item is make or buy, and a code to indicate whether or not a qualification item arises from unit design or another item must be procured for the module and/or Observatory qualification tests. Option numbers present alternate approaches to accomplishing the same function. For example, data on three different types of on-board computers reside in our data base. Weights of components can be summed to yield Observatory weight as easily as costs can be accumulated once a configuration is specified.

The configuration model consists of a listing of each component by part and option number and the quantity required by each. Figure 10-1 schematically illustrates the model as it resides in the computer. Assembling of new configurations is most easily accomplished by calling up an existing configuration closest to the one desired and editing the listing to add, modify, or delete entries until the desired configuration is arrived at. Figure 10-2 illustrates a listing for a typical module complete with recurring and nonrecurring costs. (Nonrecurring costs include the qualification module.)

10.2 COST TRADEOFFS

Cost tradeoffs conducted during this study and included here are:

- Spacecraft redundancy level
- Payload selection
- Thematic mapper scan techniques
- Low cost ground station capability
- Central data processing facility throughput capability.

Using the cost data for a baseline configuration, we have developed costs for a modular spacecraft bus capable of supporting advanced missions as well as the total EOS-A program. The baseline configuration is defined in Table 10-1. Cost increments for variations from this baseline are

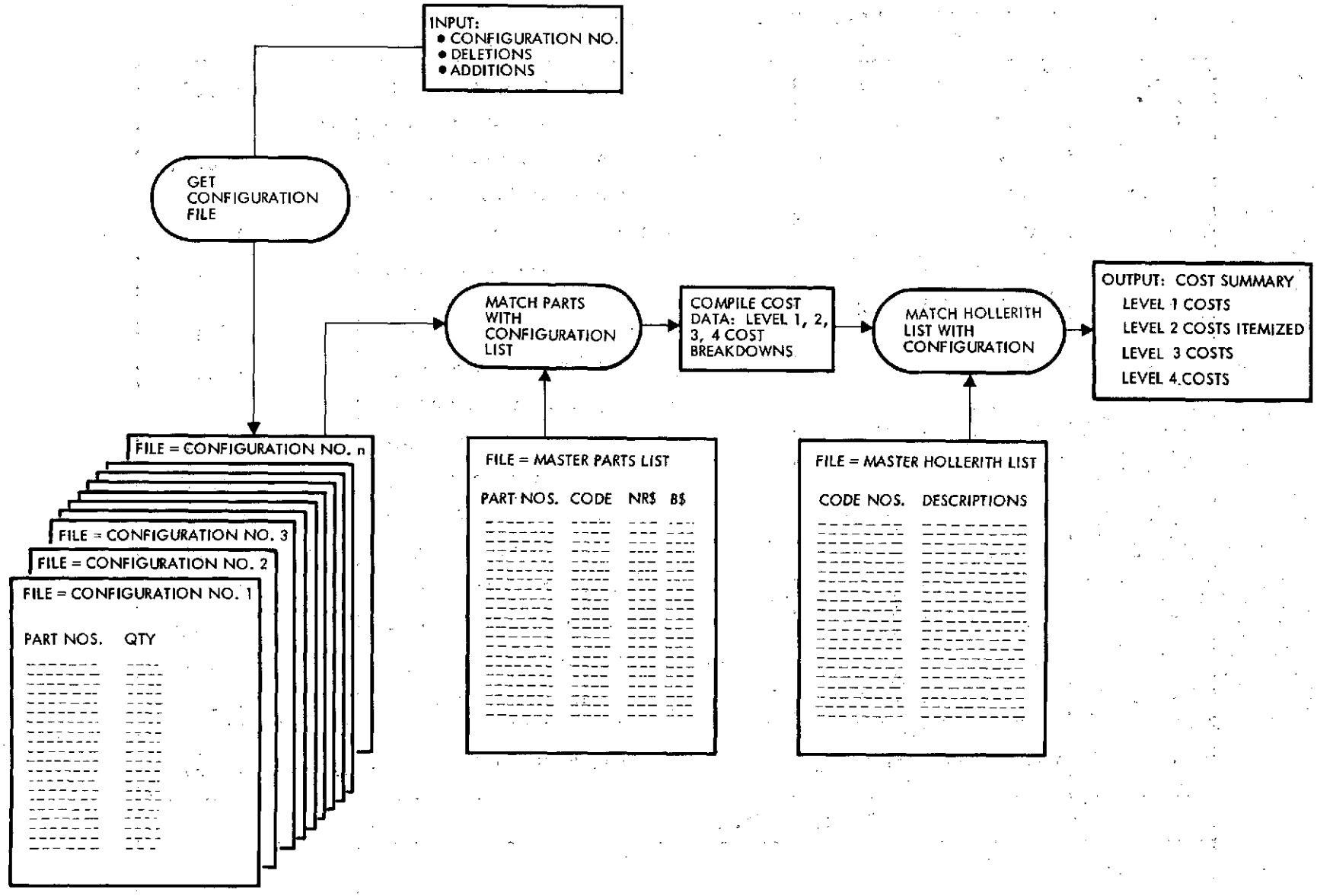

Figure 10-1. Costing Program Organization

Module Number	Module Name
3200	Communications and data handling (CDH) module
Option 5	

COMPONENT COSTS

Component Number and Option	Component Name	Quantity	Nonrecurring	Recurring
3205-1	CDH module structure	1	34.6	19.6
3206-1	CDH module thermal control	1	74.0	13.9
3207-1	S-band omni antennas	1	30.0	20.0
3208-1	S-band transponder	1	123.0	108.0
3210-1	S-band diplexer	2	41.0	32.0
3211-2	Demodulator/decoder	1	30.0	30.0
3212-1	Data interface unit	1	155.0	15.0
3213-1	Bus controller	1	160.0	20.0
3214-1	Baseband assembly	1	102.0	12.0
3215.1-1	On-board computer (CPU)	1	355.0	45.0
3215.2-1	On-board computer memory module	2	70.0	70.0
3216.1-1	Basic software	0	550.0	0
3217-1	CDH power conditioning	1	75.0	25.0
3218-1	CDH wiring harness	1	56.0	15.0
3220-1	Signal conditioning electronics	1	114.0	7.0
3221-1	Hybrid combiner	1	2.5	1.0
3223-1	RF transfer switch	1	6.5	5.5

Figure 10-2. Typical Module Summary Taken from Computer Run

Table 10-1. Payload/GDHS Configuration Options Definition

	Case							
	I*	II	III	IV	V	VI	VII	VIII
Number of spacecraft	1	1	1	1	1	1	2	1
Thematic mapper	1	1	1	1	0	0	0	0
HRPI	1	1	0	0	1	1	0	0
Multispectral scanner	0	0	1	1	1	1	2	2
VTR	0	0	2	2	2	2	4	3
All-up central data processing facility	1	0	0	0	0	0	0	0
Reduced central data processing facility	1	0	0	0	0	0	0	0
All-up one instrument plus modified ERTS processing facility	0	0	1	0	1	0	0	0
Reduced one instrument plus modified ERTS processing facility	0	0	0	1	0	1	0	0
Modified ERTS processing facility	0	0	0	0	0	0	1	1

Baseline System

- Delta structure
- Minimum redundancy
- Case I with Te' and Westinghouse
- Computer low cost ground station
- Retrieval but no resupply
- No TDRSS
- No VTR

*Baseline.

readily assembled from the data presented here. Table 10-2 provides recurring and nonrecurring hardware costs for three levels of redundancy. Backup information on each module is presented in Tables 10-3 through 10-8. Similar information for the wideband communications module is presented in Table 10-9.

A summary of the total spacecraft (bus) costs including management and other non-hardware items appears in Table 10-10. Table 10-11 provides cost data for the observatory ground support equipment. Costs are based on the equipment described in Section 8 of this report. We have reviewed the three thematic mapper approaches and they are presented in Section 5. Table 10-12 summarizes the system cost impacts for these instruments.

Our ground station studies discussed in Section 9 present an attractive design for the image processing facility. Costs for this facility are given in Table 10-13. These costs are based on a system which provides a total capability for all necessary revisions and the generation of all user products. Also included is a system that is based on a single computer. This limited system can handle much of the required corrections but fails to deliver all the required user products. It could be very attractive to NASA for R and D activities if another agency takes over the job of generating all user products. A backup hardware listing for these configurations is shown in Table 10-14.

Two low cost ground station configurations have been found attractive depending on the needs and financial capability of the user. The cost breakdown for these is presented in Table 10-15. System operating costs are given in Table 10-16.

A selection between various R and D, operational, and combined missions is shown in Table 10-17. Costs vary approximately over a two to one range. Further options can be introduced by incrementing data on this chart with data taken from other charts.

Table 10-2. Spacecraft Hardware Costs ($000)

	Basic Spacecraft		Minimum Spacecraft		Nominal Spacecraft	
	Nonrecurring	Recurring	Nonrecurring	Recurring	Nonrecurring	Recurring
Spacecraft structure	613.5	263.8	618.5	265.8	618.5	265.8
Communications and data handling	2,028.6	439.0	2,028.6	439.0	2,325.6	736.0
Electric power module	1,171.2	244.2	1,277.2	345.2	1,316.2	384.2
Attitude determination module	2,326.4	638.2	2,351.4	663.6	2,798.4	1,110.6
Actuation module	1,437.2	539.0	2,111.2	729.5	2,261.2	852.5
Solar array and drive module	1,179.9	765.0	1,232.9	862.0	1,254.9	884.0
Subtotal	8,756.8	2,889.2	9,619.8	3,305.1	10,574.8	4,233.1
Total	11,646.0		12,924.9		14,807.9	

Table 10-3. Spacecraft Structure Assembly Costs ($000)

	Basic Spacecraft			Minimum Spacecraft			Nominal Spacecraft		
	Quantity	Nonrecurring	Recurring	Quantity	Nonrecurring	Recurring	Quantity	Nonrecurring	Recurring
Basic bus structure	1	249.0	88.9	1	249.0	88.9	1	249.0	88.9
Transition ring structure	1	33.5	7.6	1	33.5	7.6	1	33.5	7.6
Adapter	1	71.0	25.2	1	71.0	25.2	1	71.0	25.2
Bus mechanisms	1	65.0	16.1	1	65.0	16.1	1	65.0	16.1
Thermal control	1	175.0	118.0	1	175.0	118.0	1	175.0	118.0
Bus harness and J-box		20.0	8.0		25.0	10.0		25.0	10.0
Total		613.5	263.8		618.5	265.8		618.5	265.8

Table 10-4. Communications and Data Handling Module Costs ($000)

	Basic Spacecraft			Minimum Spacecraft			Nominal Spacecraft		
	Quantity	Nonrecurring	Recurring	Quantity	Nonrecurring	Recurring	Quantity	Nonrecurring	Recurring
Communication and data handling module structure	1	34.6	19.6	1	34.6	19.6	1	34.6	19.6
Communication and data handling thermal control	1	74.0	13.9	1	74.0	13.9	1	74.0	13.9
S-band omni antennas	1	30.0	20.0	1	30.0	20.0	1	30.0	20.0
S-band transponder	1	123.0	108.0	1	123.0	108.0	2	231.0	216.0
S-band diplexer	2	41.0	32.0	2	41.0	32.0	1	41.0	32.0
Demodulator/decoder	1	30.0	30.0	1	30.0	30.0	2	60.0	60.0
Data interface unit	1	155.0	15.0	1	155.0	15.0	2	170.0	30.0
Bus controller	1	160.0	20.0	1	160.0	20.0	2	180.0	40.0
Baseband assembly	1	102.0	12.0	1	102.0	12.0	2	114.0	24.0
On-board computer (CPU)	1	355.0	45.0	1	355.0	45.0	2	400.0	90.0
On-board computer memory module	2	70.0	70.0	2	70.0	70.0	3	105.0	105.0
Communication and data handling power conditioning	1	75.0	25.0	1	75.0	25.0	2	100.0	50.0
Communication and data handling		56.0	15.0		56.0	15.0		56.0	15.0
Signal conditioning electronics	1	114.0	7.0	1	114.0	7.0	2	121.0	14.0
Hybrid combiner	1	2.5	1.0	1	2.5	1.0	1	2.5	1.0
RF transfer switch	1	6.5	5.5	1	6.5	5.5	1	6.5	5.5
Total		1,478.6	439.0		1 478.6	439.0		1,775.6	736.0

Table 10-5. Electric Power Module Costs ($000)

	Basic Spacecraft			Minimum Spacecraft			Nominal Spacecraft		
	Quantity	Nonrecurring	Recurring	Quantity	Nonrecurring	Recurring	Quantity	Nonrecurring	Recurring
Power module structure	1	34.6	19.6	1	34.6	19.6	1	34.6	19.6
Power thermal control	1	92.0	18.0	1	92.0	18.0	1	92.0	18.0
Power control unit	1	407.0	63.6	2	470.6	127.2	2	470.6	127.2
Battery	2	332.6	57.6	2*	350.0	70.0	2*	350.0	70.0
Diode assembly	1	12.0	2.2	1	12.0	2.2	1	12.0	2.2
Power module signal conditioning	1	29.0	12.0	1	29.0	12.0	2	41.0	24.0
Data interface unit	1	57.0	27.0	1	57.0	27.0	2	84.0	54.0
Power module harness		55.0	17.0		55.0	17.0		55.0	17.0
Secondary power and bus protection	1	140.0	25.0	2	165.0	50.0	2	165.0	50.0
Power disconnect	1	12.0	2.2	1	12.0	2.2	1	12.0	2.2
Total		1,171.2	244.2		1,277.2	345.2		1,316.2	384.2

*Change from 30 to 40 amp-hr battery

Table 10-6. Attitude Determination Module Costs ($000)

	Basic Spacecraft			Minimum Spacecraft			Nominal Spacecraft		
	Quantity	Nonrecurring	Recurring	Quantity	Nonrecurring	Recurring	Quantity	Nonrecurring	Recurring
Attitude determination structure	1	127.4	19.6	1	127.4	19.6	1	127.4	19.6
Attitude determination thermal control	1	78.0	18.0	1	78.0	18.0	1	78.0	18.0
Gyro reference assembly	3	1,030.0	240.0	3	1,030.0	240.0	6	1,270.0	480.0
Star tracker	2	154.0	138.0	2	154.0	138.0	3	223.0	207.0
Magnetometer	1	40.0	20.0	1	40.0	20.0	2	60.0	40.0
Sun sensor	1	134.0	44.0	1	134.0	44.0	1	134.0	44.0
Transfer assembly	1	880.0	62.0	1	880.0	62.0	2	942.0	124.0
Data interface unit	1	20.0	15.0	1	20.0	15.0	2	35.0	30.0
Power conditioning unit	1	225.0	25.0	2	250.0	50.0	2	250.0	50.0
Attitude determination harness		50.0	16.0		50.0	16.0		50.0	16.0
ADS signal conditioning unit	1	48.0	41.0	1	48.0	41.0	2	89.0	82.0
Total		2,326.4	638.6		2,351.4	663.6		2,798.4	1,110.6

Table 10-7. Actuation Module Costs ($000)

	Basic Spacecraft			Minimum Spacecraft			Nominal Spacecraft		
	Quantity	Nonrecurring	Recurring	Quantity	Nonrecurring	Recurring	Quantity	Nonrecurring	Recurring
Actuation module structure	1	123.2	24.0	1	123.2	24.0	1	123.2	24.0
Attitude control thermal control	1	78.0	18.0	1	78.0	18.0	1	78.0	18.0
Propulsion thermal control (cold gas)	1	32.0	6.0	1	32.0	6.0	1	32.0	6.0
Reaction wheel	3	178.0	156.0	3	178.0	156.0	3	178.0	156.0
Magnetic torquer	3	90.0	24.0	3	90.0	24.0	3	90.0	24.0
Reaction wheel electronics	3	152.0	78.0	3	152.0	78.0	6	230.0	156.0
Valve and torquer electronics	1	170.0	25.0	1	250.0	105.0	1	250.0	105.0
Cold gas system		750.0	115.0		750.0	115.0		830.0	195.0
Hydrazine propulsion system	0	0	0	1	579.0	105.5	1	609.0	108.5
Data interface unit	1	35.0	20.0	1	35.0	20.0	2	55.0	40.0
Actuation module harness		50.0	16.0		65.0	21.0		65.0	21.0
Actuation module signal conditioning	1	29.0	22.0	1	29.0	22.0	2	51.0	44.0
Total		1,437.2	539.0		2,111.2	729.5		2,261.2	852.5

Table 10-8. Solar Array and Drive Module ($000)

	Basic Spacecraft			Minimum Spacecraft			Nominal Spacecraft		
	Quantity	Nonrecurring	Recurring	Quantity	Nonrecurring	Recurring	Quantity	Nonrecurring	Recurring
Array drive structure	1	78.0	22.0	1	78.0	22.0	1	78.0	22.0
Array structure	1	180.0	70.0	1	180.0	70.0		180.0	70.0
Array thermal control	1	52.0	12.0	1	52.0	12.0		52.0	12.0
Solar array subpanel	22	46.6	484.0	24	46.6	528.0	24	46.6	528.0
Array drive and electronics	1	700.0	148.0		728.0	176.0		728.0	176.0
Data interface unit	1	20.0	15.0	1	20.0	15.0		35.0	30.0
Solar array drive power conditioning	1	75.0	25.0	2	100.0	50.0	2	100.0	50.0
Solar array harness		15.0	5.0		15.0	5.0		15.0	5.0
Array drive harness		29.3	5.0		29.3	5.0		29.3	5.0
Signal conditioning	1	12.0	7.0	1	12.0	7.0		19.0	14.0
Total		1,179.9	765.0		1,232.9	862.0		1,254.9	884.0

Table 10-9. Wideband Communications and Data Handling Cost Summary ($000)

	Basic Spacecraft			Minimum Spacecraft		
	Quantity	Nonrecurring	Recurring	Quantity	Nonrecurring	Recurring
Wideband communications module structure	1	110.1	36.1	1	110.1	36.1
Wideband communications thermal control	1	123.9	40.4	1	123.9	40.4
X-band antennas	2	160.0	50.0	2	160.0	50.0
Antenna gimbal drive	2	356.0	256.0	2	356.0	256.0
Antenna drive electronics	1	200.0	25.0	2	225.0	50.0
X-band power amplifier	2	100.0	60.0	4	160.0	120.0
QPSK modulator	1	225.0	115.0	2	340.0	230.0
Biphase modulator	1	130.0	115.0	2	245.0	230.0
X-band RF switches	3	12.2	5.4	7	19.4	12.6
Flexible waveguide	12	50.4	14.4	20	60.0	24.0
Data interface unit	1	15.0	15.0	2	30.0	30.0
Speed buffer	1	800.0	180.0	1	800.0	180.0
MODS controller	1	210.0	30.0	2	240.0	60.0
Power conditioning unit	1	50.0	25.0	2	75.0	50.0
Signal conditioning	1	11.0	6.0	2	17.0	12.0
Module harness		20.0	7.0		20.0	7.0
40 MHz bandwidth filter	1	15.0	6.6	1	15.0	6.6
256 MHz bandwidth filter	1	15.0	6.6	1	15.0	6.6
Total		2,603.6	993.5		3,011.4	1,401.3

Table 10-10. Spacecraft Cost Summary ($000)

	Basic Spacecraft		Minimum Spacecraft		Nominal Spacecraft	
	Nonrecurring	Recurring	Nonrecurring	Recurring	Nonrecurring	Recurring
Program management	955.0	327.0	1,005.0	363.0	1,195.0	465.0
Systems engineering	1,373.0	35.0	1,517.0	40.0	1,681.0	50.0
Reliability and quality assurance	1,149.0	404.0	1,269.0	462.0	1,403.0	593.0
Module integration	507.0	148.0	661.0	196.0	945.0	280.0
Module environmental test	270.0	82.0	330.0	98.0	388.0	115.0
Spacecraft integration	90.0	29.0	95.0	31.0	102.0	36.0
EGSE	2,201.0	0	2,201.0	0	2,201.0	0
MGSE	591.0	0	711.0	0	711.0	0
AOP software	530.0	0	550.0	0	610.0	0
Spacecraft hardware	8,207.0	2,889.0	9,070.0	3,305.0	10,025.0	4,233.0
Total	15,873.0	3,914.0	17,409	4,495.0	19,261.0	5,772
	19,787		21,904		25,033	

Table 10-11. Ground Support Equipment Costs ($000)

	Nonrecurring			Recurring		
	EGSE	MGSE	Total	EGSE	MGSE	Total
Communications and data handling	1,066	50	1,116	770	32	802
Electric power	197	50	247	140	32	172
Attitude determination	456	100	556	320	64	384
Actuation	132	120	252	92	80	172
Propulsion	0	120	120	0	80	80
Solar array and drive	150	171	321	85	120	205
Overall bus	200*	100	300	0	70	70
Subtotal	2,201	711	2,912	1,407	478	1,885
Wideband communications	808	100	908	566	64	630
Total payload	400*	390	790	0	274	274
Subtotal	1,208	490	1,698	566	338	904
Total	3,409	1,201	4,610	1,973	816	2,789

*Software

Table 10-12. Thematic Mapper Scanning - Technique Tradeoff ($000)

	Te	Hughes	Honeywell
Instrument nonrecurring	16,300.0	15,700.0	16,100.0
Flight instrument	6,820.0	7,200.0	6,800.0
Payload structure	666.0	666.0	666.0
Wideband communications and data handling	2,603.6	2,603.6	2,603.6
CDPF	8,175.0	8,175.0	9,020.0
LCGS	828.0	828.0	1,020.0
Total	35,392.6	35,172.6	36,209.6

Table 10-13. Central Data Processing Facility Cost Summary ($000)

	Full-Capacity System		Limited System	
	First System	Additional System	First System	Additional System
Subproject management	200	70	200	70
Subproject engineering	500	100	500	100
Module-level quality assurance	100	40	100	40
Module integration and test	170	100	170	100
Software development*	750	0	750	0
Facility modifications	200	200	125	125
Hardware	6,655	5,905	2,914	2,289
Total*	8,175	6,015	4,859	2,724

*Add $85 K to each software nonrecurring cost, $220 K to each total recurring cost, and $845 K to each total nonrecurring cost to convert Honeywell conical scan to linear output.

Table 10-14. Central Data Processing Facility Hardware Cost Summary ($000)

	Full Capacity			Reduced Capacity		
	Quantity	Nonrecurring	Recurring	Quantity	Nonrecurring	Recurring
Basic central processing unit and peripherals	3	0	921.0	1	0	307.0
32 K memory module	11	0	726.0	5	0	330.0
Laser beam recorder and interface	1	260.0	105.0	1	260.0	105.0
Dual computer-compatible tape and controller	1	10.0	124.0	1	10.0	124.0
Dual high-density digital tape and interface	10	175.0	1,560.0	3	175.0	468.0
Interactive display	1	0	60.0	1	0	60.0
Pixel interpolator	2	125.0	120.0	1	125.0	60.0
1000 MB disk system	2	0	717.0	0	0	0
400 MB disk system	0	0	0	1	0	237.0
150 MB disk system	1	0	180.0	0	0	0
Dual cartridge disk system	4	0	108.0	1	0	27.0
Fixed-head disk system	2	0	80.0	1	0	40.0
MIOP	15	0	225.0	5	0	75.0
Input output cluster	6	0	48.0	2	0	16.0
High-density multitrack recorder	3		585.0	1	0	195.0
High-density multitrack recorder interfaces	-	175.0	291.0	0	100.0	205.0
High-density digital tape matrix switch	1	5.0	40.0	1	5.0	40.0
High-density multitrack recorder matrix switch	1	0	15.0	0	0	0
Total*		750.0	5,905.0		675.0	2,289.0

*Increase each recurring value by $220 K and each nonrecurring value by $760 K to convert Honeywell conical scan to linear output.

Table 10-15. Low-Cost Ground Station Cost Summary ($000)

	Computer-Based Option		Direct-Record Option	
	First System	Additional System	First System	Additional System
Subproject management	55	25	40	15
Subproject engineering	120	7	80	5
Module-level quality assurance	9	7	6	5
Module integration and test	35	7	20	5
Facility modifications	35	35	30	30
Hardware	569	379	452	162
Total	823	460	628	222

Note: some changes noted on first five entries (those before hardware) but total is about the same; no 15 percent handling etc. on hardware.

Table 10-16. Observatory Operations ($000 per year)

	TM and HRPI	TM and MSS Plus 2 VIR's	HRPI and MSS Plus 2 VTR's	2 MSS Plus 3 VTR's	2 (1 MSS Plus 2 VTR's)
Operations					
Network	Same as ERTS	Same as ERTS	Same as ERTS	Same as ERTS	1.2 x ERTS
Control center	Same as ERTS	Same as ERTS	1.2 x ERTS	Same as ERTS	1.3 x ERTS
CDPF	ERTS + $300 K	ERTS + $300 K	ERTS + $300 K	ERTS + $300 K	ERTS + $300 K
LCGS	$100 K	$100 K	$100 K	$100 K	$120 K
Expendables					
Film products	$250 K	$375 K	$600 K	$500 K	$375 K
Magnetic tape	$3200 K	$4000 K	$4000 K	$2000 K	$2000 K

Table 10-17. Payload and Ground Data Processing System Configuration Cost Tradeoffs ($000)

	Baseline	Case						
		II	III	IV	V	VI	VII	VIII
Program management	5,980.0	-110.0	-500.0	-610.0	-300.0	-410.0	-500.0	-1,800.0
Systems engineering	8,730.0	-130.0	-200.0	-330.0	-500.0	-1,500.0	-2,000.0	-2,500.0
Reliability and quality assurance	6,650.0	-50.0	0	-50.0	-150.0	-1,000.0	-1,000.0	-2,000.0
Integration	907.0	0	0	0	0	0	+203.0	-8.0
Environmental test	2,062.0	0	0	0	0	0	-129.0	-117.0
Qual spacecraft (including AOP software)	9,620.0	0	0	0	0	0	0	0
Flight spacecraft	3,305.0	0	0	0	0	0	+3,305.0	0
Hydrazine propulsion	incl. above	0	0	0	0	0	0	0
Mechanical GSE	1,201.0	0	0	0	0	0	-100.0	-100.0
Electrical GSE	3,409.0	0	0	0	0	0	-808.0	-808.0
MSS	0	0	+4,200.0	+4,200.0	+4,200.0	+4,200.0	+8,400.0	+8,400.0
Wideband video tape recorder	0	0	+800.0	+800.0	+800.0	+800.0	+1,600.0	+1,200.0
Thematic mapper	23,120.0	0	0	0	-23,120.0	-23,120.0	-23,120.0	-23,120.0
HRPI	15,700.0	0	-15,700.0	-15,700.0	0	0	-15,700.0	-15,700.0
Contractor-supplied equipment	1,107.0	0	-570.0	-570.0	-537.0	-537.0	-1,107.0	-1,107.0
Wideband communications and data handling	3,597.0	0	+85.0	+85.0	-1,606.0	-1,606.0	-3,377.0	-3,377.0
Instrument support structure	666.0	0	0	0	0	0	+34.0	-166.0
Network mods	1,775.0	0	-585.0	-585.0	-585.0	-585.0	-1,775.0	-1,775.0
Control center	2,116.0	0	0	0	0	0	-1,616.0	-1,616.0
Central data processing	8,175.0	-2,160.0	-350.0	-1,210.0	-350.0	-1,210.0	-7,225.0	-7,225.0
Low-cost ground station	823.0	0	0	0	-823.0	-823.0	-823.0	-823.0
ΔCost		-2,450.0	-12,820.0	-13,970.0	-22,971.0	-25,791.0	-44,631.0	-52,642.0
Total	98,943.0	96,493.0	86,123.0	84,973.0	75,972.0	73,152.0	54,312.0	46,301.0